UNIVERSITÀ DEGLI STUDI FIRENZE
DICEA
DIPARTIMENTO DI INGEGNERIA CIVILE E AMBIENTALE

UAM Universidad Autónoma de Madrid

Application of hydrothermal carbonization for sewage sludge and food waste valorization

Dissertation

submitted to and approved by the

Department of Civil and Environmental Engineering

University of Florence

and

Department of Chemical Engineering

Autonomous University of Madrid

in candidacy for the

Doctoral Program in International Doctorate in Civil and Environmental Engineering (UNIFI)

34 ° Cycle curriculum Environment, Resources and Security

and

Doctoral program in Applied Chemistry (UAM)

Supervisors:

Prof. Riccardo Gori

Prof. Angel F. Mohedano

PhD candidate:

Gemma Mannarino

2022

Table of contents

Summary

Sewage sludge (SS), which is the main by-product of a Water Resources Recovery Facility (WRRF), is produced worldwide in large amounts. The rapid population growth, together with the progressive urbanization, has led to the generation of an increasing amount of SS, which is expected to continuously increase in the next future (up to an annual production of 150 – 200 million tons on a dry basis by 2050). Further, the production of other wastes, such as food waste (FW), are going to increase in the coming years. In fact, more than 2 billion tons of municipal waste have been generated worldwide and the production is estimated to increase by 70% to 2050.

Sewage sludge and food waste must be properly disposed of using the best available technologies, in accordance with the current legislation and the circular economy principles. Both wastes can be generally treated via composting, anaerobic digestion (AD), incineration, and landfilling. However, all these treatments suffer from various limitations (e.g., long treatment time, pre-treatments, and inhibition). Therefore, thermochemical technologies, such as hydrothermal carbonization (HTC), are becoming increasingly attractive to treat different types of wet biomasses (such as SS, and FW). Indeed, HTC is able to transform the feedstock in three fractions: a solid fraction (hydrochar, HC), a liquid phase (process water, PW), and a small gaseous phase.

This aim of this work was to investigate the application of HTC to treat SS or FW. In particular, the carbonization of SS has been extensively studied (**Chapter 1 – 5**), whereas only **Chapter 6** has been devoted to the treatment of FW through HTC.

Chapter 1 studies the influence of HTC reaction conditions (i.e., temperature, time, and solid content) on products (HC and PW) characteristics. Secondary SS derived from San Colombano WRRF (Florence, Italy) was collected and further treated via HTC by changing the operating conditions. Both HC and PW were characterized, pointing out that there was a relationship between HTC conditions and products characteristics. Further, the dewaterability of SS after HTC treatment was tested, showing better filtration performance than raw sludge.

Chapter 2 investigates the recovery of phosphorous (P) from HC by acid leaching. Two acids (HNO_3, and H_2SO_4) were tested, using both process water derived from SS carbonization and demineralized water as solution. Phosphorous yield (P yield) and ash content were selected as responses, with the goal to find the optimal conditions to maximize P yield while minimizing ash content. H_2SO_4 favoured P yield, but at the same time increased ash content in HC after leaching.

In **Chapter 3**, three possible valorization pathways of PW derived from HTC on SS are proposed. Six SS samples (three anaerobically digested, and three aerobically stabilized) were collected from six WRRFs in Tuscany (Italy). The potential applications of PW as fertilizer on soils, as a substrate in AD, and as an effluent to be recirculated into the WRRF were further investigated. Process water was studied both in terms of chemical characterization and of biodegradability in anaerobic and aerobic conditions. The result was that PW has potential for a future use in soils, and that a correlation between anaerobic and aerobic biodegradability can be found.

Chapter 4 is focused on the continuous anaerobic treatment of HTC-derived PW of the digested SS. For this purpose, an upflow anaerobic sludge blanket reactor (UASB) was set up for continuous treatment of PW. The reactor was first started up with only glucose, and subsequently a progressively increasing percentage of PW was added, reaching the 100 % of PW after 113 Days. Various parameters were monitored over time (e.g., biogas volume and composition, chemical oxygen demand (COD), and volatile fatty acids). A soluble COD removal up to 73 % was observed, while a specific CH_4 production equal to 202 (33) mL STP CH_4 $g^{-1}COD_{fed}$ was achieved.

Chapter 5 addresses the integration between the existing SS treatment line of San Colombano WRRF and HTC through Life Cycle Assessment analysis. HC was assumed to be energetically valorized as a solid fuel, while different treatments were proposed for PW (recirculation into the WRRF, or anaerobic digestion). In addition, phosphorous recovery from HC was also included in two of five Scenarios. Results showed that more environmental benefits occurred when including HTC into the SS treatment line (excluding three impact categories). Phosphorous recovery negatively affected the environmental performances of the proposed configurations, indicating that this process should be optimised.

Finally, **Chapter 6** investigates the application of HTC on FW. HC was chemically characterized, and since its properties resulted to fulfil the requirements of ISO/TS 17225-8, its application as biofuel was proposed. Further, PW was used as substrate in AD. The process was monitored over time in terms of soluble COD, total ammonia nitrogen, pH, alkalinity, and volatile fatty acids. The trend of recalcitrant compounds before and after AD was studied, observing that AD promoted the removal of specific refractory compounds. In addition, an energetic and economical balance of the process was carried out, evaluating the benefits produced by HTC technology.

Resumen

Los lodos de aguas residuales (SS), que son el principal subproducto de una Instalación de Recuperación de Recursos Hídricos (WRRF), se producen en todo el mundo en grandes cantidades. El rápido crecimiento de la población, junto con la urbanización progresiva, ha llevado a la generación de una cantidad creciente de SS, que se espera que aumente continuamente en el próximo futuro (hasta una producción anual de 150 a 200 millones de toneladas en base seca para 2050). Además, la producción de otros residuos, como como los de alimentos (FW), va a aumentar en los próximos años. De hecho, se han generado más de 2 mil millones de toneladas de residuos municipales en todo el mundo y se estima que la producción aumentará en un 70% hasta 2050.

Los lodos de depuradora y los residuos alimentarios deben eliminarse adecuadamente utilizando las mejores tecnologías disponibles, de acuerdo con la legislación vigente y los principios de la economía circular. Ambos residuos generalmente se pueden tratar a través del compostaje, la digestión anaeróbica (AD), la incineración y el vertido. Sin embargo, todos estos tratamientos adolecen de algunas limitaciones (por ejemplo, largo tiempo de tratamiento, la necesidad de pretratamientos y la posible inhibición de los tratamientos inhibición). Por lo tanto, las tecnologías termoquímicas, como la carbonización hidrotermal (HTC), son cada vez más atractivas para tratar diferentes tipos de biomasa húmeda (como SS y FW). De hecho, la HTC es capaz de transformar la materia prima en tres fracciones: una fracción sólida (hidrochar, HC), una fase líquida (agua de proceso, PW) y una pequeña fase gaseosa.

El objetivo de este trabajo se centró en investigar la aplicación de HTC para tratar SS o FW. En particular, la carbonización de los SS ha sido ampliamente estudiada (**Capítulo 1 – 5**), mientras que solo el **Capítulo 6** se ha dedicado al tratamiento de FW a través de HTC**.** El **Capítulo 1** estudia la influencia de las condiciones de reacción de HTC (es decir, temperatura, tiempo y contenido sólido) en las características de los productos (HC y PW). El SS secundario derivado de San Colombano WRRF (Florencia, Italia) se recolectó y trató posteriormente a través de HTC estudiando las condiciones de operación. Tanto HC como PW fueron caracterizados, señalando que había una relación entre las condiciones de HTC y las características de los productos. Además, se estudió la deshidratabilidad de

SS después del tratamiento con HTC, mostrando un mejor rendimiento de filtración que el lodo de partida.

El **Capítulo 2** investiga la recuperación de fósforo (P) a partir de HC por lixiviación ácida. Se probaron dos ácidos (HNO_3 y H_2SO_4), utilizando agua de proceso derivada de la carbonización SS y agua desmineralizada como disolvente. El rendimiento de fósforo (P) y el contenido de cenizas se seleccionaron como respuestas, con el objetivo de encontrar las condiciones óptimas para maximizar el rendimiento de P y minimizar el contenido de cenizas. El H_2SO_4 favoreció el rendimiento de P, pero al mismo tiempo aumentó el contenido de cenizas en HC después de la lixiviación.

En el **Capítulo 3**, se proponen tres posibles vías de valorización de PW derivadas de HTC en SS. Se recogieron seis muestras de SS (tres digeridas anaeróbicamente y tres estabilizadas aeróbicamente) de seis WRRF en Toscana (Italia). Se investigaron las posibles aplicaciones de PW como fertilizante en los suelos, como sustrato en DA y como efluente para ser recirculado en el WRRF. El agua de proceso se estudió tanto en términos de caracterización química como de biodegradabilidad en condiciones anaeróbicas y aeróbicas. El PW mostró potencial para un uso futuro en suelos, y que se pudo encontrar una correlación entre la biodegradabilidad anaeróbica y aeróbica.

El **Capítulo 4** se centra en el tratamiento anaeróbico continuo del PW derivado de HTC de los SS digeridos. Para este propósito, se estableció un reactor de lodos anaeróbicos de flujo ascendente (UASB) para el tratamiento continuo de PW. El reactor se puso en marcha por primera vez con solo glucosa, y posteriormente se añadió un porcentaje progresivamente creciente de PW, alcanzando el 100 % de PW después de 113 días. Se siguienron varios parámetros a lo largo del tiempo (por ejemplo, volumen y composición de biogás, demanda química de oxígeno (DQO) y ácidos grasos volátiles). Se observó una eliminación de DQO soluble de hasta el 73 %, mientras que se logró una producción específica de CH_4 igual a 202 (33) mL STP CH_4 $g^{-1}COD_{alimentado}$.

El **Capítulo 5** aborda la integración entre la línea de tratamiento de SS existente de San Colombano WRRF y HTC a través del análisis de Evaluación del Ciclo de Vida. Se asumió que el HC se valorizaba energéticamente como combustible sólido, mientras que se propusieron diferentes tratamientos para el

PW (recirculación en el WRRF, o digestión anaeróbica). Además, la recuperación de fósforo de HC también se incluyó en dos de los cinco escenarios. Los resultados mostraron que se obtuvieron más beneficios ambientales al incluir HTC en la línea de tratamiento de los SS (excluyendo tres categorías de impacto). La recuperación de fósforo afectó negativamente a los comportamientos ambientales de las configuraciones propuestas, lo que indica que este proceso debe optimizarse.

Finalmente, el **Capítulo 6** investiga la aplicación de HTC para los FW. El HC fue caracterizado químicamente, y dado que sus propiedades resultaron cumplir con los requisitos de ISO/TS 17225-8, se propuso su aplicación como biocombustible. Además, los PW se utilizó como sustrato en AD. El proceso se evalué a lo largo del tiempo en términos de DQO soluble, nitrógeno amoniacal total, pH, alcalinidad y ácidos grasos volátiles. Se estudió la tendencia de los compuestos recalcitrantes antes y después de la AD, observando que la AD promovía la eliminación de compuestos refractarios específicos. Además, se llevó a cabo un balance energético y económico del proceso, evaluando los beneficios producidos por la tecnología HTC.

Introduction

0.1 Hydrothermal carbonization for sewage sludge and food waste valorization

Hydrothermal carbonization (HTC) is a thermochemical process able to convert a wet biomass into a solid fraction (named hydrochar, HC), a liquid phase (named process water, PW), and a small gaseous part, mainly made by CO_2 and small amounts of CH_4 and CO [1]. HTC process operates in a mild range of temperatures (180 – 250 °C), within a reaction time of 1 – 12 h under self-generated pressure in subcritical water [2]. It is based on hydrolysis, dehydration, decarboxylation, condensation, polymerization, and aromatization reactions, and the mechanisms depend on the feedstock nature [3]. As a rule, HTC processes biomass with high moisture content, resulting suitable to treat substrates as sewage sludge (SS) and food waste (FW). Indeed, raw SS, which is produced by wastewater treatment, typically contains an amount of water equal to 97 – 98 % [4]. Hence, to be properly disposed of, SS usually requires further treatments (e.g., stabilization, dewatering), which are time-consuming and costly, making HTC even more attractive. The technologies currently applied for its disposal, are somehow limited. SS management includes two main routes: the organic recycling correlated with the use as fertilizers and on soils (e.g., agriculture, reclamation, composting, and mechanical biological treatment) and the recycling of energy and material (e.g., incineration, co-incineration, and alternative thermal methods) [4]. The use of SS in agriculture is promoted by EU, but its application is strictly regulated to prevent harmful consequence on soil, vegetation, animals and people, setting limitations for heavy metals (i.e., Cd, Cu, Ni, Pb, Zn, and Hg) concentrations [5]. Thermal treatments are generally characterized by a significant reduction of SS volume, the degradation of toxic components, and high energy efficiency [6]. However, these processes generally require pre-treatments to reduce the water content and they produce ash, which concentrates heavy metals from sludge, requiring proper treatments to prevent pollution of the environment [6]. Similar considerations can be carried out also about FW treatment. Food waste is a wet and heterogenous feedstock, rich in nutrients and organic matter, which is typically composted and used as fertilizers or as amendment on soils. Nevertheless, it is biologically unstable and composting requires long treatment time [7]. Further, nutrient leaching could determine water pollution and algal boom, while an incorrect management could lead to

environmental problems, such as greenhouses gas emissions [7]. Thus, HTC seems promising to overcome these limitations, especially because no pre-treatments of feedstocks are needed, being a suitable technology to treat biomass with high moisture content (> 70 %).

0.2 Characterization of HTC products

HC obtained by carbonization of biomass (e.g., SS and FW) is a solid coal-like material rich in C. Due to the dehydration and decarboxylation reactions that occur during HTC, the content of oxygen and hydrogen is reduced, resulting in a lowering of the molecular O/C and H/C ratios, as is typically reported in literature through the Van Krevelen diagram [1, 8] (**Fig. 0.1**).

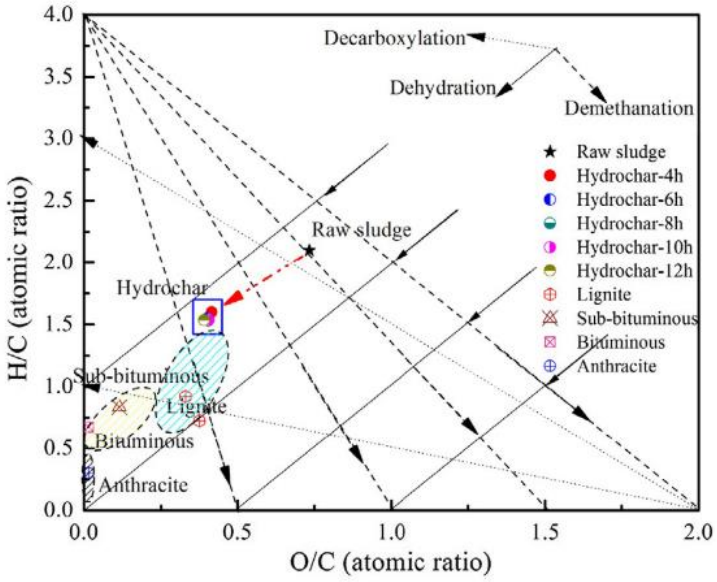

Figure 0.1 Van Krevelen diagram for raw sludge and hydrochars, in comparison with four coals (i.e., anthracite, bituminous, sub-bituminous, and lignite) [8].

Hence, HC atomic ratios resulted similar to that of lignite and subbituminous coals [9], since the majority of C is retained within the solid matrix (45 – 75 %) [10, 11]. HC characteristics are largely influenced by process conditions. Longer carbonization times increased the fixed carbon and the carbon content of HC, reducing at the same time the solid product recovery [9, 12]. Further, HC increased its hydrophobicity after long residence time, since the aromatic structure increased [8]. Temperature influences the H/C and the O/C ratios, which are reported to decrease steadily with temperature [12]. Typically, the combined effect of time and temperature is summarized in a parameter named reaction severity f [1], which turns out to be crucial in determining the quality of HC as solid fuel [13].

PW is an aqueous liquid phase containing total organic carbon (TOC), sugars and derivatives, organic acids, furanoids, and phenolic compounds [1]. The C fraction transferred from the feedstock to the liquid phase is mainly associated to the carbon solubilisation, which increases with temperature [11]. It is brown in colour, containing solids mainly into the dissolved form [14]. It is characterized by a wide range of pH values, from acidic in nature up to the neutral one [14, 15]. At temperatures higher than 180 °C and for reaction times longer than 15 minutes, Maillard reactions occur during HTC, often producing refractory compounds (e.g., pyrazines, and pyridines) [16]. Some studies have observed that a close relationship between temperature and refractory compounds can be found [17, 18]. Particularly, Zhu et al. [18] concluded that more inhibitory compounds (e.g., pyrazines, pyridines, and phenols) were detected into the liquid fraction derived by the co-HTC at 240 °C of SS and FW than that obtained at 180 °C.

0.3 Hydrochar valorization

Several studies proposed to recover HC energetically as a fuel [8, 14, 19], due to the high quality of its combustible properties. Kim et al. [19] reported that HC derived from carbonization of anaerobically digested SS at 250 ° was characterized by a higher heating value (HHV) equal to 20.2 MJ kg-1, which is comparable to that of lignite 15 – 20 MJ kg-1. They also have observed that while the volatile matter (VM) of HC decreased, the fixed carbon increased with respect to the initial SS. Thus, the fuel ratio (FC/VM) was enhanced, suggesting that the energy value of HC was higher than that of the raw feedstock [19]. Further, HC derived by HTC on food waste showed an activation energy lower than that of the raw feedstock, suggesting that it might be used as co-fuel to reduce the coal ignition temperature [14]. HC derived by HTC on SS retains the majority of heavy metals (e.g., Al, Fe, Zn, and Mn) and phosphorous (P) into its solid matrix, while alkali/alkaline earth metals (e.g., Ca, K, Mg, and Na) show a different behaviour [20, 21]. Ca and Mg are accumulated into HC since they are closely related with the presence of P in HC [22], while K and Na show a high affinity with the liquid phase, whose concentration is reported to significantly increase as exponential trend with reaction severity [20]. HC is able to concentrate most of P (> 75 %) in its structure, representing a potential P source that can be exploited [23, 24]. For the essential role of P and for its scarce availability in EU, its recovery is

becoming urgent to avoid the lack of this nutrient. Some authors have already proposed the recovery of P through acid leaching from HC derived from both SS and FW [24–27]. Despite a direct comparison among different studies is generally challenging, all authors agree in identifying the P leaching from HC as a promising route for P valorization [24–28]. As reported in literature, both organic and inorganic acids could potentially be applied to recover P from HC [25, 28, 29]. Regarding the first mentioned, it has been reported for example that citric acid behaves positively as a complexation agent for the precipitation of struvite, reaching very high P recovery yield in the acidified solution (> 94 %). Additionally, the precipitation of heavy metals is limited, and consequently the produced struvite might be considered as a fertilizer ready to use [28]. As concern inorganic acids (e.g., HNO_3, HCl, and H_2SO_4) instead, a P yield higher than 80 % was observed [24, 26]. During acid leaching, the P is transferred into the liquid phase and it could be subsequently precipitated at basic pH in the form of solid, whose composition (P, calcium, and metals) depends also by the acid used [26]. The P-rich liquid leachate might be recovered as fertilizer, in combination with proper pre- or post-treatments to increase purity [24], whereas the P-rich precipitated solid could find different applications, such as fertilizer or adsorbent, beside its use as a fuel [30, 31]. Indeed, as a consequence of acid leaching, the ash content of leachate HC is typically reduced using both HNO_3 or HCl as acids, while with high calcium hydrochars, the ash content does not decrease when H_2SO_4 is used [26]. Therefore, the use of this last acid is not preferable when the final use of the solid is as a fuel. Finally, since the specific surface area and the porosity of HC samples are generally enhanced [21], its use as absorbent material [32] and as soil amender [33] has been proposed.

0.4 Process water valorization

Available literature is mainly focused on HC applications, leaving PW and its possible valorization routes aside. Only recently, PW has been proposed as a substrate for anaerobic digestion (AD). Some studies [34–37] agree in indicating PW derived from HTC of both SS and FW as appropriate to produce biogas through AD. Most of the previous studies evaluated the biochemical methane potential of PW derived from carbonization of SS and FW performing batch tests in mesophilic conditions [34–37]. Ahmed et al. [36] reported that the specific CH_4 production of PW derived from HTC on digested SS

at 190 °C varied into the range of 84 – 142 $mLCH_4$ $g^{-1}COD_{added}$, for a residence time of 3, and 0.5 h, respectively. A similar range of CH_4 specific productions (144 – 177 $mLCH_4$ $g^{-1}COD_{added}$) was observed for the AD of PW derived from carbonization of SS collected from a full-scale membrane bioreactor treating industrial wastewater [34]. Further, in case of PW derived by HTC on food waste, a production equal to 57 $mLCH_4$ $g^{-1}COD_{added}$ was obtained, which might be affected by inhibition of specific compounds [37]. However, batch tests are performed to estimate the maximum achievable yield, which is usually higher than the specific production achieved in continuous systems [38]. However, only few works can be found about continuous anaerobic treatment of PW derived from HTC [39–41]. Liu et al. [39] performed a continuous AD experiment on PW derived from carbonization of SS through an upflow anaerobic sludge blanket reactor (UASB). The authors have tested two different ranges of organic loading rates (OLRs) (1.9 – 2.1 gCOD L^{-1} d^{-1}, and 3.7 – 4.1 gCOD L^{-1} d^{-1}) on two reactors, and they observed that a CH4 conversion efficiency of 71 % was reached, with a specific methane production of 285 mL CH_4 g^{-1} COD_{added}. Further, another work [40] investigated the anaerobic and aerobic degradation of PW derived by carbonization of SS in three-stage continuous systems. Methane concentrations from continuous AD experiments resulted in agreement with that obtained from the batch ones, which were equal to 77 vol %, and 50 – 67 vol %, respectively [40]. Further, a COD degradation equal to 58 % was obtained during the anaerobic phase, which was enhanced up to an additional percentage (35-44 %) during the aerobic one [40]. This study indicated that also aerobic conditions could promote the degradation of PW, which was suggested also by Biochemical Oxygen Demand (BOD) tests carried out in other studies on PW derived by carbonization of SS [16]. Finally, PW was proposed also as liquid fertilizer [42]. Indeed, PW derived by HTC on poultry litter showed to promote, with and without recirculation, the growth of lettuce, providing nutrients back to the soil [42].

0.5 Environmental perspective

As is reported in the above paragraphs, both HC and PW are products that can find application in different fields. Despite several works proposed HTC as environmentally beneficial to convert wastes into value-added products [43], not many studies have deeply investigated the environmental performance of HTC for SS or FW treatment [26, 43–45]. Practically, HTC could be integrated into the

treatment of SS in a Water Resources Recovery Facility (WRRF), as well as in FW treatment. However, to completely understand the effective environmental advantages of the integration of this technology into the treatment of SS or FW, the Life Cycle Assessment (LCA) analysis can be carried out. It is a useful tool to evaluate the environmental impacts and resources used through a life cycle of a product [46]. Thus, it can provide key indications about the integration of HTC technology and the traditional treatment line of these wastes. Medina-Martos et al. [44] carried out an LCA analysis comparing the integration of HTC and AD with the standalone AD for SS treatment. From this study emerged that the environmental impacts of the integrated configuration were globally reduced in comparison with the standalone configuration, due to the replacement of fossil combustibles with HC [44]. Further, another study concluded that the environmental profile of HTC for SS treatment was improved with respect to the mono-incineration of sludge [45]. Also, regarding the application of HTC on food waste, the valorization of HC through combustion significantly influences the environmental impacts, pointing out that appropriate management strategies, a clear understanding of nutrient and metals fate, and the composition of gaseous emissions are needed [43].

0.6 Objectives

The overall objective of this doctoral thesis was to evaluate the integration of HTC into SS and FW treatment, specifically focusing of PW applications. This study was carried out following these specific objectives:

- To study the influence of HTC operational conditions (temperature, time, and solid content) on characteristics of products (HC and PW) derived from HTC on SS;
- To investigate the feasibility to recover phosphorus from HC derived from HTC on SS, establishing the optimal conditions (contact time, type and concentration of acids, solid/solution ratio) with the goal to maximize the P yield and to minimize the ash content of HC after leaching;
- To evaluate the possible recovery of PW derived from HTC on SS as an effluent to be treated into a WRRF, as a substrate for anaerobic digestion, and as a liquid fertilizer to be applied on soil;
- To study the performance of continuous anaerobic treatment of PW derived from HTC on SS;

- To evaluate the environmental performance of the integration of HTC into an existing WRRF sludge treatment line through LCA analysis;
- To study the possible valorization routes of products derived from carbonization of FW.

This doctoral thesis has been carried out in the UNALAB laboratory (joint laboratory between the Department of Civil and Environmental Engineering of University of Florence and Publiacqua SpA), the laboratory of the Department of Civil and Environmental Engineering of University of Florence, and the laboratories of the Chemical Engineering Department at Autonomous University of Madrid.

0.7 References – Introduction

1. Funke, A., Ziegler, F.: Hydrothermal carbonization of biomass: A summary and discussion of chemical mechanisms for process engineering. Biofuels, Bioprod. Biorefining. 4, 160–177 (2010). https://doi.org/10.1002/bbb.198

2. Libra, A.J., Kammann, C., Funke, A., Berge, N.D., Neubauer, Y., Titirici, M.-M., Fuhner, C., Bens, O., Kern, J., Emmerich, K.-H.: Hydrothermal carbonization of biomass residuals: A comparative review of the chemistry, processes and applications of wet and dry pyrolysis. 2, 89–124 (2011). https://doi.org/10.4155/bfs.10.81

3. Pauline, A.L., Joseph, K.: Hydrothermal carbonization of organic wastes to carbonaceous solid fuel – A review of mechanisms and process parameters. Fuel. 279, 118472 (2020). https://doi.org/10.1016/j.fuel.2020.118472

4. Kacprzak, M., Neczaj, E., Fijałkowski, K., Grobelak, A., Grosser, A., Worwag, M., Rorat, A., Brattebo, H., Almas, A., Singh, B.R.: Sewage sludge disposal strategies for sustainable development. Environ. Res. 156, 39–46 (2017). https://doi.org/10.1016/j.envres.2017.03.010

5. European Commission: Protection of the Environment, and in particular of the soil, when sewage sludge is used in agriculture. Off. J. Eur. Communities. 4, 6–12 (1986)

6. Durdević, D., Trstenjak, M., Hulenić, I.: Sewage sludge thermal treatment technology selection by utilizing the analytical hierarchy process. Water (Switzerland). 12, (2020). https://doi.org/10.3390/W12051255

7. McGaughy, K., Toufiq Reza, M.: Hydrothermal carbonization of food waste: simplified process simulation model based on experimental results. Biomass Convers. Biorefinery. 8, 283–292 (2018). https://doi.org/10.1007/s13399-017-0276-4

8. He, C., Giannis, A., Wang, J.Y.: Conversion of sewage sludge to clean solid fuel using hydrothermal carbonization: Hydrochar fuel characteristics and combustion behavior. Appl. Energy. 111, 257–266 (2013). https://doi.org/10.1016/j.apenergy.2013.04.084

9. Saetea, P., Tippayawong, N.: Recovery of Value-Added Products from Hydrothermal Carbonization of Sewage Sludge. ISRN Chem. Eng. 2013, 1–6 (2013). https://doi.org/10.1155/2013/268947

10. Lu, X., Jordan, B., Berge, N.D.: Thermal conversion of municipal solid waste via hydrothermal carbonization: Comparison of carbonization products to products from current waste management techniques. Waste Manag. 32, 1353–1365 (2012). https://doi.org/10.1016/j.wasman.2012.02.012

11. Aragón-Briceño, C., Ross, A.B., Camargo-Valero, M.A.: Evaluation and comparison of product yields and bio-methane potential in sewage digestate following hydrothermal treatment. Appl. Energy. 0–1 (2017). https://doi.org/10.1016/j.apenergy.2017.09.019

12. Wang, T., Zhai, Y., Zhu, Y., Li, C., Zeng, G.: A review of the hydrothermal carbonization of biomass waste for hydrochar formation: Process conditions, fundamentals, and physicochemical properties. Renew. Sustain. Energy Rev. 90, 223–247 (2018). https://doi.org/10.1016/j.rser.2018.03.071

13. Zhao, P., Shen, Y., Ge, S., Chen, Z., Yoshikawa, K.: Clean solid biofuel production from high moisture content waste biomass employing hydrothermal treatment. Appl. Energy. 131, 345–367 (2014). https://doi.org/10.1016/j.apenergy.2014.06.038

14. Gupta, D., Mahajani, S.M., Garg, A.: Investigation on hydrochar and macromolecules recovery opportunities from food waste after hydrothermal carbonization. Sci. Total Environ. 749, 142294 (2020). https://doi.org/10.1016/j.scitotenv.2020.142294

15. Escala, M., Zumbühl, T., Koller, C., Junge, R., Krebs, R.: Hydrothermal carbonization as an energy-efficient alternative to established drying technologies for sewage sludge: A feasibility study on a laboratory scale. Energy and Fuels. 27, 454–460 (2013). https://doi.org/10.1021/ef3015266

16. Danso-Boateng, E., Shama, G., Wheatley, A.D., Martin, S.J., Holdich, R.G.: Hydrothermal carbonisation of sewage sludge: Effect of process conditions on product characteristics and methane production. Bioresour. Technol. 177, 318–327 (2015). https://doi.org/10.1016/j.biortech.2014.11.096

17. Wang, T., Zhai, Y., Zhu, Y., Peng, C., Xu, B., Wang, T., Li, C., Zeng, G.: Influence of temperature on nitrogen fate during hydrothermal carbonization of food waste. Bioresour. Technol. 247, 182–189 (2018). https://doi.org/10.1016/j.biortech.2017.09.076

18. Zhu, K., Liu, Q., Dang, C., Li, A., Zhang, L.: Valorization of hydrothermal carbonization products by anaerobic digestion: Inhibitor identification, biomethanization potential and process intensification. Bioresour. Technol. 341, 125752 (2021). https://doi.org/10.1016/j.biortech.2021.125752

19. Kim, D., Lee, K., Park, K.Y.: Hydrothermal carbonization of anaerobically digested sludge for solid fuel production and energy recovery. Fuel. 130, 120–125 (2014). https://doi.org/10.1016/j.fuel.2014.04.030

20. Wang, L., Chang, Y., Liu, Q.: Fate and distribution of nutrients and heavy metals during hydrothermal carbonization of sewage sludge with implication to land application. J. Clean. Prod. 225, 972–983 (2019). https://doi.org/10.1016/j.jclepro.2019.03.347

21. Wang, H., Yang, Z., Li, X., Liu, Y.: Distribution and transformation behaviors of heavy metals and phosphorus during hydrothermal carbonization of sewage sludge. Environ. Sci. Pollut. Res. 27, 17109–17122 (2020). https://doi.org/10.1007/s11356-020-08098-4

22. Ekpo, U., Ross, A.B., Camargo-Valero, M.A., Fletcher, L.A.: Influence of pH on hydrothermal treatment of swine manure: Impact on extraction of nitrogen and phosphorus in process water. Bioresour. Technol. 214, 637–644 (2016). https://doi.org/10.1016/j.biortech.2016.05.012

23. Hämäläinen, A., Kokko, M., Kinnunen, V., Hilli, T., Rintala, J.: Hydrothermal carbonisation of mechanically dewatered digested sewage sludge—Energy and nutrient recovery in centralised biogas plant. Water Res. 201, (2021). https://doi.org/10.1016/j.watres.2021.117284

24. Pérez, C., François, J., Stina, B., Tomas, J., Jerker, G.: Acid - Induced Phosphorus Release from Hydrothermally Carbonized Sewage Sludge. Waste and Biomass Valorization. (2021). https://doi.org/10.1007/s12649-021-01463-5

25. Volpe, M., Fiori, L., Merzari, F., Messineo, A., Andreottola, G.: Hydrothermal carbonization as an efficient tool for sewage sludge valorization and phosphorous recovery. Chem. Eng. Trans. 80, 199–204 (2020). https://doi.org/10.3303/CET2080034

26. Oliver-Tomas, B., Hitzl, M., Owsianiak, M., Renz, M.: Evaluation of hydrothermal carbonization in urban mining for the recovery of phosphorus from the organic fraction of municipal solid waste. Resour. Conserv. Recycl. 147, 111–118 (2019). https://doi.org/10.1016/j.resconrec.2019.04.023

27. Marin-Batista, J.D., Mohedano, A.F., Rodríguez, J.J., de la Rubia, M.A.: Energy and phosphorous recovery through hydrothermal carbonization of digested sewage sludge. 105, 566–574 (2020). https://doi.org/doi.org/10.1016/j.wasman.2020.03.004

28. Becker, G.C., Wüst, D., Köhler, H., Lautenbach, A., Kruse, A.: Novel approach of phosphate-reclamation as struvite from sewage sludge by utilising hydrothermal carbonization. J. Environ. Manage. 238, 119–125 (2019). https://doi.org/10.1016/j.jenvman.2019.02.121

29. Gerner, G., Meyer, L., Wanner, R., Keller, T., Krebs, R.: Sewage sludge treatment by hydrothermal carbonization: Feasibility study for sustainable nutrient recovery and fuel production. Energies. 14, (2021). https://doi.org/10.3390/en14092697

30. Zhao, X., Becker, G.C., Faweya, N., Rodriguez Correa, C., Yang, S., Xie, X., Kruse, A.: Fertilizer and activated carbon production by hydrothermal carbonization of digestate. Biomass Convers. Biorefinery. 8, 423–436 (2018). https://doi.org/10.1007/s13399-017-0291-5

31. Tasca, A.L., Mannarino, G., Gori, R., Vitolo, S., Puccini, M.: Phosphorus recovery from sewage sludge hydrochar: process optimization by response surface methodology. Water Sci. Technol. (2020). https://doi.org/10.2166/wst.2020.485

32. Puccini, M., Stefanelli, E., Hiltz, M., Seggiani, M.: Activated Carbon from Hydrochar Produced by Hydrothermal Carbonization of Wastes. Chem. Eng. Trans. 57, 169–174 (2017). https://doi.org/10.3303/CET1757029

33. Bargmann, I., Rillig, M.C., Buss, W., Kruse, A., Kuecke, M.: Hydrochar and biochar effects on germination of spring barley. J. Agron. Crop Sci. 199, 360–373 (2013). https://doi.org/10.1111/jac.12024

34. Villamil, J.A., Mohedano, A.F., Rodriguez, J.J., de la Rubia, M.A.: Valorisation of the liquid fraction from hydrothermal carbonisation of sewage sludge by anaerobic digestion. J. Chem. Technol. Biotechnol. 93, 450–456 (2018). https://doi.org/10.1002/jctb.5375

35. Ferrentino, R., Merzari, F., Fiori, L., Andreottola, G.: Coupling hydrothermal carbonization with anaerobic digestion for sewage sludge treatment: Influence of HTC liquor and hydrochar on biomethane production. Energies. 13, (2020). https://doi.org/10.3390/en13236262

36. Ahmed, M., Andreottola, G., Elagroudy, S., Negm, M.S., Fiori, L.: Coupling hydrothermal carbonization and anaerobic digestion for sewage digestate management: Influence of hydrothermal treatment time on dewaterability and bio-methane production. J. Environ. Manage. 281, 111910 (2021). https://doi.org/10.1016/j.jenvman.2020.111910

37. Zhao, K., Li, Y., Zhou, Y., Guo, W., Jiang, H., Xu, Q.: Characterization of hydrothermal carbonization products (hydrochars and spent liquor) and their biomethane production performance. Bioresour. Technol. 267, 9–16 (2018). https://doi.org/10.1016/j.biortech.2018.07.006

38. Koch, K., Hafner, S.D., Weinrich, S., Astals, S., Holliger, C.: Power and Limitations of Biochemical Methane Potential (BMP) Tests. Front. Energy Res. 8, 1–4 (2020). https://doi.org/10.3389/fenrg.2020.00063

39. Liu, S., Wang, Y., Guo, J., Wang, W., Dong, R.: Start-up and performance evaluation of upflow anaerobic sludge blanket reactor treating supernatant of hydrothermally treated municipal sludge: Effect of initial organic loading rate. Biochem. Eng. J. 166, 107843 (2021). https://doi.org/10.1016/j.bej.2020.107843

40. Weide, T., Brügging, E., Wetter, C.: Anaerobic and aerobic degradation of wastewater from hydrothermal carbonization (HTC) in a continuous, three-stage and semi-industrial system. J. Environ. Chem. Eng. 7, (2019). https://doi.org/10.1016/j.jece.2019.102912

41. Wirth, B., Reza, T., Mumme, J.: Influence of digestion temperature and organic loading rate on the continuous anaerobic treatment of process liquor from hydrothermal carbonization of sewage sludge. Bioresour. Technol. 198, 215–222 (2015). https://doi.org/10.1016/j.biortech.2015.09.022

42. Mau, V., Neumann, J., Wehrli, B., Gross, A.: Nutrient Behaviour in Hydrothermal Carbonization Aqueous Phase Following Recirculation and Reuse. Environ. Sci. Technol. 53, 10426–10434 (2019). https://doi.org/10.1021/acs.est.9b03080

43. Berge, N.D., Li, L., Flora, J.R.V., Ro, K.S.: Assessing the environmental impact of energy production from hydrochar generated via hydrothermal carbonization of food wastes. Waste Manag. 43, 203–217 (2015). https://doi.org/10.1016/j.wasman.2015.04.029

44. Medina-Martos, E., Istrate, I.R., Villamil, J.A., Gálvez-Martos, J.L., Dufour, J., Mohedano, Á.F.: Techno-economic and life cycle assessment of an integrated hydrothermal carbonization system for sewage sludge. J. Clean. Prod. 277, (2020). https://doi.org/10.1016/j.jclepro.2020.122930

45. Gievers, F., Loewen, A., Nelles, M.: Hydrothermal Carbonization (HTC) of Sewage Sludge: GHG Emissions of Various Hydrochar Applications. Springer International Publishing (2019)

46. Finnveden, G., Hauschild, M.Z., Ekvall, T., Guinée, J., Heijungs, R., Hellweg, S., Koehler, A., Pennington, D., Suh, S.: Recent developments in Life Cycle Assessment. J. Environ. Manage. 91, 1–21 (2009). https://doi.org/10.1016/j.jenvman.2009.06.018

Chapter 1

Hydrothermal carbonization of sewage sludge: influence of process conditions

Abstract

Hydrothermal carbonization (HTC) is a thermochemical process able to convert sewage sludge (SS) into a solid coal-like material (hydrochar, HC), and a liquid phase (process water, PW). Operational conditions of the process (i.e., temperature, time, and solid content of the feedstock) influences the characteristics of both HC and PW. Thus, twenty HTC reactions were carried out at various process conditions, according to an experimental plan elaborated with the Design of Experiments (DoE). Thus, yield (Y) and C yield (C_{yield}) responses have been modelled by response surface methodology (RSM) approach. The solid-liquid suspension derived from HTC (named slurry) was investigated in terms of dewaterability through specific resistance to filtration (SRF) tests. A strongly improvement in dewaterability was observed in comparison with sludge performances. Further, from analysis on solid emerged that the ash content into HC increased with severity, while volatile matter simultaneously decreased with respect to the initial raw sludge. Further, the trend of H/C and O/C ratio has been studied, in order to find a relationship with severity. Then, the distribution of C among solid, liquid, and gas phase was studied, relating it with temperature, time, and solid content. PW was characterized in terms of total ammonia nitrogen (TAN) and heavy metals. Particularly, it was observed that the concentration in PW of specific parameters (e.g., TAN, and As) increased with the rising of severity. Thus, a relationship between chemical composition of products and operational HTC conditions was found, making it possible to choose the latter according to the desired characteristics of HC and PW.

1.1 Introduction

Sewage sludge (SS) treatment represents one of the main issues of wastewater treatment network. Indeed, with the growth of population and urbanization, the generated SS is going to significantly increase. In the EU, an average of 90 g per capita of SS is generated from Water Resources Recovery Facilities (WRRFs) every day [1]. Generally, SS disposal methods includes agricultural use,

composting, incineration, and landfilling, although the latter is recently under severe limitation [2]. Indeed, despite sludge is a relevant supply of phosphorus and nitrogen, it is often contaminated with heavy metals, microorganisms, and different hazardous organic substances [3]. As a consequence, SS applications on soils have been strongly limited according to the Council Directive 86/278/EEC, which establishes limits for specific parameters (e.g., heavy metals) [4]. Thus, alternative solutions are required to meet the global need for SS treatment, protecting the environment and the human health.

In this perspective, thermal treatments are emerged as promising, with respect of circular economy principles. Particularly, hydrothermal carbonization (HTC) is arising as suitable technology to treat SS. HTC is able to treat wet biomass (e.g., SS), at mild temperatures (up to 220 °C) and within a reaction time of 1 – 10 h. The pressure is self- generated during the process, which transforms the feedstock in three fractions: a solid coal-like material (hydrochar, HC), a liquid fraction (process water, PW), and a gaseous phase (mainly made of CO_2) [5, 6].

As a rule, HC is a carbonaceous material with higher calorific values than low-grade coal, but with comparable H/C and O/C ratios [7]. Thus, HC has been proposed as an alternative fuel in previous studies [8, 9]. Further, since HC is a porous material, with surface functionality and a hydrophobic behaviour, it can find applications also as activated carbon [8, 10, 11]. Nevertheless, HC is able to retain phosphorous into his structure, suggesting its use in agriculture and horticulture applications [12]. PW is a liquid fraction rich in total organic carbon (TOC), containing sugars and derivatives, phenolic compounds, furanoids, and organic acids [13]. The energy potential of PW derived by HTC on SS has been already investigated by some authors, who proposed anaerobic digestion (AD) as a feasible pathway to valorize this fraction [14, 15]. Further, a study reports that PW derived by carbonization of poultry litter could be recirculated to improve its nutrient content and then used as fertilizer with beneficial effects on agriculture [16]. Also, it is worth pointing out that applying HTC on SS the dewaterability of sludge is strongly improved [8, 17], consequently reducing the energy required for its dehydration.

This study is aimed to deeply investigate the chemical characteristics of both HC and PW, evaluating the influence of process conditions on the obtained products. A direct comparison of PW and HC

characteristics among various studies is generally challenging, due to the differences of the initial feedstock, HTC reactors, and process conditions. Thus, this study would deepen the influence of operational HTC conditions (i.e., temperature, time, and solid content) on a single feedstock (secondary SS sludge). Therefore, twenty HTC reactions were carried out on SS in various ranges of temperature, time, and solid content, equal to 190 – 220 °C, 85 – 240 min, and 5 – 12 wt %, respectively. Then, the behaviour of characteristic parameters of HC and PW was evaluated according to process conditions, while HC yield (Y) and C yield (C_{yield}) were investigated by response surface methodology (RSM) approach, proposing relationship between severity and moisture content of the sludge [6].

Part of this work has been already published [6]:

Tasca, A.L., Stefanelli, E., Raspolli Galletti, A.M., Gori, R., Mannarino, G., Vitolo, S., Puccini, M.: Hydrothermal Carbonization of Sewage Sludge: Analysis of Process Severity and Solid Content. Chem. Eng. Technol. 43, 2382–2392 (2020). https://doi.org/10.1002/ceat.202000095

1.2 Materials and methods

1.2.1 Sewage sludge sample

SS was collected from San Colombano WRRF, which treats the urban wastewater of Florence and surroundings. The plant (Florence, Italy) is managed by Publiacqua SpA and it has a capacity of 600 000 PE (person equivalent), with a flow rate of around 200 000 m^3 d^{-1} [6]. The WRRF layout includes pre-treatments, primary settling (currently by-passed), a modified Ludzack-Ettinger denitrification-nitrification biological process, secondary settling, and final disinfection, as described more in detail by Tasca et al. [6]. Further, the sludge treatment line consists in a dynamic thickening, a mesophilic anaerobic digestion (AD), and a final dewatering step with a centrifuge. The SS investigated in this study was collected immediately before AD (solid content equal to ~ 5 wt %). As described by Tasca et al. [6], the SS characterization is reported in the following table (**Tab. 1.1**) (values are reported as average values with standard deviation in parenthesis):

Table 1.1 Sewage sludge characterization. All values are reported in wt % on dry basis (values are expressed as average on seven sewage sludge samples, with standard deviation in parenthesis).

Parameter	Measure
FC	4.49 (0.68)
VM	52.53 (1.59)
Ash	42.98 (1.12)
C	27.76 (0.60)
H	4.42 (0.17)
N	4.49 (0.27)
O	19.57 (0.48)
S	0.79 (0.07)

1.2.2 Hydrothermal carbonization

HTC reactions were performed according to Tasca et al. [6]. Briefly, a 300 mL AISI 316 stainless-steel reactor, equipped with mechanical agitator, electric heating system, thermocouple, and a pressure gauge (1- 1000 psi), was used. Temperature profile during HTC was monitored over time through a manual controller (PARR 4842). HTC trials were carried out in a different range of temperatures (190 – 220 °C), reaction times (85 – 240 min), and solid content of the feedstock (5 – 12 wt %). To reach the desired sludge solid content, samples were centrifuged (when necessary) (NEYA, mod. 16R). Approximately 200 mL of SS were loaded into the HTC reactor, then heated up to the desired temperature, maintained, and lastly cooled at room temperature. The slurry (i.e., the solid-liquid suspension derived by HTC) was then separated through a vacuum filter (Whatman n. 41). The solid HC was collected, dried at 105 °C overnight, and then stored for analysis. At the same time, the liquid PW was stored at 4 °C for further analysis.

1.2.3 Design of Experiments

As reported by Tasca et al. [6], experimental trials were planned according to the Design of Experiments (DoE), under response surface methodology (RSM) approach (see **A1.2** in **Appendix A1** for more

details about DoE). A three factorial central composite design (CCD) with six axial points and six replicates at the central point was elaborated. Temperature (A), reaction time (B), and solid content (C) were selected as independent variables (**Tab. 1.2**).

Table 1.2 Levels of factors for DoE.

Factor	Name	Unit	Min	Max
A	Temperature	°C	190	220
B	Time	min	85	240
C	Solid content	wt %	5	12

The ranges reported in **Tab. 1.2** were chosen with the aim of describing the HTC operational conditions (temperature 180 – 250 °C, time 1 - 10 h, and solid content > 5 wt %) usually reported in literature [5]. Indeed, as can be observed in **Tab. 1.3**, trials were carried at operational conditions representative of these ranges, but also at extreme conditions (e.g., time equal to about 32 minutes (Run 11), and temperature high than 220 °C (Run 13)).

Actual values are reported in coded notification using the following equation (**equation 1.1)**:

$$x_i = \frac{X_i - X_0}{\Delta X_i} \quad (1.1)$$

where x_i is the dimensionless codified value for each independent variable, X_i is the actual value, X_0 is the value of each factor at the central point, and ΔX_i is the difference between the levels for each factor. Axial points were calculated in codified notation according to **equation 1.2**:

$$\alpha = 2^{k/4} \quad (1.2)$$

where α is the axial point, and k is the number of factors. To reduce the effect of uncontrolled factors, the experimental sequence was randomized. The experimental plan is reported in **Tab. 1.3**:

Table 1.3 Experimental plan elaborated by DOE.

Run	Temperature (°C)	Time (min)	Solid content (%)
1	220.00	85.00	5.00
2	190.00	240.00	12.00
3	205.00	162.50	8.50
4	220.00	240.00	5.00
5	190.00	85.00	5.00
6	205.00	162.50	2.61
7	190.00	240.00	5.00
8	220.00	85.00	12.00
9	205.00	292.84	8.50
10	205.00	162.50	8.50
11	205.00	32.16	8.50
12	205.00	162.50	8.50
13	230.23	162.50	8.50
14	205.00	162.50	8.50
15	220.00	240.00	12.00
16	205.00	162.50	8.50
17	179.77	162.50	8.50
18	190.00	85.00	12.00
19	205.00	162.50	14.39
20	205.00	162.50	8.50

Yield (Y) and carbon yield (C_{yield}) were selected as responses to assess the HTC's performance. These two parameters were calculated using the following equations:

$$Y\,(\%) = \frac{\text{mass}_{\text{dry HC}}}{\text{mass}_{\text{dry sludge}}} \cdot 100 \quad (1.3)$$

$$C_{\text{yield}}\,(\%) = Y \cdot \frac{C_{\text{dry HC}}}{C_{\text{dry sludge}}} \cdot 100 \quad (1.4)$$

Where $C_{dry\ HC}$ and $C_{dry\ sludge}$ represent the concentration of C on dry basis in hydrochar and sludge, respectively.

The responses were fitted using a second-order polynomial regression model, as described by Tasca et al. [6]. The equation used is reported below:

$$Y_i = a_0 + b_1x_1 + b_2x_2 + b_3x_3 + b_{12}x_1x_2 + b_{13}x_1x_3 + b_{23}x_2x_3 + c_1x_1^2 + c_2x_2^2 + c_3x_3^2 \quad (1.5)$$

Where Y_i is the predicted response, x_i are the coded values of the process variables, a_0 is the constant coefficient, b_i is the linear coefficient, b_{ij} represents the interaction, and c_i is the quadratic coefficient. Analysis of variance (ANOVA) was applied to verify the statistical significance of the obtained regression, and the software Design Expert® 11 (Stat-Ease) was used to develop the design of the experiments (DoE/RSM procedures).

1.2.4 Dewaterability

The dewaterability of raw sludges and slurries was evaluated by specific resistance to filtration (SRF). It describes the resistance to filtration of a theoretical sludge panel, with a unitary weight in dry solids per unit of the filtering surface [18]. Dewaterability tests were performed according to Pontoni et al. [18]. The slurry volume derived by HTC was filtered in a Buchner funnel using filter paper (Whatman n. 41) applying a negative pressure of 49 kN m^{-2}. The pressure was kept constant regulating system for the entire duration of the test. The first volume was discarded, and then it was recorded at constant interval of time. The SRF (m kg^{-1}) parameter was calculated using the following equation (**equation 1.6)**:

$$SRF = \frac{2\,P\,A^2}{\mu C} \cdot b \quad (1.6)$$

Where P is the applied differential pressure (N m^{-2}), A is the filtration area (m^2), μ is the viscosity of the filtrate (kg m^{-1} s^{-1}) (assumed equal to the viscosity of water) [19] , C was calculated according to

equation 1.7, and b is the slope of the discharge curve (s m^{-6}). This curve is experimentally determined, plotting the values of filtered volume *V* observed at time *t* on the x-axis and the ratio $t\ V^{-1}$ on the y-axis (**Fig. A1.1** in **Appendix A1**).

$$C = \frac{C_0\ C_c}{C_c - C_0} \tag{1.7}$$

Where C_0 and C_c are the solid concentration (kg m^{-3}) in the raw sludge and in the sludge panel on the filter after filtration.

1.2.5 Characterization

Thermogravimetric analyzer TGA TA Q500 (TA Instruments, USA) was used to carry out the proximate analyses of raw sludge and HC. Samples were weighted and then heated from 30 °C to 900 °C at 10 °C min^{-1}, under N_2 flow (100 vol %, 100 mL min^{-1}). The weight loss of the sample from 30 to 105 °C, and from 105 to 900 °C were measured to determine the moisture and the volatile matter, respectively. The same protocol was applied under airflow (100 mL min^{-1}) to determine the ash content. The fixed carbon was calculated by difference. Elemental analysis (C, H, N, and S content) was determined using the TruSpec Micro CHN analyzer, in agreement with the ASTM D5373 method. Samples were combusted at 950 °C in an oxygen-rich atmosphere, then the gas was subjected to a next oxidation stage at 850 °C. Thus, ash was collected and combustion products were treated into a furnace: part of them was directed to the infrared detection C, H, and S, while the remaining amount was passed over high-purity copper to eliminate the oxygen not consumed for N determination. Helium was used as carrier gas. Both proximate and elemental analysis procedure were also reported in detail by Tasca et al. [6]. The higher heating value (HHV) was calculated according to the following equation [6]:

$$\text{HHV (MJ kg}^{-1}) = (84\ \text{C\%} + 277.65\ \text{H\%} + 25\ \text{S\%} + 15\ \text{N\%} - 26.5\ \text{O\%}) \cdot 0.00419 \tag{1.8}$$

Where C%, H%, S%, N%, and O% represent the content of each element expressed as wt % on dry basis.

Investigated parameters were studied also considering the combined effect of temperature and time, using the severity (*f*), which was calculated according to the **equation 1.9** [6, 20]:

$$f = 50\, t^{0.2} e^{\frac{-3500}{T}} \quad (1.9)$$

where t is treatment time (s), and T is the temperature maintained during the reaction (K).

The effect of the different solid concentration of raw sludge loaded into the reactor was associated with severity, in order to evaluate their influence on the investigated parameters.

Determination of total phosphorous (TP) and heavy metals on HC was performed according to the CNR IRSA method [21], and EPA 3051A + EPA 6020B [22, 23], respectively.

PW was investigated in terms of total organic carbon (TOC), TP, total ammonia nitrogen (TAN), and heavy metals according to the CNR IRSA 5040, CNR IRSA 4110, EPA 350.1, and EPA 3010A + EPA 6020B, respectively [23–27].

Mass balances of each element (total phosphorous (TP), and heavy metals (hm)) was developed via the following equations:

$$\text{HC mass}_{\text{TP,hm}}(\text{mg}) = \text{HC concentration}_{\text{TP,hm}}\left(\frac{\text{mg}}{\text{kg DM}}\right) \cdot \text{mass}_{\text{HC}}(\text{g DM}) \cdot \frac{10^{-3}\,\text{g}}{\text{kg}} \quad (1.10)$$

$$\text{PW mass}_{\text{TP,hm}}(\text{mg}) = \text{PW concentration}_{\text{TP,hm}}\left(\frac{\text{mg}}{\text{L}}\right) \cdot \text{PW volume (L)} \quad (1.11)$$

where mass_{HC} is the mass of dried HC, and PW volume is the volume of PW obtained after vacuum filtration of slurry.

Mass balances of C was carried out according to Aragon – Briceño et al. [28]. Since gas was not directly measured, the amount of C in gas phase was calculated by difference.

1.3 Results and Discussion

1.3.1 HC characterization

In **Tab. 1.4** results derived from proximate and elemental analysis are reported. Further, also HHV, yield, and C_{yield} values are visible.

Table 1.4 Parameters derived from HC characterizations (proximate analysis, elemental analysis, HHV, yield, and C_{yield})

			Proximate analysis			Elemental analysis							
Run	**f**	**Solid content**	**FC**	**VM**	**Ash**	**C**	**H**	**N**	**O[1a]**	**S**	**HHV**	**Yield**	**C_{yield}**
	-	**wt %**	**wt %**	**wt %**	**wt %**	**wt %**	**wt %**	**wt %**	**wt %**	**wt %**	**MJ kg^{-1}**	**wt %**	**wt %**
1	0.228	5.00	4.02	34.16	61.82	20.67	3.31	1.98	11.47	0.75	10.04	57.61	43.79
2	0.177	12.00	4.74	37.29	57.96	22.34	3.53	2.62	12.70	0.85	10.80	62.17	51.07
3	0.207	8.50	4.22	35.13	60.64	20.83	3.35	2.28	12.38	0.52	10.03	56.07	42.95
4	0.280	5.00	4.33	33.73	61.94	21.00	3.34	2.01	11.09	0.62	10.22	55.25	41.86
5	0.144	5.00	4.41	39.08	56.51	21.87	3.75	2.54	14.68	0.65	10.64	57.98	45.73
6	0.207	2.61	3.67	34.41	61.92	19.71	3.50	1.79	12.48	0.60	9.78	52.97	37.66
7	0.177	5.00	4.27	34.49	61.23	20.09	3.44	2.12	12.53	0.59	9.87	58.61	43.52
8	0.228	12.00	5.21	36.08	58.71	22.70	3.44	2.68	11.70	0.77	10.93	59.58	49.99
9	0.233	8.50	4.72	35.85	59.43	22.32	3.43	2.52	11.54	0.78	10.78	56.99	47.02
10	0.207	8.50	4.70	38.00	57.30	23.86	3.77	2.72	11.70	0.65	11.70	56.67	46.87
11	0.150	8.50	4.26	39.79	55.95	23.55	3.78	2.94	13.20	0.58	11.45	63.15	53.71
12	0.207	8.50	3.23	38.45	58.32	23.32	3.63	2.70	11.41	0.62	11.38	58.88	49.59
13	0.299	8.50	3.43	34.24	62.34	22.58	3.44	2.26	8.81	0.58	11.16	57.22	46.67
14	0.207	8.50	3.38	37.80	58.82	23.30	3.65	2.66	10.97	0.61	11.44	59.80	50.33
15	0.280	12.00	4.55	34.53	60.92	22.52	3.45	2.66	9.88	0.57	11.05	61.39	49.96
16	0.207	8.50	4.05	37.38	58.58	22.90	3.56	2.93	11.46	0.57	11.16	60.78	50.30
17	0.138	8.50	3.77	39.22	57.01	22.53	3.75	2.95	12.87	0.88	11.12	61.65	50.20
18	0.144	12.00	3.99	40.65	55.36	23.84	3.85	3.47	12.83	0.66	11.71	68.06	58.62
19	0.207	14.39	5.66	38.58	55.76	24.16	3.59	3.33	12.53	0.63	11.55	67.84	58.24
20	0.207	8.50	3.69	35.39	60.92	22.14	3.44	2.60	10.42	0.49	10.83	60.36	47.48

[1a] Calculated by difference O =100 - (C+H+N+S+Ash)

For all experimental trials, HC was charcterized by an increase of ash content with respect to the raw sludge, which was equal to 42.98 (1.12) wt % (expressed as average value of 7 samples with standard deviation in parenthesis). An enhancement of ash content could be associated to the loss of VM during HTC reactions and also to the partition of the organic fraction between HC and PW [6, 8]. In **Fig. 1.1** is described the ash content behaviour for all the trials (reported as average of tests performed with the same solid load):

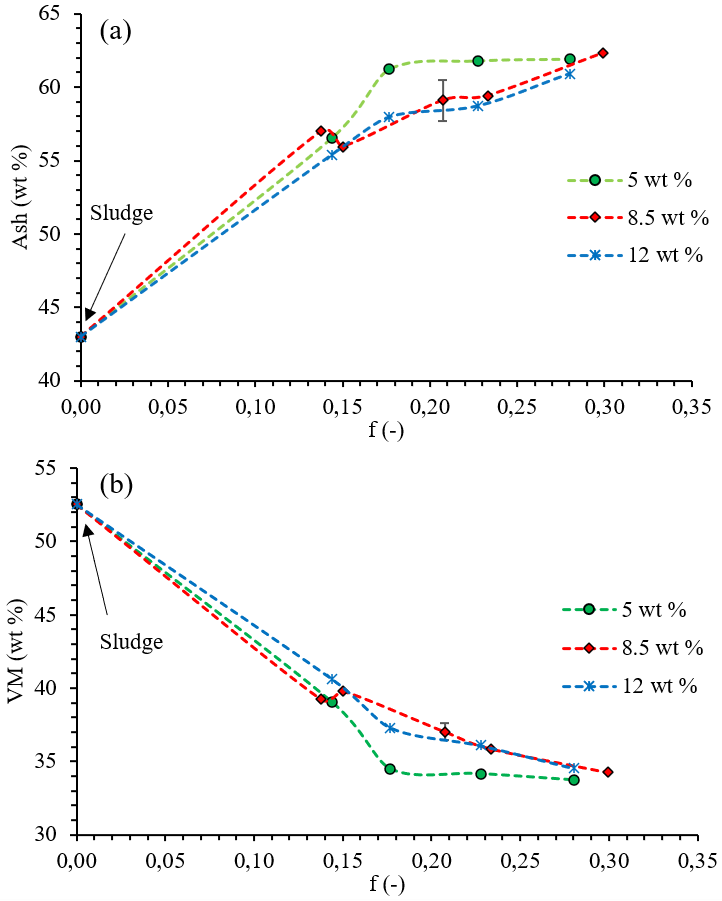

Figure 1.1 Ash (a) and VM (b) behaviour of HC derived from HTC experiments.

Further, the ash content increased also with the enhancement of severity, resulting higher with the reduction of the solid content. Indeed, with the increase of severity, both precipitation of inorganics and solubilization of the organic fraction are promoted [6]. Conversely, VM showed

opposite trends than those observed for ash. Indeed, all HC samples resulted in a VM content lower than that of raw sludge, which was equal to 52.53 (1.59) wt % (expressed as average value of 7 samples with standard deviation in parenthesis). The VM decreased more with the reduction of the solid content, since it is partially converted into CO_2 and soluble products [6]. A reduction of C, H, N, and O content was observed for all HC in comparison with sludge, which was characterized by a content of 27.76 (0.60), 4.42 (0.17), 4.49 (0.27), and 19.57 (0.48) wt %, respectively (expressed as average value of 7 samples with standard deviation in parenthesis). In most of cases, also S content of sludge (0.79 (0.07)) resulted higher than that retained into HC. In **Fig. 1.2** are reported the H/C and O/C atomic ratio for each solid content of loaded sludge [6].

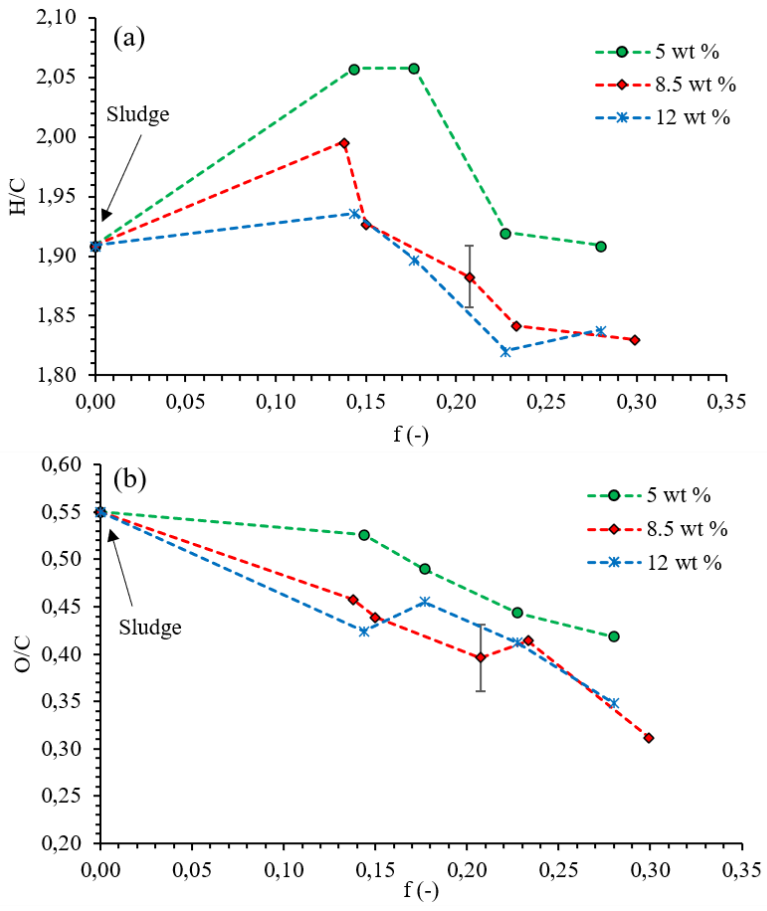

Figure 1.2 H/C (a) and O/C (b) atomic ratio for raw sludge and HC.

As severity increase, H/C and O/C decreased with the increase of the solid content of sludge. At low severity, the H/C ratio increased with respect to the raw sewage sludge, due to the

solubilization of C [6]. At high severity, the concentration of C into the solid matrix increased, and consecutively both H/C and O/C ratios were reduced. It indicated that the HTC reaction was effective, due to the dehydration, decarboxylation, as well as hydrolysis [8]. The H/C and O/C atomic ratio varied between 1.82 – 2.06, and 0.31 – 0.53, respectively. These values are similar to those reported by Peng et al. [9] for HC derived from carbonization of dewatered SS in a different range of temperature (180 – 300 °C), and times (30 – 480 min). However, these atomic ratios were not close to that of lignite region (i.e., H/C in the range 0.8 – 1.3, and O/C ratio in the interval of 0.2 – 0.38) [29]. This fact could be related to the presence of a significant content of ash into the HC [9]. Further, high H/C ratios suggested that a not condensed aromatic structure has been formed during HTC reaction [30].

1.3.2 Y and C_{yield}

HC yield varied between 52.97 and 68.06 wt %, while C_{yield} was comprised in a wider range equal to 37.66 and 58.62 wt %. Generally, similar range of HC yield (49 – 73 wt %) are reported in literature performing HTC on sludge [28, 31, 32].

The RSM analysis defined the model describing Y and C_{yield} responses. Thus, a linear relationship between variables has been proposed [6]:

$$\text{Yield} = 74.27613 - 0.099779A - 0.015284B + 0.978111C \quad (1.12)$$

$$C_{yield} = 58.76256 - 0.094083A - 0.021729B + 1.45106C \quad (1.13)$$

Where A is the temperature, B is the time, and C is the solid content.

As can be observed in **equation 1.12 and 1.13**, a linear relationship occurred among independent variables. Details about analysis of variance (ANOVA) can be found in the published manuscript [6]. Briefly, from ANOVA analysis emerged that temperature, time, and solid content were all significant (p-value < 0.05), while the lack of fit was not significant (p-value > 0.1), indicating a good predictivity of the models. Further, it was observed that severity had not an appreciable influence on the two responses (Y, and C_{yield}), while an average decrease of the two responses can

be observed with the increase of both temperature and time [6]. However, temperature proved to significantly influence the HTC reactions. Further, the solid content showed an appreciable influence on the responses (i.e., Y, and C_{yield} were enhanced with the increase of the solid content). 3-D graphs of response surface can be consulted on the published article [6].

1.3.3 Dewaterability

The SRF results obtained performing dewaterability tests on raw sludge and slurry samples is reported in **Fig. 1.3:**

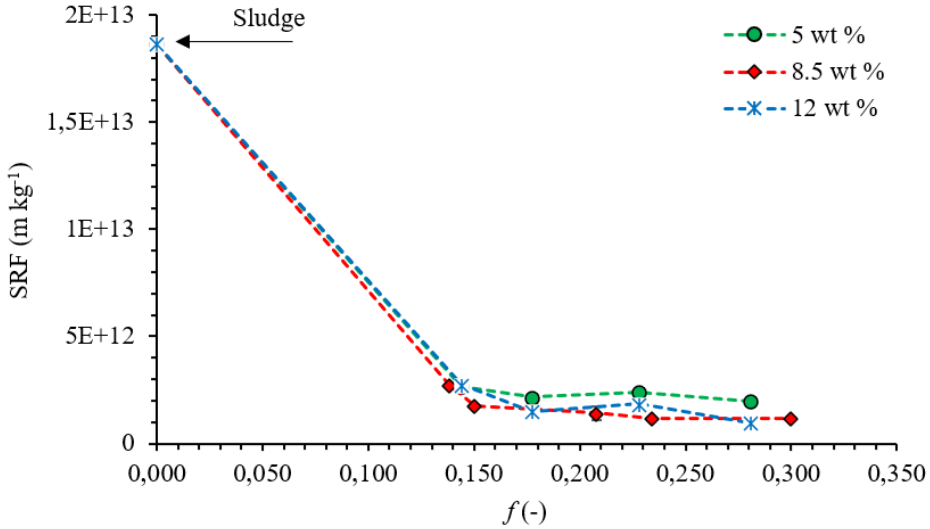

Figure 1.3 Specific resistance to filtration (SRF) test (m kg^{-1}) performed on raw sludge and slurry samples according to severity *f* (-) and solid content.

As can be observed in **Fig. 1.3**, SRF of slurry samples strongly decreased with respect to the raw sludge, indicating that HTC significatively promotes the dewaterability of sludge, regardless of severity. Indeed, dewaterability of sludge was strongly improved after HTC even at low severity, without depending by the solid content of the feedstock. About this, HTC is reported to play a main role in sludge dewaterability [17, 33]. Particularly, reaction time of 1 h and temperatures above 150 °C are recommended to improve this properties [17, 34]. Indeed, HTC is able to weak the bond between water and solid particle, transforming the surface water into interstitial and free

water, which is also the main form of which water is present processing sludge by HTC at temperatures above 180 °C [33]. Thus, free water can be removed just by compression, strongly reducing the time and the energy consumptions of thermal drying [6].

1.3.4 C distribution

In **Fig. 1.4** is reported the C distribution among HC, PW, and gas phase. Values are reported as average of measurements on tests performed at the same temperature (different conditions of time and solid content) (**Fig. 1.4a**), for the same reaction time (different conditions of temperature and solid content) (**Fig. 1.4b**), and with the same solid content (different conditions of temperature and time) (**Fig. 1.4c**):

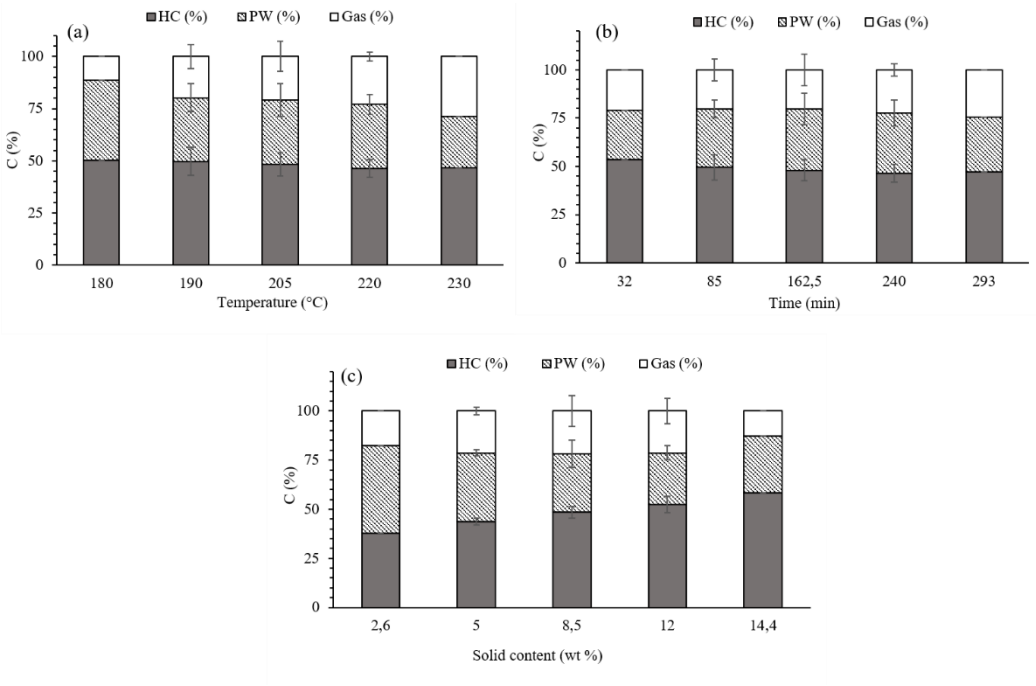

Figure 1.4 Carbon distribution (%) among HC, PW, and gas phase. Results are reported as average value of different trials performed at the same temperature (a), time (b), and solid content (c).

As can be observed in **Fig. 1.4a**, the C distribution was influenced by temperature. Indeed, as temperature rose, C in gas phase increased (from the 11.4 % at 180 °C up to the 28.8 % at 230 °C). Subsequently, the C percentage in HC decreased with temperature (from 50.2 % at 180 °C

up to the 46.7 % at 230 °C). Further, the C percentage in PW varied in the range 30.4 – 38.4 %. The presence of C in PW is mainly related to the products of Millard and Browning reactions, which determines the dissolution of low molecular weight carbonaceous compounds [35]. Further, the percentage of C in gas phase is appreciable at 220, and 230 °C, due to the fact that with higher temperatures the conversion of C into gas form might be promoted. Conversely, time proved to not have a relevant impact on C distribution, as can be observed in **Fig. 1.4b**. Additionally, the increased of solid content favoured the concentration of C into the solid matrix, as can be concluded from **Fig. 1.4c**. At the same time, the concentrations of C into liquid and gas phase were reduced.

1.3.5 TAN and phosphorous

PW was characterized in terms of TAN. Interestingly, a relationship between this parameter and severity was found, as reported in **Fig. 1.5**:

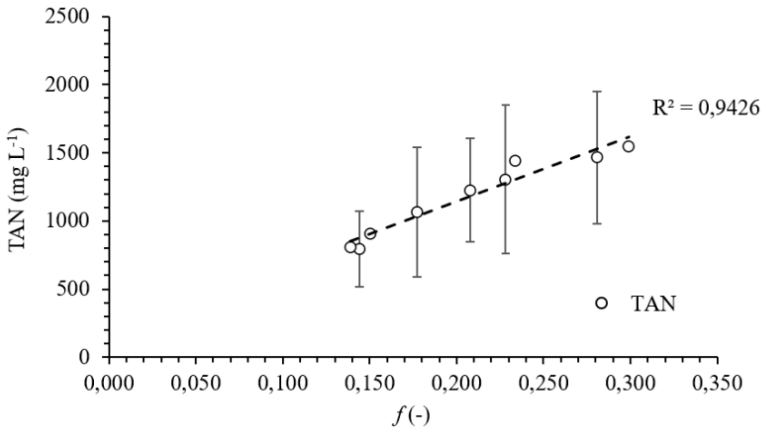

Figure 1.5 Total ammonia nitrogen (TAN) concentration in PW according to severity *f* (-).

As can be observed in **Fig. 1.5**, as the severity increased, TAN concentration into process water was enhanced. It might find explanation in the fact that in severe conditions (e.g., high temperature and long reaction time) the transformation of nitrogen in the form of TAN in the liquid phase could be promoted. Indeed, is reported that deamination occurred at higher temperature and longer reaction time, and consequently, proteins could be hydrolysed to peptide,

individual proteins, and amino acids, which were then converted into fatty acid and ammonia [36, 37].

Further, total phosphorous (TP) resulted to be mainly retained into the solid matrix (data not shown). Indeed, the percentage distribution of TP into the solid matrix was higher than 90 % for all investigated samples, suggesting that HC can play a potential role in phosphorous recovery.

1.3.6 Heavy metals

Heavy metals like Pb, Cd, Ni, Zn, and Cu were mainly accumulated into hydrochar [6]. Indeed, percentages higher than 70 % were observed into HC for the all-aforementioned metals. However, heavy metals are generally reported to be immobilized into the solid matrix, as is reported in previous studies [3, 38]. Specifically, the enrichment of Cu, Zn, and Cr into HC could be associated to their the low water solubility and cation exchange capacity, which determine their dissolution and then precipitation [6, 39].

Further, it was noted that a clear correlation occurred between the concentration of arsenic (As) into PW and severity.

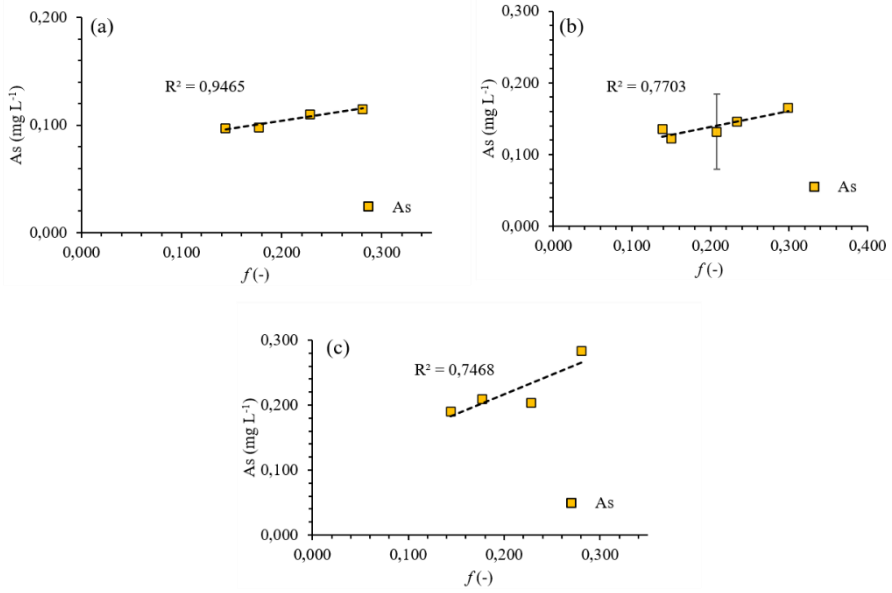

Figure 1.6 Arsenic (As) concentration in PW according to severity *f* (-).

As can be observed in **Fig. 1.6**, As concentration is related to the severity of HTC reaction, as its concentration was enhanced as the severity increased. A similar trend of As was observed by Wang et al. [37], who reported that also other metals (e.g., Cd, Pb, Hg, and Cr) shows the same behaviour. Thus, a deep characterization of PW is generally needed, in order to define its proper application.

1.4 Conclusion

The results reported in this study pointed out that HTC operational conditions (i.e., severity, and solid content) strongly influenced the characteristics of products derived from carbonization (both solid and liquid fraction). Specifically, severity resulted to impact on ash and volatile matter content of hydrochar, which increased and decreased, respectively, as severity increased. Further, dewaterability of slurry derived from HTC was definitely enhanced respect to the raw sludge regardless of HTC conditions. Further, C distribution proved to be influenced by temperature and solid content of HTC reaction, while time proved to not affect this parameter. Also, TP was mainly retained into the solid matrix, outlining a potential route for its valorization. Lastly, specific parameters, such as TAN and As resulted to be related with severity, being their concentrations rising with the increase of severity. Hence, this study demonstrated that, according to the desired characteristics of hydrochar and process water, operational conditions could be properly set-up.

1.5 Supplementary information A1

Supplementary information is included into the **Appendix A1**.

1.6 References – Chapter 1

1. Durdević, D., Trstenjak, M., Hulenić, I.: Sewage sludge thermal treatment technology selection by utilizing the analytical hierarchy process. Water (Switzerland). 12, (2020). https://doi.org/10.3390/W12051255
2. Kelessidis, A., Stasinakis, A.S.: Comparative study of the methods used for treatment and final disposal of sewage sludge in European countries. Waste Manag. 32, 1186–1195 (2012). https://doi.org/10.1016/j.wasman.2012.01.012
3. Escala, M., Zumbühl, T., Koller, C., Junge, R., Krebs, R.: Hydrothermal carbonization as an energy-efficient alternative to established drying technologies for sewage sludge: A

feasibility study on a laboratory scale. Energy and Fuels. 27, 454–460 (2013). https://doi.org/10.1021/ef3015266

4. European Commission: Protection of the Environment, and in particular of the soil, when sewage sludge is used in agriculture. Off. J. Eur. Communities. 4, 6–12 (1986)

5. Libra, A.J., Kammann, C., Funke, A., Berge, N.D., Neubauer, Y., Titirici, M.-M., Fuhner, C., Bens, O., Kern, J., Emmerich, K.-H.: Hydrothermal carbonization of biomass residuals : A comparative review of the chemistry , processes and appolications of wet and dry pyrolysis. 2, 89–124 (2011). https://doi.org/10.4155/bfs.10.81

6. Tasca, A.L., Stefanelli, E., Raspolli Galletti, A.M., Gori, R., Mannarino, G., Vitolo, S., Puccini, M.: Hydrothermal Carbonization of Sewage Sludge: Analysis of Process Severity and Solid Content. Chem. Eng. Technol. 43, 2382–2392 (2020). https://doi.org/10.1002/ceat.202000095

7. Danso-Boateng, E., Shama, G., Wheatley, A.D., Martin, S.J., Holdich, R.G.: Hydrothermal carbonisation of sewage sludge: Effect of process conditions on product characteristics and methane production. Bioresour. Technol. 177, 318–327 (2015). https://doi.org/10.1016/j.biortech.2014.11.096

8. Kim, D., Lee, K., Park, K.Y.: Hydrothermal carbonization of anaerobically digested sludge for solid fuel production and energy recovery. Fuel. 130, 120–125 (2014). https://doi.org/10.1016/j.fuel.2014.04.030

9. Peng, C., Zhai, Y., Zhu, Y., Xu, B., Wang, T., Li, C., Zeng, G.: Production of char from sewage sludge employing hydrothermal carbonization: Char properties, combustion behavior and thermal characteristics. Fuel. 176, 110–118 (2016). https://doi.org/10.1016/j.fuel.2016.02.068

10. Akarsu, K., Duman, G., Yilmazer, A., Keskin, T., Azbar, N., Yanik, J.: Sustainable valorization of food wastes into solid fuel by hydrothermal carbonization. Bioresour. Technol. 292, (2019). https://doi.org/https://doi.org/10.1016/j.biortech.2019.121959

11. Puccini, M., Stefanelli, E., Hiltz, M., Seggiani, M.: Activated Carbon from Hydrochar Produced by Hydrothermal Carbonization of Wastes. Chem. Eng. Trans. 57, 169–174 (2017). https://doi.org/10.3303/CET1757029

12. Oliver-Tomas, B., Hitzl, M., Owsianiak, M., Renz, M.: Evaluation of hydrothermal carbonization in urban mining for the recovery of phosphorus from the organic fraction of municipal solid waste. Resour. Conserv. Recycl. 147, 111–118 (2019). https://doi.org/10.1016/j.resconrec.2019.04.023

13. Funke, A., Ziegler, F.: Hydrothermal carbonization of biomass: A summary and discussion of chemical mechanisms for process engineering. Biofuels, Bioprod. Biorefining. 4, 160–177 (2010). https://doi.org/10.1002/bbb.198

14. Villamil, J.A., Mohedano, A.F., Rodriguez, J.J., de la Rubia, M.A.: Valorisation of the liquid fraction from hydrothermal carbonisation of sewage sludge by anaerobic digestion. J. Chem. Technol. Biotechnol. 93, 450–456 (2018). https://doi.org/10.1002/jctb.5375

15. Ferrentino, R., Merzari, F., Fiori, L., Andreottola, G.: Coupling hydrothermal carbonization with anaerobic digestion for sewage sludge treatment: Influence of HTC liquor and hydrochar on biomethane production. Energies. 13, (2020). https://doi.org/10.3390/en13236262

16. Mau, V., Neumann, J., Wehrli, B., Gross, A.: Nutrient Behavior in Hydrothermal Carbonization Aqueous Phase Following Recirculation and Reuse. Environ. Sci. Technol. 53, 10426–10434 (2019). https://doi.org/10.1021/acs.est.9b03080

17. Ahmed, M., Andreottola, G., Elagroudy, S., Negm, M.S., Fiori, L.: Coupling hydrothermal carbonization and anaerobic digestion for sewage digestate management: Influence of hydrothermal treatment time on dewaterability and bio-methane production. J. Environ. Manage. 281, 111910 (2021). https://doi.org/10.1016/j.jenvman.2020.111910

18. Pontoni, L., Fabbricino, M., Frunzo, L., Pirozzi, F., Esposito, G.: Biological stability and dewaterability of CAS and MBR sludge. Desalin. Water Treat. (2016)

19. Marinetti, M.: CONDIZIONAMENTO E DISIDRATAZIONE FANGHI. PhD thesis - Politec. di Milano. (2007)

20. Suwelack, K.U., Wüst, D., Fleischmann, P., Kruse, A.: Prediction of gaseous, liquid and solid mass yields from hydrothermal carbonization of biogas digestate by severity parameter. Biomass Convers. Biorefinery. 6, 151–160 (2016). https://doi.org/10.1007/s13399-015-0172-8

21. IRSA, CNR, I. di ricerca sulle acque: Quaderno n. 64 - METODI ANALITICI PER I FANGHI, (1985)

22. United States Environmental Protection Agency: Method 3051A - Microwave Assisted Acid Digestion of Sediments, Sludges, Soils, and oils. Washington, DC. (2007)

23. United States Environmental Protection Agency: EPA Method 6020B - Inductively Coupled Plasma-Mass Spectrometry. Washington, (2014)

24. IRSA, CNR, I. di ricerca sulle acque, APAT: Method 5040 - Carbonio organico totale, (2003)

25. IRSA, CNR, I. di ricerca sulle acque, APAT: Method 4110 A2 - Fosforo totale, (2003)

26. United States Environmental Protection Agency: EPA Method 350.1 - Determination of ammonia nitrogen by semi-automated colorimetry. (1993)

27. United States Environmental Protection Agency: Method 3010A - Acid Digestion of Aqueous Samples and Extracts for Total Metals for Analysis by FLAA or ICP Spectroscopy. (1992)

28. Aragón-briceño, C., Ross, A.B., Camargo-valero, M.A.: Evaluation and comparison of product yields and bio-methane potential in sewage digestate following hydrothermal treatment. Appl. Energy. 0–1 (2017). https://doi.org/10.1016/j.apenergy.2017.09.019

29. Park, S.W., Jang, C.H.: Characteristics of carbonized sludge for co-combustion in pulverized coal power plants. Waste Manag. 31, 523–529 (2011).

https://doi.org/10.1016/j.wasman.2010.10.009

30. Tasca, A.L., Puccini, M., Gori, R., Corsi, I., Galletti, A.M.R., Vitolo, S.: Hydrothermal carbonization of sewage sludge: A critical analysis of process severity, hydrochar properties and environmental implications. Waste Manag. 93, 1–13 (2019). https://doi.org/10.1016/j.wasman.2019.05.027

31. Gaur, R.Z., Khoury, O., Zohar, M., Poverenov, E., Darzi, R., Laor, Y., Posmanik, R.: Hydrothermal carbonization of sewage sludge coupled with anaerobic digestion: Integrated approach for sludge management and energy recycling. Energy Convers. Manag. 224, 113353 (2020). https://doi.org/10.1016/j.enconman.2020.113353

32. Arauzo, P.J., Atienza-Martínez, M., Ábrego, J., Olszewski, M.P., Cao, Z., Kruse, A.: Combustion characteristics of hydrochar and pyrochar derived from digested sewage sludge. Energies. 13, 1–15 (2020). https://doi.org/10.3390/en13164164

33. Wang, L., Li, A., Chang, Y.: Relationship between enhanced dewaterability and structural properties of hydrothermal sludge after hydrothermal treatment of excess sludge. Water Res. 112, 72–82 (2017). https://doi.org/10.1016/j.watres.2017.01.034

34. Bougrier, C., Delgenès, J.P., Carrère, H.: Effects of thermal treatments on five different waste activated sludge samples solubilisation, physical properties and anaerobic digestion. Chem. Eng. J. 139, 236–244 (2008). https://doi.org/10.1016/j.cej.2007.07.099

35. Danso-Boateng, E., Holdich, R.G., Shama, G., Wheatley, A.D., Sohail, M., Martin, S.J.: Kinetics of faecal biomass hydrothermal carbonisation for hydrochar production. Appl. Energy. 111, 351–357 (2013). https://doi.org/10.1016/j.apenergy.2013.04.090

36. Chen, H., Rao, Y., Cao, L., Shi, Y., Hao, S., Luo, G., Zhang, S.: Hydrothermal conversion of sewage sludge: Focusing on the characterization of liquid products and their methane yields. Chem. Eng. J. 357, 367–375 (2019). https://doi.org/10.1016/j.cej.2018.09.180

37. Wang, L., Chang, Y., Liu, Q.: Fate and distribution of nutrients and heavy metals during hydrothermal carbonization of sewage sludge with implication to land application. J. Clean. Prod. 225, 972–983 (2019). https://doi.org/10.1016/j.jclepro.2019.03.347

38. Langone, M., Basso, D.: Process waters from hydrothermal carbonization of sludge: Characteristics and possible valorization pathways. Int. J. Environ. Res. Public Health. 17, 1–31 (2020). https://doi.org/10.3390/ijerph17186618

39. Jakubus, M., Czekała, J.: Heavy Metal Speciation in Sewage Sludge. Polish J. Environ. Stud. 10, 245–250 (2001)

Chapter 2

Phosphorous recovery from hydrochar derived by hydrothermal carbonization of sewage sludge

Abstract

The recycle and recovery of phosphorous (P) is becoming necessary for satisfying the future P demand and for environmental protection. Wastewaters and by-products wastewater, as sewage sludge (SS), represent an important P-source, which can be exploited. In this direction, hydrothermal carbonization (HTC) is arising as a suitable technology to treat SS, promoting also P recovery. In this study, leaching tests using both nitric and sulfuric acids were performed at different operational conditions: pH (1 – 3.5), leaching time (30 – 240 minutes), and solid/liquid ratio (5 – 20 wt %). Trials were performed using process water derived by HTC and demi water as solution. Experimental responses were elaborated according to the Design of Experiments method, under Response Surface Methodology approach. Results were then optimized with the goal of maximizing the P yield and minimizing the ash content of HC after leaching. Phosphorous recovery results in high P yield (> 60 wt %), applying both nitric and sulfuric acid with PW and demi-water. While H_2SO_4 proved to be more efficient than HNO_3 to leach P from HC, the latter determine an HC with better fuel properties after leaching (low ash content). Optimal conditions were identified at lowest pH, while the leaching time did not show a relevant influence. Lastly, the effect of temperature has been investigated, proving that the room temperature is optimal to carry out leaching tests.

2.1 Introduction

Phosphorous (P) is an essential nutrient for life of all organisms [1], but its availability on earth is scarce, as in only few countries (China, Vietnam, Kazakhstan, and United States) P sources are present [2]. Thus, since its global supply is limited and it cannot be replaced by any other element, P has been listed among critical raw materials since 2017 from European Commission [2]. The P

demand is mainly related to its use as fertilizer in agriculture (~ 82 %), whereas a small quantity is used for animal feed production or in industrial, medical, and textile applications [3]. Because of the world population will growth by 2050, and subsequently the related agricultural production, the P demand will strongly increase [4].

P-fertilizers are produced by mining mineral phosphate rocks, which naturally contains some hazardous chemical elements (e.g., Cd, Pb, Cr, and As) that contributes to the environmental pollution [5, 6]. Further, P release in freshwater generally promotes eutrophication, which ultimately determines a loss in biodiversity and species [3]. Thus, to find alternative P sources is becoming extremely important, in order to avoid the excessive exploitation of P deposits and to limit the environmental pollution.

Wastewater and by-products of wastewater treatment (e.g., sewage sludge (SS), and ash) represent significant P-sources [1]. Indeed, for example, the P content in SS (~ 8 wt %) is comparable to that into phosphate rock (6.5 – 17.9 % P) [6, 7]. Additionally, SS ash is reported to contain P into a similar range (4 – 12 % P) [6, 8]. Thus, different technologies (biological and chemical) have been developed to recover P from wastewater streams, transferring it from the liquid to the solid phase. Among biological treatment, the enhanced biological phosphorous removal (EBPR) is the most widely applied. The process is based on specific microorganisms (PAO – polyphosphate accumulating organisms), which consume phosphate from wastewater for their growth under anaerobic and aerobic/anoxic conditions [9]. Conversely, chemical treatment uses cations of metal salts to precipitate P and subsequently recover it [10]. Besides these technologies, thermal treatments (e.g., incineration, and pyrolysis) also promote P recovery from SS. Indeed, after thermal treatments, P is generally concentrated into the solid matrix. Then, it can be easily leached using acids, and lastly precipitated using a base [11].

Among thermal treatments, hydrothermal carbonization (HTC) can play a key role as suitable technology to recover P from SS. HTC can process biomass (e.g., SS) in water under autogenous pressure and temperature at the lower region of liquefaction process [12]. Applying HTC on SS,

three fractions are obtained: a solid coal-like material (hydrochar, HC), a liquid phase (process water, PW), and a small gaseous fraction. Particularly, P is generally reported to be concentrated into HC, showing a good affinity with solid phase [13, 14]. Some studies have already investigated the P recovery from HC derived from SS, proposing acid leaching as feasible pathway [15–17]. In these works, two types of acids (H_2SO_4, HCl) and different operational conditions have been tested. All authors agreed that high P recovery yield (> 70 wt %) can be obtained. Accordingly, also Oliver-Tomas et al. [18] reported that P yield higher than 95 wt % can be obtained leaching P from HC derived by the organic fraction of municipal solid waste with HNO_3, H_2SO_4, and HCl. Further, HNO_3 was selected as preferred acid in terms of fuel properties, since sulfur and chlorine content increased after leaching. Thus, the main idea of this study was to evaluate the optimal leaching conditions (type of acid, pH, leaching time, and solid/solution ratio) in order to obtain the highest P yield and to reduce the ash content. Leaching experiments were carried out on HC derived from SS using HNO_3 and H_2SO_4 acids, and using as solution PW or demi water. Trials were planned according to the Design of Experiments method, under the Response Surface Methodology approach. Part of this work has been already published [19]:

Tasca, A.L., Mannarino, G., Gori, R., Vitolo, S., Puccini, M., 2020. Phosphorus recovery from sewage sludge hydrochar: process optimization by response surface methodology. Water Sci. Technol. https://doi.org/10.2166/wst.2020.485

2.2 Acid leaching test with process water - Materials and methods

2.2.1 Hydrochar and process water

Hydrochar pellets were obtained by processing secondary SS derived by Naquera's Water Resources Recovery Facility (WRRF) (managed by Aguas de Valencia) at HTC Ingelia full-scale plant. The WRRF has a capacity of 5000 population equivalent, treating an average flow of 1500 $m^3\ d^{-1}$. The treatment train consists of pre-treatments, primary clarification, and conventional activated sludge process. SS (moisture of 82 %) was processed in HTC batch conditions (200 – 210 °C, 3 h), previously adding an ultra-high molecular weight cationic flocculant (ZETAG

8167), in order to improve sludge dewaterability and to increase its solid content. After HTC, the slurry (a solid-liquid mixture) was directed to a grinder, a hydro cyclone, and then to a vibrating screen to remove inert solids. The suspension was then separated into the solid hydrochar (HC) and process water (PW) by a filter press, and then the HC was thermally dried and lastly pelletized.

2.2.2 Phosphorous extraction

Before P extraction experiments, HC pellets were ground by an electric mortar mill and then sieved (< 212 μm) to obtain a homogenous sample. After, HC powder was dried at 105 °C overnight before analysis. Leaching tests were carried out according to Oliver-Tomas et al. [18] and Tasca et al. [19]. Briefly, 50 mL of PW were placed into a 100 mL beaker together with dried HC. The HC quantity was weighted according to the desired S/L (% wt) ratio. The solid-liquid suspension was then mixed for 15 – 20 minutes to homogenize the slurry. The pH of suspension was measured, and subsequently the selected acid (nitric/sulfuric acid) was added through a glass graduated pipette in order to reach the desired pH. Nitric acid ($HNO_3 \geq 65$ %, Honeywall Fluka) and sulfuric acid (H_2SO_4 at 97 %, Honeywall Fluka) were used. The acidified mixture was stirred at 20 °C for the time required for each run and then separated by filtration using filter paper (No. 1 Whatman). Hence, the final P-rich acidified liquid fraction was collected and chemically characterized using analytical kits. The solid was washed with demi water for three times using an amount of water equal to 3 times the weight of the initial solid and then it was dried overnight. Further, the effect of temperature was evaluated performing six preliminary leaching runs at three different temperatures (20, 40 and 60 °C) and at different S/L ratios (10 and 20 wt %).

2.2.3 Design of Experiments with process water

The Design of Experiments (DoE) is an approach method able to systematically analyse the significant elements and the objectives of an experiment. It mainly results in an experimental plan of randomized runs. The DoE can predict the effects of an input variation on the outputs, elaborating a probabilistic mathematical model able to predict the responses. Thus, it reduces the

systematic error and it allows to estimate the related experimental error. In this study, DoE was elaborated under the RSM (Response Surface Methodology) approach. The software Design Expert 11 (Stat-Ease) was used to develop the experimental plan. Three key parameters were selected as initial variables according to Tasca et al. [19] and values are reported **Tab. 2.1**:

Table 2.2 Levels of factors for DoE with PW.

Factor	Name	Unit	Min	Max
A	pH prior leaching	-	1	3.5
B	Leaching time	min	30	240
C	S/L ratio[2a]	wt %	5	20

[2a] the S/L ratio was calculated as the weight of dry HC on the weight of solution (PW + HC) in all runs.

The choice of the initial variables and the explanation of factors level are described in detail by Tasca et al. [19]. Phosphorous extraction yield (named P yield) and ash content of HC after acid leaching were selected as target responses. P yield was calculated according to **equation 2.1**:

$$P_{yield}\ (wt\ \%) = \frac{P_L - P_{PW}}{P_{HC}} \cdot 100 \qquad (2.1)$$

where: P_L is the amount of phosphorus (mg) in the acidified process water after leaching, P_{PW} is the amount of phosphorus (mg) in process water, and P_{HC} is the amount of phosphorus (mg) in the hydrochar before acid leaching.

Ash content (wt % on dry basis) were measured by incineration in a muffle furnace or by thermogravimetric analysis (TGA) in air at 900 °C.

In this study, two experimental plans were elaborated using the DoE methodology. The first one (PW - nitric acid), expected 34 trials (**Tab. 2.2**), whereas the second one (PW - sulfuric acids) involved 20 runs (**Tab. 2.3**). In both cases, a two-level RSM plan, CCD (Central composite

Design) and FCC (Face Centered Design) was elaborated. For PW - nitric acid plan, factorial points (8) as well axial points (6) were replicated twice, in addition to the 6 central points. Instead, in case of PW - sulfuric acid, neither factorial nor axial points were replicated.

Table 2.3 Experimental plan of 34 runs carried out using PW - nitric acid.

Run	pH	Time (min)	S/L (wt %)
1	2.25	135	12.5
2	2.25	135	12.5
3	1	240	20
4	2.25	240	12.5
5	3.5	30	20
6	1	30	20
7	2.25	135	20
8	1	135	12.5
9	1	135	12.5
10	2.25	135	20
11	2.25	30	12.5
12	2.25	135	5
13	3.5	135	12.5
14	3.5	30	20
15	3.5	30	5
16	1	30	5
17	2.25	30	12.5
18	2.25	135	12.5
19	2.25	135	12.5
20	3.5	240	5
21	1	30	5
22	2.25	135	5
23	3.5	240	20
24	1	240	5
25	1	30	20
26	3.5	240	5
27	3.5	135	12.5
28	2.25	135	12.5

29	3.5	240	20
30	1	240	5
31	2.25	135	12.5
32	3.5	30	5
33	1	240	20
34	2.25	240	12.5

Table 2.4 Experimental plan of 20 runs carried out using PW – sulfuric acid.

Run	pH	Time (min)	S/L (wt %)
1	3.5	240	20
2	2.25	30	12.5
3	3.5	30	5
4	3.5	30	20
5	2.25	135	12.5
6	2.25	135	12.5
7	2.25	135	12.5
8	1	30	5
9	2.25	135	20
10	2.25	240	12.5
11	1	240	20
12	3.5	240	5
13	1	30	5
14	2.25	135	12.5
15	1	135	12.5
16	2.25	135	5
17	2.25	135	12.5
18	2.25	135	12.5
19	1	240	5
20	3.5	135	12.5

2.2.4 Characterization

HC after leaching was characterized in terms of elemental analysis (C, H, N) and of moisture, volatile matter, and fixed carbon as reported in detail by Tasca et al. [20]. PW before leaching, as

well as acidified process waters, were chemically characterized in terms of P, orthophosphate (Orto-P), total ammonia nitrogen (TAN), and chemical oxygen demand (COD). These parameters were measured using analytical kits [19] or by standard methods (CNR IRSA 4110 A2 for P [21], CNR IRSA 4020 for Orto-P [22], EPA 350.1 for TAN [23], and ISO 15705 for COD [24]). In case of analytical kits, samples were properly diluted to comply measurements range and blanks were performed to avoid interferences. Further, concentration of several metals (i.e., Al, As, Ba, Cd, Cr, Fe, Mn, Hg, Pb, Cu, Zn, Ca, Mg, K, and Na) were measured according to EPA 3010A, and EPA 6020B [25, 26]. Additionally, P content in HC was measured [27]. Lastly, P concentrated in HC was fractionated applying a procedure widely used for soils and sediments, named SMT protocol [28].

2.3 Preliminary leaching tests with effect of temperature

In order to evaluate the influence of temperature on acid leaching tests, six experiments at three different temperatures (20, 40, and 60 °C) were carried out [19]. In **Tab. 2.4** are reported the operating conditions of each run and the resulted P yield (wt %).

Table 2.5 Preliminary tests on temperature influence.

Run	Temperature (°C)	pH	Time (min)	S/L (wt %)	HNO_3 added (mL)	P yield (wt %)
1	20	2.25	135	10	1.8	23.45
2	40	2.25	135	10	1.9	27.70
3	60	2.25	135	10	1.4	6.47
4	20	2.25	135	20	2.1	12.22
5	40	2.25	135	20	1.5	3.96
6	60	2.25	135	20	1.4	3.05

As can be observed in **Tab. 2.4**, P yield (wt %) decreased with the increase of temperature. Thus, all tests were carried out at the lowest temperature (i.e., 20 °C). It might find explanation in the heat generated during exothermic reactions, which occur during acid leaching tests. Therefore,

the P recovery process resulted to be independent of the reaction temperature, as also assessed by Oliver-Tomas et al. [18].

2.4 Results of tests with nitric acid

2.4.1 P yield and ash content

In **Tab. 2.5** are reported all data measured during acid leaching tests with HNO_3 under DoE procedure.

Table 2.6 Experimental data on DoE carried out with nitric acid.

Run	HC weight (g)	Volume HNO_3 (mL)	pH slurry prior acidification	pH slurry post acidification	pH slurry post leaching	pH leachate	Final HC weight (g)	TP of PW (mg L^{-1})
1	7.14	1.9	6.63	2.28	2.28	3.33	6.9829	592.5
2	7.14	1.9	6.57	2.31	2.31	3.32	6.8789	590.0
3	12.50	4.1	6.53	1.05	1.05	2.33	10.2164	3075.0
4	7.14	1.9	6.62	2.29	2.29	3.29	6.2282	580.0
5	12.50	1.7	6.45	3.58	3.58	3.99	11.706	547.5
6	12.50	3.8	6.56	1.04	1.04	1.75	10.0301	3175.0
7	12.50	2.5	6.41	2.22	2.22	3.29	11.3112	787.5
8	7.14	2.9	6.56	1.08	1.08	1.93	5.7338	2342.5
9	7.14	2.9	6.61	1.08	1.08	2.01	5.8735	2455.0
10	12.50	2.5	6.41	2.23	2.23	3.13	11.2017	802.5
11	7.14	1.9	6.72	2.26	2.26	2.85	6.4114	562.5
12	2.63	1.5	6.83	2.19	2.19	2.69	2.317	432.5
13	7.14	1.2	6.65	3.51	3.51	4.26	6.6003	152.8
14	12.50	1.6	6.38	3.48	3.48	4.12	11.5095	267.5
15	2.63	0.9	6.93	3.48	3.48	3.91	2.4776	94.3
16	2.63	1.9	6.71	1.05	1.05	1.49	2.1936	985.0
17	7.14	1.7	6.64	2.22	2.22	3.22	6.4239	412.5
18	7.14	1.9	6.96	2.27	2.27	3.5	6.4082	537.5
19	7.14	2.0	6.78	2.23	2.23	3.33	6.3951	585.0
20	2.63	1.2	6.83	3.4	3.4	3.87	2.5902	209.8
21	2.63	2.0	7.08	1.08	1.08	1.52	2.2198	975.0
22	2.63	1.6	6.83	2.22	2.22	2.84	2.3791	470.0
23	12.50	2.1	6.68	3.48	3.48	4.04	11.9742	747.5

24	2.63	2.1	6.87	1.09	1.09	1.73	2.1627	965.0
25	12.50	4.0	6.65	1.08	1.08	1.99	10.2892	3250.0
26	2.63	1.2	6.87	3.44	3.44	3.81	2.4247	186.3
27	7.14	1.9	6.85	3.45	3.45	4.04	6.4512	472.5
28	7.14	2	6.86	2.26	2.26	3.47	6.3764	625.0
29	12.50	1.8	6.56	3.53	3.53	3.97	11.7457	597.5
30	2.63	1.9	6.92	1.08	1.08	1.8	2.1957	842.5
31	7.14	2.1	6.81	2.21	2.21	3.36	6.4322	715.0
32	2.63	1.2	6.93	3.46	3.46	3.82	2.4467	147.0
33	12.50	3.9	6.79	1.08	1.08	2.27	10.2934	2875.0
34	7.14	2.0	6.90	2.26	2.26	3.49	6.4132	402.5

The results of P yield (wt %) and ash content (wt %) are reported in **Tab. 2.6**:

Table 2.7 Responses of DoE with nitric acid.

P yield (wt %)	**Ash content (wt %)**
12.88	25.57
12.82	24.67
41.85	20.16
12.59	25.83
6.74	28.93
42.99	20.79
10.05	25.20
54.35	17.98
57.00	16.85
10.25	26.18
12.19	25.53
24.72	24.15
2.67	28.36
3.05	28.93
3.60	26.79
59.57	19.21
8.68	25.85
11.61	25.56
12.73	26.24

10.78	26.05
59.06	20.22
27.11	22.62
9.44	28.11
58.55	16.09
44.18	19.63
9.32	26.23
10.11	26.38
13.66	25.42
7.41	28.34
50.63	18.29
15.77	24.81
6.90	25.01
38.96	20.51
8.51	25.05

Results described in **Tab. 2.6** are referred to a concentration of P in PW equal to 36.38 mg L^{-1}, in HC equal to 31450 mg P $kg_{dry\ HC}$, and to an ash content in HC equal to 30.97 wt %. As can be directly observed in **Tab. 2.6**, P yield varied in the range 2.67 – 59.57 wt %, and the ash content decreased up to the 48 % with respect of the initial HC ash content (pH = 1, time of 240 min, and S/L ratio of 5 wt %). Indeed, low pH resulted to reduce the ash content on HC. Regarding the P recovery yield, higher values (up to 90 wt %) were reported for acid leaching tests on HC derived from SS [17]. Nevertheless, in that study, P from HC has been leached using a 4 M HCl solution instead of PW. Additionally, HCl proved to be the more efficient acid for P recovery [18]. Thus, it is reasonable to assume that similar results could be obtained using a pure acid solution, instead of acidified PW. Here, HNO_3 was selected as acid, since it showed to be efficient for recovering P recovery from HC, by not adding sulfur or chlorine to the solid matrix [18]. This aspect is fundamental in the perspective of using HC as solid fuel. Indeed, after leaching, the ash content of HC is generally reduced, improving its combustible quality. Conversely, the addition of sulfur or chlorine made its fuel properties worse. As concluded by Oliver-Tomas et al. [18], nitric acid

proved to be appropriate to improve solid fuel characteristics of HC derived by organic fraction of municipal solid waste, fulfilling also the requirements defined by ISO 17225-8. Similar ash reductions (equal to 50 %) were observed by Marin Batista et al. [15], recovering P from HC derived by digestate using HCl.

In **Fig. 2.1a** P yield (wt %) is reported as a function of pH for runs with the same S/L ratio (wt %) (average of trials with different leaching times), while in **Fig. 2.1b** trials were clustered according to leaching time (at different S/L ratios).

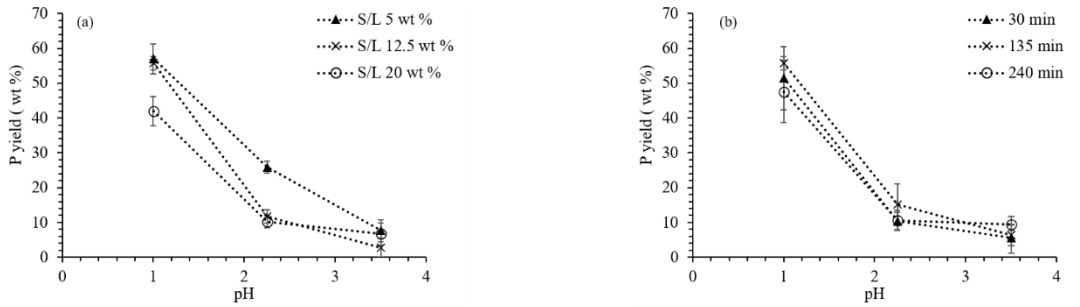

Figure 2.1 P yield (wt %) as a function of pH for runs with the same S/L ratio (a), and with equal leaching time (b) using PW and nitric acid.

P yield (wt %) increased with the decreasing of pH, while it decreased with the increase of S/L ratio (**Fig. 2.1a**). Since P yield resulted in different values for each pH tested, this parameter seemed to be the most relevant during leaching tests. Indeed, to obtain a complete dissolution of P associated with iron, a pH lower than 1.5 has to be reached [29]. Differently, P yield resulted to be independent by leaching time, since similar P recovery were obtained for trials with the same pH.

2.4.2 Characterization of leachate

During acid leaching tests on HC, other compounds, as metals and cations, were dissolved into the acidified solution together with P. In the perspective of recovering the acidified PW in agriculture or to produce struvite [30], its chemical characterization must be known.

In **Tab. 2.7**, are reported the chemical characterizations of PW prior leaching, of leachate derived by run 16 (at which corresponded the highest P yield), and of leachate obtained by run 9 (in which the highest P concentration was measured).

Table 2.8 Chemical characterization of PW prior leaching, and leachates from Run 16 and Run 9 using PW and nitric acid (values are reported as average of three determinations with standard deviation in brackets).

	PW[2a]	**Run 16**[2a]	**Run 9**[2a]
pH	7.4 (0.1)	1.49 (0.1)	2.01 (0.1)
Al (mg L^{-1})	1.33 (0.33)	209 (52)	512 (130)
As (mg L^{-1})	0.227 (0.057)	0.166 (0.042)	0.361 (0.090)
Ba (mg L^{-1})	0.135 (0.032)	5.70 (1.4)	7.10 (1.7)
Cd (mg L^{-1})	< 0.0025	0.0197 (0.0045)	0.0560 (0.013)
Cr (mg L^{-1})	0.170 (0.041)	0.081 (0.020)	0.182 (0.044)
Fe (mg L^{-1})	26 (6.5)	121 (30)	440 (110)
Mn (mg L^{-1})	0.53 (0.13)	7.90 (1.9)	20.00 (4.8)
Hg (mg L^{-1})	< 0.00075	0.00157 (0.00047)	0.00160 (0.00048)
Pb (mg L^{-1})	< 0.0025	0.690 (0.17)	1.150 (0.28)
Cu (mg L^{-1})	0.0300 (0.0069)	2.920 (0.0025)	5.700 (1.4)
Zn (mg L^{-1})	0.152 (0.037)	35.40 (8.5)	139.00 (33)
Ca (mg L^{-1})	1010 (240)	3890 (930)	9000 (2200)
Mg (mg L^{-1})	248 (60)	520 (130)	1661 (400)
K (mg L^{-1})	610 (150)	567 (140)	730 (170)
Na (mg L^{-1})	403 (97)	445 (110)	590 (140)

[2a] Standard deviation of n = 3 measure is reported in parenthesis.

As can be observed in **Tab. 2.7**, for most of the investigated compounds, the concentration increased in the leachate in comparison with PW. With the exception of As, Cr and K, this behaviour was observed for all other metals and cations. Particularly, an increase in Al and Fe concentration was observed for both runs, together with the increase of Ca in leachate of Run 16 and 9. The presence of these compounds might be an indication about the forms in which P is in HC. Indeed, Ca could be associated to apatite forms, while Al, Fe and Mn might suggest the

presence of oxides and hydroxides [28]. Indeed, as can be observed in **Fig. 2.2**, apatite (AP) resulted to be the biggest fraction of inorganic P (IP) in HC.

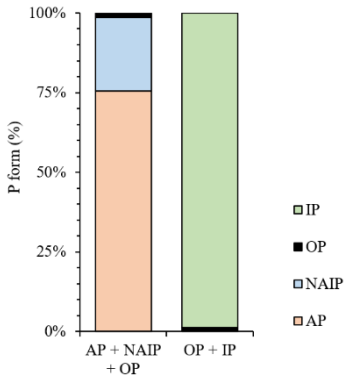

Figure 2.2 P speciation in HC among apatite form (AP), non-apatite form (NAIP), organic phosphorus (OP), and inorganic phosphorous (IP).

Considering the concentrations of Al, Ca, Fe, and Mg, in acidified PW of all trials (as can be observed in **Figure 2.3**), it was evident that Al, Fe and Mn needed low pH to be effectively dissolved into the liquid phase, while Ca was easily transferred into PW also at pH of 2 - 3. Thus, HC containing P mainly in apatite form, might need less acid volume than those containing oxides/hydroxides of Al and Fe.

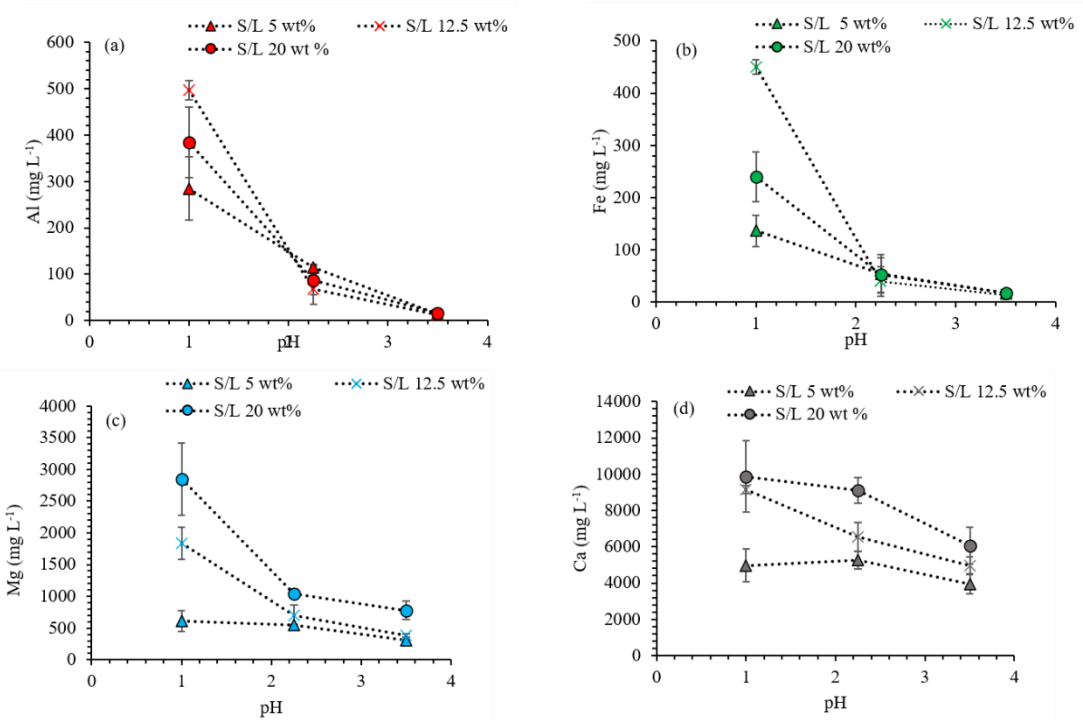

Figure 2.3 Al (a), Fe (b), Mg (c), and Ca (d) concentrations in acidified PW with nitric acid (expressed as average values of trials in same conditions of pH and S/L ratio, but different leaching time).

Further, since HC contains only inorganic orthophosphate [31], it resulted the most relevant P form (76 – 100 %) in acidified PW [19]. Additionally, the leachates showed a COD loss up to 19 %, whereas positive and negative variations were detected for TAN (- 7 to 39 %). These variations could be related to the oxidizing effect of nitric acid [19].

2.4.3 Design of Experiment results with nitric acid and process water

2.4.3.1 P yield

The analysis of variance (ANOVA) carried out on the P yield response is reported in **Tab. 2.8.**

Table 2.9 Analysis of variance and determination coefficients for P yield response (nitric acid – PW).

	Sum of Squares	df	Mean Square	F-value	p-value	
Model	12343.36	10	1234.34	223.00	<0.0001	significant
A-pH	2429.31	1	2429.31	438.89	<0.0001	
B-Tempo	0.0603	1	0.0603	0.0109	0.9178	
C-Rapporto S/L	248.24	1	248.24	44.85	<0.0001	
AB	65.94	1	65.94	11.91	0.0022	
AC	195.18	1	195.18	35.26	<0.0001	
A^2	1357.05	1	1357.05	245.17	<0.0001	
B^2	114.75	1	114.75	20.73	0.0001	
C^2	45.46	1	45.46	8.21	0.0087	
A^2C	48.44	1	48.44	8.75	0.0070	
AB^2	38.85	1	38.85	7.02	0.0143	
Residual	127.31	23	5.54			
Lack of Fit	17.27	4	4.32	0.7454	0.5730	not significant
Pure Error	110.04	19	5.79			
Cor Total	12470.67	33				

Model statistics	
R^2	0.9898
Adjusted R^2	0.9854
Predicted R^2	0.9746

From ANOVA analysis emerged that the experimental data were well fitted by a quadratic model with the addition of semi-cubic terms. This model was significant (p-value < 0.05), whereas the lack of fit (i.e., the lack of adaptation of the model) was not significant (p-value > 0.1), indicating a good prediction of the response [19]. Additionally, the determination coefficient (R^2) confirmed the prediction ability of the model. Notably, the B-factor (i.e., time) showed a p-value > 0.1, resulting not significant for the model. Nevertheless, the quadratic terms (AB, AB^2, and B^2), derived by the interaction of terms, appeared significative for the response. The *Cor Total* explains the variation around the mean of observations. This amount is partially explained by *Model* value, while the *Residual* interprets the rest. In **equation 2.2** is reported the equation of the model in coded form:

$$\text{P yield (wt \%)} = 14.32 - 24.64\ A + 0.0549\ B - 7.88\ C + 2.03AB + 3.49\ AC + 15.91\ A^2 - 4.63\ B^2 + 2.91C^2 + 3.89\ A^2C + 3.48\ AB^2 \quad (2.2)$$

Where A, B, C represent the input variables, i.e., pH, time, and S/L ratio respectively. Coefficients are reported through coded notation, in which parameters varies between +1 (high level) and -1 (low level). Coded coefficients are obtained using the following equation (**equation 2.3**):

$$\text{Coded} = \frac{2\ (\text{Actual setting} - \text{Average actual setting})}{\text{Range between low and high actual settings}} \quad (2.3)$$

Where actual setting represents the parameters reported in conventional measure unit, while coded values are normalized into the same range, pointing out the influence on the response by a single factor or by their interactions.

As can be observed in **Fig. 2.4**, predicted values of responses calculated by the model and experimental values were severely distributed on the line, pointing out that the model is moderately predictive.

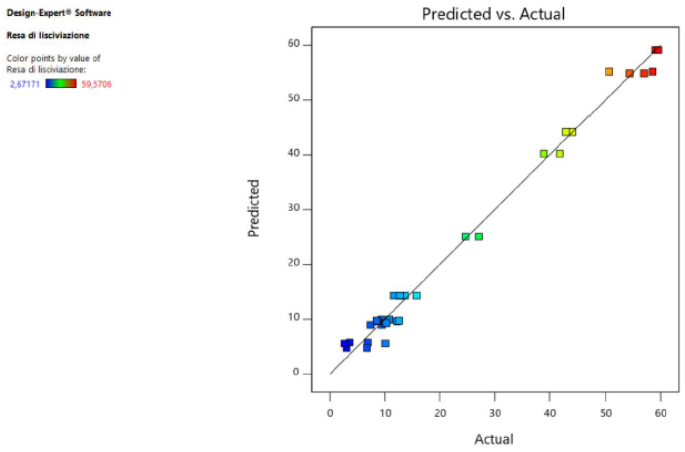

Figure 2.4 Comparison between predicted and actual values for P yield response for nitric acid and PW.

Further, in **Fig. 2.5** the 3-D graphs of the response are reported [19].

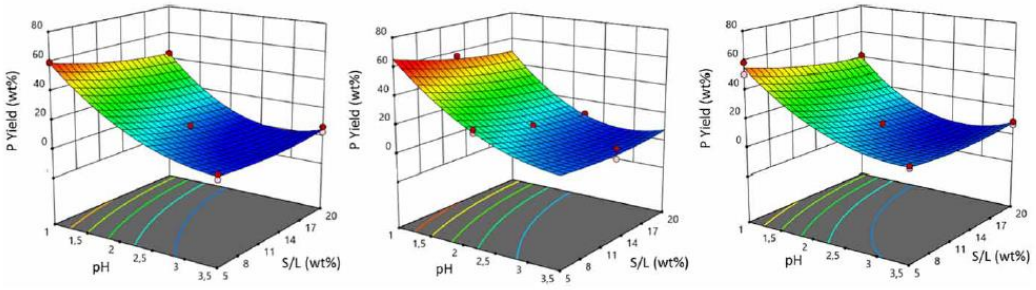

Figure 2.5 3-D graphs for P yield response for B-Time equal of 30, 135, and 240 minutes on the left, centre, and right, respectively (red points represents the design points above the predicted values, and pink points are the design points below the predicted values) for nitric acid and PW.

As can be observed in **Fig. 2.5**, the pH proved to significantly influence the P yield, since it increased as pH decreased. At pH = 1, the P yield increased with S/L ratio decreasing, whereas the latter showed a little influence on the response at pH = 3.5. The leaching time seemed to not alter the P yield, even though a slightly higher P yield was observed for the intermediate leaching time (135 min) at pH = 1.

2.4.3.2 Ash content

As reported in **Tab. 2.9**, the ANOVA analysis was developed also on ash content.

Table 2.9 Analysis of variance and determination coefficients for ash content response for nitric acid and PW.

	Sum of Squares	df	Mean Square	F-value	p-value	
Model	420.70	10	42.07	70.64	<0.0001	significant
A-pH	98.97	1	98.97	166.17	<0.0001	
B-Tempo	1.93	1	1.93	3.24	0.0850	
C-Rapporto S/L	24.45	1	24.45	41.05	<0.0001	
AB	0.9366	1	0.9366	1.57	0.2224	
AC	0.5461	1	0.5461	0.9170	0.3482	
BC	0.7229	1	0.7229	1.21	0.2820	
A^2	35.80	1	35.80	60.10	<0.0001	
B^2	3.34	1	3.34	5.61	0.0267	
ABC	3.23	1	3.23	5.42	0.0291	
AB^2	3.23	1	3.23	5.43	0.0289	
Residual	13.70	23	0.5956			
Lack of Fit	2.15	4	0.5374	0.8841	0.4921	not significant
Pure Error	11.55	19	0.6078			
Cor Total	434.40	33				
Model statistics						
R^2	0.9685					
Adjusted R^2	0.9548					
Predicted R^2	0.9218					

A quadratic model with semi-cubic terms proved to the best fitting of the ash content response, as reported above for P yield. This model was significant (p-value < 0.05), whereas the lack of fit was not significant (p-value > 0.1), indicating a good prediction of the response [19]. It was also confirmed by the value of the determination coefficient (R^2). Time (factor B) (p-value > 0.05), and the combined terms of AB, AC, and BC resulted to be not significative for the response (p-value > 0.1), but these terms were however included in the model, as the terms ABC and AB^2 were significant. In **equation 2.4** is reported the coded equation of the model:

$$\text{Ash content (wt \%)} = 24.98 + 4.97\,A - 0.3107B + 1.11\,C + 0.2419AB + 0.1848\,AC + 0.2126BC - 2.43\,A^2 + 0.7424\,B^2 - 0.4490ABC - 1.01AB^2 \quad (2.4)$$

Where A, B, C represent the input variables, i.e., pH, time, and S/L ratio respectively.

The model resulted moderately predictive, as is shown in **Fig. 2.6.**

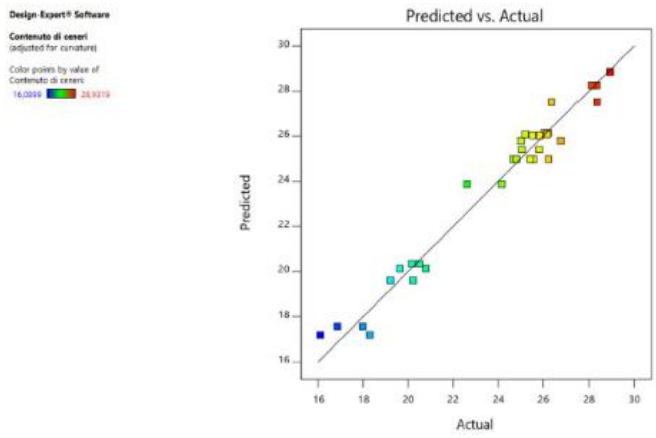

Figure 2.6 Comparison between predicted and actual values for ash content response for nitric acid and PW.

In **Fig. 2.7** are depicted the 3-D surfaces of the ash content response [19].

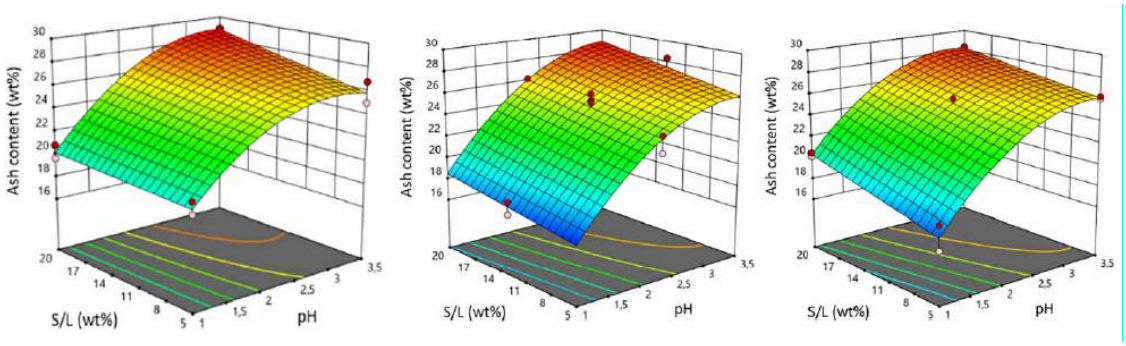

Figure 2.7 3-D graphs for ash content response for B-Time equal of 30, 135, and 240 minutes on the left, centre, and right, respectively (red points represents the design points above the predicted values, and pink points are the design points below the predicted values) for nitric acid and PW.

The ash content of the leached solid decreased at low pH, which was the most significant factor on the response. Further, the ash content linearly decreased with the reduction of the S/L ratio (the quadratic term C^2 is not present in the **equation 2.4**). As for P yield, leaching time did not show a relevant influence on the ash content, even though its decrease was observed with an increasing leaching time and low pH (equal to 1).

2.4.3.3 Optimization

A multi-objective optimization of the selected responses was developed by relating to the obtained parametric model [19]. The optimization was carried out in the perspective of defining the optimal conditions (pH, time, and S/L ratio) to maximize the P yield and to minimize the ash content. Results of the optimization are reported in **Fig. 2.8**:

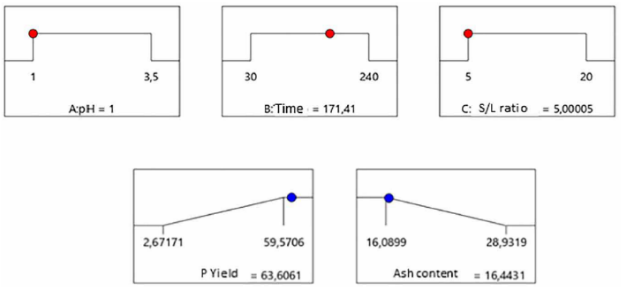

Figure 2.8 Multi-objective optimization for nitric acid and PW.

A pH equal to 1, a S/L ratio of 5 wt %, and an intermediate leaching time of about 171 minutes were optimal to improve both P yield and ash content. In practice, the quantity of nitric acid required to obtain a pH of 1 might be not feasible, and a more precise compromise could be found. An additional optimization was carried out by fixing a S/L ratio of 12.5 wt %, which is a representative value for slurry obtained by HTC process. The optimization results are reported in **Fig. 2.9**:

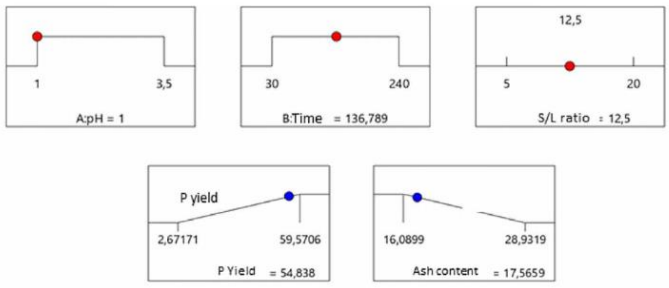

Figure 2.9 Multi-objective optimization with a fixed S/L ratio (12.5 wt %) for nitric acid and PW.

The lowest pH resulted to be the optimal also in this case, where the optimal leaching time decreased up to about 140 minutes.

2.5 Results of tests with sulfuric acid

2.5.1 P yield and ash content

In **Tab. 2.10** is reported the whole data set collected during acid leaching tests with H_2SO_4 under DoE procedure.

Table 2.10 Experimental data on DoE carried out with sulfuric acid.

Run	HC weight (g)	Volume of H_2SO_4 (mL)	pH slurry prior acidification	pH slurry post acidification	pH slurry post leaching	pH leachate	Final HC weight (g)	TP of PW (mg L^{-1})
1	12.51	1.1	6.98	3.36	3.89	3.94	13.0891	680
2	7.15	1.1	7.23	2.34	2.98	2.9	78.609	990
3	2.67	0.6	7.57	3.47	3.65	3.74	31.682	200
4	12.53	1.05	6.72	3.5	3.96	3.88	129.508	391
5	7.18	1	7.01	2.26	3.09	3.1	75.993	1220
6	7.2	0.98	7.17	2.24	3.07	3.03	76.257	1250
7	7.26	1	7.26	2.35	3.13	3.12	77.618	1190
8	2.64	1.12	7.15	1.06	1.16	1.21	30.098	740
9	12.53	1.3	6.98	2.31	3.2	3.23	131.137	1450
10	7.14	0.95	6.4	2.29	3.16	3.31	75.834	1030
11	12.51	1.9	6.76	1.05	1.43	1.46	127.988	4020
12	2.62	0.6	7.53	3.46	3.84	3.9	30.227	289
13	12.55	1.85	6.93	1.04	1.36	1.46	129.827	3720
14	7.15	0.95	6.91	2.29	3.05	3.17	75.594	1140
15	7.14	1.43	6.99	1.06	1.36	1.43	74.193	2250
16	2.64	0.7	7.65	2.25	2.94	3.02	3.059	560
17	7.17	1	6.87	2.31	3.02	3.1	75.849	1160
18	7.15	1	6.91	2.28	3.08	3.08	75.959	1190
19	2.68	1.14	7.56	1.05	1.19	1.16	31.128	1080
20	7.14	0.8	7.26	3.4	3.88	3.88	75.377	513

The results of P yield (wt %) and ash content (wt %) are reported in **Tab. 2.11**:

Table 2.11 – Responses of DoE with sulfuric acid.

P yield (wt %)	Ash content (wt %)
9.76	28.75
25.43	29.37
10.36	32.71
5.19	29.09
31.47	29.35
32.22	29.74
30.32	29.97
50.95	32.67
21.9	29.72
26.45	29.85
62.99	27.95
17.11	31.78
57.61	28.01
29.39	29.31
60.2	29.04
36.84	32.25
29.89	29.91
30.78	29.8
74.43	32.59
12.37	30.48

Results reported in **Tab. 2.11** are referred to a concentration of P in PW equal to 57 mg L^{-1}, in HC equal to 26300 mg P $kg_{dry\ HC}$, and to an ash content in HC equal to 26.33 wt %. As can be directly observed in **Tab. 2.11**, P yield varied in the range 5.19 – 74.43 wt % and ash content increased up to the 24 % with respect of the initial HC ash content (pH = 1, time of 30 min, and S/L ratio of 5 wt %). The maximum value of P yield using sulfuric acid resulted higher than those obtained with nitric acid, whereas no reductions of ash content were observed using sulfuric acid. Limited studies were found regarding the comparison of different acids on P leaching performance of HC. Nitric, sulfuric, hydrochloric, citric and oxalic acid were generally applied to recover P from HC, while only few studies compared their performances [32]. A recent study [16]

assesses that H_2SO_4 proved to be more efficient than HCl to remove P from HC, with P yields recovery in a range of 80 – 100%. They also reported that the highest P recovery was observed at low temperature of HTC process (180 °C), whereas higher temperatures (215, and 250 °C) were characterized by slower P release. Since here HC was obtained by a hydrothermal reaction carried out at ~ 200 °C, the P yield might be affected also by the high reaction temperature.

HC after leaching were generally characterized by higher content of ash respect to the initial one (**Tab. 2.11**). It might find explanation in the precipitation of calcium sulfate ($CaSO_4$) on HC [18], which has a low solubility product. This aspect can be related to the use of sulfuric acid instead of nitric one. Thus, even though sulfuric acid is more efficient and cheaper than nitric acid, appropriate evaluations have to be developed in order to define the final application of leached HC.

In **Fig. 2.10** is reported the P yield (wt %) as a function of pH and S/L ratio (average of trials with different leaching times).

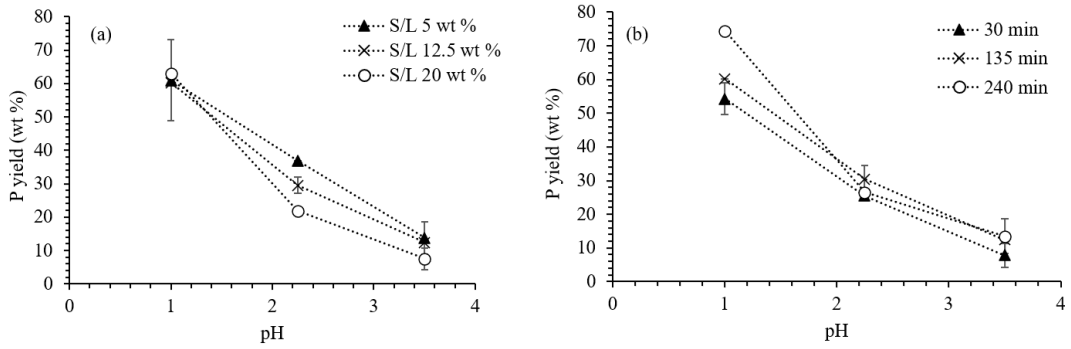

Figure 2.10 P yield (wt %) as a function of pH for runs with the same S/L ratio (a), and with equal leaching time (b) using PW and sulfuric acid.

As can be observed in **Fig. 2. 10a**, P yield decreased with the pH reduction and with the increase of S/L ratio, showing a trend similar to trials with nitric acid. Nevertheless, no relevant differences can be noted among different P yields at pH equal to 1. In this case, time proved to have an

influence on P yield, since longer leaching time (i.e., 240 min) promoted higher P yields (**Fig. 2. 10b**).

2.5.2 Characterization of leachate

In **Tab. 2.12**, are reported the chemical characterizations of PW prior leaching, of leachate derived by Run 19 (at which corresponded the highest P yield), and of leachate obtained by Run 11 (in which the highest P concentration was measured).

Table 2.12 Chemical characterization of PW prior leaching, and leachates from Run 19 and Run 11 using PW and sulfuric acid.

	PW[2b]	**Run 19**[2b]	**Run 11**[2b]
pH	7.00	1.16	1.46
Al (mg L^{-1})	0.78	170	570
As (mg L^{-1})	0.174	0.276	0.450
Ba (mg L^{-1})	0.04	0.61	0.08
Cd (mg L^{-1})	< 0.0025	0.024	0.104
Cr (mg L^{-1})	0.187	0.43	0.98
Fe (mg L^{-1})	19.60	241	860
Mn (mg L^{-1})	0.389	7.90	40.2
Hg (mg L^{-1})	0.00106	< 0.00075	< 0.00075
Pb (mg L^{-1})	< 0.0025	0.226	0.269
Cu (mg L^{-1})	< 0.0025	8.2	23.1
Zn (mg L^{-1})	0.092	36.5	181
Ca (mg L^{-1})	1520	392	440
Mg (mg L^{-1})	216	460	1230
K (mg L^{-1})	760	980	1390
Na (mg L^{-1})	314	383	470

[2b] Standard deviation of n = 3 measure is not available.

An increase of Fe and Al concentrations was observed in leachates respect to their content in PW (**Tab. 2.12**). Nevertheless, Ca significantly decreased its content in leachates, supporting the hypothesis of calcium sulfate precipitation.

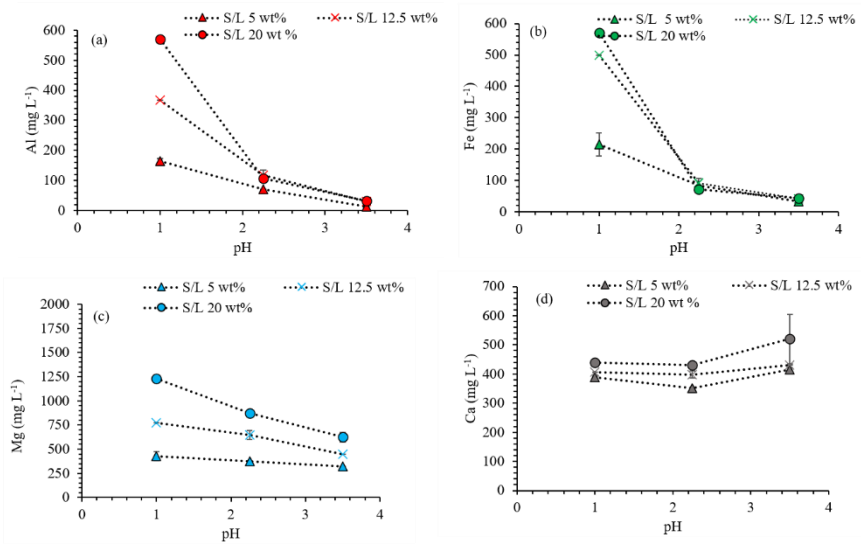

Figure 2.11 Al (a), Fe (b), Mg (c), and Ca (d) concentrations in acidified PW with sulfuric acid (expressed as average values of trials in same conditions of pH and S/L ratio, but different leaching time).

Considering the concentrations of Al, Ca, Fe, and Mg, in acidified PW of all runs (as can be observed in **Fig. 2. 11**), it was evident that Al and Fe needed low pH to be effectively dissolved into the liquid phase, while in case of Mg the same trend is slightly detectable. Conversely, since Ca precipitated as calcium sulfate, a no visible correlation with pH can be observed (**Fig. 2.11d**).

Also in this case, orthophosphate resulted the most relevant P form (63– 100 %) in acidified PW. Similarly, the leachates showed a COD loss up to 22 %, whereas positive and negative variations were detected for TAN (- 1 to 18 %).

2.5.3 Design of Experiment results with sulfuric acid and process water

2.5.3.1 P yield

The ANOVA analysis was developed on P yield response and results are reported in **Tab. 2.13.**

Table 2.13 Analysis of variance and determination coefficients for P yield response (sulfuric acid – PW).

	Sum of Squares	df	Mean Square	F-value	p-value	
Model	0.1217	12	0.0101	1313.84	<0.0001	significant
A-pH	0.0121	1	0.0121	1564.61	<0.0001	
B-Tempo	7.57E-03	1	7.57E-03	0.9809	0.3550	
C-Rapporto S/L	0.0066	1	0.0066	856.92	<0.0001	
AB	0.0031	1	0.0031	402.47	<0.0001	
AC	0.0052	1	0.0052	679.14	<0.0001	
BC	0.0001	1	0.0001	15.91	0.0053	
A^2	0.0017	1	0.0017	221.92	<0.0001	
B^2	0.0006	1	0.0006	77.36	<0.0001	
C^2	0.0002	1	0.0002	20.50	0.0027	
ABC	0.0006	1	0.0006	75.33	<0.0001	
A^2B	0.0010	1	0.0010	132.13	<0.0001	
AB^2	0.0008	1	0.0008	100.29	<0.0001	
Residual	0.0001	7	7.72E-03			
Lack of Fit	7.45E-03	2	3.72E-03	0.3996	0.6902	not significant
Pure Error	0.0000	5	9.32E-03			
Cor Total	0.1217	19				
Model statistics						
R^2	0.9996					
Adjusted R^2	0.9988					
Predicted R^2	0.9903					

Experimental data were fitted by a quadratic model with the addition of semi-cubic terms. This model was significant (p-value < 0.05), whereas the lack of fit (i.e., the lack of adaptation of the model) was not significant (p-value > 0.1), indicating a good prediction of the response. Additionally, R^2 confirmed the prediction ability of the model. The B-factor (i.e., time) showed a p-value > 0.1, resulting not significant for the model. Nevertheless, the quadratic terms (A^2B, AB, AB^2, and B^2), derived by the interaction of terms, appeared significant for the response. In this specific case, the response was obtained using the following equation:

$$y' = \frac{1}{\sqrt{y}} \tag{2.5}$$

where y is the response and y' is the transformed one.

The response transformation through the root square is generally needed when the error (residue) is a function of response and, in particular, it is recommended when a proportional relationship among data can be observed.

In **equation 2.6** is reported the equation of the model in coded form:

$$\text{P yield (wt \%)} = 0.1810 + 0.0777\,A - 0.0019\,B + 0.0275\,C - 0.0197\,AB + 0.0256\,AC - 0.0039\,BC + 0.0250\,A^2 + 0.0147\,B^2 + 0.0076\,C^2 - 0.0085\,ABC - 0.0252\,A^2B + 0.0220\,AB^2 \quad (2.6)$$

Where A, B, C represent the input variables, i.e., pH, time, and S/L ratio, respectively.

Predicted values of the responses calculated by the model and experimental values resulted severely distributed on the line, pointing out that the model is moderately predictive.

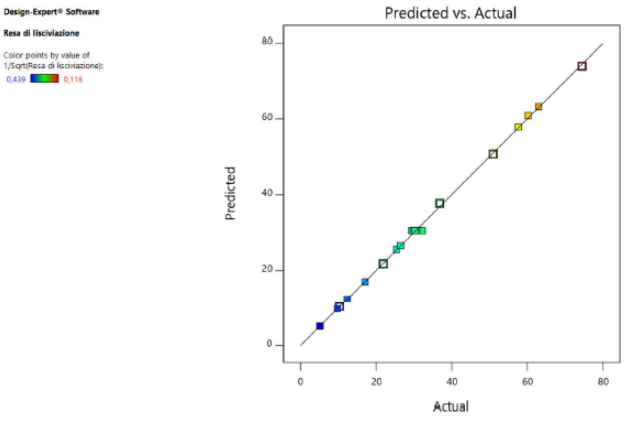

Figure 2.12 Comparison between predicted and actual values for P yield response in case of sulfuric acid and PW.

Further, in **Fig. 2.13** the 3-D graphs of P yield are reported.

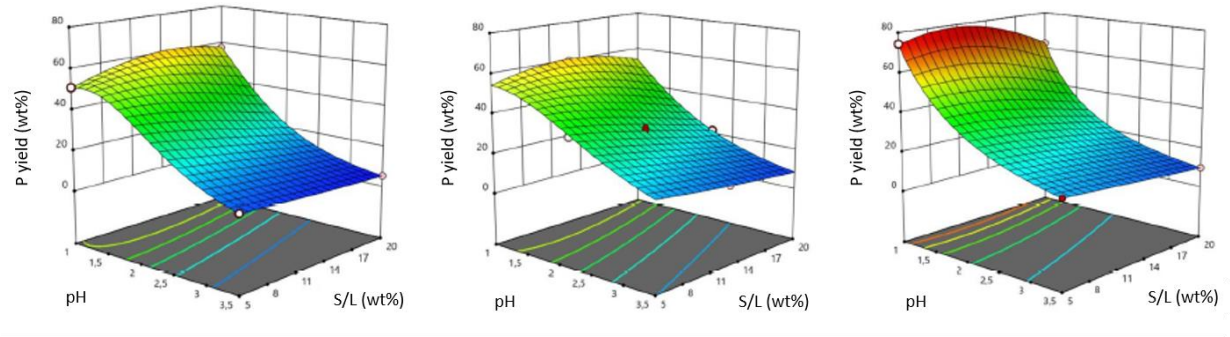

Figure 2.13 3-D graphs for P yield response for B-Time equal of 30, 135, and 240 minutes on the left, centre, and right, respectively (red points represents the design points above the predicted values, and pink points are the design points below the predicted values) for sulfuric acid and PW.

As can be observed in **Fig. 2.13**, P yield increased with the decrease of pH, as was previously observed in **2.4.3.1.** For pH equal to 1, the P yield increased when S/L ratio assumed intermediate values, while it seemed to not have a relevant influence when pH is higher than 1. Leaching time showed an influence on P yield higher than tests with nitric acid, especially with low value of pH.

2.5.3.2 Ash content

As reported in **Tab. 2.14**, the ANOVA analysis was carried out also on ash content.

Table 2.14 Analysis of variance and determination coefficients for ash content response for sulfuric acid and PW.

	Sum of Squares	df	Mean Square	F-value	p-value	
Model	40.45	6	6.74	46.55	<0.0001	significant
A-pH	0.6443	1	0.6443	4.45	0.0549	
C-Rapporto S/L	3.22	1	3.22	22.26	0.0004	
AC	0.8896	1	0.8896	6.14	0.0277	
A^2	0.156	1	0.156	1.08	0.3182	
C^2	3.21	1	3.21	22.18	0.0004	
A^2C	0.8358	1	0.8358	5.77	0.032	
Residual	1.88	13	0.1448			
Lack of Fit	1.48	8	0.1855	2.32	0.184	not significant
Pure Error	0.399	5	0.0798			
Cor Total	42.34	19				
Model statistics						
R^2	0.9555					
Adjusted R^2	0.935					
Predicted R^2	0.8175					

A quadratic model with the addition of only one semi-cubic term proved to the best model to fit the ash content response. This model was significant (p-value < 0.05), whereas the lack of fit was not significant (p-value > 0.1), indicating a good prediction of the response. As can be observed in **Tab. 2.14**, the leaching time (factor B) and its interactions were discarded from the model, since its influence on the response was negligible. In **equation 2.7** is reported the equation of the model in coded form:

$$\text{Ash content (wt \%)} = 29.37 + 0.2538\,A - 1.27\,C + 0.3335\,AC - 0.2208\,A^2 + 1.00\,C^2 - 0.7227\,A^2C \quad (2.7)$$

Where A, and C represent the input variables, i.e., pH, and S/L ratio, respectively.

The model showed an acceptable prediction capacity, since both modelled and experimental values were close to the line (**Fig. 2.14**).

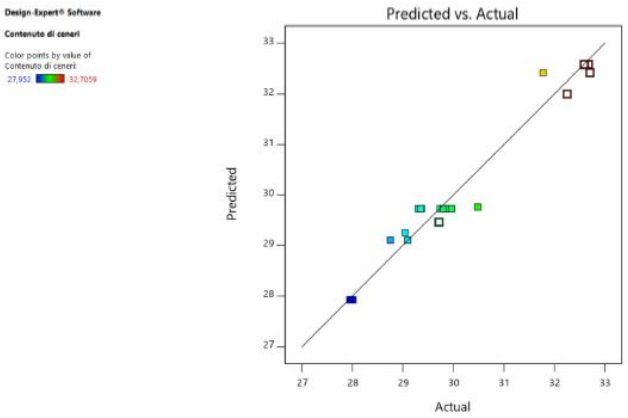

Figure 2.14 Comparison between predicted and actual values for ash content response for sulfuric acid and PW.

In **Fig. 2.15** is reported the 3-D surface of the ash content response.

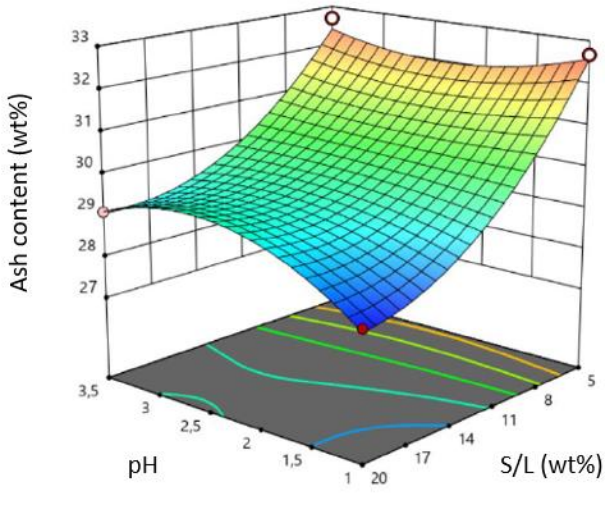

Figure 2.15 3-D graphs for ash content response (red points represents the design points above the predicted values, and pink points are the design points below the predicted values) for sulfuric acid and PW.

The S/L ratio resulted to be the factor that mainly influence the response, since a clear increase of ash content can be observed with a reduction of S/L ratio. Further, at low pH the ash content decreased at high S/L ratio.

2.5.3.3 Optimization

Also in this case, a multi-objective optimization of the selected responses was performed. It was carried out in the perspective of defining the optimal conditions (pH, time, and S/L ratio) to maximize the P yield and to minimize the ash content. Results of the optimization are reported in **Fig. 2.16**:

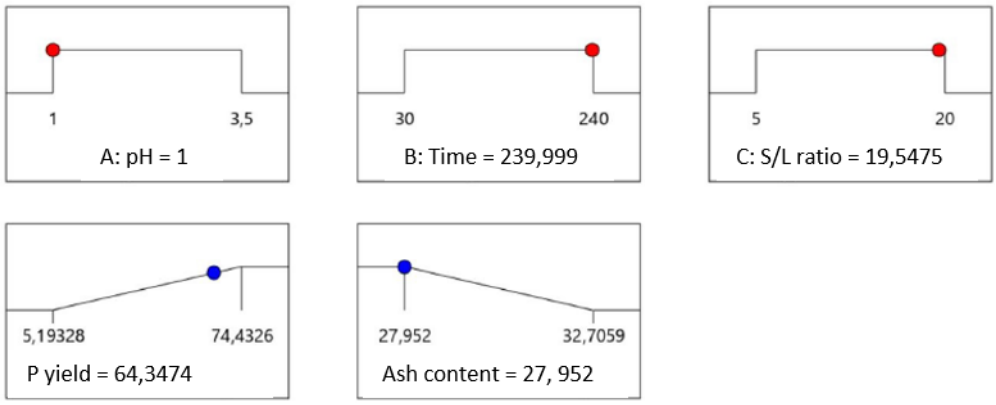

Figure 2.16 Multi-objective optimization for sulfuric acid and PW.

An additional optimization was carried out by fixing a S/L ratio of 12.5 wt %, which is a representative value for slurry obtained by HTC process. The optimization results are reported in **Fig. 2.17**:

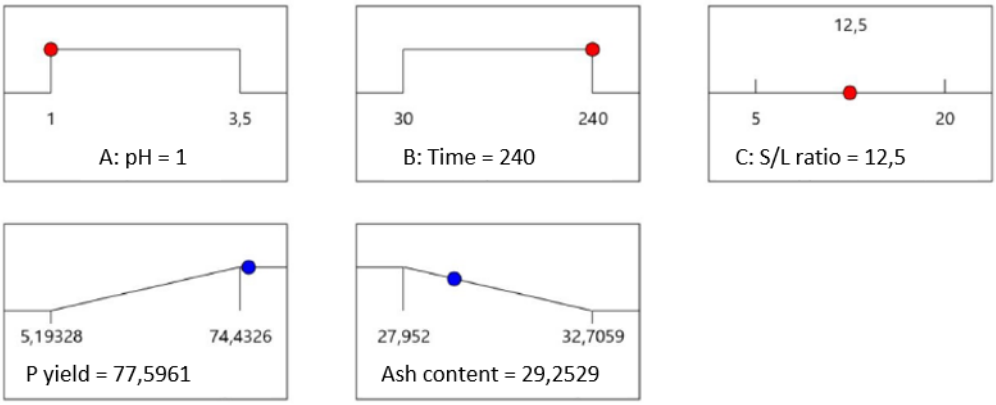

Figure 2.17 Multi-objective optimization with a fixed S/L ratio (12.5 wt %).

The lowest pH resulted to be optimal in both cases, while the longest time resulted the best. With a fixed S/L ratio (**Fig. 2.17**), a sensibly higher P yield than those reported in **Fig. 2.16** was obtained, while only a slight increase in ash content was observed.

2.5.4 Thermogravimetric analysis (TGA)

TGA analysis was carried out as depicted in **2.2.4** on leached HC with sulfuric acid and on HC prior leaching. In **Fig. 2.18** are reported the thermogravimetric curves of the initial HC and of Run 15 (pH 1, S/L ratio 12.5, and time 135 min), 18 (pH 2.25, S/L ratio 12.5, and time 135 min), and 4 (pH 3.5, S/L ratio 20, and time 30 min).

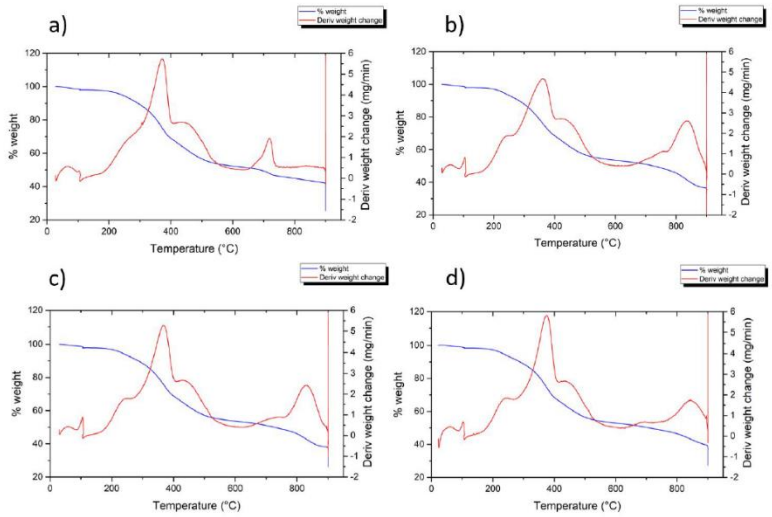

Figure 2.18 Thermogravimetric curves (TG) and differential thermogravimetric (DTG) of specific samples: initial HC (a), leached HC of Run 15 (b), of Run 18 (c), and of Run 4 (d).

Initial weight loss up to 105 °C represents the loss of moisture, which accounted around the 2 % of the total mass of the sample, confirming the hydrophobicity of HC. The DTG curves showed a clear peak around 350 °C, while two more small peaks can be observed before and after it, related to the volatilization of volatile materials. Another significant peak can be noted over 800 °C, where the decomposition of organic material occurred.

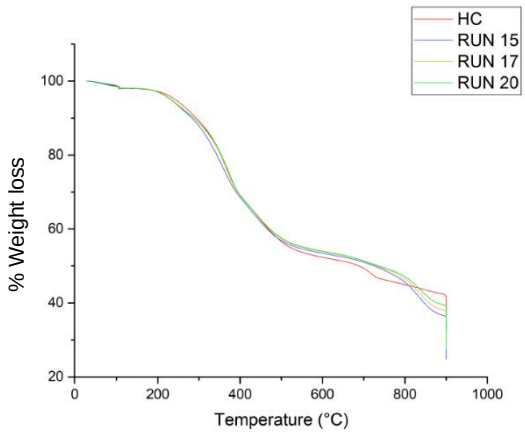

Figure 2.19 Comparison of TGA curves obtained for HC leached at different pH.

In **Fig. 2.19** are reported the TGA curves of HC leached at different pH. Curves showed a similar trend, especially in the zone of volatile matter. The Run 15 (pH 1) was the HC with the most rapid decomposition over the 800 °C. All leached HC were characterized by a more significant weight loss than the initial one, which might be related to the presence of calcium sulfate occurred during the leaching tests.

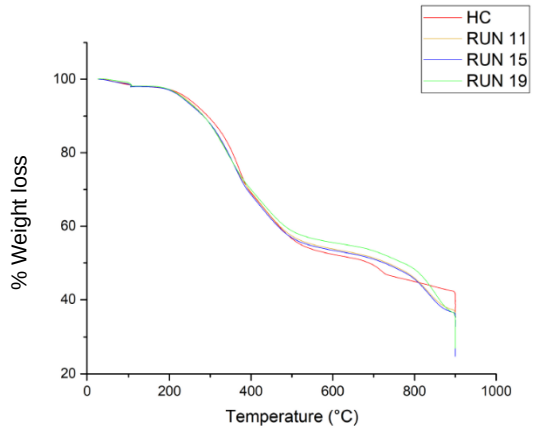

Figure 2.20 Comparison of TGA curves obtained for HC leached at different S/L ratio.

In **Fig. 2.20** is reported the weight loss of HC leached at different S/L ratio. The Run 19 (S/L equal to 5) showed a smaller loss of volatile material than Run 15 (S/L equal to 12.5) and 11 (S/L equal to 20). As can be observed in **Fig. 2.19**, the three HC after leaching were characterized by a higher weight loss than the initial one.

2.6 Acid leaching test with demi water - Materials and methods

2.6.1 Design of Experiments with demi water

A new DOE with demi water instead of PW and with both sulfuric and nitric acid has been developed. Leaching tests were carried out as described previously in **2.2.2**.

Four key parameters were chosen as initial variables and values are reported **Tab. 2.15**:

Table 2.15 Levels of factors for DoE with demi water.

Factor	Name	Unit	Min	Max
A	pH prior leaching	-	1	3.5
B	Leaching time	min	30	240
C	S/L ratio[2b]	wt %	5	20
D	Type of acid	-	HNO_3	H_2SO_4

[2b] the S/L ratio was calculated as the weight of dry HC on the weight of solution (demi water + HC) in all runs.

Since the number of independent variables is limited (i.e., 4) a two-level RSM plan, CCD (Central composite Design) and FCC (Face Centered Design) with one replicate of 8 (2^3) factorial points was elaborated. A plan of 40 trials was elaborated.

Phosphorous extraction yield (P yield) and ash content of HC after acid leaching were selected as target responses. P yield was calculated according to **equation 2.8**:

$$\text{P yield (wt \%)} = \frac{P_L}{P_{HC}} \cdot 100 \quad (2.8)$$

where: P_L is the amount of phosphorus (mg) in the acidified process water after leaching and P_{HC} is the amount of phosphorus (mg) in hydrochar before acid leaching.

Ash content (wt % on dry basis) were measured by incineration in a muffle furnace.

Table 2.16 Experimental plan of 40 runs carried out using demi water.

Run	pH	Time (min)	S/L (wt %)	Type of acid
1	2.25	135	12.5	H_2SO_4
2	1	240	5	HNO_3
3	3.5	240	5	HNO_3
4	2.25	240	12.5	HNO_3
5	2.25	135	5	HNO_3
6	2.25	30	12.5	HNO_3
7	3.5	240	20	HNO_3
8	2.25	135	12.5	HNO_3
9	2.25	30	12.5	H_2SO_4
10	1	135	12.5	H_2SO_4
11	2.25	135	12.5	H_2SO_4
12	2.25	135	20	H_2SO_4
13	3.5	240	5	H_2SO_4
14	2.25	135	12.5	H_2SO_4
15	3.5	30	5	HNO_3
16	2.25	135	12.5	H_2SO_4
17	1	30	5	HNO_3
18	1	30	5	H_2SO_4
19	2.25	240	12.5	H_2SO_4
20	1	30	20	H_2SO_4

21	2.25	135	12.5	H_2SO_4
22	3.5	30	5	H_2SO_4
23	2.25	135	20	HNO_3
24	1	240	5	H_2SO_4
25	3.5	30	20	H_2SO_4
26	1	240	20	HNO_3
27	3.5	135	12.5	H_2SO_4
28	1	240	20	H_2SO_4
29	2.25	135	12.5	HNO_3
30	2.25	135	12.5	HNO_3
31	2.25	135	12.5	HNO_3
32	2.25	135	12.5	HNO_3
33	2.25	135	5	H_2SO_4
34	1	135	12.5	HNO_3
35	2.25	135	12.5	HNO_3
36	3.5	135	12.5	HNO_3
37	2.25	135	12.5	H_2SO_4
38	3.5	30	20	HNO_3
39	3.5	240	20	H_2SO_4
40	1	30	20	HNO_3

2.6.2 Pre-washing

With the aim of simulating the washing of HC after the separation by filter press, the solid was washed with demi water prior leaching tests. The pre-washing has the goal to remove residues of PW retained into HC. It was carried out with demi water in a 3:1 ratio respect to the initial weight of solid for three times. Dried HC (granulometry < 212 μm) was mixed with demi water in a beaker in a 3:1 ratio. After a homogeneous mixing, the solid was separated through a filter, and then two more washing were performed. Lastly, the solid was dried at 105 °C, collected and stored at 4 °C until further use.

2.7 Results of tests with demi water

In the following tables (**Tab. 2.17 and 2.18**) are reported the data obtained by experimental trials. P content in HC resulted equal to 22 800 mg $kg^{-1}_{dryHC.}$

Table 2.17 Responses of DoE with demi water.

Run	P yield (wt %)	Ash content (wt %)
1	25.65	26.32

2	77.66	12.55
3	9.65	20.74
4	19.08	18.83
5	21.91	18.75
6	20.13	18.42
7	4.08	21.82
8	19.98	18.69
9	25.36	26.47
10	68.19	26.53
11	24.23	25.77
12	20.81	26.73
13	13.65	20.41
14	24.40	26.07
15	10.01	20.63
16	24.50	26.24
17	63.25	13.05
18	64.54	23.32
19	25.47	25.61
20	63.40	26.7
21	25.32	26.28
22	13.72	20.07
23	13.57	19.22
24	73.27	23.53
25	6.47	26.51
26	60.17	13.38
27	8.50	25.63
28	66.20	26.34
29	20.50	18.6
30	19.59	18.51
31	22.84	18
32	23.67	17.71
33	27.31	24
34	62.73	13.11
35	20.81	18.5
36	4.95	21.52
37	23.5	26.09
38	4.39	21.86
39	9.00	26.8
40	60.13	13.51

Data about experiments are reported in detail **Tab. 2.18**. About 50 g of demi water were added in each test, with a pH equal to 5.52 (average of 40 values).

Table 2.18 Experimental data on DoE carried out with demi water and both sulfuric and nitric acid.

Run	HC weight (g)	Volume of acid (mL)	pH slurry prior acidification	pH slurry post acidification	pH slurry post leaching	pH leachate	Final leached solution (g)	Final HC weight (g)	TP of PW (mg L^{-1})
1	7.15	0.4	6.58	2.15	3.33	3.32	26.7725	7.0541	827.5
2	2.64	0.8	6.63	1.02	1.15	1.24	41.1213	2.1185	917.5
3	2.63	0.26	6.65	3.54	4.36	4.32	38.2052	2.3418	114.75
4	7.15	0.93	6.53	2.32	3.37	3.33	34.9223	6.3824	610.0
5	2.65	0.35	6.64	2.33	3.44	3.44	41.1118	2.3549	262.5
6	7.15	0.96	6.37	2.32	2.81	2.87	38.3462	6.3166	642.5
7	12.5	1.05	6.31	3.57	4.13	4.19	29.9014	11.4945	227.5
8	7.16	1.01	6.42	2.19	3.06	3	36.4505	6.2854	637.5
9	7.16	0.38	6.4	2.23	2.89	2.95	26.8813	7.0318	820.0
10	7.14	0.83	6.3	1.07	1.29	1.32	24.5466	6.9759	2182.5
11	7.14	0.4	6.3	2.29	3.38	3.35	28.3303	7.0172	780.0
12	12.51	0.68	6.19	2.26	3.35	3.35	22.7699	12.4301	1167.5
13	2.65	0.13	6.52	3.41	4.35	4.4	39.0789	2.3848	164.5
14	7.17	0.41	6.37	2.24	3.30	3.29	27.8284	7.0771	790.0
15	2.65	0.28	6.69	3.41	3.92	3.83	42.8106	2.3992	120.25
16	7.16	0.41	6.33	2.28	3.36	3.41	26.2575	7.0665	792.5
17	2.66	0.8	6.53	1.02	1.15	1.15	43.0956	2.1729	755.0
18	2.66	0.6	6.55	1.03	1.09	1.02	40.6872	2.5077	772.5
19	7.15	0.42	6.43	2.25	3.51	3.56	24.8992	7.0358	820.0
20	12.51	1.29	6.23	1.07	1.34	1.33	21.7502	12.2442	3525
21	7.15	0.42	6.35	2.27	3.35	3.35	27.4101	7.0717	817.5
22	2.65	0.11	6.63	3.4	3.89	3.9	41.0266	2.3957	165.4
23	12.53	1.62	6.27	2.3	3.07	3.04	31.8017	11.1132	750.0

24	2.65	0.6	6.71	1	1.06	1.13	35.4214	2.471	872.5
25	12.5	0.5	6.3	3.53	4.13	4.2	28.7164	12.3866	365.0
26	12.53	2.65	6.21	1.09	1.60	1.72	32.8185	10.2547	3250.0
27	7.16	0.3	6.4	3.51	4.42	4.4	32.3574	6.9705	275.0
28	12.5	1.3	6.11	1.03	1.32	1.37	25.6023	12.3756	3675.0
29	7.15	0.95	6.33	2.28	3.06	3.12	38.0862	6.3485	655.0
30	7.14	0.98	6.37	2.31	3.09	3.09	37.2912	6.3201	625.0
31	7.15	1.03	6.4	2.2	2.94	2.98	37.7793	6.2924	727.5
32	7.17	1.05	6.34	2.15	2.85	2.89	37.5718	6.2994	755.0
33	2.66	0.17	6.64	2.26	3.34	3.48	37.8215	2.5318	330.0
34	7.16	1.68	6.31	1.04	1.42	1.41	38.8064	5.8792	1980.0
35	7.14	1	6.41	2.3	3.00	3.07	37.2898	6.268	662.5
36	7.15	0.61	6.44	3.58	4.21	4.21	37.1092	6.5322	159.5
37	7.15	0.4	6.44	2.25	3.43	3.42	28.0945	7.0585	760.0
38	12.51	1.03	6.26	3.57	3.99	3.95	33.5453	11.5623	244.0
39	12.52	0.5	6.29	3.54	4.37	4.37	26.1429	12.3473	507.5
40	12.5	2.72	6.29	1.06	1.38	1.49	33.1713	10.3254	3250

P yield was firstly analyzed clustering the results according to the S/L ratio and the type of acid (**Fig. 2.21**).

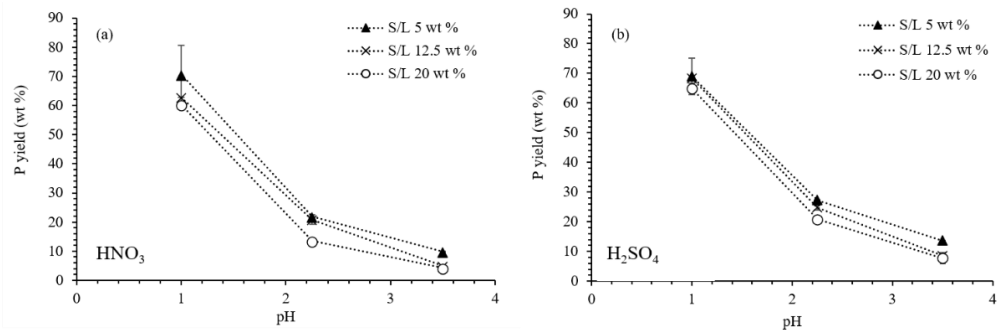

Figure 2.21 P yield (wt %) as a function of pH for runs with the same S/L ratio with demi water and nitric acid (a), and sulfuric acid (b).

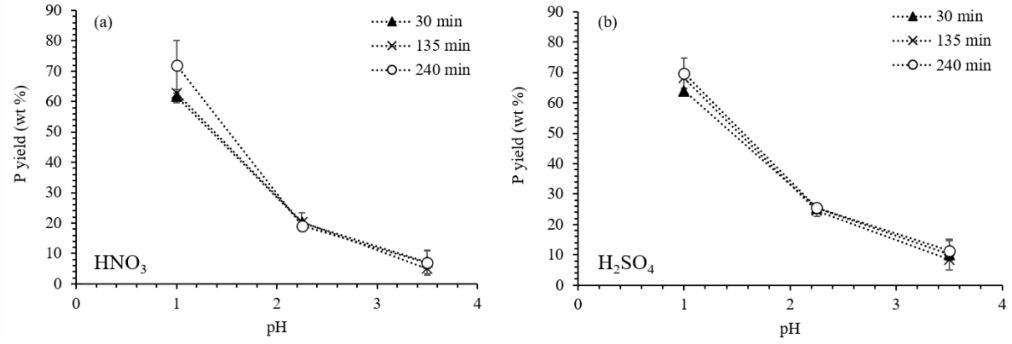

Figure 2.22 P yield (wt %) as a function of pH for runs with the same leaching time with demi water and nitric acid (a), and sulfuric acid (b).

As can be observed in **Fig. 2.21**, P yield increase with the pH reduction, while it decreased with the increase of the S/L ratio. However, a small influence of S/L ratio was observed among tests. It might be related to the low concentration of dissolved substances in solution, which promoted a high concentration gradient during leaching. P yield showed similar patterns for both acids, resulting slightly higher in case of sulfuric acid. Time proved to have a small impact on P yield response for both acids, even though the highest P yield was observed at the longest leaching time. HC after leaching with nitric acid showed a lower content of ash in comparison to the initial one (24.59 wt %). Conversely, it was characterized by a higher ash content than HC prior leaching

in case of sulfuric acid, confirming that calcium sulfate precipitation might occur. As a rule, ash content decreased with pH reduction, with a minimum value when S/L was equal to 5. Indeed, diluted systems allows a higher reduction of ash content, since the liquid phase promotes the solubilization of inorganic compounds.

2.7.1 Characterization of leachates with demi water

Concentrations of metals and other elements of acidified solutions are reported in **Tab. 19.** In the following table, a comparison between two acidified PW obtained at the same process conditions (pH = 1, S/L ratio = 5 wt %, time = 240 minutes, and H_2SO_4 as acid) but with different solvent (demi water in one case and PW in the other one) is reported.

Table 2.19 - Chemical characterization of leachates derived from Run 19 (PW and sulfuric acid, see **Tab. 2.12**) and Run 24 (demi water and sulfuric acid).

	Run 19 (PW - H_2SO_4) [2c]	**Run 24 (Demi water - H_2SO_4)** [2c]
pH	1.16	1.13
P yield (% wt)	74.43	73.27
P (mg L^{-1})	1080	790
COD (mg L^{-1})	56100	3640
Al (mg L^{-1})	170	185
As (mg L^{-1})	0.276	0.079
Cd (mg L^{-1})	0.024	0.0372
Cr (mg L^{-1})	0.43	0.173
Fe (mg L^{-1})	241	200
Mn (mg L^{-1})	7.90	7.40
Hg (mg L^{-1})	< 0.00075	< 0.00075
Ni (mg L^{-1})	0.60	0.188
Pb (mg L^{-1})	0.226	0.207
Cu (mg L^{-1})	8.2	11.3
Zn (mg L^{-1})	36.5	53
Ca (mg L^{-1})	392	570

Mg (mg L^{-1})	460	181
K (mg L^{-1})	980	47
Na (mg L^{-1})	383	11.3

[2c] Standard deviation of n = 3 measure is not available.

As can be immediately noted, the COD concentration was pretty different between the two samples. Indeed, the PW itself contained a relevant quantity of organic substances, which significantly contributed to the COD concentration. As concern the concentration of heavy metals, no relevant differences were noted between the two runs. Particularly, Ni concentration resulted three times higher with PW than with demi water. Alkaline and alkaline earth metals (e.g., Na, K, and Mg) in acidified demi water resulted in lower concentrations than PW, since during HTC these elements are preferably distributed into the liquid phase.

2.7.2 Design of Experiment results with demi water

2.7.2.1 P yield

The ANOVA analysis was carried out on P yield output and results are reported in **Tab. 2.20.**

Table 2.20 Analysis of variance and determination coefficients for P yield response (demi water – HNO_3/H_2SO_4 acid).

	Sum of Squares	df	Mean Square	F-value	p-value	
Model	19207,24	9	2134,14	611,17	<0.0001	significant
A-pH	16538,40	1	16538,40	4736,26	<0.0001	
B-Tempo	36,01	1	36,01	10,31	0,0031	
C-Rapporto S/L	222,78	1	222,78	63,80	<0.0001	
D-Tipo di acido	138,45	1	138,45	39,65	<0.0001	
AB	36,59	1	36,59	10,48	0,0029	
AC	2,06	1	2,06	0,5902	0,4484	
BC	19,45	1	19,45	5,57	0,0250	
A^2	2180,56	1	2180,56	624,47	<0.0001	
ABC	32,94	1	32,94	9,43	0,0045	
Residual	104,76	30	3,49			
Lack of Fit	88,24	20	4,41	2,67	0,0563	not significant
Pure Error	16,51	10	1,65			
Cor Total	19312,00	39				

Model statistics	
R^2	0,9946
Adjusted R^2	0,9929
Predicted R^2	0,9877

From ANOVA analysis resulted that the experimental data were well fitted by a quadratic model with the addition of semi-cubic terms. This model was significant (p-value < 0.05), whereas the lack of fit (i.e., the lack of adaptation of the model) was not significant (p-value > 0.1). Additionally, the determination coefficient (R^2) confirmed the prediction ability of the model. Notably, the D-factor (i.e., Type of acid) did not show significant interaction terms. Thus, the models elaborated for the two acids will be shown with the same surface response, but translated on vertical axis. In **equation 2.9** is reported the equation of the model in the coded form:

$$\text{P yield (wt \%)} = 22.43 - 28.76\,A + 1.34\,B - 3.34\,C + 1.86D - 1.51AB + 0.3589\,AC - 1.10\,BC + 14.77\,A^2 + 1.43\,ABC \quad (2.9)$$

Where A, B, C represent the input variables, i.e., pH, time, and S/L ratio, respectively.

As can be observed in **Fig. 2.23,** predicted values of responses calculated by the model and experimental values were severely distributed on the line, pointing out that the model is moderately predictive.

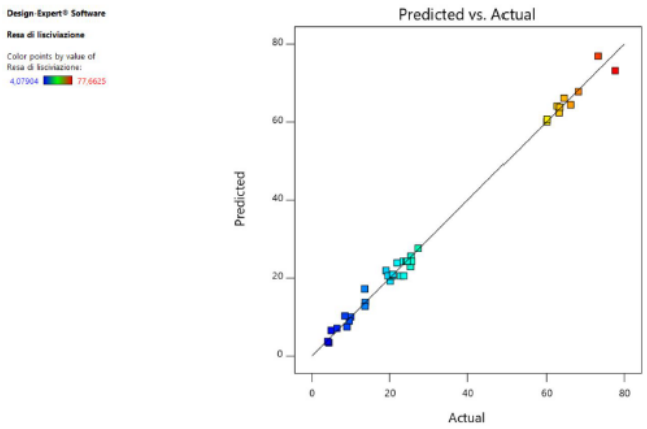

Figure 2.23 Comparison between predicted and actual values for P yield response for demi water and HNO_3 and H_2SO_4.

Graphs of 3-D surfaces describing P yield responses with both nitric and sulfuric acids are reported below (**Fig. 2.24**):

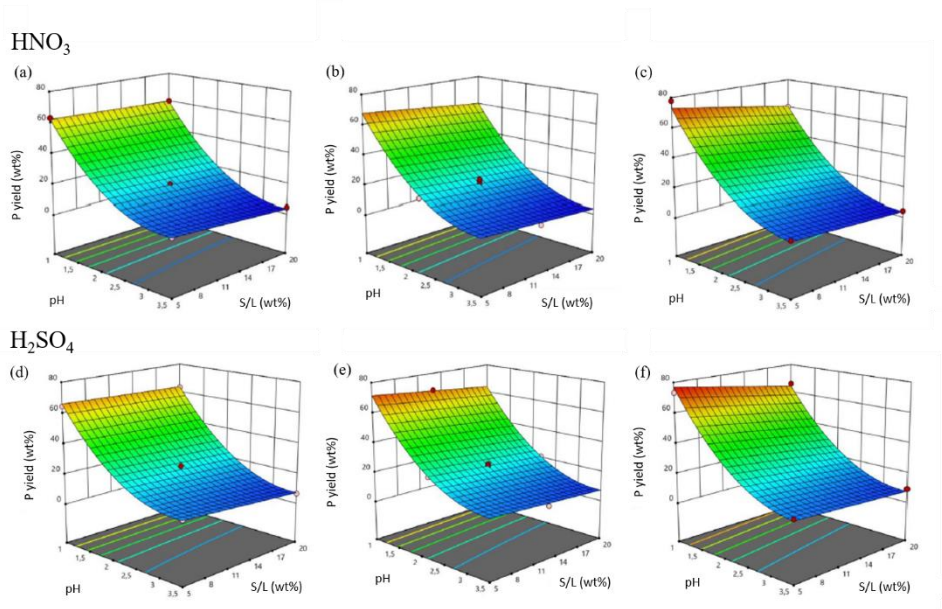

Figure 2.24 3-D graphs for P yield response for B-Time equal of 30, 135, and 240 minutes (a), (b), and (c), respectively, in case of demi water - HNO3 acid and (d), (e), and (f), respectively, in case of demi water - H_2SO_4 acid (red points represents the design points above the predicted values, and pink points are the design points below the predicted values).

As can be observed in **Fig. 2.24**, the type of acid did not influence the shape of surfaces, but it determined only their absolute values. In case of sulfuric acid, the P yield resulted higher of 3 % than those obtained with nitric. Further, as was previously reported, P yield increased with the reduction of pH, reaching its maximum value for a pH equal to 1 and a S/L ratio of 5 wt %.

2.7.2.2 Ash content

The ANOVA analysis was carried out on ash content output and results are reported in **Tab. 2.21.**

Table 2.21 Analysis of variance and determination coefficients for ash content response (demi water – HNO_3/H_2SO_4 acid).

	Sum of Squares	df	Mean Square	F-value	p-value	
Model	798,82	11	72,62	389,54	<0.0001	significant
A-pH	57,73	1	57,73	309,67	<0.0001	
C-Rapporto S/L	33,32	1	33,32	178,75	<0.0001	
D-Tipo di acido	266,30	1	266,30	1428,48	<0.0001	
AC	3,68	1	3,68	19,72	0,0001	
AD	115,07	1	115,07	617,25	<0.0001	
CD	15,65	1	15,65	83,96	<0.0001	
A^2	6,63	1	6,63	35,54	<0.0001	
C^2	1,86	1	1,86	9,99	0,0038	
ACD	1,99	1	1,99	10,66	0,0029	
A^2D	1,17	1	1,17	6,30	0,0182	
C^2D	3,77	1	3,77	20,25	0,0001	
Residual	5,22	28	0,1864			
Lack of Fit	4,25	18	0,2363	2,44	0,0756	not significant
Pure Error	0,9671	10	0,0967			
Cor Total	804,04	39				
Model statistics						
R^2	0,9935					
Adjusted R^2	0,9910					
Predicted R^2	0,9848					

From ANOVA analysis resulted that the experimental data were well fitted by a quadratic model with the addition of semi-cubic terms. This model was significant (p-value < 0.05), whereas the lack of fit (i.e., the lack of adaptation of the model) was not significant (p-value > 0.1). Additionally, the determination coefficient (R^2) confirmed the prediction ability of the model. Notably, the B-factor (i.e., Time) proved to be not significant for the response, thus it was removed for the model formulation. Conversely, interaction factors containing the D-factor (i.e., Type of acid) were present in the model, while they were not detected for P yield equation. In the following equation (**equation 2.10**) is reported is reported the model in the coded form:

$$\text{Ash content (wt \%)} = 22.35 + 1.70\,A + 1.29\,C + 3.87\,D + 0.4794\,AC - 2.40\,AD + 0.8846\,CD - 1.02\,A^2 - 0.5394\,C^2 + 0.3525\,ACD + 0.4283\,A^2D - 0.7680\,C^2D \quad (2.10)$$

Where A, C, and D represent the input variables, i.e., pH, S/L ratio, and type of acid, respectively.

As can be observed in **Fig. 2.25,** predicted values of responses calculated by the model and experimental values were severely distributed on the line, pointing out that the model is moderately predictive.

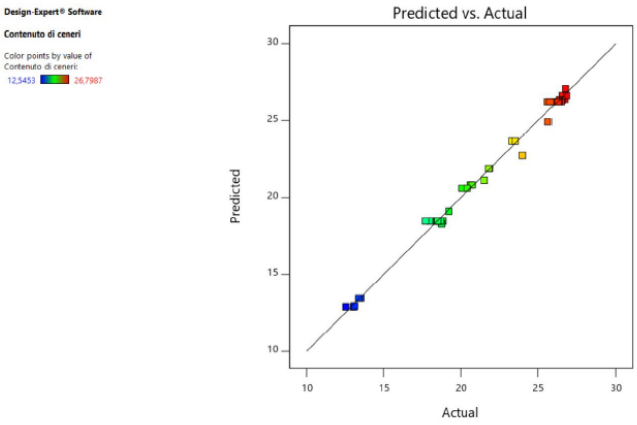

Figure 2.25 Comparison between predicted and actual values for ash content response in case of demi water and HNO_3/H_2SO_4.

3-D surfaces reporting the ash content response with both nitric and sulfuric acids are reported in **Fig. 2.26**.

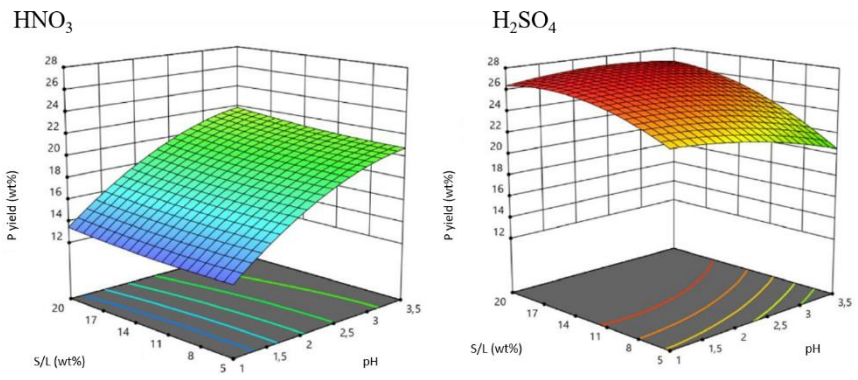

Figure 2.26 3-D graphs for ash content response in case of demi water - HNO_3/H_2SO_4 acid.

As emerged in **Fig. 2.26**, the ash content on the solid HC after leaching with nitric acid decreased with the reduction of pH, which is the factor that mainly influenced this response. Further, it also decreased with the reduction of the S/L ratio.

2.7.2.3 Optimization

Also in this case, a multi-objective optimization of the selected responses was performed. It was carried out in the perspective of defining the optimal conditions (pH, time, S/L ratio, and type of acid) to maximize the P yield and to minimize the ash content. Results of the optimization are reported in **Fig. 2.27**:

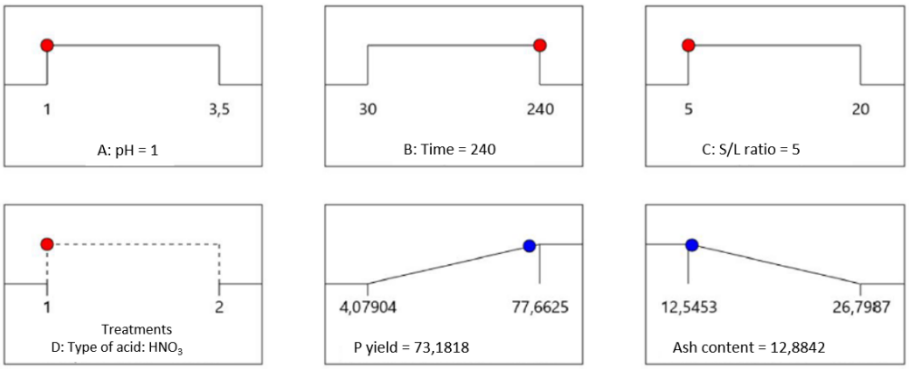

Figure 2.27 Multi-objective optimization for demi water and HNO_3/H_2SO_4 acid.

The optimization pointed out the optimal condition (pH equal to 1, leaching time of 240 minutes, and a S/L ratio of 5 wt %). The optimal acid resulted HNO_3, since it was the only one that promoted an ash content reduction.

2.7.3 Mass loss

One of the main effects of acid leaching was the reduction of ash on HC. At the same time, the dry mass of HC resulting after leaching decreased with respect to the initial one. These two variations were not coincident, since an organic component was loss during the experiments, going from the solid to the liquid phase. For each test, the mass of dry HC was weighted before

and after leaching, and the mass loss was calculated according to the following equation (**equation 2.11**):

$$\text{Mass loss (wt \%)} = \frac{\text{Mass}_{\text{HC initial}} - \text{Mass}_{\text{HC final}}}{\text{Mass}_{\text{HC initial}}} \quad (2.11)$$

Where $\text{Mass}_{\text{HC initial}}$ and $\text{Mass}_{\text{HC final}}$ are the mass of dry HC before and after leaching test, respectively. A mass loss up ~ 20 % was observed (**Fig. 2.28**). The reduction of mass increased with the pH, while S/L ratio seemed to not have a relevant influence.

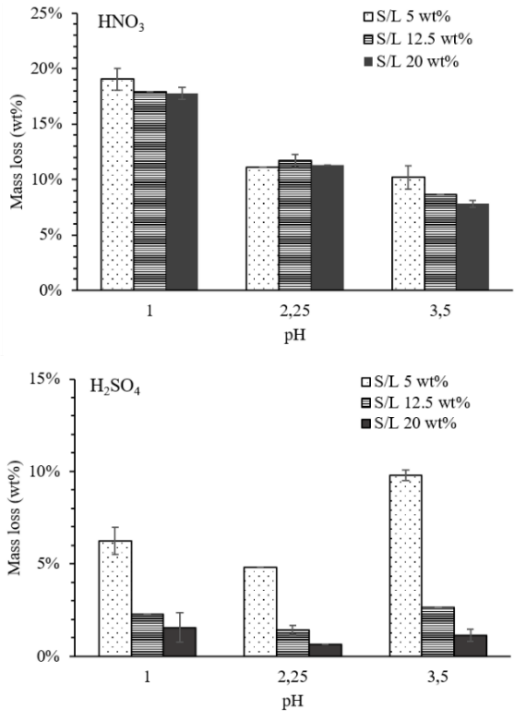

Figure 2.28 Mass loss (wt %) of HC due to the acid leaching with nitric and sulfuric acid.

In case of nitric acid, the mass loss increases with the reduction of pH, while the differences related to the S/L ratio were not appreciable. This trend was confirmed by the pattern of the ash content. A different behaviour was observed in case of sulfuric acid. Indeed, the S/L ratio resulted the most significant factor, with its decrease the mass loss increased. Indeed, at high S/L ratio, the amount of acid required to reach a determined pH increased, promoting the precipitation of calcium sulfate, which reduced significantly the mass loss. Further, when pH was equal to 3.5, a

higher mass loss was observed, since a limited precipitation of calcium sulfate occurred (the amount of acid added was the smallest).

2.7.4 Acid consumptions

Comparing the quantity of acids required by leaching tests with both PW and demi water, it was clear that tests with PW required an amount of acid generally higher than trials carried out with demi water (~ 2 times). It might find explanation in the fact that part of the acid was consumed by organic and inorganic substances contained into PW, subsequently requiring higher amounts of acid. Further, the average pH of PW was equal to 7, while that of demi water was generally lower, around 5.5. However, the acid consumption depends also by the S/L ratio, since the acidification occurred during slurry mixing. A higher S/L ratio required a higher volume of acid, since some reactions started immediately. In the following figure, the acid consumption is reported in function of pH (average of values at different S/L ratio).

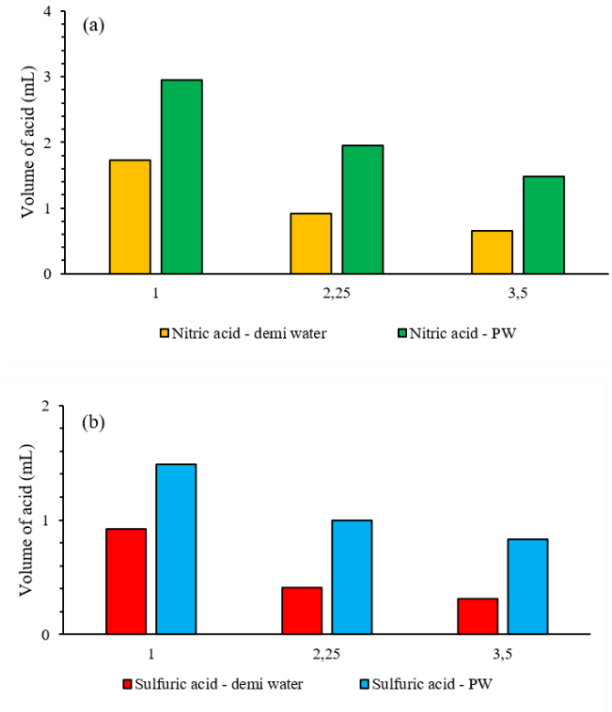

Figure 2.29 Comparison of acid consumption in case of PW and demi water with nitric acid (a), and sulfuric one (b).

2.8 Conclusions

This study demonstrated that acid leaching was an efficient method to recover phosphorous from HC. Among the three investigated key factors (pH, leaching time, and S/L ratio), the pH proved to mostly influenced the P yield response. A low S/L ratio seemed to promote the P leaching, while time resulted to be not relevant. A temperature of 20 °C was identified as the optimal to perform these tests. Interestingly, the use of H_2SO_4 determined an increase of ash content on HC after acid leaching, which could be related to calcium sulfate precipitation. Differently, the ash content decreased using HNO_3, suggesting that the application of this acid is preferable, with the perspective of valorizing HC as combustible. During experiments with demi water, it resulted that a slightly higher (~ 3 %) P yield response could be achieved using sulfuric acid instead on nitric one. Nevertheless, the multi-objective optimization on trials performed with demi water pointed out that a P yield of 73 wt % and an ash content lower than 13 wt % can be obtained at pH equal to 1, with a leaching time of 240 minutes, and a S/L ratio of 5 wt %. Also, in case of using

nitric/sulfuric acid and PW, a pH equal to 1 was identified as the optimal. Additionally, demi water reduced the acid required by the process in comparison with PW. However, it is worth to point out that during acid leaching also other elements were solubilized besides P. Particularly, Fe, Al, and Ca showed a behaviour similar to that of P, since they are bonded together into the solid matrix. A special attention must be focused on Pb, Cu, Zn, and Cd which are solubilized during acid leaching. These compounds could affect the possible application of leachate in agriculture. Hence, a detailed chemical characterization of this fraction must be carried out in order to evaluate its possible application as fertilizer.

2.9 References - Chapter 2

1. Cornel, P., Schaum, C.: Phosphorus recovery from wastewater : needs , technologies and costs. 1069–1076 (2009). https://doi.org/10.2166/wst.2009.045
2. European Commission: Communication from the Commission to the European Parliament, the Council, the Eurpean Economic and Social Committee and the Committee of the Regions on the 2017 list of Critical Raw Materials for the EU. Off. J. Eur. Union. COM(2017), 8 (2017)
3. Cieslik, B., Konieczka, P.: A review of phosphorus recovery methods at various steps of wastewater treatment and sewage sludge management . The concept of " no solid waste generation " and analytical methods. 142, 1728–1740 (2017). https://doi.org/10.1016/j.jclepro.2016.11.116
4. Zhou, K., Barjenbruch, M., Kabbe, C., Inial, G., Remy, C.: Phosphorus recovery from municipal and fertilizer wastewater: China's potential and perspective. J. Environ. Sci. (China). 52, 151–159 (2017). https://doi.org/10.1016/j.jes.2016.04.010
5. Dissanayake, C.B., Chandrajith, R.: Phosphate Mineral Fertilizers, trace metals and human health. J. Natl. Sci. Found. Sri Lanka. 37, 153–165 (2009). https://doi.org/10.4038/jnsfsr.v37i3.1219
6. Luyckx, L., Geerts, S., Van Caneghem, J.: Closing the phosphorus cycle: Multi-criteria techno-economic optimization of phosphorus extraction from wastewater treatment sludge ash. Sci. Total Environ. 713, 135543 (2020). https://doi.org/10.1016/j.scitotenv.2019.135543
7. Shiba, N.C., Ntuli, F.: Extraction and precipitation of phosphorus from sewage sludge. Waste Manag. 60, 191–200 (2017). https://doi.org/10.1016/j.wasman.2016.07.031
8. Fang, L., Li, J. shan, Guo, M.Z., Cheeseman, C.R., Tsang, D.C.W., Donatello, S., Poon, C.S.: Phosphorus recovery and leaching of trace elements from incinerated sewage sludge ash (ISSA). Chemosphere. 193, 278–287 (2018). https://doi.org/10.1016/j.chemosphere.2017.11.023

9. Yuan, Z., Pratt, S., Batstone, D.J.: Phosphorus recovery from wastewater through microbial processes. Curr. Opin. Biotechnol. 23, 878–883 (2012). https://doi.org/10.1016/j.copbio.2012.08.001

10. Morse, G.K., Brett, S.W., Guy, J.A., Lester, J.N.: Review: Phosphorus removal and recovery technologies. Sci. Total Environ. 212, 69–81 (1998). https://doi.org/10.1016/S0048-9697(97)00332-X

11. Donatello, S., Cheeseman, C.R.: Recycling and recovery routes for incinerated sewage sludge ash (ISSA): A review. Waste Manag. 33, 2328–2340 (2013). https://doi.org/10.1016/j.wasman.2013.05.024

12. Libra, A.J., Kammann, C., Funke, A., Berge, N.D., Neubauer, Y., Titirici, M.-M., Fuhner, C., Bens, O., Kern, J., Emmerich, K.-H.: Hydrothermal carbonization of biomass residuals : A comparative review of the chemistry , processes and appolications of wet and dry pyrolysis. 2, 89–124 (2011). https://doi.org/10.4155/bfs.10.81

13. Escala, M., Zumbühl, T., Koller, C., Junge, R., Krebs, R.: Hydrothermal carbonization as an energy-efficient alternative to established drying technologies for sewage sludge: A feasibility study on a laboratory scale. Energy and Fuels. 27, 454–460 (2013). https://doi.org/10.1021/ef3015266

14. Hämäläinen, A., Kokko, M., Kinnunen, V., Hilli, T., Rintala, J.: Hydrothermal carbonisation of mechanically dewatered digested sewage sludge—Energy and nutrient recovery in centralised biogas plant. Water Res. 201, (2021). https://doi.org/10.1016/j.watres.2021.117284

15. Marin-Batista, J.D., Mohedano, A.F., Rodríguez, J.J., De la Rubia, M.A.: Energy and phosphorous recovery through hydrothermal carbonization of digested sewage sludge. Waste Manag. 105, 566–574 (2020). https://doi.org/10.1016/j.wasman.2020.03.004

16. Pérez, C., François, J., Stina, B., Tomas, J., Jerker, G.: Acid - Induced Phosphorus Release from Hydrothermally Carbonized Sewage Sludge. Waste and Biomass Valorization. (2021). https://doi.org/10.1007/s12649-021-01463-5

17. Volpe, M., Fiori, L., Merzari, F., Messineo, A., Andreottola, G.: Hydrothermal carbonization as an efficient tool for sewage sludge valorization and phosphorous recovery. Chem. Eng. Trans. 80, 199–204 (2020). https://doi.org/10.3303/CET2080034

18. Oliver-Tomas, B., Hitzl, M., Owsianiak, M., Renz, M.: Evaluation of hydrothermal carbonization in urban mining for the recovery of phosphorus from the organic fraction of municipal solid waste. Resour. Conserv. Recycl. 147, 111–118 (2019). https://doi.org/10.1016/j.resconrec.2019.04.023

19. Tasca, A.L., Mannarino, G., Gori, R., Vitolo, S., Puccini, M.: Phosphorus recovery from sewage sludge hydrochar: process optimization by response surface methodology. Water Sci. Technol. (2020). https://doi.org/10.2166/wst.2020.485

20. Tasca, A.L., Stefanelli, E., Raspolli Galletti, A.M., Gori, R., Mannarino, G., Vitolo, S., Puccini, M.: Hydrothermal Carbonization of Sewage Sludge: Analysis of Process Severity and Solid Content. Chem. Eng. Technol. 43, 2382–2392 (2020).

https://doi.org/10.1002/ceat.202000095

21. IRSA, CNR, I. di ricerca sulle acque, APAT: Method 4110 A2 - Fosforo totale, (2003)

22. CNR IRSA: 4020 Determinazione di anioni (fluoruro, cloruro, nitrito, bromuro, nitrato, fosfato e solfato) mediante cromatografia ionica. APAT Man, 29. (2003)

23. United States Environmental Protection Agency: EPA Method 350.1 - Determination of ammonia nitrogen by semi-automated colorimetry. (1993)

24. ISO: Water quality — Determination of the chemical oxygen demand index ISO 15705. (2002)

25. United States Environmental Protection Agency: Method 3010A - Acid Digestion of Aqueous Samples and Extracts for Total Metals for Analysis by FLAA or ICP Spectroscopy. (1992)

26. United States Environmental Protection Agency: EPA Method 6020B - Inductively Coupled Plasma-Mass Spectrometry. Washington, (2014)

27. IRSA, CNR, I. di ricerca sulle acque: Quaderno n. 64 - METODI ANALITICI PER I FANGHI, (1985)

28. Pardo, P., Lòpez-Sànchez, J.F., Rauret, G.: Relationships between phosphorus fractionation and major components in sediments using the SMT harmonised extraction procedure. Anal Bioanal Chem. 376, 248–254 (2003). https://doi.org/10.1007/s00216-003-1897-y

29. Monea, M.C., Lohr, D.K., Meyer, C., Preyl, V., Xiao, J., Steinmetz, H., Schonberger, H., Drenkova-Tuhtan, A.: Comparing the leaching behavior of phosphorus , aluminum and iron from post-precipitated tertiary sludge and anaerobically digested sewage sludge aiming at phosphorus recovery. J. Clean. Prod. 247, (2020). https://doi.org/10.1016/j.jclepro.2019.119129

30. Shi, Y., Luo, G., Rao, Y., Chen, H., Zhang, S.: Hydrothermal conversion of dewatered sewage sludge : Focusing on the transformation mechanism and recovery of phosphorus. Chemosphere. 228, 619–628 (2019). https://doi.org/10.1016/j.chemosphere.2019.04.109

31. Huang, R., Tang, Y.: Speciation Dynamics of Phosphorus during (Hydro)Thermal Treatments of Sewage Sludge. Environ. Sci. Technol. 49, 14466–14474 (2015). https://doi.org/10.1021/acs.est.5b04140

32. Liu, H., Hu, G., Basar, I.A., Li, J., Lyczko, N., Nzihou, A., Eskicioglu, C.: Phosphorus recovery from municipal sludge-derived ash and hydrochar through wet-chemical technology: A review towards sustainable waste management. Chem. Eng. J. 417, 129300 (2021). https://doi.org/10.1016/j.cej.2021.129300

Chapter 3

Characterization of hydrothermal carbonization process water for optimizing the recovery of energy and valuable materials from sewage sludge

Abstract

Process water (PW) derived from hydrothermal carbonization (HTC) of sewage sludge (SS) is generally overlooked as a potential source of energy and valuable materials. This study was aimed to investigate three possible applications of PW: as fertilizer on soils, as a substrate in anaerobic digestion to recover energy from biogas, and as an effluent with suitable characteristics to be treated into a Water Resources Recovery Facility (WRRF). Thus, six samples of digested SS produced by six different WRRFs (located in Tuscany, Italy) were selected. PW was obtained from HTC performed at 220 °C, for 85 min, and with a 15 wt % of solid content. It was firstly chemically characterized in terms of nutrients (carbon, nitrogen, and phosphorus), and heavy metals (As, Cd, Cr, Cu, Hg, Mo, Pb, and Zn), and then its chemical composition was compared with specific regulation limits (e.g., Regulation (EU) 2019/1009). Thus, even though its application as fertilizer resulted critical for some parameters (e.g., Cr), it seemed a promising resource for soil application. Further, PW was studied in terms of anaerobic and aerobic biodegradability. The first one was investigated performing Biomethane Potential tests (BMP), resulting variable into the range 54 – 78 %. Further, the second one was studied by both Biochemical Oxygen Demand (BOD) and respirometric assays. From these tests emerged that the aerobic biodegradability varied in the range of 71 – 79 %, and 65 – 85 %, respectively. Thus, this study suggested that PW could be potentially used as fertilizers, as well as could be treated by anaerobic/aerobic processes.

3.1 Introduction

Sewage sludge (SS) is the main by-product of wastewater treatment; in 2010 its amount was equal to 11.5 million tons on dry basis in EU27 in 2010 [1], and it was expected to reach up 13.0 million tons in 2020 due to the improvement of wastewater collection system and growing population. Further, considering the economic aspects, sludge disposal accounted about 50 – 60 % of the total operating costs of a WRRF (Water Resources Recovery Facilities) [2].

SS is a mixture of valuable compounds (e.g., organic carbon, phosphorous and nitrogen) and hazardous materials (e.g., heavy metals, organic pollutants, and pathogens). Hence, its application in agriculture is now under increasing restrictions [3]. Further, SS treatment is currently limited also in landfill, because of the potential pollution risk for soil and water, besides the scarcity of available space [3]. In addition, the EU Directive on circular economy support the recovery of wastes, such as SS, promoting its application in agriculture while respecting the limits set on heavy metals concentration [4]. Furthermore, traditional thermal treatments, as pyrolysis and gasification, are generally applied to manage SS, but they usually require feedstock pre-treatments to reduce the moisture content. In addition, the final product needs generally a later improvement to find applications [2]. Thus, SS management is becoming worldwide an urgent issue.

Besides disposal strategies, different valorization pathways can be followed to manage SS. In particular, hydrothermal carbonization (HTC) is gaining attention as suitable technology to treat SS. HTC is a thermochemical process able to convert a biomass feedstock in three products: a carbonaceous solid matrix (hydrochar, HC), a liquid phase (process water, PW), and a negligible gaseous fraction. During this process, temperature generally ranges between 180 and 300 °C, under self-generated pressure of saturated vapor (2 – 10 MPa) [5].

HTC technology is characterized by several advantages in comparison to other processes. HC is a storage of carbon, with fuel properties that can replace the equivalent products from fossil sources. Indeed, HC can find applications as bio-combustible, as well as soil amendment and low-cost adsorbent [6]. Further, HC is a source of recoverable nutrients (P and N), while PW contains

dissolved complex organic substances, which can be recovered to produce organo-mineral fertilizers.

Thus, a deep and detailed investigation on HTC products (PW and HC) is needed. HC has been studied since the first HTC applications, as the process has been initially designed to convert organic residues in a fuel from renewable resources. Far fewer studies were dedicated to PW, which however is of extreme interest, especially in case of sewage sludge. Indeed, SS contains the correct moisture amount to be directly processed by HTC, not necessarily requiring PW recirculation into the process. Furthermore, to improve the process sustainability, valorization of PW is definitely needed. Therefore, a more in-depth characterization of this fraction is required, also based on SS characteristics, which are directly dependent on qualitative characteristics of the incoming wastewater into the WWRF and on operating conditions of the plant.

Several previous studies have already investigated the distribution of nutrient and heavy metal between solid and liquid fractions obtained processing SS with HTC [7–10], also focusing on the feasibility of using PW for land application [11]. As a rule, P is mainly retained in the solid HC in high percentage (> 65 %), N is differently distributed between HC (15 – 50 %) and PW (up to 48 %) [8, 10] and heavy metals result to be mainly retained in HC [7]. Some researchers have already investigated also the CH_4 potential production of anaerobic digestion of PW derived by HTC on sewage sludge, demonstrating that good specific methane yield can be achieved [8, 12, 13].

This study is aimed to provide a further contribution to the aforementioned investigation about HTC on sewage sludge, in particular outlining three possible PW valorization pathways. The first one is the application on soils as fertilizers, the second one is the energetic valorization through anaerobic digestion (AD), and the last one is the PW treatment into the WRRF train.

Accordingly, both products of processing raw sludges in an HTC reactor (HC and PW) were properly characterized in order to: (i) carry out C, N, P mass balance and their distribution between

HC and PW, (ii) characterize PW in view of its utilization for the production of organic-mineral liquid fertilizers (iii) assess the biodegradable fraction of COD in both aerobic and anaerobic conditions.

3.2 Materials and methods

3.2.1 Digested and dewatered sludge

Digested and dewatered sewage sludge samples were collected from six WRRFs located in the Tuscany region (Italy). Three of the six sludges investigated were anaerobically digested (An1 (a), An2 (b), An3 (c)), while the other three were aerobically stabilized (Ae1 (d), Ae2 (e), Ae3 (f)) respectively sampled from the plants a) – f) whose layout is depicted in **Fig. 3.1**. All selected WRRFs mainly treat urban wastewater, relying on activated sludge process.

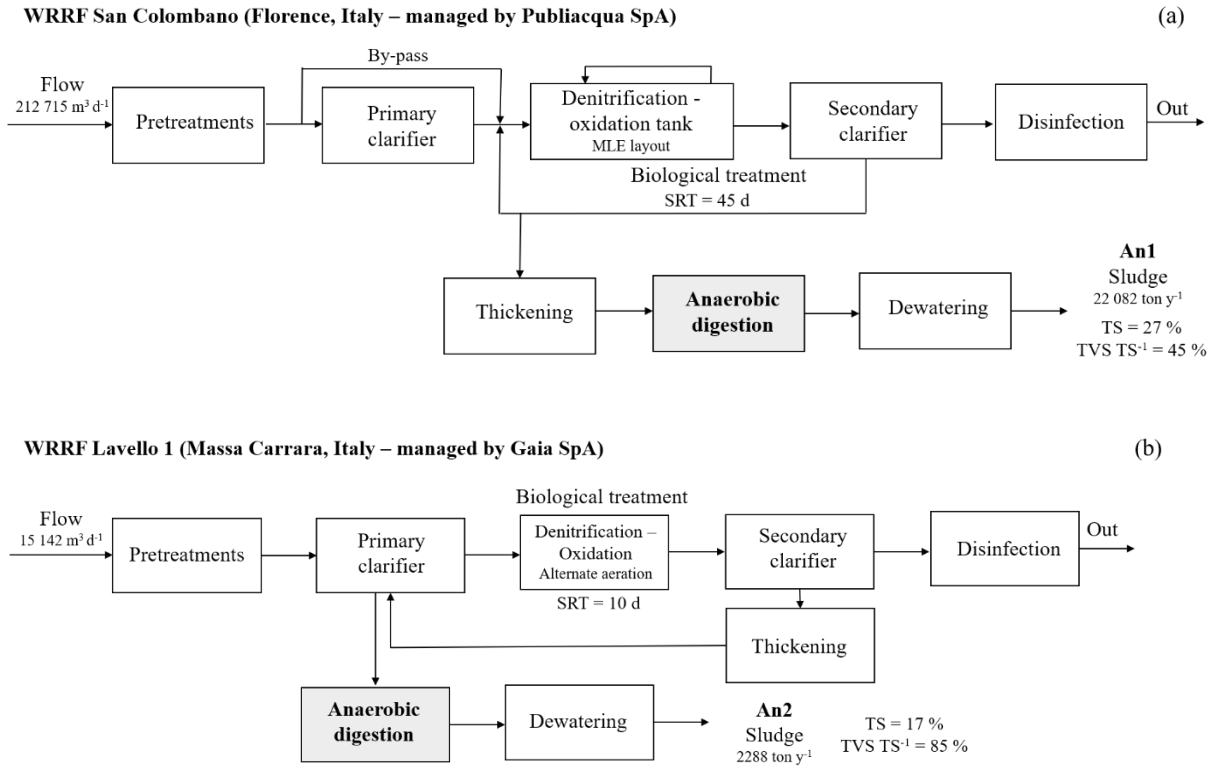

WRRF Rivellino (Livorno, Italy – managed by ASA SpA) (c)

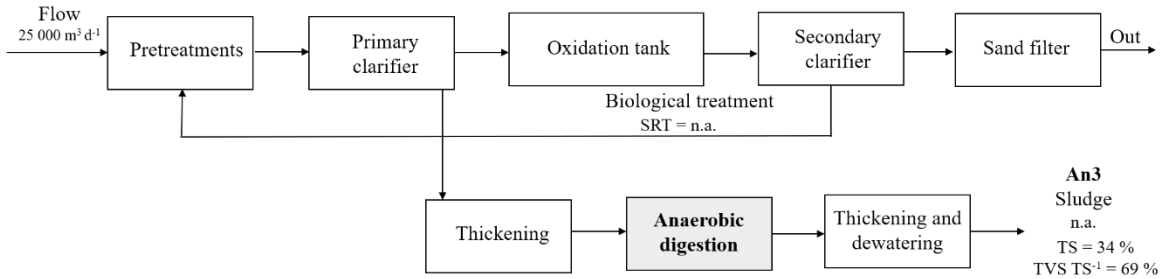

WRRF San Jacopo (Pisa, Italy – managed by Acque SpA) (d)

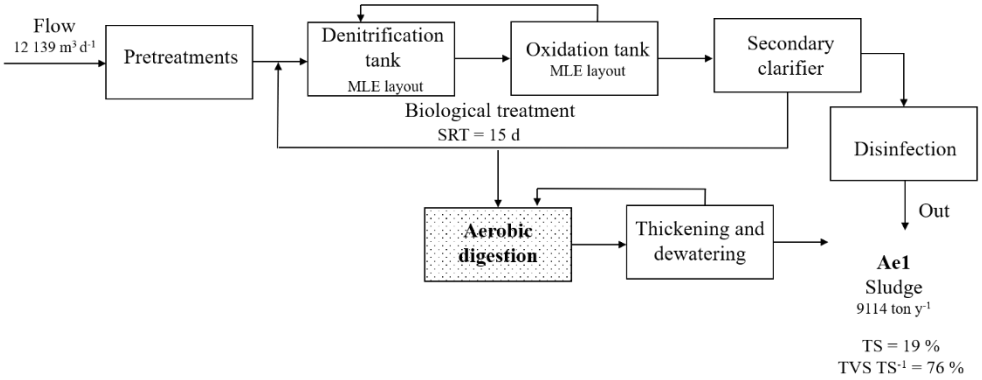

WRRF San Giovanni (Grosseto, Italy – managed by Acquedotto del Fiora SpA) (e)

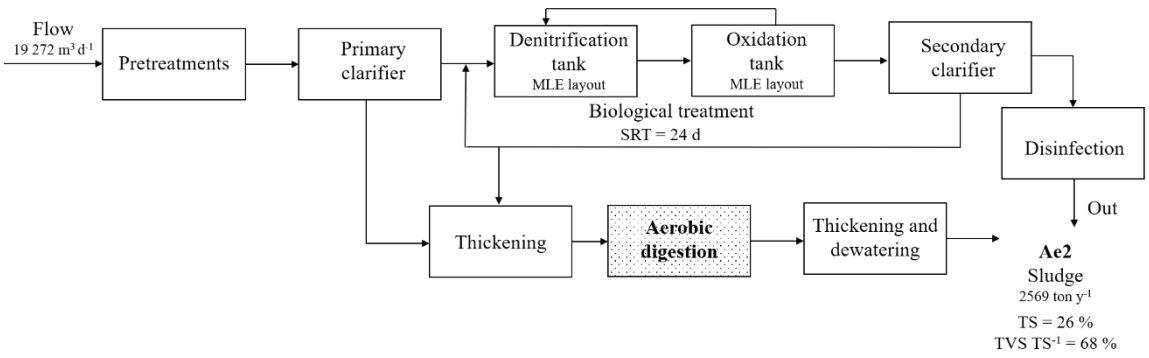

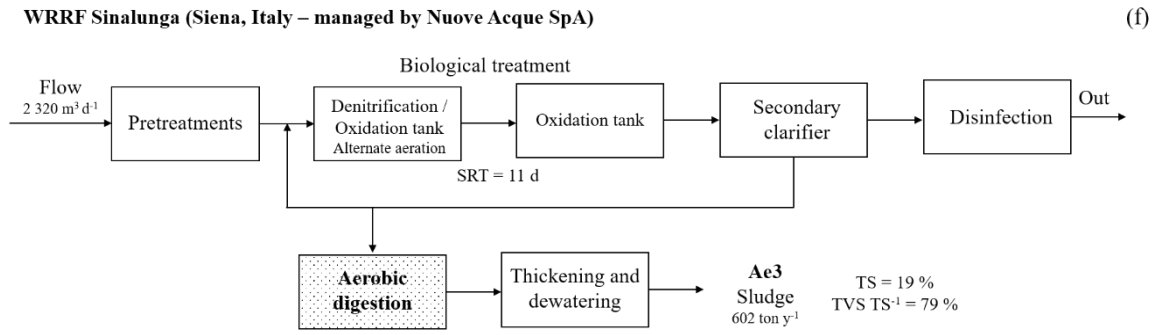

Figure 3.1 Plant schemes of studied WRRFs: (a) San Colombano; (b) Lavello 1; (c) Rivellino; (d) San Jacopo; (e) San Giovanni; (f) Sinalunga.

3.2.2 Hydrothermal carbonization

HTC was carried out in an AISI 316 stainless-steel reactor with a capacity of 300 mL, equipped with a mechanical agitator, electric heating system, thermocouple, and a pressure gauge (1-1000 psi). The reactor temperature was monitored by a manual controller PARR 4842 [14]. All sludge samples were diluted with demi-water to reach a desired total solids (TS) concentration equal to 15 wt %. HTC experimental tests were conducted at same process conditions of temperature and time for all samples, 220 °C and 85 minutes, respectively. About 200 g of SS were loaded into the vessel, and then heated up to the desired temperature, maintained, and decreased to room temperature. After treatment, slurries were vacuum filtered (Whatman n° 41) in order to separate hydrochar (HC) and process water (PW). PW was then collected and kept at 4 °C until further use, and hydrochar was dried at 105 °C until constant weight. The dried solid was then weighted and stored in sealed containers until characterization was carried out.

3.2.3 Analytical methods

TS and volatile solids (VS) of SS were determined according to the standard methods 2540B and 2540E [15]. The elemental composition (C, H, N, and S) of SS and hydrochars was determined by CHNS analyser (TruSpec Micro CHN analyzer) [14]. Total phosphorus (TP) on solid samples was determined according to the method CNR IRSA 9 (1985). Pb, Cd, Mo, Cu, Zn, and K on

liquid samples were determined according to EPA 3010A (1992) and EPA 6020B (2014). Further, PW from HTC treatment was characterized in terms of total organic carbon (TOC) by APAT CNR IRSA 5040 (2003) and of total phosphorous by APAT CNR IRSA 4110 A2 (2003). Total nitrogen (TN), ammonium ($N\text{-}NH_4^+$), and total chemical oxygen demand (COD) on liquid samples were measured using commercial analytical kits (LCK 238, LCK 303, and LCK 614 respectively) (Hach-Lange), after dilution (1: 100, 1: 200, and 1: 250) with Milli-Q water to comply the measurement range of the kits. All parameters were determined on nonfiltered solutions, except for $N\text{-}NH_4^+$ which was measured after filtration (0.1 µm in PES) (Sartorius). No interferences were observed according to product specifications.

3.2.4 C, N, P mass balance

Mass balance of N and P was developed via **equation 3.1** and **3.2**:

$$\text{HC mass}_{\text{N,P}}(\text{mg}) = \text{HC concentration}_{\text{N,P}}\left(\frac{\text{mg}}{\text{kg DM}}\right) \cdot \text{mass}_{\text{HC}}(\text{ g DM}) \cdot \frac{10^{-3}\,\text{g}}{\text{kg}} \quad (3.1)$$

$$\text{PW mass}_{\text{N,P}}(\text{mg}) = \text{PW concentration}_{\text{N,P}}\left(\frac{\text{mg}}{\text{L}}\right) \cdot \text{PW volume (L)} \quad (3.2)$$

where mass_{HC} is the mass of dried HC, and PW volume is the volume of PW obtained after vacuum filtration of slurry.

Mass balance of C was carried out according to Aragon – Briceño et al. [16]. Since gas was not directly measured, the amount of C in gas phase was estimated by difference.

3.2.5 Biodegradability in anaerobic conditions

Anaerobic biodegradability was assessed through Biomethane Potential Tests (BMPs) operated in batch conditions. All experiments were performed in 330 mL glass bottles with two lateral openings sealed by a rubber septum for biogas sampling. Bottles were equipped with a respirometric-manometric sensor (Oxitop®, WTW) on the top. The anaerobic inoculum was collected from a mesophilic full-scale anaerobic digester of San Colombano WRRF (managed by Publiacqua SpA, Florence, Italy). An inoculum-to-substrate ratio (ISR) equal to 2 on COD basis

was selected for all tests according to Villamil et al. [13]. Amounts of substrate and inoculum were chosen considering the pressure limitation of the OxiTop® system (1350 hPa absolute pressure). Neither buffer nor basal medium containing micro- and macro- nutrients were dosed to the mix. Water collected from the effluent of San Colombano plant was added in all trails to ensure a homogeneous mixing. pH (sensION$^+$ PH31, Hach) of each test was checked before starting AD experiments to be within the range 7 – 7.5. If not, it was corrected adding HCl 1 M. Tests were performed in triplicate and blanks with no substrate were run to determine the background methane production from the inoculum. At the beginning of each experiment, the empty space of the bottle was purged with N_2 for 10 minutes in order to ensure anaerobic conditions. Bottles were kept in a thermostatic incubator (WTW, TS 606/4-i) and continuously mixed on magnetic stirrers at 37 °C (± 1 °C). The time-course of pressure was recorded directly by OxiTop® system. To avoid overpressure due to the heating of air from ambient to mesophilic temperature, the pressure into bottles was exhausted after 2 hours. Experiments were then re-started, and they lasted until no significant changes were observed in pressure [17]. Biogas production was determined by manometric method [18], and its composition (CO_2, and CH_4) was regularly assessed by gas-chromatography (Varian, CP-4900 Micro GC), assuming biogas as a binary mixture of CO_2 and CH_4. CH_4 percentages in biogas were then corrected according to [19], using the **equation 3.3**:

$$\%\ CH_{4\ dry} = \%\ CH_{4\ wet}\ (1 - \frac{Pvap}{Pamb + P\ headspace}) \quad (3.3)$$

where $\%CH_{4\ dry}$ is the methane content in dry gas conditions, $\%CH_{4\ wet}$ is the analysed methane content in wet conditions, P_{vap} is the water vapor pressure at 37 °C (62.74 mbar) and P_{amb} is the ambient pressure which was set at a constant value of 1013.25 mbar (the experiment was carried out at around the sea level). Final CH_4 volumes (B_{o_exp}) are referred to standard conditions (STP) (0 °C, 1 atm).

The fraction of COD effectively converted in CH_4 during AD experiments was calculated according to **equation 3.4 and 3.5** [20]:

$$B_{o\_Th} = \left(350 \frac{\text{STP mL } CH_4}{\text{g } COD_{added}}\right) \cdot \text{g } COD_{added} \quad (3.4)$$

$$bCOD_{an}(\%) = \frac{B_{o\_Exp}}{B_{o\_Th}} \cdot 100 \quad (3.5)$$

where COD_{added} is the COD added into AD test referred only to the substrate, 350 STP mL CH_4 g COD^{-1} is the stoichiometric conversion of COD in CH_4, and B_{o_Exp} is the volume of methane (NmL CH_4) measured at the end of the BMP test.

3.2.6 Biodegradability in aerobic conditions

Biodegradability in aerobic conditions was assessed using both the ultimate biochemical oxygen demand (UBOD) and respirometric tests.

3.2.7 Biochemical Oxygen Demand (BOD) tests

UBOD of PW was determined carrying out BOD experiments at 20 days. Trials were performed in duplicate in glass bottle (1140 mL) provided by two lateral openings sealed by a rubber septum. Samples were characterized in terms of COD and then diluted (1: 200, and 1: 400) with Milli- Q water. Based on COD concentration, diluted samples were placed in bottles according to the volume directly calculated by controller (OC 110, OxiTop®, WTW). NaOH pellets were placed in bottle headspace to trap CO_2. 1 M phosphate buffer (0.5 mol K_2HPO_4 e 0.5 mol KH_2PO_4) was added in order to avoid pH deviations during experiments (Standard Methods 8.04 BOD 5210 D). Nitrapyrin (TCMP Nitrification Inhibitor for BOD, Formula 2533™, Hach) was selected to inhibit nitrification according to product features. Active sludge was drawn from oxidation tank of San Colombano WRRF (Florence, Italy) and it was added in order to inoculate a mass (calculated as g of total suspended solid (TSS)) equal to the 3 % of the sample COD. The initial pH was always included in range 7.2 – 8. Samples were aerated with air for 10 minutes to reach non-limiting

dissolved oxygen conditions, and then placed at 20 °C under continuous mixing. Output of these trials is the measurement of the BOD_{20}.

Then, UBOD was calculated using **equation 3.6** [21]**:**

$$BODt = UBOD\ (1 - e^{-kt}) \quad (3.6)$$

Where BODt is the BOD value at time t (d), UBOD is the ultimate BOD value, k is the first-order reaction rate constant (d^{-1}) and t is the time (d).

UBOD (mg O_2 L^{-1}) and k (d^{-1}) were estimated minimizing the sum of square differences between the experimental and the theoretical values. Thus, the values which best approximate the experimental values were determined. Then, UBOD modelled value of each experiment was corrected subtracting the BOD contribute due to only the biomass [22]. Finally, the biodegradable COD was calculated according to the following equation (**equation 3.7**) [21]:

$$bCOD_{\_mod} = \frac{1}{1-fp}\ UBOD \quad (3.7)$$

where $bCOD_{\_mod}$ (mg O_2 L^{-1}) represents the fraction of the biodegradable COD and f_p (-) the fraction on non-biodegradable organic matter produced from endogenous decay and here set at 0.08 [23].

The non-biodegradable COD ($nbCOD_{\_mod}$) was subsequently obtained by difference between COD of the sample and $bCOD_{\_mod}$. Considering the characteristics of PW, we assumed that all COD was soluble, neglecting the particulate fraction. Finally, at the end of the test, the soluble and non-biodegradable COD was also experimentally determined by measuring the COD on the filtered sample (0.1 μm PES filter), using an analytical kit (LCK 1414 and 614, Hach). This value ($nbCOD_{\_exp}$), net of the concentration of COD brought by nitrapirin, was then compared with $nbCOD_{\_mod}$. Lastly, the experimental biodegradable COD ($bCOD_{\_exp}$) was then calculated using the following equation (**equation 3.8**):

$$bCOD_{\_exp} = COD - nbCOD_{\_exp} \quad (3.8)$$

Where all parameters were already defined above.

3.2.8 Respirometric tests

Activated sludge samples were drawn from oxidation tanks of Calice WWRF (managed by G.I.D.A. SpA, Prato, Italy). The plant treats urban (30 %) and industrial textile (70 %) sewage wastewater and truck-transported liquid waste. Sludge samples were preliminarily aerated overnight and then transferred into a 2 L batch reactor equipped with a pH probe (Polilyte Plus PHI Arc 120, Hamilton), and a DO sensor (VisiWater DO Arc 120 FC10, Hamilton). Trials were carried out at pH-stat (7.5 – 7.9) dosing acid (HCl) or basic solution (NaOH), and at DO-stat (5 – 6 mg O_2 L^{-1}) conditions, aerating with an air diffuser and a membrane pump (NMP 830 KNDC, KNF). Allylthiourea (ATU) was also added to inhibit nitrification (15 mg ATU L^{-1}). Data (e.g., pH, DO, and temperature) were collected automatically by a software system. DO concentrations (mg O_2 L^{-1}) were recorded every 5 s, and the oxygen uptake rates (OUR) (mg O_2 L^{-1} h^{-1}) were calculated with the downward slopes of a DO curve (y-axis) on time (h) (x-axis). PW samples were added in order to maintain a ratio of 0.05 between substrate – biomass in terms of COD. Firstly, only the endogenous oxygen respiration ($OUR_{\_end}$) was observed. Then, after PWs sample addition, the oxygen consumption pointed out the exogenous respiration ($OUR_{\_es}$) due to the COD biodegradation. Finally, bCOD was calculated taking into account only the exogenous respiration, according to **equation 3.9**:

$$bCOD_{\_resp} = \frac{1}{1-Y_h} \cdot \int OUR_{\_es} \cdot \frac{V_R+V_S}{V_S} \quad (3.9)$$

where $OUR_{\_es}$ is the O_2 consumption due to the COD biodegradation, Y_h is the heterotrophic yield of the biomass (0.786), V_R is the sludge volume before sample spike, and V_S is the spiked sample. The yield factor Y_h was measured experimentally, developing a specific respirometric tests with multiple spikes of sodium acetate (data not shown).

The biodegradable COD fraction obtained from respirometric tests was calculated as:

$$\mathrm{bCOD_{ae\_resp}}(\%) = \frac{\mathrm{bCOD\_resp}}{\mathrm{TCOD}} \cdot 100 \quad (3.10)$$

3.3 Results and Discussion

3.3.1 C, N, and P distribution

Carbon content of hydrochars obtained by hydrothermal treatment of different sludges varied in a wider range (19.4 – 49.6 wt %) than those reported in literature by Marin Batista et al. [24] (30.8 – 32.6 wt %), and by Arauzo et al. [25] (25.6 – 27.9 wt %), who carried out HTC tests on an anaerobically digested sewage sludge varying operational conditions. This fact could be associated to many factors such as reactor design, process conditions, and solid loadings which affect the results [10]. However, it is important to highlight that the main reason might be due to the different feedstock itself, which is produced by selected WRRFs with different configurations both in the mainstreams and sewage sludge treatment line, capacity, and operational conditions. Indeed, a good correlation with the VSS of sewage sludge loaded into the reactor was found (**Fig. 3.2**).

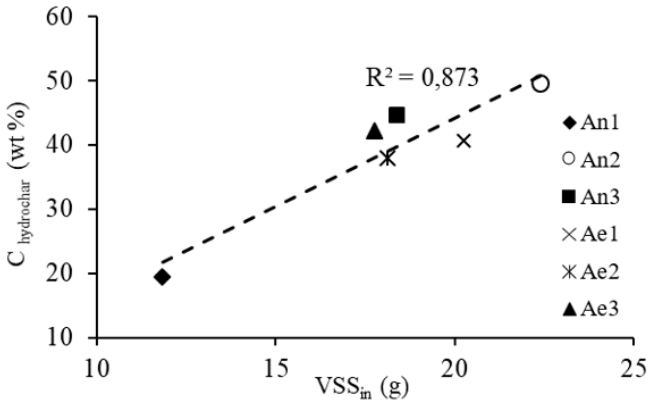

Figure 3.2 Relation between carbon content in HC ($C_{hydrochar}$ wt%) and the content of VSS loaded into HTC reactor.

Fig. 3.2 demonstrates that a linear correlation between the VSS content of sludge loaded into the HTC reactor and the carbon retained in HC can be found. Thus, with a good determination coefficient, once the volatile solid content in sludge is known, the carbon content in hydrochar

could be predicted in this specific HTC operational conditions. The C, N and P balances among the solid, liquid, and gaseous fraction are reported in **Fig. 3.3.**

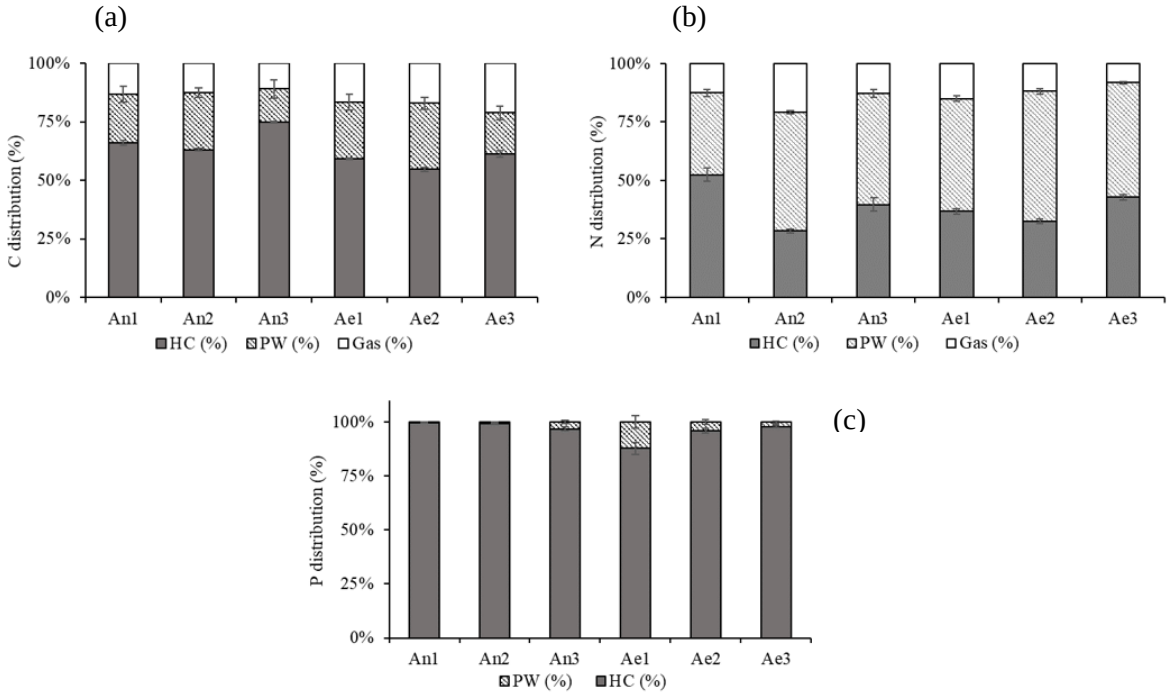

Figure 3.3 C, N, and P distribution in hydrochar, process water, and gas.

As depicted in **Fig. 3.3a**, C is mainly retained within solid fraction (55 – 75 %), while PW can hold lower C percentages (14 – 28 %). The gas fraction varied in the range 11 – 21 %, showing higher values in case of aerobic digested sewage sludge (17 – 21 %) rather than in anaerobic digested ones (11 – 13 %). Comparable values of C distribution percentage (i.e., ≅ 60, 20, and 20 % for hydrochar, process water, and gas, respectively) were reported in literature by Danso-Boateng et al. [26] for hydrothermal carbonization of primary sludge at 200 °C for 4 h. Indeed, high temperatures (> 200 °C) could promote the C transfer to the liquid phase, due to the carbon solubilisation during Maillard and Browning reactions [26, 27].

In **Fig. 3.3b** is reported the nitrogen balance among HC, PW, and gas fraction. N is heterogeneously distributed between solid (28 – 53 %) and liquid fraction (35 – 56 %), while a nitrogen loss in the gas phase was observed. The presence of N in gas could be related to its volatilisation of nitrogen, which might occur during HTC at high temperature and long retention

time. These results are in accordance with the percentage of N in gas (3 – 20 %) reported for HTC treatment of digestate (210 – 250 °C, 30 – 120 minutes) [8]. Except for the case of An1, all the analyzed samples showed that residual N in PW was higher than that in HC. Indeed, N is gradually released into the aqueous phase at temperature higher than 160 °C, due to the decomposition of organic nitrogen [8, 28].

The P distribution among HC and PW is reported in **Fig. 3.3c**. Despite the high variability of P concentrations in the initial sludge samples, whose concentration varied between 8 500 – 42 600 mg $kg^{-1}_{dry\ feedstock}$, HTC proved to concentrate almost the entire P content in the solid phase (percentages higher than 90 % for all samples), regardless of the content of initial P. which shows that the fraction.

3.3.2 Process water characterization

Tab. 3.1 summarizes the heavy metals concentrations detected in PW samples (expressed as mg kg^{-1}_{dry} with standard deviations in parenthesis), in comparison with the limits defined by Regulation (EU) 2019/1009 about the market of EU fertilising products (organic, mineral-organic, and inorganic) based on macro-elements [29].

Table 3.1 Heavy metals concentrations in PW samples (all values are expressed in mg kg^{-1}_{dry}), total nutrients (wt %), and specific regulation limits.

Sample	As	Cd	Cr	Cu[3a]	Hg	Mo	Pb	Zn	N P K[3b]
An1	9.78 (2.46)	0.06	34.82 (8.48)	1.68 (0.39)	0.19 (0.06)	1.09 (0.13)	0.29 (0.10)	2.86 (0.67)	0.34
An2	5.73 (1.44)	0.06	10.55 (2.64)	0.32 (0.07)	0.02 (0.01)	1.22 (0.03)	0.07 (0.02)	1.51 (0.36)	0.70
An3	8.51 (2.12)	0.06	15.77 (3.78)	1.86 (0.43)	0.02	0.70 (0.16)	0.49 (0.11)	5.09 (1.22)	0.33
Ae1	12.50 (3.19)	0.06	16.18 (3.92)	0.43 (0.10)	0.01	1.15 (0.27)	0.15 (0.05)	4.68 (1.13)	0.77

Ae2	14.71 (3.62)	0.06	11.09 (2.71)	0.97 (0.22)	0.06 (0.02)	0.60 (0.14)	0.12 (0.04)	4.34 (1.04)	0.77
Ae3	8.05 (1.92)	0.06	9.77 (2.30)	1.57 (0.38)	0.05 (0.02)	0.88 (0.21)	0.12 (0.04)	2.95 (0.71)	0.91
EU 2019/1009	40[3c]	1.5[3d]	2[3e]	300[3f]	1	-	120	800[3g]	3[3h]
Italy 75/2010[3i]	-	-	-	-	-	-	30	-	-
USA 40 CFR Part 503	75	85	-	4300	57	75	840	7500	-

Standard deviations are reported in parenthesis.

[3a] Concentrations values are referred to the total Cr;

[3b] Values considers the sum nutrients as $N + P_2O_5 + K_2O$ (wt %);

[3c] EU regulation refers this value to the only inorganic As;

[3d] the value is referred to the only organic fertilizer, different values could be considered (3 for $P_2O_5 < 5\%$, and 60 for $P_2O_5 > 5\%$);

[3e] EU regulation refers to the Cr (VI) individually;

[3f] the value refers to organic fertilizer, in other cases the limit is 600 mg kg^{-1}_{dry};

[3g] the value refers to organic fertilizer, otherwise the limit is 1500 mg kg^{-1}_{dry};

[3h] the lower limit for total nutrients in organic fertilizers;

[3i] there are additional specific limitations for different fertilizers categories.

EU regulation establishes limits also for Ni (100 mg kg^{-1}_{dry} for inorganic, and < 50 mg kg^{-1}_{dry} in other cases) and for biuret (not detected for organic, and 12 g kg^{-1}_{dry} in other cases). Even though the sum of nutrient's concentration is below the minimum amount for organic fertilizers defined by 2019/1009, all PW samples results to comply As, Cd, Cu, Hg, Mo, Pb, and Zn limits. Differently, total Cr concentrations resulted above 2 mg kg^{-1}_{dry}, which is the maximum amount permitted for Cr (VI) by EU regulation. Therefore, the limit could be respected if only Cr (VI) was considered. Although products derived from char are not yet fully authorized by EU

regulation, the characteristics of PW demonstrated its suitability as fertilizer. Indeed, PW derived by hydrothermal treatment of poultry litter has shown to promote lettuce growth by fertigation, also improving its nutrients concentration by recirculation [30]. Accordingly, even if nutrients (**Tab. 3.1**) resulted < 3% for all samples, PW could be recirculated into the HTC reactor to concentrate N, P, and K to upgrade its fertilizing properties. The Italian legislative decree (75/2010) proposed Pb as the limiting concentration of heavy metals for organic and mineral-organic fertilizer. For all samples, this limitation was respected. Further, all standards defined by US regulation were complied. Concentrations reported in **Tab. 3.1** were mostly in agreement with values described for PW derived by HTC (at 210 °C for 60 min and 300°C for 180 min) of no-stabilized and dewatered sewage sludge by Wang et al. [11]. They reported similar concentrations of Cd, Cu, Hg, and Pb to those described in this study, while higher concentration of As and Cr were here detected. However, heavy metals concentrations are strongly influenced by initial feedstock characteristics and severity of reaction [11], making a direct comparison with other studies challenging.

3.3.3 Methane yields and anaerobic biodegradability

Specific CH_4 yields for each PW sample are shown in **Fig. 3.4**. In this study, first-order (**equation 3.11**) and modified Gompertz models (**equation 3.12**) were selected to fit experimental data to predict the final CH_4 production of AD tests [31]. OriginPro (9.1 version) was used to model the experimental data to following kinetic equations.

$$G(t) = G_{max} \cdot [1 - \exp(-k \cdot t)] \quad (3.11)$$

$$G(t) = G_{max} \cdot \exp\left(-\exp\left(\left(\frac{R_m \cdot \exp(1)}{G_{max}}\right) \cdot (\lambda - t) + 1\right)\right) \quad (3.12)$$

In **equation 3.11**, G(t) is the CH_4 production at time t (d), G_{max} is the maximum methane production (mL CH_4 STP g COD^{-1}_{added}), k is the specific rate constant (d^{-1}), and t is the digestion time at which the methane production is calculated. In **equation 3.12**, R_m is the maximum methane

production rate (mL CH_4 STP g COD^{-1}_{added} d^{-1}) and λ is the lag time (d), while all other variables were already defined above.

Table 3.2 Key parameters of equations applied to model experimental data.

Sample	Model	G_{max} (mL CH_4 STP $g^{-1}COD_{added}$)	k (d^{-1})	R_m (mL CH_4 STP $gCOD^{-1}_{added}$ d^{-1})	λ (d)	R^2 (-)	$bCOD_{an}$ (%)
PW An1	First-order	228 ± 4	0.109 ± 0.015	-	-	0.999	64
PW An2	Modified Gompertz	195 ± 4	-	7.258 ± 0.961	6.376 ± 1.832	0.999	54
PW An3	Modified Gompertz	217 ± 2	-	6.656 ± 0.338	4.324 ± 0.853	0.999	61
PW Ae1	Modified Gompertz	280 ± 5	-	6.397 ± 0.233	7.918 ± 0.635	0.999	74
PW Ae2	Modified Gompertz	214 ± 1	-	9.524 ± 0.260	8.290 ± 0.399	0.999	61
PW Ae3	Modified Gompertz	296 ± 4	-	6.937 ± 0.218	8.736 ± 0.533	0.999	78

All parameters are expressed as modelled values ± standard error.

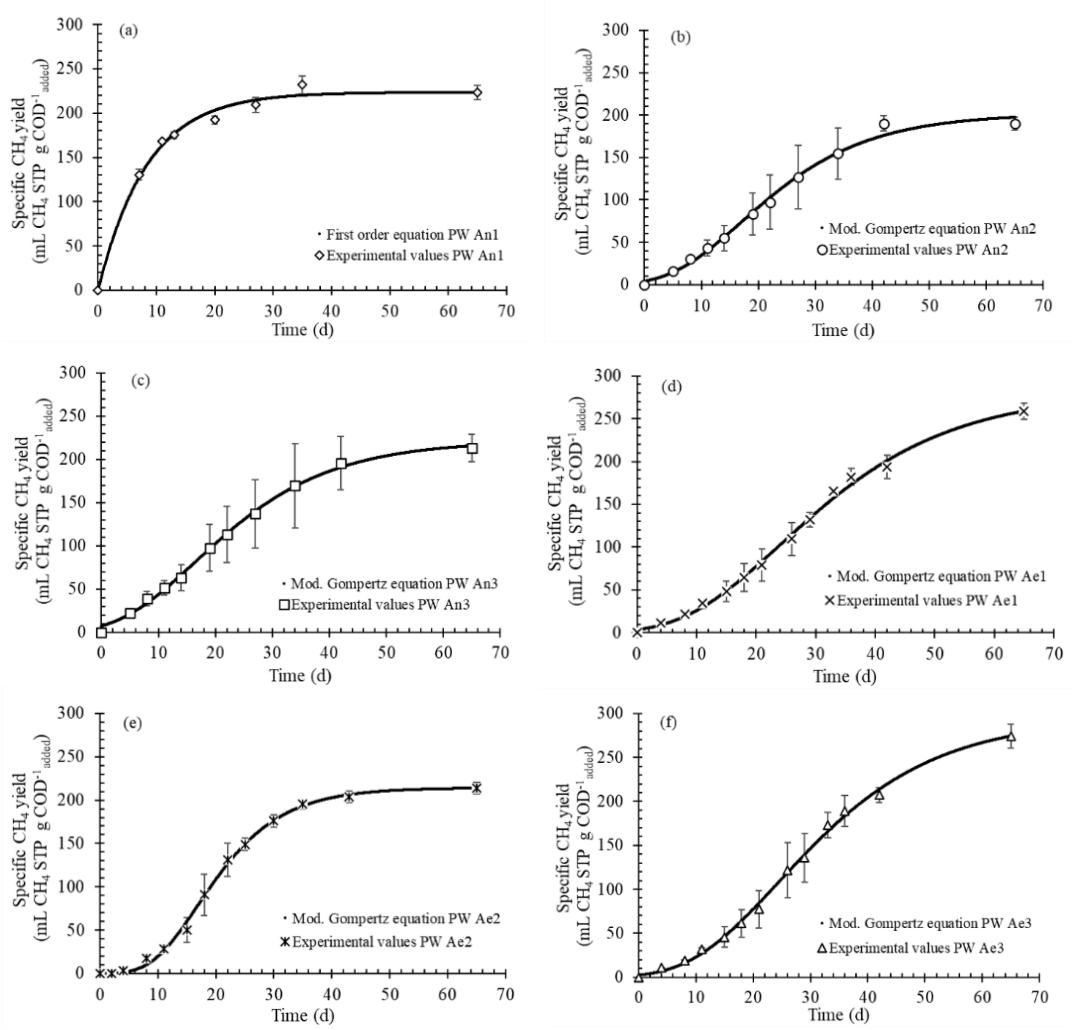

Figure 3.4 Specific CH_4 productions for PW derived by HTC of An1 (a), An2 (b), An3 (c), Ae1 (d), Ae2 (e), Ae3 (f).

PW derived from Ae1 and Ae3 resulted in higher CH_4 production (expressed as average values of n=3 determination with standard deviations in parenthesis, and equal to 259 (9), and 274 (14) mL CH_4 STP $g^{-1}COD_{added}$, respectively) than other PW samples. This may be explained by the presence of organic substances, which can be still partially biodegradable after aerobic stabilization. Nevertheless, also PW from HTC on An1 resulted in a considerable CH_4 yield (223 (8) mL CH_4 STP $g^{-1}COD_{added}$). Indeed, in the case of An1, experimental data were fitted by the first-order equation with a high coefficient of determination (**Tab. 3.2**), indicating that no lag-phase is needed to quickly convert the organic matter in anaerobic conditions. Thus, BMP test on

PW from HTC of An1 sludge revealed that no acclimatization phase was required for the anaerobic inoculum in this specific condition. This could be due to the fact that the anaerobic biomass used as inoculum in all tests was directly collected from anaerobic digesters of the WRRF which produces An1 sludge. The value of the first-order kinetic constant (**Tab. 3.2**) was higher than those reported for PW derived by HTC of sewage sludge processed at 208 °C for 1 h (0.031 – 0.048 d^{-1}) [12], and similar to those described by Marin-Batista et al. [32] for PW obtained by HTC of cow manure (0.074 – 0.130 d^{-1}). Observing the modified Gompertz equation parameters, is noted that lag-phase varied in a range of around 4 – 9 d. Clearly, PW from HTC on anaerobic sludges (An2, and An3) showed shorter lag-phase values (4 – 6 d) than those observed during BMP tests on PW derived from carbonization of aerobically stabilized samples (7 – 9 d). This suggests that the anaerobic biomass needed longer time to hydrolyze the organic substances in PW derived from aerobically treated SS than anaerobically. Similar lag-phase values were described by Ferrentino et al. [13], testing different mixture of hydrochar and process water derived by HTC on sewage sludge together with primary and secondary sludge (0.3 – 7.3 d). Overall, experimental specific CH_4 productions varied in the following range (expressed as average values of n=3 determination with standard deviations in parenthesis): 190 (8) – 274 (14) mL CH_4 STP $g^{-1}COD_{added}$ for An2, and Ae3, respectively. Comparable methane yields (228 – 301 mL CH_4 $g^{-1}COD$) were observed for PW obtained by HTC on anaerobic sludge digestate at 250 °C for 30 minutes at different solid concentration of feedstock (2.5 – 30 wt. %) [10]. Specific CH_4 production described in **Fig. 3.4b, 3.4c, 3.4e** showed similar trend. In these BMP tests, G_{max} resulted really close to the experimental methane yields at day 65, which showed a 3 % maximum difference. Differently, **Fig. 3.4d** and **3.4f** resulted in a G_{max} higher than 7 % of experimental value at day 65, suggesting that the maximum CH_4 production is still not reached at the end of the experiment. Lastly, anaerobic biodegradability ($bCOD_{an}$ (%)) varied between 54 and 78 % for An2, and Ae3, respectively. These values were slightly lower than anaerobic biodegradability determined by Aragon-Briceno et al.[10] (75 – 89 %), using experimental data from BMP test of PW derived by HTC on sewage sludge and theoretical values by Boyle's equations.

3.3.4 Biochemical Oxygen Demand (BOD) tests and aerobic biodegradability

In **Fig. 3.5** are reported the pattern of O_2 consumptions during BOD experiments for each PW investigated.

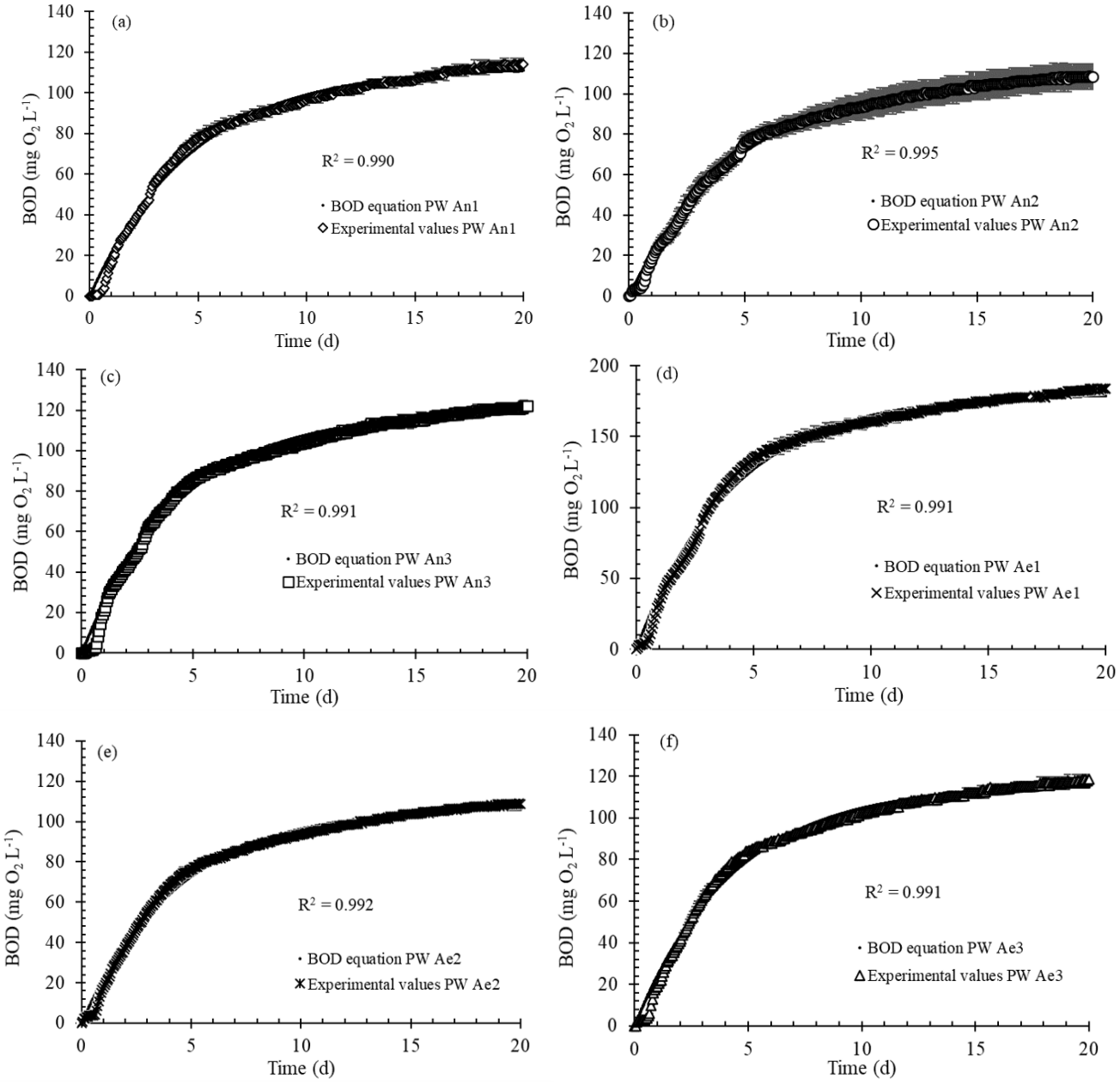

Figure 3.5 O_2 consumption during BOD tests on PW derived by HTC of An1 (a), An2 (b), An3 (c), Ae1 (d), Ae2 (e), Ae3 (f).

Considering the dilution factor, BOD varied in the range 23 – 47 g O_2 L^{-1}. Modelled data fitted by BOD equation described experimental values with a high coefficient of determination (R^2 > 0.990 in all experiments). Values of k constant varied between 0.21 – 0.25 d^{-1}, resulting included in the range of values generally reported for untreated wastewater (0.12 – 0.46 d^{-1}) [22]. Further, the COD/BOD_5 ratio varied between 1.88 and 2.09, indicating a significant content of easily biodegradable organic matter [33]. PW samples achieved high percentage of biodegradable COD (71 - 79 %). Interestingly, the COD biodegradability in aerobic conditions seemed to be independent by the type of SS treated by HTC. Differently, the COD biodegradable fraction determined experimentally ($bCOD_{\_exp}$) at the end of BOD tests, demonstrated to underestimate modelled values ($bCOD_{\_mod}$) in all tests. Indeed, considering experimental data, bCOD varied in a lower range (62 - 72 %), however confirming a good aerobic biodegradability of PW.

3.3.5 Respirometric tests and aerobic biodegradability

Respirograms of PW samples are reported in **Fig. 3.6**.

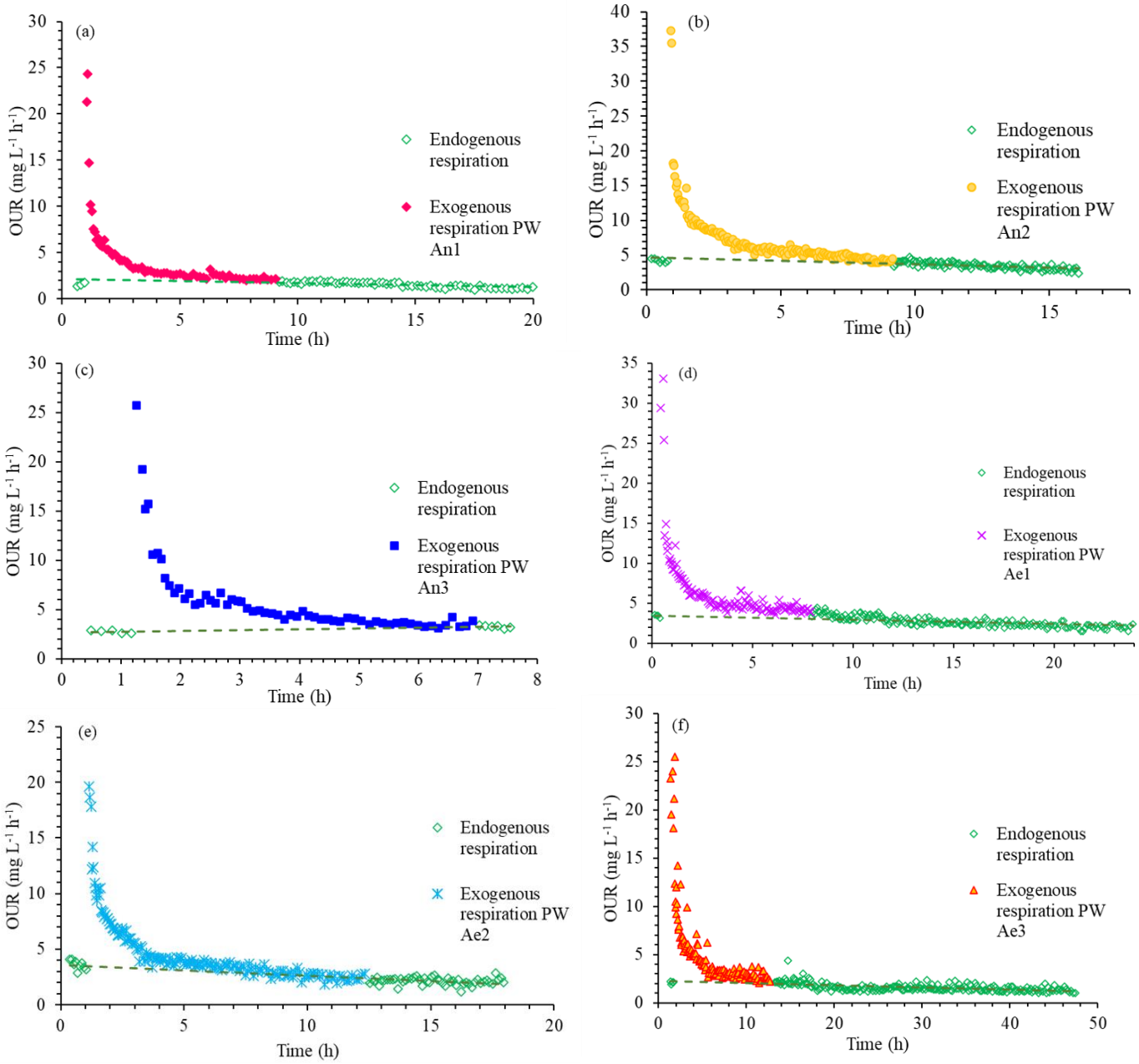

Figure 3.6 Oxygen uptake rate (OUR) during respirometric tests on PW derived by HTC of An1 (a), An2 (b), An3 (c), Ae1 (d), Ae2 (e), Ae3 (f).

One main sharp peak after sample's spike can be observed in all tests, defining areas under the curve with similar shape. This suggests that the aerobic respiration of biomass occurred immediately for all tested samples. No other evident peaks can be noted and, subsequently to the first peak, OUR trend assumed a decreasing behaviour, depicting an exogenous area within 10 hours of starting the tests. Respirograms confirmed that PW derived by HTC of sewage sludge is biodegradable in aerobic conditions, with a wide bCOD range (65 - 85 %). Hence, the biodegradability identified by respirometric test showed a good agreement with results obtained by BOD tests.

3.3.6 Comparison

Comparing the percentages of $bCOD_{\_mod}$, $bCOD_{\_exp}$, and $bCOD_{\_resp}$ derived from experimental tests, can be concluded that PW is biodegradable in aerobic conditions regardless of original feedstock processed by HTC, with bCOD percentages higher than 60 % for all investigated samples (**Fig. 3.7**).

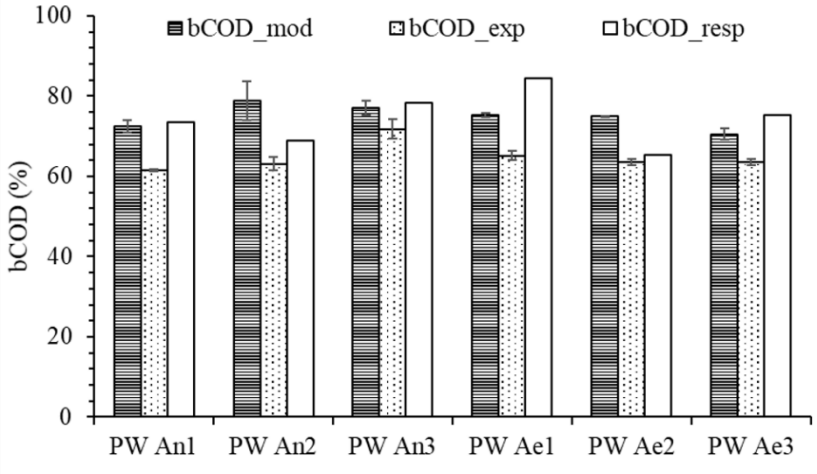

Figure 3.7 Comparison of biodegradable COD (bCOD) percentages obtained by BOD test ($bCOD_{\_mod}$, $bCOD_{\_exp}$), and respirometric tests $bCOD_{\_resp}$ on PW obtained by HTC on An1 (a), An2 (b), An3 (c), Ae1 (d), Ae2 (e), Ae3 (f).

As is shown in **Fig. 3.7**, $bCOD_{\_exp}$ resulted generally in lower bCOD percentages than $bCOD_{\_mod}$ and $bCOD_{\_resp}$ values. The maximum distance of these latter parameters from $bCOD_{\_exp}$ resulted equal to 30 % for PW Ae1 in case of $bCOD_{\_resp}$, while the minimum error (7 %) was revealed for $bCOD_{\_mod}$ in case of PW An3. However, all resulted bCOD values are in agreement in identifying a good biodegradability of PW in aerobic conditions, pointing out the feasibility to treat this liquid fraction directly in WRRF water treatment line. Even though BOD experiments could be affected by the dilution effect, which could promote the biodegradability of PW reducing microorganism inhibition, respirometric tests have confirmed the range of bCOD values. The distance among results could firstly find explanation in the food/microorganism ratio, which is completely different between BOD (F/M = 30) and respirometric tests (F/M = 0.05). Additionally, a different biomass has been used during tests. While an activated sludge from oxidation tank from a WRRF treating domestic wastewater was used as inoculum in BOD tests, a biomass collected from oxidation tanks of a WRRF that treats also industrial wastewater was selected for respirometric experiments. Thus, this biomass might be acclimatized to degrade specific compounds usually hard to remove, helping their biodegradability [34]. This aspect could promote the degradation of PW, which is a complex liquid matrix generally containing recalcitrant compounds [35].

Further, while no clear correlation was found between anaerobic ($bCOD_{\_an}$) and aerobic biodegradability ($bCOD_{\_exp}$ and $bCOD_{\_resp}$), a linear relationship between $bCOD_{\_an}$ and $bCOD_{\_mod}$ has been identified (**Fig. 3.8**).

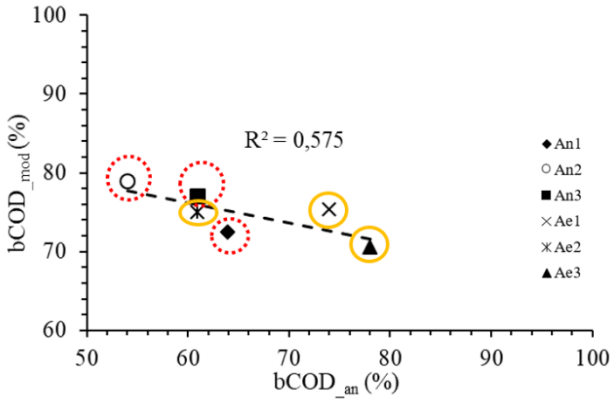

Figure 3.8 Linear correlation between $bCOD_{\_an}$ (%) and $bCOD_{\_mod}$ (%) of PW derived by HTC on anaerobically digested SS (highlighted by dotted line) and aerobically stabilized SS (highlighted by continuous line).

Generally, positive linear correlations were reported in literature between aerobic and anaerobic biodegradability of waste. Bayard et al. [36] identified a linear correlation ($R^2 = 0.725$) between aerobic biodegradability determined by BOD values (at day 28) and anaerobic one (at day 60) for different organic fractions of residual municipal solid waste. Furthermore, Argiz et al. [37] described a solid linear correlation between biodegradability determined performing BMP and respirometric tests of seven different waste streams (six liquid effluents derived from industry and wastewater/waste treatment, and one solid sample obtained from a mixture of primary and secondary sewage sludge from an urban WRRF). Here, a negative correlation is proposed between anaerobic and aerobic biodegradability. No previous work has deeply investigated biodegradability of PW in aerobic and anaerobic conditions. Thus, it is challenging to compare these results with other studies, also considering some aspects such as feedstock characteristic and HTC process conditions. However, it must be underlined that PW derived by anaerobically digested SS revealed higher biodegradability in aerobic tests, while PW obtained by HTC on aerobically stabilized SS are easily degraded in anaerobic environment. Thus, it can be concluded that aerobic/anaerobic treatment on sludge before HTC process influences the biodegradability of PW.

3.4 Conclusion

Anaerobic/aerobic stabilization of raw SS had not a relevant impact on C, N and P distribution between HC and PW derived by HTC treatment. Gas losses estimated by C balance indicated that higher losses could occur carrying out HTC on aerobically digested SS. Even though some parameters of PW (e.g., Cr) could be critical for its utilization as fertilizer, its chemical composition suggests that its use on soil could be feasible in the future. However, this pathway is

not straight forward, and more investigations are needed to fully understand the effect of PW on soil, plants, and their growth. Further, anaerobic/aerobic biodegradability was in agreement in identifying a biodegradable COD fraction comprised between 50 and 80 % for all investigated cases. It suggests that both anaerobic digestion and aerobic treatment in WRRF line of PW might be applied on this fraction. Interestingly, an inverse trend was observed between anaerobic/aerobic stabilization of sludge and anaerobic/aerobic biodegradability of PW. It indicates that processing anaerobic digestate SS by HTC, in terms of biodegradability an aerobic treatment of PW would be then preferred, while vice versa would be optimal for aerobically stabilized SS.

3.5 References – Chapter 3

1. Samolada, M.C., Zabaniotou, A.A.: Comparative assessment of municipal sewage sludge incineration , gasification and pyrolysis for a sustainable sludge-to-energy management in Greece. Waste Manag. 34, 411–420 (2014). https://doi.org/10.1016/j.wasman.2013.11.003
2. Medina-Martos, E., Istrate, I.R., Villamil, J.A., Gálvez-Martos, J.L., Dufour, J., Mohedano, Á.F.: Techno-economic and life cycle assessment of an integrated hydrothermal carbonization system for sewage sludge. J. Clean. Prod. 277, (2020). https://doi.org/10.1016/j.jclepro.2020.122930
3. Wang, L., Chang, Y., Li, A.: Hydrothermal carbonization for energy-efficient processing of sewage sludge: A review. Renew. Sustain. Energy Rev. 108, 423–440 (2019). https://doi.org/10.1016/j.rser.2019.04.011
4. European Commission: The implementation of EU waste legislation, including the early warning report for Member States at risk of missing the 2020 preparation for re-use/recycling target on municipal waste. Brussels, 24.9.2018 COM(2018) 656 Final. (2018)
5. Tasca, A.L., Puccini, M., Gori, R., Corsi, I., Galletti, A.M.R., Vitolo, S.: Hydrothermal carbonization of sewage sludge: A critical analysis of process severity, hydrochar properties and environmental implications. Waste Manag. 93, 1–13 (2019). https://doi.org/10.1016/j.wasman.2019.05.027
6. Fang, J., Zhan, L., Ok, Y.S., Gao, B.: Minireview of potential applications of hydrochar derived from hydrothermal carbonization of biomass. J. Ind. Eng. Chem. 57, 15–21 (2018). https://doi.org/10.1016/j.jiec.2017.08.026
7. Gerner, G., Meyer, L., Wanner, R., Keller, T., Krebs, R.: Sewage sludge treatment by hydrothermal carbonization: Feasibility study for sustainable nutrient recovery and fuel production. Energies. 14, (2021). https://doi.org/10.3390/en14092697

8. Aragón-Briceño, C.I., Grasham, O., Ross, A.B., Dupont, V., Camargo-Valero, M.A.: Hydrothermal carbonization of sewage digestate at wastewater treatment works: Influence of solid loading on characteristics of hydrochar, process water and plant energetics. Renew. Energy. 157, 959–973 (2020). https://doi.org/10.1016/j.renene.2020.05.021

9. Hämäläinen, A., Kokko, M., Kinnunen, V., Hilli, T., Rintala, J.: Hydrothermal carbonisation of mechanically dewatered digested sewage sludge—Energy and nutrient recovery in centralised biogas plant. Water Res. 201, (2021). https://doi.org/10.1016/j.watres.2021.117284

10. Escala, M., Zumbühl, T., Koller, C., Junge, R., Krebs, R.: Hydrothermal carbonization as an energy-efficient alternative to established drying technologies for sewage sludge: A feasibility study on a laboratory scale. Energy and Fuels. 27, 454–460 (2013). https://doi.org/10.1021/ef3015266

11. Wang, L., Chang, Y., Liu, Q.: Fate and distribution of nutrients and heavy metals during hydrothermal carbonization of sewage sludge with implication to land application. J. Clean. Prod. 225, 972–983 (2019). https://doi.org/10.1016/j.jclepro.2019.03.347

12. Ferrentino, R., Merzari, F., Fiori, L., Andreottola, G.: Coupling hydrothermal carbonization with anaerobic digestion for sewage sludge treatment: Influence of HTC liquor and hydrochar on biomethane production. Energies. 13, (2020). https://doi.org/10.3390/en13236262

13. Villamil, J.A., Mohedano, A.F., Rodriguez, J.J., de la Rubia, M.A.: Valorisation of the liquid fraction from hydrothermal carbonisation of sewage sludge by anaerobic digestion. J. Chem. Technol. Biotechnol. 93, 450–456 (2018). https://doi.org/10.1002/jctb.5375

14. Tasca, A.L., Stefanelli, E., Raspolli Galletti, A.M., Gori, R., Mannarino, G., Vitolo, S., Puccini, M.: Hydrothermal Carbonization of Sewage Sludge: Analysis of Process Severity and Solid Content. Chem. Eng. Technol. 43, 2382–2392 (2020). https://doi.org/10.1002/ceat.202000095

15. APHA (American Public Health Association): APHA Standard methods for examination of water and wastewater. (2005)

16. Aragón-briceño, C., Ross, A.B., Camargo-valero, M.A.: Evaluation and comparison of product yields and bio-methane potential in sewage digestate following hydrothermal treatment. Appl. Energy. 0–1 (2017). https://doi.org/10.1016/j.apenergy.2017.09.019

17. Pabòn Pereira, C.P., Castanares, G., Van Lier, J.B.: An OxiTop protocol for screening plant material for its biochemical methane potential (BMP). Water Sci. Technol. 66, 1416–1423 (2012). https://doi.org/10.2166/wst.2012.305

18. Rozzi, A., Remigi, E.: Methods of assessing microbial activity and inhibition under anaerobic conditions: A literature review. Rev. Environ. Sci. Biotechnol. 3, 93–115 (2004). https://doi.org/10.1007/s11157-004-5762-z

19. Valero, D., Montes, J.A., Rico, J.L., Rico, C.: Influence of headspace pressure on methane production in Biochemical Methane Potential (BMP) tests. Waste Manag. 48, 193–198 (2016). https://doi.org/10.1016/j.wasman.2015.11.012

20. Raposo, F., Fern, V., Rubia, M.A. De, Borja, R., B, F., Fern, M., Frigon, J.C., Cavinato, C., Demirer, G., Fern, B., Menin, G., Peene, A., Scherer, P., Torrijos, M., Uellendahl, H., Wierinck, I., Wilde, V. De: Biochemical methane potential (BMP) of solid organic substrates : evaluation of anaerobic biodegradability using data from an international interlaboratory study. . Chem. JTechnol. Biotechnol. 86, 1088–1098 (2011). https://doi.org/10.1002/jctb.2622

21. Roeleveld, P.J., Van Loosdrecht, M.C.M.: Experience with guidelines for wastewater characterisation in The Netherlands. Water Sci. Technol. 45, 77–87 (2002). https://doi.org/10.2166/wst.2002.0095

22. Metcalf, Eddy, &: Wastewater engineering : treatment and reuse. Fourth edition / revised by George Tchobanoglous, Franklin L. Burton, H. David Stensel. Boston : McGraw-Hill, [2003] ©2003 (2013)

23. Jeppsson, U.: A General Description of the Activated Sludge Model No . 1 (ASM1). Components. 1, 1–16 (1996). https://doi.org/10.1007/s00540-017-2318-2

24. Marin-Batista, J.D., Mohedano, A.F., Rodríguez, J.J., De la Rubia, M.A.: Energy and phosphorous recovery through hydrothermal carbonization of digested sewage sludge. Waste Manag. 105, 566–574 (2020). https://doi.org/10.1016/j.wasman.2020.03.004

25. Arauzo, P.J., Atienza-Martínez, M., Ábrego, J., Olszewski, M.P., Cao, Z., Kruse, A.: Combustion characteristics of hydrochar and pyrochar derived from digested sewage sludge. Energies. 13, 1–15 (2020). https://doi.org/10.3390/en13164164

26. Danso-Boateng, E., Holdich, R.G., Shama, G., Wheatley, A.D., Sohail, M., Martin, S.J.: Kinetics of faecal biomass hydrothermal carbonisation for hydrochar production. Appl. Energy. 111, 351–357 (2013). https://doi.org/10.1016/j.apenergy.2013.04.090

27. Danso-Boateng, E., Shama, G., Wheatley, A.D., Martin, S.J., Holdich, R.G.: Hydrothermal carbonisation of sewage sludge: Effect of process conditions on product characteristics and methane production. Bioresour. Technol. 177, 318–327 (2015). https://doi.org/10.1016/j.biortech.2014.11.096

28. Huang, J., Wang, Z., Qiao, Y., Wang, B., Yu, Y., Xu, M.: Transformation of nitrogen during hydrothermal carbonization of sewage sludge: Effects of temperature and Na/Ca acetates addition. Proc. Combust. Inst. 38, 4335–4344 (2021). https://doi.org/10.1016/j.proci.2020.06.075

29. Parlament, E.: Regolamento (UE) 1009/2019. 1009, 1–114 (2019)

30. Mau, V., Neumann, J., Wehrli, B., Gross, A.: Nutrient Behavior in Hydrothermal Carbonization Aqueous Phase Following Recirculation and Reuse. Environ. Sci. Technol. 53, 10426–10434 (2019). https://doi.org/10.1021/acs.est.9b03080

31. Zhao, C., Yan, H., Liu, Y., Huang, Y., Zhang, R., Chen, C., Liu, G.: Bio-energy conversion performance, biodegradability, and kinetic analysis of different fruit residues during discontinuous anaerobic digestion. Waste Manag. 52, 295–301 (2016). https://doi.org/10.1016/j.wasman.2016.03.028

32. Marin-Batista, J.D., Villamil, J.A., Qaramaleki, S. V, Coronella, C.J., Mohedano, A.F., de la Rubia, M.A.: Energy valorization of cow manure by hydrothermal carbonization and anaerobic digestion. Renew. Energy. 160, 623–632 (2020). https://doi.org/10.1016/j.renene.2020.07.003

33. Płuciennik-Koropczuk, E., Myszograj, S.: New approach in COD fractionation methods. Water (Switzerland). 11, 1–12 (2019). https://doi.org/10.3390/w11071484

34. Fongsatitkul, P., Elefsiniotis, P., Yamasmit, A., Yamasmit, N.: Use of sequencing batch reactors and Fenton ' s reagent to treat a wastewater from a textile industry. 21, 213–220 (2004). https://doi.org/10.1016/j.bej.2004.06.009

35. Chen, H., Rao, Y., Cao, L., Shi, Y., Hao, S., Luo, G., Zhang, S.: Hydrothermal conversion of sewage sludge: Focusing on the characterization of liquid products and their methane yields. Chem. Eng. J. 357, 367–375 (2019). https://doi.org/10.1016/j.cej.2018.09.180

36. Bayard, R., Benbelkacem, H., Gourdon, R., Buf, P.: Characterization of selected municipal solid waste components to estimate their biodegradability re. 216, 4–12 (2018). https://doi.org/10.1016/j.jenvman.2017.04.087

37. Argiz, L., Reyes, C., Belmonte, M., Franchi, O., Campo, R., Fra-Vàzquez, A., Val del Rìo, A., Mosquera-Corral, A., Campos, J.L.: Assessment of a fast method to predict the biochemical methane potential based on biodegradable COD obtained by fractionation respirometric tests. 269, (2020). https://doi.org/10.1016/j.jenvman.2020.110695

Chapter 4

Performance of upflow anaerobic sludge blanket (UASB) reactor treating process water derived from hydrothermal carbonization of sewage sludge

Abstract

A continuous anaerobic treatment of process water (PW) derived from hydrothermal carbonization (HTC) of sewage sludge (SS) has been here investigated. To this end, an upflow anaerobic sludge blanket (UASB) reactor was set-up. The reactor operated over a period of 131 days with a constant organic loading rate equal to 5 gCOD L^{-1} d^{-1}. The start-up was carried out by feeding only glucose and then an increasing percentage of PW has been added over time. In the last phase, only diluted PW was fed into the reactor. During the experiment both reactor's influent and effluent were monitored for chemical oxygen demand (COD), volatile fatty acids (VFA), total nitrogen (TN), and total ammonia nitrogen (TAN), as well as biogas production and composition. The evolution of the biomass microbial community and its particle size was evaluated at the beginning and at the end of the experiment. The start-up strategy proved to be successfully, since a good CH_4 production was observed (202 (33) mL STP CH_4 $g^{-1}COD_{fed}$). The COD removal percentage decreased linearly with the increase of PW percentage, reaching a minimum value equal to 73 %. VFA, TN, and TAN values suggested that the process was stable over time. The microbial analysis community showed that Firmicutes, Synergistetes, Bacteroidota, and Chloroflexi were the dominant phyla of bacteria, while the granulometric study highlighted that the diameter of the 50 % of particle increased at the end of the experiment with respect to the initial one.

4.1 Introduction

Hydrothermal carbonization (HTC) has been recently proposed as suitable technology to treat different types of biomasses. It is a thermochemical process tested for the first time by Bergius in

1913 [1]. The process is able to convert a wet feedstock (e.g., sewage sludge, SS) into a solid carbonaceous matrix (hydrochar), an aqueous phase (named process water, PW), and very small gas fraction (usually in the range 1-5 % on a dry mass basis), operating at temperatures of 180 – 250 °C under autogenous pressure and with retention time of 1 – 12 h [2].

Many studies have already investigated the application of HTC on different wastes: SS, digestate, food waste, paper waste, green waste, and olive mill waste [*inter alia* 3–6]. Because of the urgent needed required by SS disposal [7], some scientific studies have pointed out HTC as an appropriate technology for SS treatment. Indeed, the application of HTC on SS produces a solid with high fuel properties (hydrochar) and a biogas rich in methane [8], whom can be energetically valorized.

While chemical properties of hydrochar derived by SS have been widely investigated in literature for energetical purposes [9, 10], PW was generally neglected. Just in the last few years, some studies have investigated its possible valorization through anaerobic digestion (AD). Indeed, its application as a substrate in AD seemed to be promising to recover thermal energy through biogas production and valorization [11, 12]. High specific CH_4 yields (84 - 235 mL STP CH_4 $g^{-1}COD_{added}$) are reported for PW derived by HTC of digestate during AD batch tests [13], whereas only few studies about continuous anaerobic treatment of PW can be found.

Wirth et al. [14] have tested anaerobic digestion of PW derived by HTC (at 200 °C for 6 h) of SS running two continuously-fed anaerobic filters (AF) in mesophilic and thermophilic conditions. No relevant differences were observed between reactors, since both of them yielded up to 0.18 L_{CH4} g COD^{-1} (value expressed in standard conditions). They also observed that methanogenesis was the limiting step in AD process, significantly slower than hydrolysis. Further, long term stability was investigated over 500 days by a two steps AD configuration followed by an aerobic step [15]. They found similar results between CH_4 yields derived from both continuous and batch tests. They further observed that AD batch tests resulted generally in higher (77 %) methane percentage in biogas than continuous experiment (50 – 67 %). Lastly, Liu et al. [16] have

investigated the continuous AD of PW derived from SS running two UASB reactors at different organic loading rates (OLRs). They observed good performances of UASB reactor, with a high methane conversion efficiency (71 %). Further, they suggested also to impose a low organic loading rate (OLR) to start-up the reactor (1.9 – 2.1 gCOD L^{-1} d^{-1}).

Here, UASB technology has been selected to treat PW derived by HTC on SS. Indeed, UASB is the most widely used high-rate anaerobic system to process different industrial wastewaters, because of its flexibility and versatility [17]. UASB reactor proved to achieve the highest efficiency processing wastewater with mainly soluble components [18]. Therefore, since PW contains only limited amount of particulate and soluble COD is by far the most abundant fraction present in the liquid fraction [19], this technology seems to be promising for this application.

In this study, the aim was to evaluate the performance of a UASB reactor treating PW derived by HTC on SS at constant OLR, in order to evaluate its stability and its adaptation performance. The OLR was maintained at 5 gCOD L^{-1} d^{-1} for the whole experimentation (with the exception of the first 5 days when the COD load was equal to 1 gCOD L^{-1} d^{-1}). The UASB was firstly fed with glucose only, and then increasing percentage of PW were introduced up to reach the 100%. As a future following research step, the capability of the UASB reactor to operate at higher and various OLRs should be explored. Additionally, microbial community structure was monitored over time, with the purpose of evaluating the stability of the reactor and observing the dynamic of the biomass system.

4.2 Materials and methods

4.2.1 Process water of hydrothermally carbonized sewage sludge and anaerobic granular inoculum

Two hundred kg of anaerobically digested and dewatered SS (with TS (total solids) of 22.7 (0.9) wt % and VS (volatile solids) TS^{-1} ratio equal to 64.3 (3.9) % and pH of 6.9 (0.2)) were firstly diluted with water (200 kg) and $CaCl_2$ (7.2 kg), and then hydrothermally carbonized at 210 °C for around 30 minutes in a continuous pilot scale plant. Operational temperature and time were

selected depending on the practical operation of the pilot plant. $CaCl_2$ was added to improve the dewaterability of the solid-liquid suspension derived by HTC treatment (slurry). This mixture was pumped into a filter press recovering a cake with 38 % of TS, together with 40 L of process water (PW). Before use, PW was filtered (50 µm in nylon and 1 µm in PE) to partially remove solid content and then stored at 4 °C until further use. The principal goal was to obtain a sufficient homogeneous PW sample for the entire duration of the experimentation. Main PW characteristics (i.e., total COD (TCOD), soluble COD (SCOD), total organic carbon (TOC), dissolved organic carbon (DOC), total nitrogen (TN), total ammonia nitrogen (TAN), nitric nitrogen ($N\text{-}NO_3^-$), nitrous nitrogen ($N\text{-}NO_2^-$), concentrations of different VFAs (volatile fatty acids), conductivity, TS, and VS) are reported in **Table 4.1.** Analytical methods applied for the determination of the above-mentioned parameters are reported in the section **4.2.3.**

Table 4.1 – Chemical characterization of process water.

Parameters	Measure[4a]	Parameters	Measure[4a]
TCOD (g L^{-1})	29.6 (4.4)	Acetic acid (mg L^{-1})	930 (540)
SCOD (g L^{-1})	29.0 (4.4)	Propionic acid (mg L^{-1})	240 (140)
TOC (g L^{-1})	10.5 (1.9)	Butyric acid (mg L^{-1})	270 (160)
DOC (mg L^{-1})	10.1 (2.0)	Valeric acid (mg L^{-1})	< 100
TN (mg L^{-1})	1450 (290)	pH	7.4 (0.1)
TAN (mg L^{-1})	1140 (140)	Conductivity (mS cm^{-1})	15.8 (1.8)
$N\text{-}NO_3^-$ (mg L^{-1})	< 0.280	$N\text{-}NO_2^-$ (mg L^{-1})	< 0.015
TS (g L^{-1})	25.12 (0.08)	VS (g L^{-1})	18.12 (0.04)

[4a] Standard deviation of n = 3 measure is reported in parenthesis.

As can be observed in **Tab. 4.1**, VFA measurements were affected by high values of standard deviations, which might be related to the complexity of the PW sample. Anaerobic granular sludge was collected from an industrial full-scale UASB reactor and used as inoculum for lab-scale experiment. Inoculum characteristics were as follows (values are reported as average value

of n = 2 determinations): 9.71 (0.73) wt % TS, 70.03 (0.82) % VS TS^{-1}, pH 7.50 (0.1) and conductivity 9.65 (0.100) mS cm^{-1}.

4.2.2 Experimental set-up and operational conditions

A 5.4 L continuous-flow UASB reactor made with polymethyl methacrylate was designed for this study. The reactor was 710 mm tall, with a 90 mm as internal diameter circular cross section, which widens in the upper part up to 200 mm to facilitate the outlet sample collection, as depicted in **Fig. 4.1**.

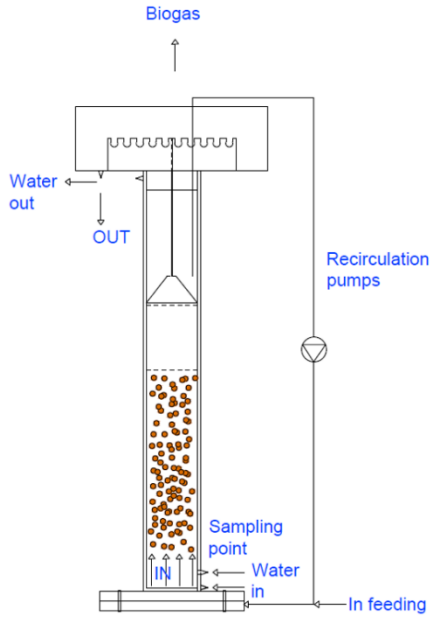

Figure 4.1 UASB reactor configuration scheme at lab-scale.

Approximately 1.6 kg of anaerobic granular sludge were filled into the UASB reactor for the start-up. The feeding was driven across the bottom of the reactor by a peristaltic pump and evenly distributed through the radially assigned holes in the bottom base. The flow moved upward, with the contribution of a recirculation flow rate, achieved through two peristaltic pumps, in order to ensure an appropriate upflow velocity around 0.8 m h^{-1}. The experiment was carried out at constant temperature (37 ± 1 °C), which was kept uniform by an external jacket filled with hot water circulating in a water bath. Biogas collected from the gas-solid-liquid separator on top of the reactor was directed to a gas counter (Apparatebau MilliGascounter with a 3.16 mL drum

volume, Ritter). Biogas was then collected into a 10 L gas bag (multi-layer foil gas samplings bags, Supelco) before analysis. In the first days (1 – 6 days), the start-up was preformed feeding only glucose (1 gCOD L^{-1}) with an organic loading rate (OLR) of 1 gCOD L^{-1} d^{-1}. Then, the OLR was increased up to 5 gCOD L^{-1} d^{-1}, and it was maintained constant for the whole duration of the experiment. A first start-up phase with only glucose and with an OLR equal to 5 gCOD L^{-1} d^{-1} was carried out up to day 48 (start-up phase). The hydraulic retention time (HRT) was set at 24 h. The concentration of the feeding was kept constant at 5 g COD L^{-1} and the flow was accordingly regulated, referring to the only biomass volume (around 1.6 L). PW was gradually introduced, replacing glucose with PW in increasing amounts step by step. The substitution was carried out on COD basis and the performed phases were as reported in **Tab. 4.2:**

Table 4.2 Phase of UASB reactor experimentation.

Phase	Period (d)	Inlet characteristics[4b]
I	48 – 61	10 % PW + 90 % glucose
II	62 – 70	20 % PW + 80 % glucose
III	71 – 85	30 % PW + 70 % glucose
IV	86 – 91	40 % PW + 60 % glucose
V	92 – 103	50 % PW + 50 % glucose
VI	104 – 112	75 % PW + 25 % glucose
VII	113 – 131	100 % PW

[4b]Percentages are expressed on COD basis.

To maintain the desired COD concentration in each period, demi water was added to adequately dilute the sample. In phase VII, a 1:5 dilution was carried out. In addition, pH buffer ($NaHCO_3$ as 1 g L^{-1}) was added to the feeding, together with a basal medium of macro- and micro- nutrients

solution (1 mL L^{-1}) [12]. Samples of the effluent were collected and analysed for at least 3 consecutive days (i.e., 3 times the HRT value) before changing the OLR. Methane production of UASB reactor was calculated using **equation 4.1:**

$$CH_4 production_{exp}\left(L_{CH_4} d^{-1}\right) = \frac{volume_{biogas}(L) \cdot \%\, CH_4}{Time\ (d)} \cdot \frac{T_{STP}}{T_o} \quad (4.1)$$

where volume $_{biogas}$ is the measured volume of biogas (L), time is the measuring time (d), % CH_4 is the concentration of methane in biogas, T_{STP} and T_o are the temperatures in standard (0 °C) and operational conditions (37 °C), respectively.

The volumetric CH_4 production was further compared with the theoretical value, calculated on the basis of COD removal (neglecting the COD consumed for microbial growth), according to **equation 4.2:**

$$CH_4\ production_{th}\left(L\ STP_{CH_4}\ d^{-1}\right) = COD_{removed}\left(\frac{g\ COD}{L}\right) \cdot Q_{fed}\left(\frac{L}{d}\right) \cdot 0.35\ \left(\frac{L\ STP_{CH_4}}{g\ COD}\right) \quad (4.2)$$

4.2.3 Analytical methods

TS and VS were measured according to the standard methods 2540B and 2540E [20].

Concerning raw PW characterization, the following methods were applied: TCOD and SCOD (on filtered sample at 0.45 µm) were determined by ISO 15705 [21], TOC and DOC by method 5040 [22]. TN, N-NO_3^-, N-NO_2^- and TAN (i.e., N-NH_4^+) were measured according to APAT 4060, APAT 4020 and APAT 4050 [23–25], and EPA 350.1 [26], respectively. VFA were determined by EPA 3580A and EPA 8260D [27, 28]. Conductivity and pH were measured according to APAT 2060 [29].

Conversely, effluent analysis was performed on filtered sample (0.45 µm, nylon filter). On this sample, the following parameters were measured using analytical kits (Hach – Lange, Germany) widely applied in wastewater treatment sector: SCOD (LCK 1414, 614), TN (LCK 138, 238), TAN (LCK 305, 303). Samples were properly diluted with demi water to comply the range of

measurement. Conductivity and pH were measured using the pH 7 Vio Sensor (XS instruments). Acetic, propionic and isovaleric acids were measured according to Baldi et al. [30].

Gas composition (H_2, O_2, N_2, CH_4, CO_2, H_2S) was analyzed by a gas-chromatograph (3000 Micro GC, INFICON, Switzerland) as described by Baldi et al. [30].

4.2.4 Anaerobic digestion test in batch conditions

AD digestion tests were carried out on PW also in batch conditions (see details in **Chapter 3**). Tests lasted 35 days in mesophilic temperature (37 ± 1 °C). Runs were performed in 330 mL glass bottles, applying an inoculum to substrate ratio equal to 2 on COD basis [12]. Inoculum was collected from a full-scale anaerobic digester of a Water Resources Recovery Facility (WRRF) treating mainly municipal wastewater (San Colombano WRRF managed by Publiacqua SpA, Florence, Italy). No buffer and neither macro- or micro- nutrients solution were added to the mixture. Pressure was monitored over time through Oxitop® (WTW, Germany) manometric sensors for all duration of the experiments. Data about the first two hours were discarded, in order to eliminate the pressure jump related to the increase of temperature. Then, using data about pressure trend, biogas volume was calculated in standard conditions (0 °C and 1 atm). Its composition (CO_2 and CH_4) was then analyzed through a gas chromatograph (Varian, CP-4900 Micro GC) and data were reported in dry conditions according to Valero et al. [31].

4.2.5 Microbial and granulometric biomass analysis

Taxonomy of granules over time was analyzed by Fundació Fisabio (Valencia, Spain). Samples were collected during the start-up period, and at phases V, VI, VII. In more detail, a 50 mL syringe was inserted into the sampling point located at the bottom of the reactor, then the biomass sample was collected after a careful mixing. Particle size distribution of biomass granules was determined using the software Image ProPlus® at the beginning and at the end of the experiment.

4.3 Results and Discussion

4.3.1 Biogas composition and production

Biogas composition in terms of CH_4, CO_2 and H_2 concentrations (%) is reported in **Fig. 3.2a**. In **Fig. 3.2b** is further depicted the methane production derived by experimental data (**equation 3.1**), in comparison with the theoretical CH_4 production calculated starting from the removal of COD (**equation 3.2**).

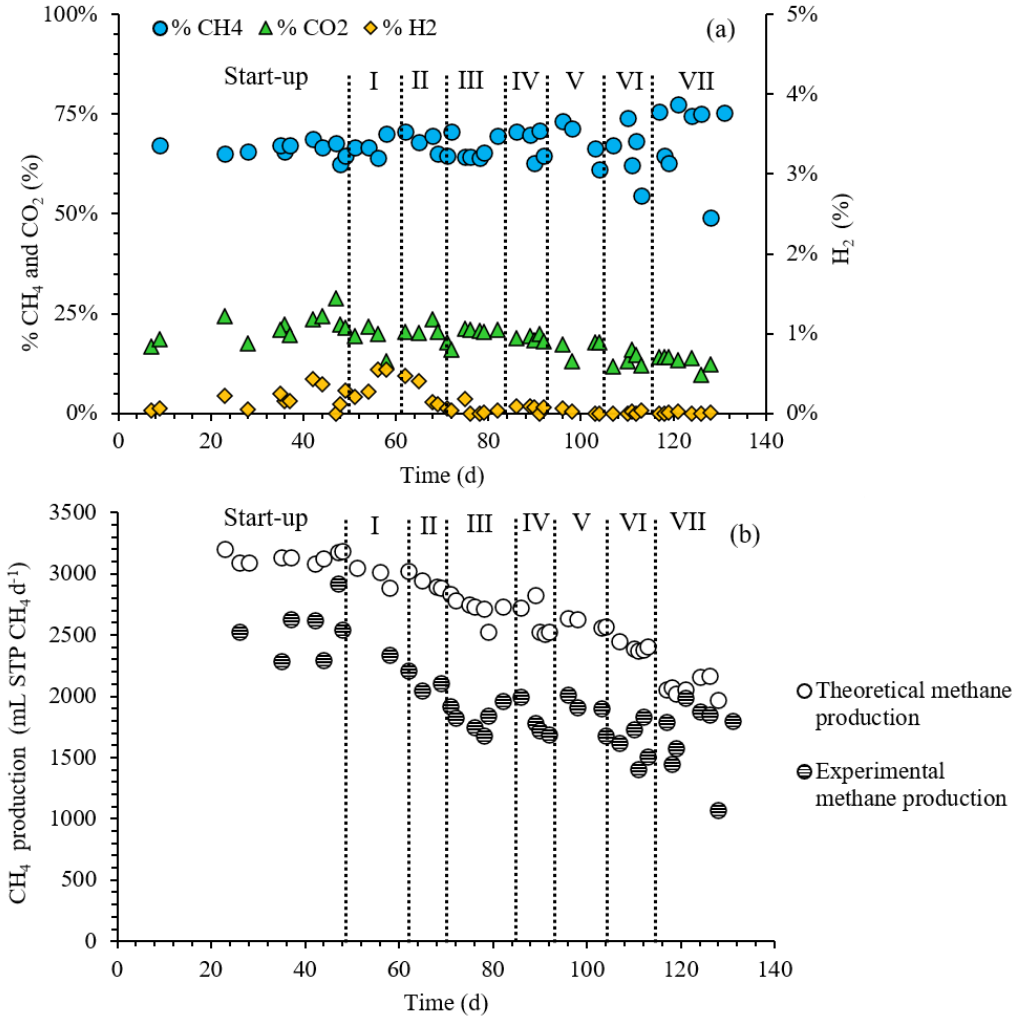

Figure 3.2 CH_4, CO_2 and H_2 concentrations in biogas over time (a). CH_4 production measured experimentally, in comparison with the CH_4 production calculated theoretically (b). Each dotted line sets the end of the phase indicated on the graph.

No relevant changes in biogas composition were observed over time. CH_4 concentration in biogas proved to be stable, showing a slight increase with the addition of PW on average basis. Indeed, CH_4 percentage reached a value of around 66 % (2) (expressed as average value of n = 10 determinations over time with standard deviation in parenthesis) in start-up phase, reaching up to 69 % (10) (expressed as average value of n = 8 determinations in time with standard deviation in parenthesis) in phase VII. As can be observed in **Fig. 3.2a**, variability in CH_4 concentrations gradually increased with the addition of PW. CO_2 resulted in a decreasing pattern with the addition of PW (from about 22 % to 13 % in start-up and phase VII, respectively), while H_2 reached a maximum concentration of 0.6 % in phase I and was no longer detectable in phases VI – VII. Further, H_2S concentrations resulted lower than 0.07 % in all cases. These values comparable with those usually detected in biogas produced by AD sewage sludge (0.05 – 0.25 %) [32]. Remaining gases (i.e., O_2 and N_2) were identified in small percentages (~ 15 %) in all samplings. Their presence was mainly caused by the biogas collection system.

In **Fig. 3.2b** is reported the methane production derived by experimental measurements. A slight decreasing pattern in the theoretical CH_4 production can be observed from start-up phase to phase VII, as expected by the reduction the content of biodegradable COD by the introduction of PW derived by HTC. CH_4 yield measured experimentally confirmed this trend, but underestimating the theoretical value. Percentage ratio between experimental and theoretical CH_4 production varied between 54 – 97 %, suggesting that biogas collection system was not completely efficient during the experiment. It might be attributed to the three-phase separator, which could not be able to catch the whole biogas produced, together with biogas losses of the collection system. Further, neither the specific CH_4 production resulted in an evident pattern, assuming an average value of 202 (33) mL STP $CH_4\ g^{-1}COD_{fed}$ (referred to the only phase VII and expressed as average value of n = 9 determinations in time with standard deviation in parenthesis). Values in the same range (100 - 350 mL STP $CH_4\ g^{-1}COD_{fed}$) are reported by Liu et al. [16], treating PW derived by HTC

applied on sewage sludge from municipal wastewater treatment running UASB reactors at different OLRs (in the range of 2 – 4.5 gCOD L^{-1} d^{-1}). Similar CH_4 yield (180 mL STP CH_4 $g^{-1}COD_{fed}$) was reported for continuous treatment by anaerobic filter (AF) on PW derived from a demonstration-scale HTC plant treating municipal sewage sludge (200 °C for 6 hours) [14].

Anaerobic digestion batch tests confirmed the value of specific CH_4 production obtained by continuous UASB experiments on PW. Indeed, CH_4 yield reached a production of 198 (12) mL STP CH_4 $g^{-1}COD_{fed}$ at day 35. It indicated that no relevant changes occurred in CH_4 production switching from batch to continuous operation mode. In **Fig. 3.3** is reported the experimental curve of CH_4 specific production observed during batch tests. Further, data were fitted with the modified Gompertz equation, as described in detail in **Chapter 3**.

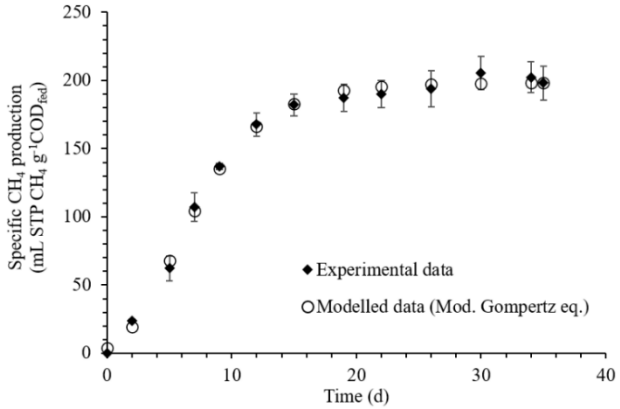

Figure 3.3 Specific CH_4 yield observed during batch AD tests in batch conditions on PW.

4.3.2 COD

Fig. 3.4a shows the influent and effluent COD concentrations over time. In addition, in **Fig. 3.4b** collects the linear correlation between the COD removal and the percentage of COD added as PW to maintain OLR equal to 5 gCOD L^{-1} d^{-1}.

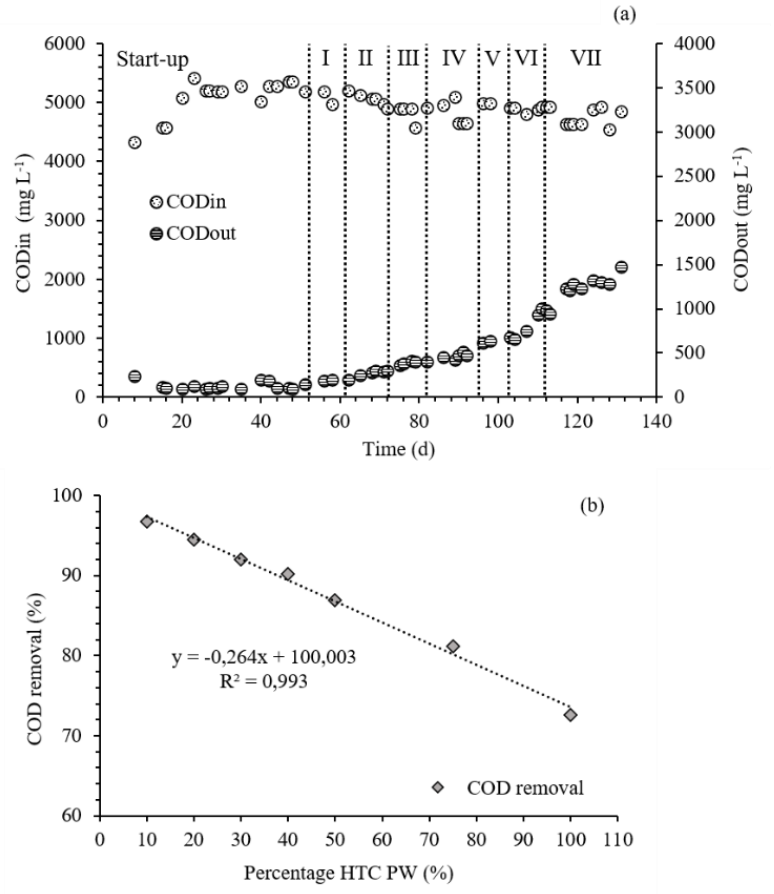

Figure 3.4 COD concentration trend in influent and effluent of UASB reactor (a). Linear correlation between COD removal (%) and percentage of PW added as COD into the influent (b).

COD concentration in the influent was maintained constant at 5 gCOD L^{-1}, since PW was progressively diluted to maintain HRT equal to 24 h for the whole duration of the experiment. COD in the effluent increased during time, because of the addition of PW. Indeed, the COD removal decreased from about 97 % in the start-up phase to around 73 % in phase VII. As can be observed in **Fig. 3.4b**, the COD removal decreased linearly with the introduction of increasing percentage of PW, with a high determination coefficient (R^2 = 0.993). This result might suggest that no inhibition occurred feeding the UASB reactor with only PW, but rather it could indicate that the biodegradable fraction of PW is equal to 73 %. Weide et al. [15] obtained lower values (58 %) of COD anaerobic degradation. In that study, PW was obtained by processing a mixture of sewage sludge and wood in a pilot-scale HTC plant and then treated by a continuous two-stage

anaerobic digesters configuration. However, UASB reactors operating in mesophilic conditions are generally reported to have an efficiency in the range 64 – 87 % treating municipal wastewater [17], in agreement with COD removal observed in this study. Indeed, these results are comparable with COD degradation percentage determined by Wirth et al. [14] for AF treating PW derived by HTC on municipal sludge. They reported values of COD removal of about 75 – 100 % in mesophilic conditions, pointing out that COD over time could be strongly affected by microbial growth, sorption processes, and sludge formation [14]. These COD removal percentages are in agreement with other studies performing differently anaerobic digestion on PW derived by HTC on sludge. Indeed, specific soluble COD removal efficiency of 78 – 86 % are reported for batch anaerobic digestion tests on PW derived by HTC on digested and dewatered sludge [13].

4.3.3 VFA, TN, TAN and pH

The concentrations of acetic, propionic and isovaleric acids (expressed as mg COD L^{-1}) in the effluent, together with the ratio between the sum of the three VFAs and SCOD, from phase IV, are presented in **Fig. 3.5**. Indeed, from this stage onwards, a relevant percentage of PW was added (40 % of PW as COD), which could lead to an AD process inhibition. Therefore, it became necessary to measure VFA concentration in the effluent, in order to evaluate the stability of AD process.

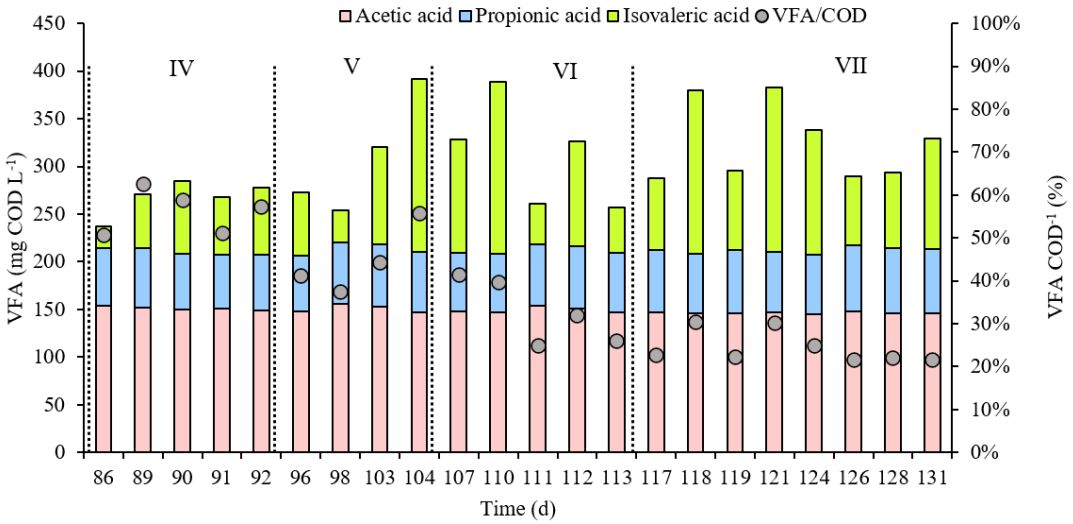

Figure 3.5 Acetic, propionic and isovaleric acids profile over time in the effluent of UASB reactor.

The VFA profile remained rather constant over time. Only isovaleric acid increased its concentration in some cases, starting from phase V. The ratio between VFA and COD decreased over time, with the increasing percentage of PW added in the feeding. It might suggest that the non-biodegradable COD content increased with the addition of PW, and consequently the ratio VFA COD^{-1} decreased significantly. Even though butyric, caproic/isocaproic, and valeric acids were not measured during this experiment, the VFA concentration (expressed as the sum of acetic, propionic, and isovaleric acid in mgCOD L^{-1}) resulted in all cases lower than 400 mgCOD L^{-1}. Typically, it is not easy to define a *normal* VFA level into a reactor [33], since many variables (e.g. type of feedstock, reactor configuration, and operating conditions) must be considered. However, the VFA concentrations detected appeared do not appear to be inhibitory for the AD process studied.

Fig. 3.6 shows the concentrations in both influent and effluent of TN (TN_{in} and TN_{out}, respectively) and TAN (TAN_{in} and TAN_{out}, respectively).

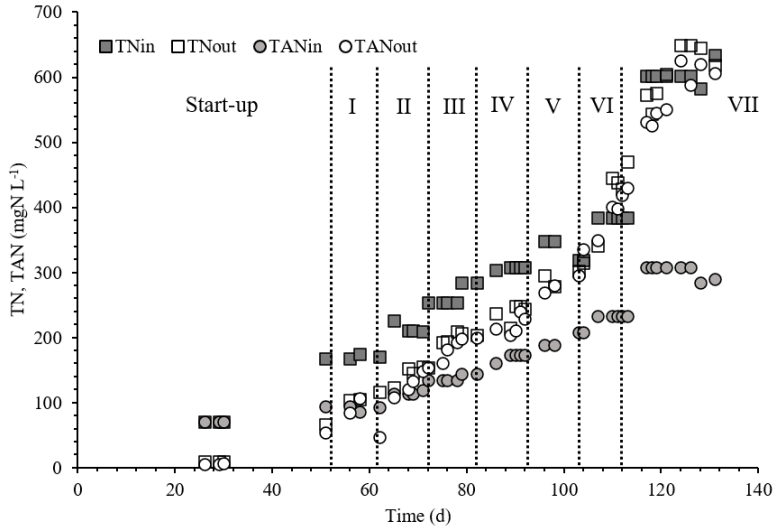

Figure 3.6 Total nitrogen (TN) and total ammonia nitrogen (TAN) concentrations into the influent and the effluent of UASB reactor**.**

TN_{in} and TAN_{in} are introduced into the UASB reactor via a macro-nutrient solution in addition to PW, which contains both. The TN and TAN content increased with the progressive addition of PW. Since both $N\text{-}NO_3^-$ and $N\text{-}NO_2^-$ concentration are negligible in PW (**Tab. 3.1**), the difference between TN and TAN was mainly organic N. TN_{out} is almost coincident in the most of cases with TAN_{out}, indicating that the whole N in the effluent was found in the form of ammonia. TN was removed from start-up to stage V, with decreasing removal efficiency with the addition of PW (from 87 to 10 %). Conversely, in the last two stages of the experiment, TN_{out} resulted higher than TN_{in}. Losses in TN balance may be linked to the formation of free ammonia (FAN) in gas phase, which could occur at operational conditions of 35 °C and pH in the range of 7 – 8.5 on the basis of TAN concentration [34]. Thus, TN resulted strongly dependent by feeding composition. Further, TAN_{out} is in almost all cases higher than TAN_{in}. The increase in TAN concentration might find explanation in the degradation of N-containing organic matter [16]. Indeed, in phase VII, TAN_{out} reached values in the range 526 – 625 mgN L^{-1}, while TAN_{in} concentration was around 300 mgN L^{-1}. However, TAN concentration was maintained lower than inhibitory range reported in literature of 1.7 – 14 g L^{-1} [16, 35].

The pH of the influent and the effluent remained slightly basic over time, varying between 7.2 – 8.4, whereas the alkalinity was not measured.

4.3.4 Microbial and granulometric analysis community

From microbial analysis emerged that Bacteria were the most abundance domain (> 94 %) in all samples. Further, a percentage of ~ 4 % of Archaea was detected in biomass granules sampled during phases V – VII. More in detail, Halobacterota represents the main phylum of Archaea (around 85 %) in all samples collected during phases V – VII, while the remaining biomass was identified in the phylum of Euryarcheota. More thoroughly, the latter resulted to be mainly composed of the genus of *Methanobacterium* (> 93 %), while the most abundant Halobacterota genus was *Methanosaeta* (> 84 %).

In **Fig. 4.7** is reported the phyla classification of bacteria.

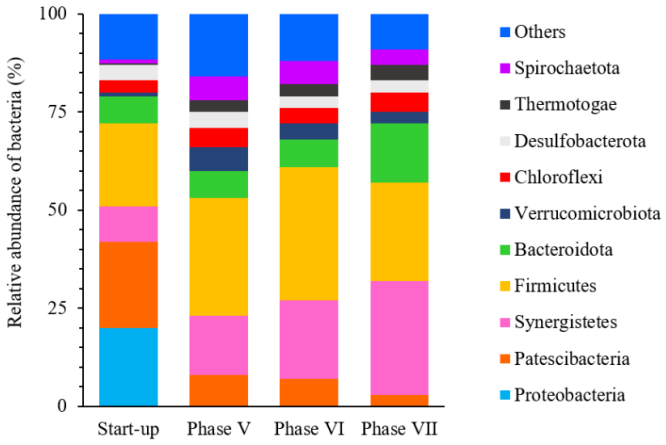

Figure 4.7 Bacterial structure community (phylum level) of UASB biomass collected during start-up period, and during phases V, VI, and VII.

As can be observed in **Fig. 4.7**, Proteobacteria (20 %), Patescibacteria (22 %) and Firmicutes (21 %) were the most abundant phyla into the biomass during the start-up period. A significant relative abundance of Proteobacteria into the inoculum was observed also by Doloman et al. [36] running an UASB reactor for microalgal and sodium acetate treatment. In subsequent samples collected during phases V – VII, Proteobacteria disappeared completely, while Patescibacteria

strongly decreased their abundance (> 3 % in phase VII). At the same time, the relative abundance of Firmicutes increased over time (with a maximum of 34 % at phase VI), together with Synergistetes and Bacteroidota phyla, which accounted 29, and 15 %, respectively, at phase VII. Small abundance of Chloroflexi (~ 5 %) was detected in samples collected during phase V – VII. A similar bacterial structure of granules (Firmicutes, Synergistetes, Bacteroidota, and Chloroflexi) was described also by Liu et al. [16] running an UASB reactor treating PW derived from HTC on SS. Each bacterial phylum is associated to a specific function in anaerobic digesters: Bacteroidota, Chloroflexi, and Firmicutes have a fundamental role into the conversion of the organic matter, while Synergistetes are mainly responsible for methane production [16, 37, 38]. Further, Thermotogae phylum increased over time, accounting a percentage equal to 0.4 % during the start-up period up to an abundance of 4 % during Phase VII. Their presence was already reported during mesophilic AD [39].

In **Fig. 4.8** the particle size distributions of granules at the beginning and at the end of the experiment is reported.

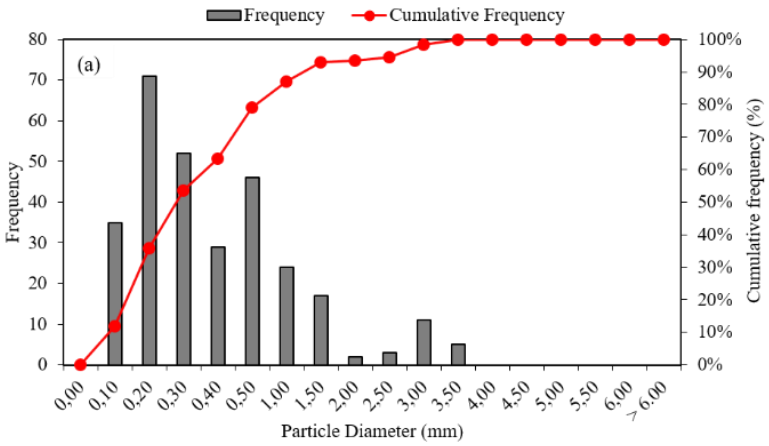

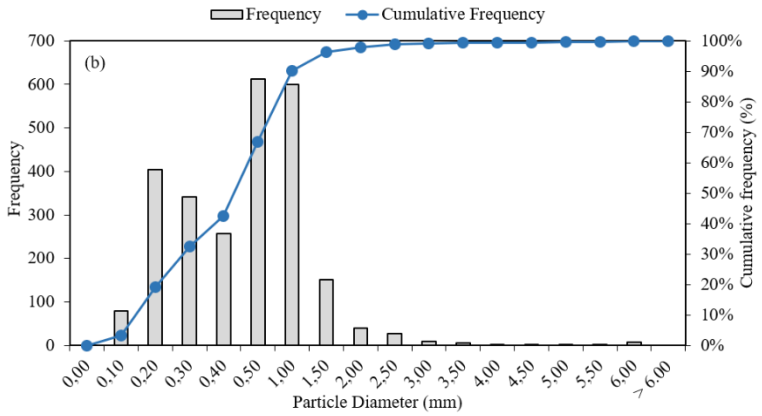

Figure 4.8 Particle size distribution of granules at the beginning (Day 0) (a) and at the end of the experiment (Day 131) (b).

The characteristics diameters D10, D50, and D90 of granules at Day 0 were 178, 371, and 1655 µm, respectively. Further, at the end of the experiment, D10, D50, and D90 were equal to 232, 584, and 1477 µm, respectively. As can be observed in **Fig. 4.8**, the particle size distribution changed comparing the granulometric curves at Day 0 and at Day 131. Particularly, the D50 indicated that the 50 % of particles was characterized by a diameter smaller than 371 µm at Day 0, and smaller than 584 µm at Day 131. Thus, it suggested that the average particle size of granules increased over time. Further, the granulometric distribution resulted mostly comprised into the range (0.1 – 1.50 mm) at Day 131, while a diversified distribution can be observed for granules at Day 0 (0.1 – 3.5 mm). The distribution described at the end of the experiment was comparable to that reported for a full-scale UASB reactor treating a slaughterhouse wastewater [40]. They reported a particle size distribution of 0.6 – 1.5 mm, which could be associated to a dynamic balance between growing and decaying processes [40].

4.4 Conclusions

In this study, the treatment of PW from HTC-treated SS with a constant OLR of 5 gCOD L^{-1} d^{-1} was evaluated in a UASB reactor for 131 days. The strategy to start-up the reactor with glucose alone, increasing progressively the percentage of PW on a COD basis over time proved to be

effective. High experimental specific CH_4 productions were observed over time, although these values resulted in some cases in appreciable differences with the theoretical ones. The UASB reactor resulted in high COD removal percentage (73 %) operating with only PW as a feeding, in agreement with the COD fraction removed AD batch tests (89 %) on the same substrate. The COD removal efficiency linearly decreased with the addition of PW, while no VFAs accumulation was observed over time, indicating the absence of inhibitory phenomena. TAN in the effluent increased over time with the addition of PW, however maintaining the concentration below the inhibition condition. Firmicutes, Synergistetes, Bacteroidota, and Chloroflexi were identified are the most abundant bacterial microorganisms in granules, which showed a particle size distribution included into the range 0.1 – 1.50 mm. Therefore, all the monitored parameters agreed in identifying UASB as a promising technology to valorize PW through anaerobic digestion. Nevertheless, future research could test the removal of PW dilution, in addition to also macro- and micro- nutrients.

4.5 References – Chapter 4

1. Zhang, J. hong, Lin, Q. mei, Zhao, X. rong: The hydrochar characters of municipal sewage sludge under different hydrothermal temperatures and durations. J. Integr. Agric. 13, 471–482 (2014). https://doi.org/10.1016/S2095-3119(13)60702-9
2. Libra, A.J., Kammann, C., Funke, A., Berge, N.D., Neubauer, Y., Titirici, M.-M., Fuhner, C., Bens, O., Kern, J., Emmerich, K.-H.: Hydrothermal carbonization of biomass residuals : A comparative review of the chemistry , processes and appolications of wet and dry pyrolysis. 2, 89–124 (2011). https://doi.org/10.4155/bfs.10.81
3. Benavente, V., Fullana, A., Berge, N.D.: Life cycle analysis of hydrothermal carbonization of olive mill waste: Comparison with current management approaches. J. Clean. Prod. 142, 2637–2648 (2017). https://doi.org/10.1016/j.jclepro.2016.11.013
4. Gupta, D., Mahajani, S.M., Garg, A.: Effect of hydrothermal carbonization as pretreatment on energy recovery from food and paper wastes. Bioresour. Technol. 285, 121329 (2019). https://doi.org/10.1016/j.biortech.2019.121329
5. Owsianiak, M., Ryberg, M.W., Renz, M., Hitzl, M., Hauschild, M.Z.: Environmental Performance of Hydrothermal Carbonization of Four Wet Biomass Waste Streams at Industry-Relevant Scales. ACS Sustain. Chem. Eng. 4, 6783–6791 (2016). https://doi.org/10.1021/acssuschemeng.6b01732
6. Zhao, P., Shen, Y., Ge, S., Yoshikawa, K.: Energy recycling from sewage sludge by

producing solid biofuel with hydrothermal carbonization. Energy Convers. Manag. 78, 815–821 (2014). https://doi.org/10.1016/j.enconman.2013.11.026

7. Kelessidis, A., Stasinakis, A.S.: Comparative study of the methods used for treatment and final disposal of sewage sludge in European countries. Waste Manag. 32, 1186–1195 (2012). https://doi.org/10.1016/j.wasman.2012.01.012

8. Villamil, J.A., Mohedano, A.F., Martín, J.S., Rodriguez, J.J., Rubia, M.A. De: Anaerobic co-digestion of the process water from waste activated sludge hydrothermally treated with primary sewage sludge . A new approach for sewage sludge management. Renew. Energy. 146, 435–443 (2020). https://doi.org/10.1016/j.renene.2019.06.138

9. Gerner, G., Meyer, L., Wanner, R., Keller, T., Krebs, R.: Sewage sludge treatment by hydrothermal carbonization: Feasibility study for sustainable nutrient recovery and fuel production. Energies. 14, (2021). https://doi.org/10.3390/en14092697

10. Kim, D., Lee, K., Park, K.Y.: Hydrothermal carbonization of anaerobically digested sludge for solid fuel production and energy recovery. Fuel. 130, 120–125 (2014). https://doi.org/10.1016/j.fuel.2014.04.030

11. Aragón-briceño, C., Ross, A.B., Camargo-valero, M.A.: Evaluation and comparison of product yields and bio-methane potential in sewage digestate following hydrothermal treatment. Appl. Energy. 0–1 (2017). https://doi.org/10.1016/j.apenergy.2017.09.019

12. Villamil, J.A., Mohedano, A.F., Rodriguez, J.J., de la Rubia, M.A.: Valorisation of the liquid fraction from hydrothermal carbonisation of sewage sludge by anaerobic digestion. J. Chem. Technol. Biotechnol. 93, 450–456 (2018). https://doi.org/10.1002/jctb.5375

13. Ahmed, M., Andreottola, G., Elagroudy, S., Negm, M.S., Fiori, L.: Coupling hydrothermal carbonization and anaerobic digestion for sewage digestate management: Influence of hydrothermal treatment time on dewaterability and bio-methane production. J. Environ. Manage. 281, 111910 (2021). https://doi.org/10.1016/j.jenvman.2020.111910

14. Wirth, B., Reza, T., Mumme, J.: Influence of digestion temperature and organic loading rate on the continuous anaerobic treatment of process liquor from hydrothermal carbonization of sewage sludge. Bioresour. Technol. 198, 215–222 (2015). https://doi.org/10.1016/j.biortech.2015.09.022

15. Weide, T., Brügging, E., Wetter, C.: Anaerobic and aerobic degradation of wastewater from hydrothermal carbonization (HTC) in a continuous, three-stage and semi-industrial system. J. Environ. Chem. Eng. 7, (2019). https://doi.org/10.1016/j.jece.2019.102912

16. Liu, S., Wang, Y., Guo, J., Wang, W., Dong, R.: Start-up and performance evaluation of upflow anaerobic sludge blanket reactor treating supernatant of hydrothermally treated municipal sludge: Effect of initial organic loading rate. Biochem. Eng. J. 166, 107843 (2021). https://doi.org/10.1016/j.bej.2020.107843

17. Dutta, A., Davies, C., Ikumi, D.S.: Performance of upflow anaerobic sludge blanket (UASB) reactor and other anaerobic reactor configurations for wastewater treatment: A comparative review and critical updates. J. Water Supply Res. Technol. - AQUA. 67, 858–884 (2018). https://doi.org/10.2166/aqua.2018.090

18. Mainardis, M., Buttazzoni, M., Goi, D.: Up-flow anaerobic sludge blanket (Uasb) technology for energy recovery: A review on state-of-the-art and recent technological advances. Bioengineering. 7, (2020). https://doi.org/10.3390/bioengineering7020043

19. Lucian, M., Volpe, M., Merzari, F., Wüst, D., Kruse, A., Andreottola, G., Fiori, L.: Hydrothermal carbonization coupled with anaerobic digestion for the valorization of the organic fraction of municipal solid waste. Bioresour. Technol. 314, 123734 (2020). https://doi.org/10.1016/j.biortech.2020.123734

20. APHA (American Public Health Association): APHA Standard methods for examination of water and wastewater. (2005)

21. ISO: Water quality — Determination of the chemical oxygen demand index ISO 15705. (2002)

22. CNR, IRSA: 5040 Carbonio organico disciolto. APAT Man, 29. 3, (2003)

23. CNR IRSA: 4060 Azoto totale e fosforo totale. APAT Man, 29. (2003)

24. CNR IRSA: 4020 Determinazione di anioni (fluoruro, cloruro, nitrito, bromuro, nitrato, fosfato e solfato) mediante cromatografia ionica. APAT Man, 29. (2003)

25. CNR IRSA: 4050 Azoto nitroso. APAT Man, 29. (2003)

26. United States Environmental Protection Agency: EPA Method 350.1 - Determination of ammonia nitrogen by semi-automated colorimetry. (1993)

27. Environmental Protection Agency: 3580A Waste dilution. (1992)

28. Environmental Protection Agency: 8260D Volatile Organic Compounds by Gas Chromatography/Mass Spectrometry (GC/MS), (2018)

29. CNR IRSA: 2060 pH. APAT Man, 29. (2003)

30. Baldi, F., Pecorini, I., Iannelli, R.: Comparison of single-stage and two-stage anaerobic co-digestion of food waste and activated sludge for hydrogen and methane production. Renew. Energy. 143, 1755–1765 (2019). https://doi.org/10.1016/j.renene.2019.05.122

31. Valero, D., Montes, J.A., Rico, J.L., Rico, C.: Influence of headspace pressure on methane production in Biochemical Methane Potential (BMP) tests. Waste Manag. 48, 193–198 (2016). https://doi.org/10.1016/j.wasman.2015.11.012

32. Vu, H.P., Nguyen, L.N., Wang, Q., Ngo, H.H., Liu, Q., Zhang, X., Nghiem, L.D.: Hydrogen sulphide management in anaerobic digestion: A critical review on input control, process regulation, and post-treatment. Bioresour. Technol. 346, 126634 (2022). https://doi.org/10.1016/j.biortech.2021.126634

33. Franke-Whittle, I.H., Walter, A., Ebner, C., Insam, H.: Investigation into the effect of high concentrations of volatile fatty acids in anaerobic digestion on methanogenic communities. Waste Manag. 34, 2080–2089 (2014). https://doi.org/10.1016/j.wasman.2014.07.020

34. Yenigün, O., Demirel, B.: Ammonia inhibition in anaerobic digestion: A review. Process

Biochem. 48, 901–911 (2013). https://doi.org/10.1016/j.procbio.2013.04.012

35. Chen, Y., Cheng, J.J., Creamer, K.S.: Inhibition of anaerobic digestion process: A review. Bioresour. Technol. 99, 4044–4064 (2008). https://doi.org/10.1016/j.biortech.2007.01.057

36. Doloman, A., Soboh, Y., Walters, A.J., Sims, R.C., Miller, C.D.: Qualitative Analysis of Microbial Dynamics during Anaerobic Digestion of Microalgal Biomass in a UASB Reactor. Int. J. Microbiol. 2017, (2017). https://doi.org/10.1155/2017/5291283

37. Krakat, N., Schmidt, S., Scherer, P.: Potential impact of process parameters upon the bacterial diversity in the mesophilic anaerobic digestion of beet silage. Bioresour. Technol. 102, 5692–5701 (2011). https://doi.org/10.1016/j.biortech.2011.02.108

38. St-Pierre, B., Wright, A.D.G.: Comparative metagenomic analysis of bacterial populations in three full-scale mesophilic anaerobic manure digesters. Appl. Microbiol. Biotechnol. 98, 2709–2717 (2014). https://doi.org/10.1007/s00253-013-5220-3

39. Nesbø, C.L., Dlutek, M., Zhaxybayeva, O., Doolittle, W.F.: Evidence for existence of "mesotogas," members of the order Thermotogales adapted to low-temperature environments. Appl. Environ. Microbiol. 72, 5061–5068 (2006). https://doi.org/10.1128/AEM.00342-06

40. Del Nery, V., Pozzi, E., Damianovic, M.H.R.Z., Domingues, M.R., Zaiat, M.: Granules characteristics in the vertical profile of a full-scale upflow anaerobic sludge blanket reactor treating poultry slaughterhouse wastewater. Bioresour. Technol. 99, 2018–2024 (2008). https://doi.org/10.1016/j.biortech.2007.03.019

Chapter 5

Environmental Life Cycle Assessment of hydrothermal carbonization of sewage sludge and its products valorization pathways

This Chapter has been submitted for publication in a modified and revised version by the authors:

G. Mannarino[a], S. Caffaz[b], R. Gori[a], L. Lombardi[c]

[a] Department of Civil and Environmental Engineering, University of Florence, via di S. Marta 3, 50139 Florence (Italy)

[b] Publiacqua SpA, Via Villamagna 90/c, 50126, Florence, Italy

[c] Niccolò Cusano University, Via Don Carlo Gnocchi, 3, 00166 Rome, Italy

Abstract

This study is aimed at evaluating through Life Cycle Assessment (LCA) the environmental performances of an integrated system of an existing Water Resources Recovery Facility (WRRF) and a hypothetical hydrothermal carbonization (HTC) plant applied to the generated sewage sludge (SS). Beside the valorisation of the solid product (hydrochar, HC) as a fuel substituting lignite, the possibility to valorize also the liquid fraction (process water, PW) derived by the HTC, by anaerobic digestion to produce biogas, is here proposed and analysed. Additionally, phosphorus recovery from HC, prior its use, by acid leaching with nitric acid is also suggested and evaluated. Thus, four integrated scenarios, based on SS carbonization, are proposed and compared with the current SS treatment, based on composting outside of the WRRF (Benchmark scenario).

The proposed scenarios, based on HTC, show improved performances with respect to the benchmark one, for thirteen of sixteen considered impact indicators.

For the Climate Change (CC) indicator, the two HTC scenarios are able to reduce the impacts up to – 98 %, with respect to the Benchmark. Further, the introduction of anaerobic digestion of PW proves to reduce impacts more than other configurations in eleven on sixteen impact categories. On the contrary, the introduction of phosphorus recovery process negatively affects the values for most of indicators. Thus, possible solutions to improve the integration of this process are outlined (e.g., the use of sulfuric acid instead of nitric one, or the application of a different ratio between solid and acidified solution during acid leaching of HC to recover phosphorus).

Statement of novelty

The novelty of this study relies in the evaluation of the environmental sustainability of HTC technology to treat sewage sludge (SS) at industrial scale, including some modifications with respect to the basic HTC process, namely the valorisation of the process water (PW), by anaerobic digestion, and recovery of the phosphorus (P) contained in the HC. Results are useful to understand the environmental sustainability of these specific modifications (PW anaerobic digestion is always beneficial, while P recovery deteriorates the environmental performance of the overall process), but more generally it is stressed the importance of evaluating innovative technologies at the early stage of development, also proposing alternatives, to obtain larger environmental benefits.

5.1 Introduction

Scientific research in sustainable technologies and renewable energies is becoming of increasing relevance year by year. Because of the exploitation of fossils resources, new solutions are urgently needed, with the perspective to achieve the EU goal of net-zero greenhouse gas (GHGs) emissions by 2050 [1, 2]. Specifically in wastewater sector, innovative, safe and environmentally friendly strategies have to be found. Indeed, sewage sludge (SS), which is the main by-product of Water Resources Recovery Facilities (WRRF), needs a proper and careful management, since, besides the importance of health and environmental protection, a considerable amount of GHGs is produced by its treatment and disposal [3].

In this framework, hydrothermal carbonization (HTC) is gaining attention as suitable technology to treat SS. During HTC, the feedstock is heated up to mild temperature (150 – 250 °C) under autogenic pressure (up to 20 bars) and in subcritical water conditions. Within short retention time (1 - 12 hours), the biomass in converted in three fractions: a solid-coal matrix (hydrochar, HC), a liquid fraction (process water, PW) and a small amount of gas (mainly composed by CO_2) [4]. Its main advantage is the ability to process biomass with a high moisture content (75 – 99 %) (such as SS) without any pre-treatments [5]. Therefore, it becomes straightaway to think to an integration of HTC in SS treatment line of WRRFs. Indeed, even though HTC is not so new, its application to SS has been proposed only in the last few years, as it is demonstrated by the increasing number of scientific publications starting from 2008 [1].

It is extremely interesting to answer the interrogative about the effective environmental advantage of the HTC application, as well as the benefit from an economic viewpoint. Some studies already evaluated the environmental performance of HTC on SS through life cycle assessment (LCA). Specifically, Medina-Martos et al. [6] compared through LCA the environmental performances of two alternative scenarios for SS treatment. The first one expects the standalone anaerobic digestion (AD) of a mixture of secondary and primary SS, while the second one includes HTC of secondary SS combined with AD of both primary SS and PW derived by HTC process. They found that the integrated strategy generally reduces the environmental impacts, in comparison with the sole AD configuration, thanks to the valorization of HC, able to replace fossil fuels. Further, the recovery of PW by anaerobic co-digestion with primary sewage sludge allows minimizing the impact of liquid fraction, whose treatment generally imposes a relevant environmental load [7]. Further, other LCA studies support the sustainability of HTC in comparison to other technologies to treat SS [8, 9]. In detail, HTC treatment on SS (anaerobically digested) proved to save more CO_2 emissions than mono-incineration, in particular using HC for energy purpose instead of in agriculture/horticulture [8]. Further, HTC process for anaerobically digested and dewatered SS treatment resulted in better environmental performances than co-

incineration with municipal solid waste, landfill and mono-incineration according to Wang et al. [9]. Finally, another work reported that the no advantages in global warming potential (GWP) are offered by HTC process on SS (both digested and non-digested) in comparison with its direct agricultural and energy valorization in German conditions [10].

It is worth pointing out that some LCA studies evaluated the environmental performances of the application of HTC on different types of feedstocks (e.g., food waste, garden/green waste, poultry litter and olive pomace) [11–14]. All the aforementioned studies are in agreement to identify the attractive role of HTC in biowaste treatment. However, the direct comparison among these different LCA studies is challenging, due to several factors, such as operational HTC conditions, feedstock, valorization pathways, assumptions and system boundary.

It is well note that P is a key nutrient essential resource for organism growth in nature and its recovery is necessary. Indeed, since 2017 it is listed among critical raw materials by EU commission, due to its scarcity in Europe [15]. Several studies investigated acid leaching of P from HC at laboratory scale, concluding that P recovery is concretely efficient [16–18]. However, from LCA perspective, the environmental performance of P recovery from HC derived by HTC of the organic fraction of municipal solid waste seems not very convenient [18], being the assumed P extraction process the limiting factor to achieve sustainable environmental performances, pointing out the necessity to optimize this process.

The novelty proposed in the present study relies in the introduction of P recovery process, in addition to HTC, to a SS treatment line of a WRRF. Moreover, the contribution of this study is to evaluate the environmental performance of a complete integrated system between SS treatment line, HTC process, AD of PW and P recovery from HC and to point out its potential application on a real scale.

In this study, the LCA is carried out in reference to an Italian case study WRRF - San Colombano WRRF (Florence), managed by Publiacqua SpA. The selected WRRF is a conventional activated

sludge plant with a modified Ludzack-Hettinger process for N removal, chemical P precipitation and anaerobic digestion for sludge stabilization and can be therefore considered representative of state-of-the art of large WRRFs in EU. The current SS treatment line of the plant processes only secondary SS, since the primary settling is by-passed due to a low C/N ratio in the influent. San Colombano treats mainly urban wastewater of Florence and surroundings and it is the biggest WRRF in Tuscany for capacity (600 000 population equivalent and SS production of 17 066 t y^{-1} on wet basis as average value of 2017-2018). Specific data about equipment and consumptions of SS treatment line are available at the time of writing and therefore used in this study. Digested SS are presently sent outside of the plant for final treatment, namely composting with other substrates, representing the current situation. In addition, four further scenarios are hypothesized integrating the HTC, two of which also including P recovery process. Data about HTC, anaerobic digestion of PW and P recovery process are gained by experimental work, on the specific substrates, and specifically used in this study.

5.2 Materials and methods

The LCA is developed according to the phases identified by ISO 14040:2006 (ISO, 2006) and ISO 14044:2006 (ISO, 2006): goal and scope definition, inventory analysis, impact assessment and interpretation (reported in Section 3).

5.2.1 Goal and scope

The aim of this study is to carry out an environmental comparison of the following five scenarios of SS treatment:

- *Benchmark scenario:* anaerobic digestion of SS, representing the current situation; the digested sludge is sent for composting elsewhere
- *HTC scenario*: anaerobic digestion of SS and further local HTC of digested sludge
- *HTC + AD scenario*: anaerobic digestion of SS, further local HTC and final anaerobic digestion of PW

- *HTC + AD + P_{dry} scenario:* anaerobic digestion of SS, further local HTC and final anaerobic digestion of PW; P recovery from dried HC through acid leaching with HNO_3
- *HTC + AD + P_{wet} scenario:* anaerobic digestion of SS, further local HTC and final anaerobic digestion of PW; P recovery from wet HC through acid leaching with HNO_3.

5.2.2 System boundaries and plant process layout

System boundaries of the five treatment scenarios include the thermochemical HTC process, the energy production from biogas, the dewatering treatment of HC solid fraction, the AD of PW, the P recovery process, and the final treatment by aerobic post-composting (where expected). In order to provide a wider picture of the treatment systems and their impacts, and to account for the small modifications that apply when HTC is integrated, the upstream SS treatment line, starting from secondary SS and including the SS anaerobic digestion, is also accounted for in all five scenarios. Inventory data of HC yield, biogas production from PW and its composition, as well as P recovery from HC, are retrieved from experimental data. Assumptions for each of the previously mentioned scenario are deeply illustrated in the following and compared with literature values (given in detail in the inventory).

Within the system boundaries, the production processes for utilities, fuels, chemicals and manufactured materials entering the processes and the related generated emissions are included. CO_2 emissions from the combustion of biogas and HC, HTC and the composting process are of biogenic origin and assumed not contributing to Global Warming [19]. The treatment of produced wastewater supernatant from pre-treatments and dewatering stages is considered and included within the system. However, the possible nutrients contribution of supernatants to SS treatment line, once recirculated in the WRRF, is excluded from the analysis.

Impacts caused by the construction of plants and auxiliary machines are not included within the system boundaries, since they are assumed to be relatively low [19].

Recovered materials or energy produced as by-products, specifically HC, compost, P, thermal energy (TE), and electric energy (EE) are accounted for by expanding the system boundaries to

include avoided primary productions due to material and/or energy recovered from SS. Particularly, the energy produced by the PW anaerobic digestion process is credited assuming it displaces EE and TE produced through an internal combustion engine (ICE). Concerning HC, P and compost, it is assumed that they can replace lignite and fertilisers, as better detailed in the inventory.

Calculations are performed for the total flow rate of produced SS, equal to 1477 m^3 d^{-1}. However, the functional unit adopted for the comparison is the treatment of 1 t of SS, characterized by total solids (TS) and total volatile solids (TVS) contents equal to 0.9 % as wet weight and 56% of TS on dry basis respectively, which represents the average value obtained in the year 2020 from the monitoring activity carried out by the plant operators.

Background data for fuels, chemicals and manufactured materials, avoided materials and energy (lignite, heat, fertilizers, etc.), and for wastewater treatment are retrieved from the database Ecoinvent 3.6 [20].

5.2.3 Inventory analysis

In this phase, mass and energy flows across system boundary are evaluated to quantitively describe the studied systems. Current real data about San Colombano SS treatment line is provided by the study case plant, while information about HTC reactor, process water AD and P recovery from hydrochar are collected from experimental laboratory tests and in some cases from literature. Details are also provided in the **Appendix A2**.

5.2.3.1 Benchmark scenario

In the Benchmark scenario (**Fig. 5.1**), secondary SS is firstly thickened by centrifugation and then it is sent to the anaerobic digesters with the organic loading rate (OLR) and the specific gas production (SGP) indicated in **Tab. 5.1** and derived from real operation data (year 2020), in agreement with literature values for sludge [21]. Before AD, a dosage of ferrous chloride ($FeCl_2$) into the sludge is accounted, promoting ferrous sulphide (FeS) precipitation to avoid the hydrogen sulphide (H_2S) formation in the biogas. Therefore, no SO_2 emissions are considered from biogas

combustion. Digestate is then dewatered by centrifugation, adding polyelectrolyte, and then it is processed by composting outside Tuscany region, according to the information provided by Publiacqua, considering a transportation distance equal to 300 km. Composting emissions are accounted for CH_4 and N_2O and equal to 2.9 $kg_{CO2\ eq.}\ t^{-1}_{dry\ sludge}$ and 0.2 $kg_{CO2\ eq.}\ t^{-1}_{dry\ sludge}$, respectively [22].

The produced biogas is mainly recovered in a boiler to produce TE for digesters heating. However, the biogas only partially covers the digesters thermal energy demand. From the data provided by the plant, an average value around 4 % of biogas is combusted in a flare (as excess in some period of the year), while natural gas is withdrawn from national grid when the biogas is not sufficient (average annual consumption equal to 8 % of produced biogas). Emission factors for a boiler powered by natural gas for NO_x, CO, PM, and VOC are taken into account [23] for both biogas and natural gas combustion. CH_4 losses are also considered: losses from biogas plant, assuming an average value of 3.7 % [24], and losses of biogas flare, considering a value equal to 1 % [25]. A specific rate of solid removal for the composting process is assumed, together with a specific EE consumption of composting process (**Tab. 5.1**).

Main operational parameters and assumptions are reported in **Tab. 5.1**, while EE and TE consumptions of the system are provided by the study case plant.

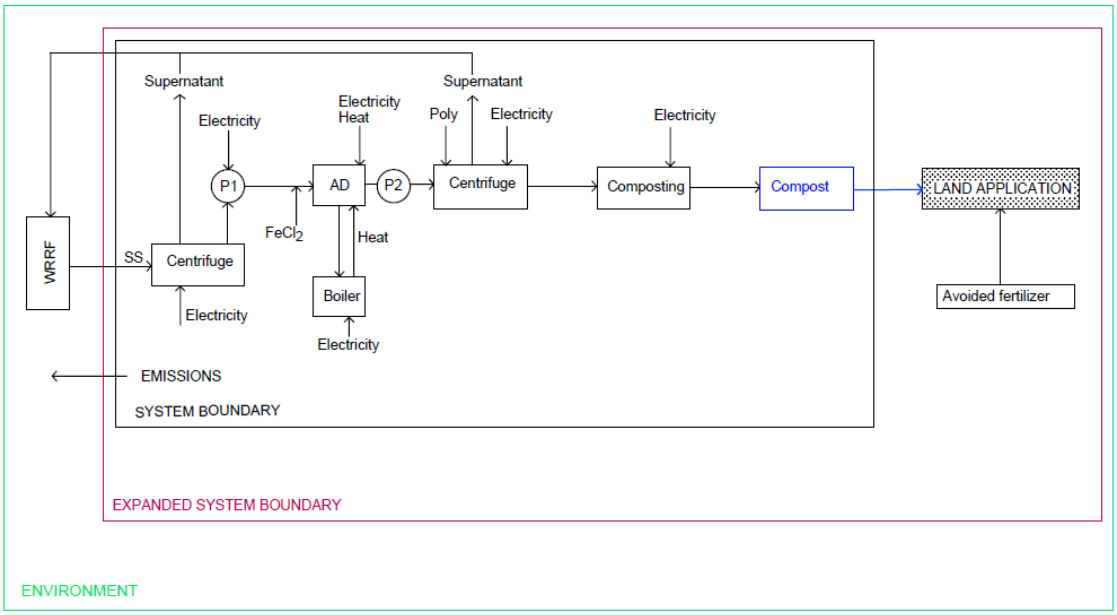

Figure 5.1 Scheme of the Benchmark scenario.

Table 5.10 Operating parameters for the Benchmark scenario

Parameters related to material streams			
Q_{out} yield respect to the incoming SS of first thickening (Centrifuge 1)	27	vol %	5a
TS after SS first centrifuge	4	wt %	5a
$FeCl_2$ consumption	0.05	kg $t^{-1}_{wet\ sludge\ in}$	5a
Digester volume	4800	m^3	5a
Number of digesters	3	-	5a
HRT (hydraulic retention time)	36	d	5a
OLR (organic loading rate)	0.53	kg TVS $m^{3\text{-}1}$ d^{-1}	5a
SGP (specific gas production)	0.21	m^3 kg TVS^{-1}_{fed}	5a
CH_4 content in biogas	64	vol %	5a
Q_{out} yield respect to the incoming SS of second centrifuge	15	vol %	5a
TS after SS second centrifuge	20	wt %	5a

Polyelectrolyte consumption for digestate	1.3	$kg_{poly}\ t^{-1}_{digestate}$	[5a]
TS removal yield during composting	70	%	[26]
Parameters related to energy streams			
EE consumption SS treatment line	2.55	$kWh\ t^{-1}_{sludge\ in}$	[5a]
Specific EE self-consumption from boiler	0.42	$\frac{kWh}{Nm^{3\ -1}_{produced}}$	[23]
TE consumption SS treatment line	0.88	$kWh\ t^{-1}_{sludge\ in}$	[5a]
Lower Heating Value (LHV) CH_4	9.78	$kWh\ Nm^{3-1}$	-
Boiler efficiency	85	%	[27]
Specific EE consumption for composting	70	$kWh\ t^{-1}_{TSdigestate}$	[28]

[5a] Data provided by the plant.

5.2.3.2 HTC scenario

In the HTC scenario (**Fig. 5.2**), an integration between the existing SS treatment line of San Colombano WRRF and HTC process is proposed, considering a hypothetical industrial layout. According to laboratory data on HTC, digested SS is supposed to enter the HTC reactor with a TS content of 15 wt %. Thus, a 6 % of the centrifuge inlet flow by-passes the centrifuge itself and then it is mixed with the exiting stream, to reach the desired solid concentration. Mass balance of the HTC process is carried out according to C yield (%) derived by laboratory data (see **Paragraph A2.1.1** of the **Appendix A2** for details). In the hypothetical industrial layout, digested SS is pre-heated up to 200°C before entering into the continuous HTC reactor, passing through a heat exchanger in which the hot solid-liquid mixture (slurry) out of HTC is recirculated. Thus, SS is further heated up the operational temperature, assumed 220°C, by a heater – externally fired - and then processed by the HTC unit. The reactor is sized as a continuous one, able to assure the required reaction time (85 min). TE is supplied to the HTC reactor as well, to balance the heat losses. Hence, exiting slurry is sent to a filter press for HC and PW separation. HC is dried to

remove the residual moisture and then pelletized to be easily stored, while PW is supposed to be recirculated into a WRRF to be treated (inventoried according to the appropriate ecoinvent process). Main operational parameters and assumptions are reported in **Tab. 5.2**, while EE and TE consumptions of the system are calculated as reported in detail in **Paragraph A2.1.2** of the **Appendix A2.** The TE required for the externally fired heater and for the HTC reactor heating is supplied by natural gas combustion. The produced HC is assumed to be sent for energy recovery to an external user. HC valorization depends on its lower heating value (LHV), which was equal to 8.1 MJ $kg^{-1}_{dry\ HC}$ (see **Chapter 1** for HHV formula; the LHV was calculated from that value but excluding the contribute of water heat vaporization).

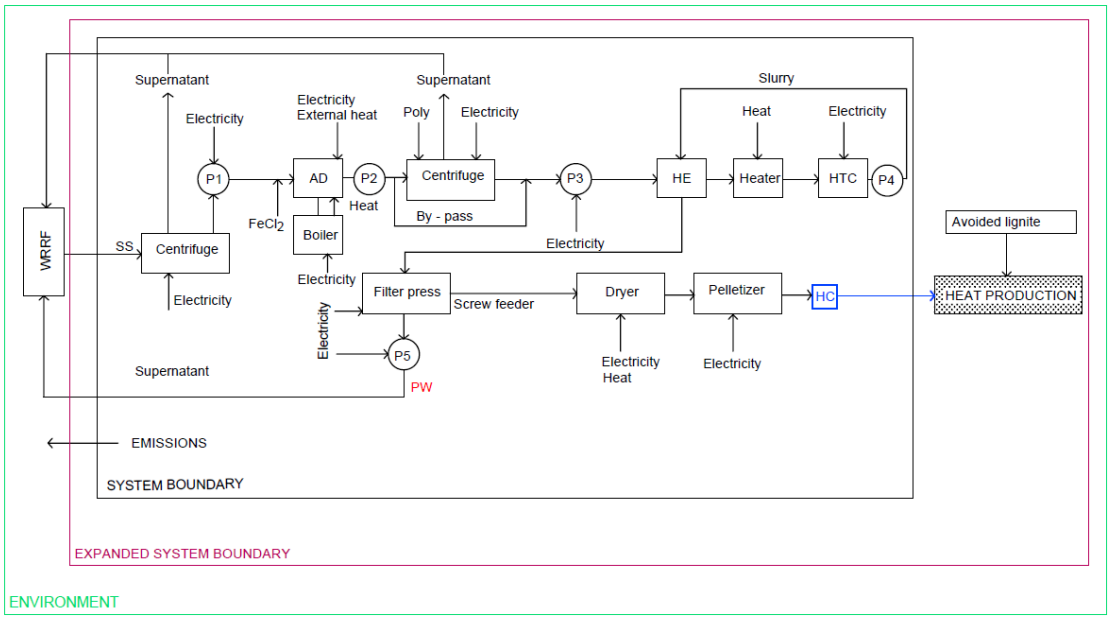

Figure 5.2 Scheme of the HTC scenario.

Table 5.11 Operating parameters for the HTC scenario

Parameters related to material streams			
C_{sludge}	22.5	wt %	**Chapter 3**
C_{HC}	19.4	wt %	**Chapter 3**
C_{PW}	13600	$mg_{TOC}\ L^{-1}$	**Chapter 3**

CO_2 in gas phase during HTC	92	vol %	[29]
CO in gas phase during HTC	8	vol %	[29]
TS_{HC} after filter press	60	wt %	[30]
HC yield	76.6	wt %	**Chapter 3**
TS_{PW}	4	wt %	[16]
TS_{HC} after drying	92	wt %	[30]
Parameters related to energy streams			
Time $_{HTC}$	85	min	**Chapter 3**
Temperature $_{HTC}$	220	°C	**Chapter 3**
Specific EE filter press	45	kWh $t^{-1}_{dry\ HC}$	[30]
Specific EE pelletizer	51	kWh $t^{-1}_{dry\ HC}$	[31]

5.2.3.3 HTC+AD scenario

In HTC+AD scenario, SS treatment line, HTC, and slurry post-treatments are exactly the same assumed in the previous scenario. The only difference relies in PW treatment. In this scenario, PW is anaerobically treated in a dedicated anaerobic digester. Process scheme is the same depicted in **Fig. 5.2,** but PW, after anaerobic digestion, is directly sent to a centrifuge to separate supernatant from digestate (**Fig. 5.3**). The first one is then directed to a WRRF to be treated, while the digestate is treated by composting. Assumptions about composting are the same described for the Benchmark scenario. The specific methane production of PW is obtained by experimental anaerobic digestion tests, resulting in agreement with specific CH_4 production reported in literature for AD on process water derived by HTC on digested SS [32, 33]. Biogas produced during AD of PW is valorized into an ICE to produce both EE and TE (efficiencies equal to 39 and 42 %, respectively). The ICE stack emissions (NO_x, CO, particulate matter) are calculated according to Asunis et al [34]. CO_2 emissions from biogas combustion are not considered, since carbon is generated by a renewable carbon source. CH_4 fugitive emissions of AD process are

assumed equal to 3.7 % of the produced biogas [24]. Main PW characteristics and operational parameters are reported in **Table 5.3,** while detailed information about EE and TE consumptions of the system are described in **Paragraph A2.2.2** of the **Appendix A2**. Composting process of digestate is inventoried similarly to the previous case.

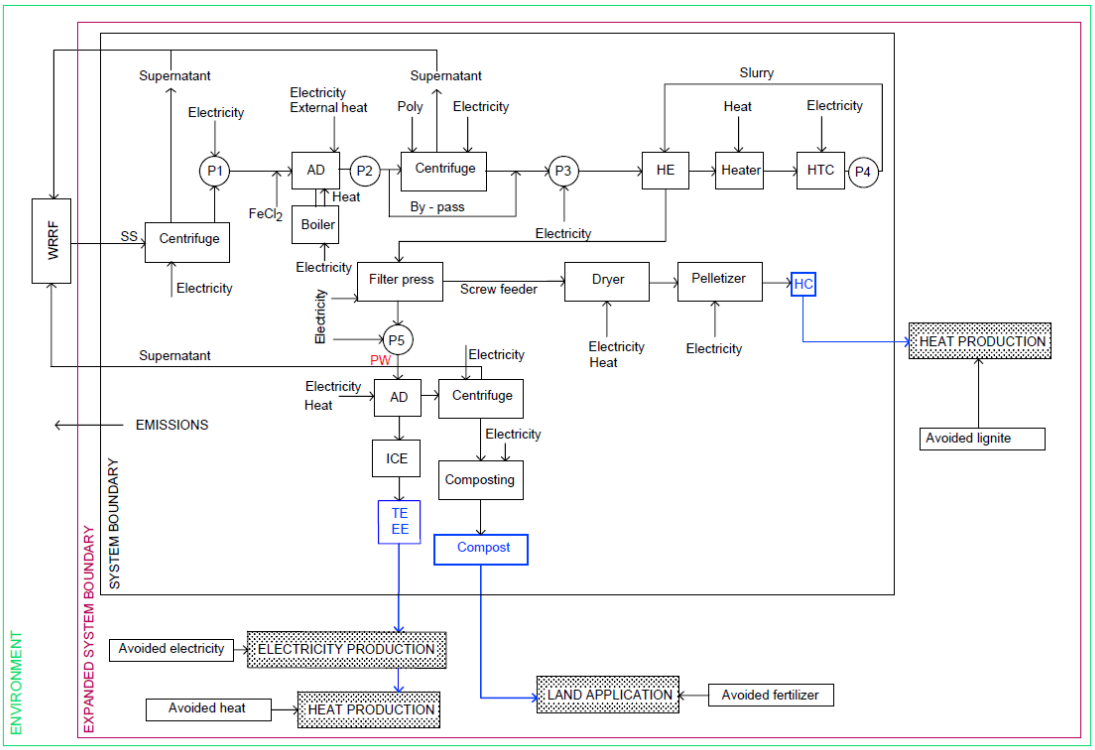

Figure 5.3 Scheme of the HTC + AD scenario.

Table 5.12 Operating parameters for HTC + AD scenario.

Parameters related to material streams			
COD	31000	mg L^{-1}	**Chapter 3**
SMP (specific methane production)	0.192	Nm^3 CH_4 $kg^{-1}COD_{fed}$	**Chapter 3**
CH_4 content in biogas	71	vol %	**Chapter 3**
$TS_{digestate}$	2	wt %	**Chapter 3**

Specific polyelectrolyte consumption	18	kg t^{-1}_{TS}	[35]
TS_{out} centrifuge	20	wt %	[35]
Parameters related to energy streams			
Specific EE centrifuge	5	kWh t^{-1}	[35]

5.2.3.4 HTC + AD + P_{dry} scenario

In the HTC + AD + P_{dry} scenario (**Fig. 5.4**), P recovery from dried HC is introduced. Here, acid leaching with nitric acid (HNO_3) in water is proposed to recover P from HC. Thus, the process scheme is exactly the same depicted in the previous scenario, except for post-treatments of HC after drying. In this scenario, dried HC is directly sent to a grinder to homogenize the sample. Then, it is directed to a mixer, where HNO_3 acid and water are added to HC, to leach P from solid fraction to the liquid phase. Quantity of HNO_3 acid and water are assumed according to laboratory conditions (**Tab. 5.4** and **Paragraph A2.3.1** of the **Appendix A2**). P experimentally recovered resulted equal to 78 % of P retained in HC, in agreement with P yield reported in literature [17, 36]. Acidified suspension is then separated by a filter press and HC is dried and pelletized. Experimental data and EE consumptions, as well as TE requirements are described in detail in **Paragraph A2.3.2** of the **Appendix A2**. In **Tab. 5.4** the main assumptions are reported. The separated P leachate is assumed to be used directly in agricultural land, even though post treatments and/or fertilizers production processes are generally recommended [37].

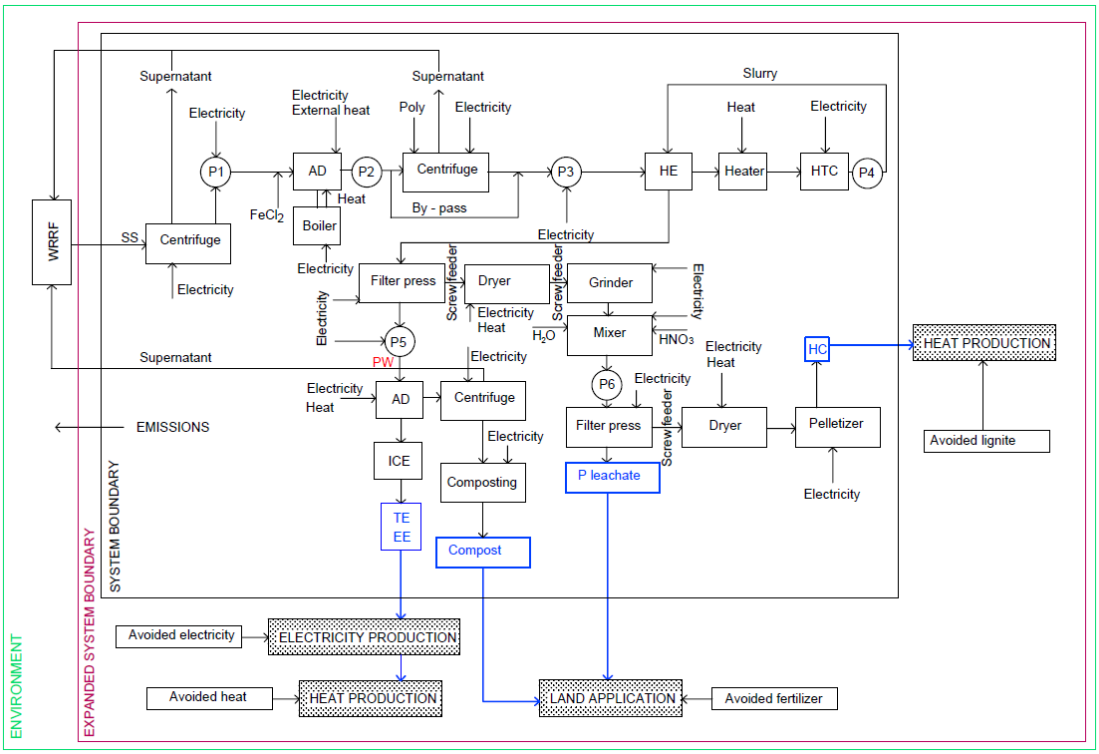

Figure 5.4 Scheme of the HTC + AD + P_{dry} scenario.

Table 5.13 Operating parameters for the HTC + AD + P_{dry} scenario

Parameters related to material streams			
HNO_3 title	65	%	**Chapter 2**
HNO_3 HC_{dry}^{-1} ratio	0.30	mL HNO_3 g^{-1}_{dryHC}	**Chapter 2**
Solid solution^{-1} ratio	5	%	**Chapter 2**
Time of mixing during leaching	240	min	**Chapter 2**
HC mass loss after leaching	17	%	**Chapter 2**
Parameters related to energy streams			
Specific EE grinder	16	kWh t^{-1}	[38]

5.2.3.5 HTC + AD + P_{wet} scenario

In HTC + AD + P_{wet} scenario, P recovery from wet HC is included. After slurry separation by filter press in PW and HC, the latter (TS equal to 60 %) is directly sent to P recovery process. P

recovery steps are exactly the ones described above, with similar considerations for each unit. Nevertheless, only a single dryer is considered in this scenario, since HC is not dried before P recovery process (**Fig. 5.5**). Therefore, TE requirements are reduced. Details on calculations are reported in **Paragraphs A2.4.1** and **A2.4.2** of the **Appendix A2.**

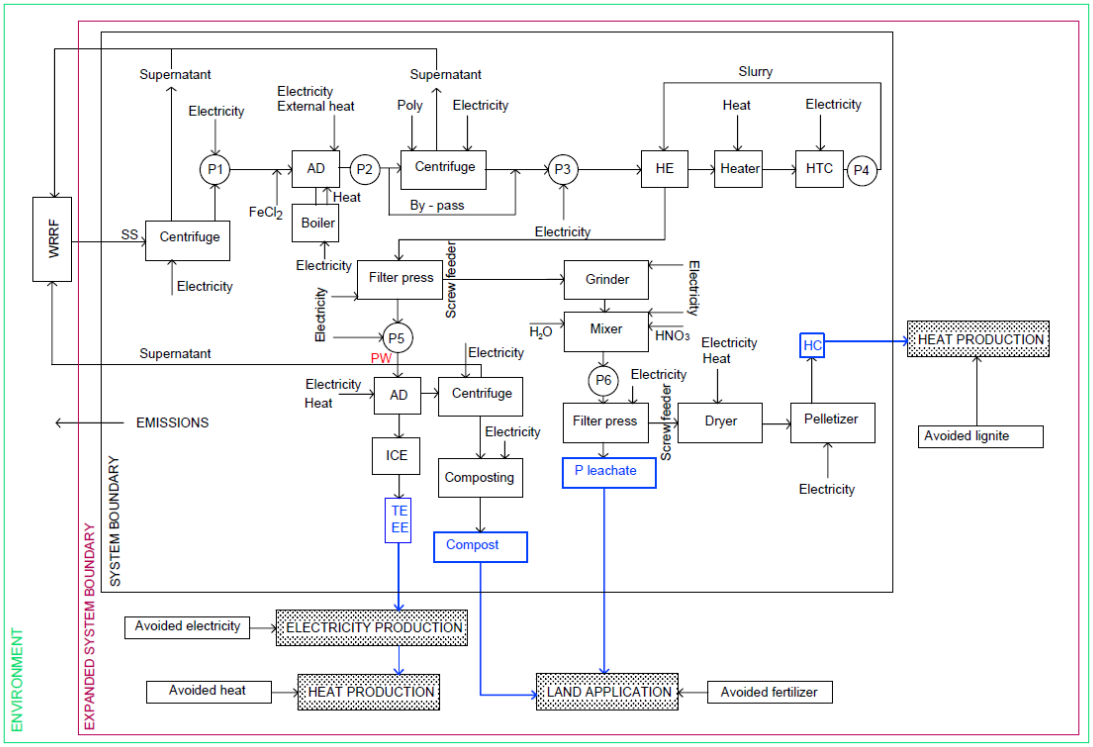

Figure 5.5 Scheme of the HTC + AD + P_{wet} scenario.

5.2.4 Summary of inputs/outputs

The following table (**Tab. 5.5**) reports the inputs/outputs quantitative flows for the investigated scenarios expressed per functional unit (1 t of SS).

Table 5.14 Input/output quantitative flows for each investigated process and sub-process.

			Benchmark	*HTC*	*HTC + AD*	*HTC + AD + P_{dry}*	*HTC + AD + P_{wet}*
SS treatment line	Electric energy	kWh $t^{-1}_{sludge\ in}$	3.011	3.011	3.011	3.011	3.011
	Thermal energy [5b]	kWh $t^{-1}_{sludge\ in}$	0.879	0.879	0.879	0.879	0.879
	$FeCl_2$	kg $t^{-1}_{sludge\ in}$	4.67E-02	4.67E-02	4.67E-02	4.67E-02	4.67E-02
	Polyelectrolyte	kg $t^{-1}_{sludge\ in}$	3.60E-01	3.38E-01	3.38E-01	3.38E-01	3.38E-01
	Wastewater to WRRF	m^3 $t^{-1}_{sludge\ in}$	0.960	0.946	0.946	0.946	0.946
	NOx emission	kg $t^{-1}_{sludge\ in}$	3.13E-03	3.13E-03	3.13E-03	3.13E-03	3.13E-03
	CO emission	kg $t^{-1}_{sludge\ in}$	9.40E-04	9.40E-04	9.40E-04	9.40E-04	9.40E-04
	Biogenic CO_2 emission	kg $t^{-1}_{sludge\ in}$	1.43E+00	1.43E+00	1.43E+00	1.43E+00	1.43E+00
	PM emission	kg $t^{-1}_{sludge\ in}$	8.50E-05	8.50E-05	8.50E-05	8.50E-05	8.50E-05
	VOC emission	kg $t^{-1}_{sludge\ in}$	6.15E-05	6.15E-05	6.15E-05	6.15E-05	6.15E-05
	CH_4 emission	kg $t^{-1}_{sludge\ in}$	3.12E-02	3.12E-02	3.12E-02	3.12E-02	3.12E-02
HTC process	Electric energy	kWh $t^{-1}_{sludge\ in}$	0	0.085	0.085	0.085	0.085
	Thermal energy	kWh $t^{-1}_{sludge\ in}$	0	1.681	1.681	1.681	1.681
	Biogenic CO_2 emission	kg $t^{-1}_{sludge\ in\ in}$	0	4.57E-02	4.57E-02	4.57E-02	4.57E-02
	CO emission	kg $t^{-1}_{sludge\ in}$	0	2.53E-03	2.53E-03	2.53E-03	2.53E-03
Filter press + Dryer + Pelletizer	Electric energy	kWh $t^{-1}_{sludge\ in}$	0	0.750	0.750	0.697	0.667
	Thermal energy	kWh $t^{-1}_{sludge\ in}$	0	6.105	6.105	6.105	5.041
	Wastewater to WRRF	m^3 $t^{-1}_{sludge\ in}$	0	0.043	0	0	0
P recovery process	Electric energy	kWh $t^{-1}_{sludge\ in}$	0	0	0	0.473	0.386
	Water	kg $t^{-1}_{sludge\ in}$	0	0	0	113.067	113.067
	HNO_3 solution	kg $t^{-1}_{sludge\ in}$	0	0	0	1.650	1.650
	Water solution	kg $t^{-1}_{sludge\ in}$	0	0	0	0.888	0.888
	Thermal energy	kWh $t^{-1}_{sludge\ in}$	0	0	0	5.041	0.386
Avoided Lignite from HC	Avoided lignite (HC)	kWh $t^{-1}_{sludge\ in}$	0	13.481	13.481	13.481	13.481

Avoided P from leachate	P-rich leachate (avoided P)	kg P t^{-1} $_{sludge\ in}$	0	0	0	0.258	0.258
Process water AD	Electric energy	kWh $t^{-1}_{sludge\ in}$	0	0	0.037	0.037	0.037
	Thermal energy	kWh $t^{-1}_{sludge\ in}$	0	0	0.115	0.115	0.115
	NOx emission	kg $t^{-1}_{sludge\ in}$	0	0	1.73E-04	1.73E-04	1.73E-04
	CO emission	kg $t^{-1}_{sludge\ in}$	0	0	2.87E-04	2.87E-04	2.87E-04
	Biogenic CO_2 emission	kg $t^{-1}_{sludge\ in}$	0	0	4.83E-01	4.83E-01	4.83E-01
	PM emission	kg $t^{-1}_{sludge\ in}$	0	0	6.61E-06	6.61E-06	6.61E-06
	CH_4 emission	kg $t^{-1}_{sludge\ in}$	0	0	6.75E-03	6.75E-03	6.75E-03
Avoided energy from process water AD	Avoided thermal energy	kWh $t^{-1}_{sludge\ in}$	0	0	1.011	1.011	1.011
	Avoided electric Energy	kWh $t^{-1}_{sludge\ in}$	0	0	0.939	0.939	0.939
Centrifuge	Electric energy	kWh $t^{-1}_{sludge\ in}$	0	0	0.212	0.212	0.212
	Wastewater to WRRF	m^3 t^{-1} $_{sludge\ in}$	0	0	0.038	0.038	0.038
Composting	Electric energy	kWh $t^{-1}_{sludge\ in}$	0.547	0	0.057	0.057	0.057
	CH_4 emission	kg $t^{-1}_{sludge\ in}$	1.85E-04	0	1.91E-05	1.91E-05	1.91E-05
	N_2O emission	kg $t^{-1}_{sludge\ in}$	1.57E-06	0	1.63E-07	1.63E-07	1.63E-07
	Biogenic CO_2 + H_2O emission	kg $t^{-1}_{sludge\ in}$	3.52E+01	0	3.63E+00	3.63E+00	3.63E+00
	Transport	tkm t^{-1} $_{sludge\ in}$	1.17E+01	0	1.21 E+00	1.21E+00	1.21E+00
Avoided fertilizer from composting	Avoided fertilizer (as N)	kg $t^{-1}_{sludge\ in}$	0.0751	0	0.0133	0.0133	0.0133
	Avoided fertilizer (as P_2O_5)	kg $t^{-1}_{sludge\ in}$	0.2289	0	0.0056	0.0056	0.0056
	Avoided fertilizer (as K_2O)	kg $t^{-1}_{sludge\ in}$	0.0045	0	0.0012	0.0012	0.0012

[5b] it refers to the net consumed energy from the national gas grid

5.2.5 System expansion

HC production is calculated equal to 0.63 $t_{dry\ HC}\ t^{-1}_{dry\ sludge\ in}$ for both HTC and HTC + AD scenarios, and equal to 0.52 $t_{dry\ HC}\ t^{-1}_{dry\ sludge\ in}$ for both HTC + AD + P_{dry} and HTC + AD + P_{wet}, respectively. Indeed, 17% mass loss is registered after leaching for P extraction. However, the LHV of the HC after leaching similarly increases by the same percentage, keeping substantially constant the energy content between the entering and exiting streams (13.481 kWh $t^{-1}_{sludge\ in}$).

The produced HC is assumed to be used entirely as bio-fuel, substituting a similar solid fuel, lignite, which is displaced on equivalent basis of energy content. Hence, the production of this amount of lignite is prevented (production process gained from ecoinvent) together with the related CO_2 emissions from combustion of lignite (thus assuming that the other emissions from combustion of lignite and HC are the same, mainly depending on the type of combustion device) [23]. The stoichiometric factor equal to 2.02 kg CO_2 per kg lignite is used for the climate change (CC) impact calculation.

The EE produced from biogas in AD of PW is assumed to be recovered into the national grid, while the TE is directed to a thermal user close to the plant, displacing heat generated by natural gas boilers [23]. The TE produced by biogas through AD of secondary SS is recovered to satisfy the energy requirement of anaerobic digesters in sludge treatment line. However, it is not sufficient to cover the whole heat demand. Hence, natural gas is withdrawn from national grid when the biogas is not sufficient. The appropriate ecoinvent record for TE is selected.

For the compost produced by aerobic stabilization of SS in the Benchmark scenario, a typical distribution of nutrients from direct chemical analysis of a sample of anaerobically digested SS provided by the plant is considered: 32 g N kg TS^{-1}, 98 g P_2O_5 kg TS^{-1} and 2 g K_2O kg TS^{-1}. For digestate derived by AD of process water in HTC + AD, HTC + AD + P_{dry} and HTC + AD + P_{wet} scenarios, a nutrient distribution is assumed based on literature (for K_2O content) [39] and on the stoichiometric elemental composition of biomass (for N and P_2O_5 content) [40]: 55 g N kg TS^{-1}, 23 g P_2O_5 kg TS^{-1} and 5 g K_2O kg TS^{-1}. Compost is assumed to be used in substitution of mineral

fertiliser with the same nutrients content (93%) or without any replacement (7%) [41]. For N fertilizer, P fertilizer and K fertilizer, the proper ecoinvent records are used.

For P extracted from HC by acid leaching, the substitution of P fertilizer is assumed (considering the appropriate ecoinvent record). Indeed, even though information about acid leachate composition is scarce, especially regarding metals content, recovered P in solution is assumed to be applied on land, exploiting its fertilizer potential.

From thickening and dewatering processes, supernatant rich in nutrients is obtained, which is recirculated to the biological oxidation tanks of the WRRF and then treated (according to the proper ecoinvent process) [23]. N and P contained in supernatant could provide nutrients, increasing their content into secondary SS, and subsequently into the produced digestate. However, since data are extremely variable and no complete information are available about these parameters, no other advantage on the compost produced is considered for this specific case study.

5.2.6 Impact assessment method

The Environmental Footprint (EF) 3.0 method [42] developed by the Joint Research Centre of European Commission, is selected to perform the Life Cycle Impact Assessment (LCIA), with its 16 impact categories: Climate change (CC) in kg CO2 eq.; Ozone depletion (OD) in kg CFC-11 eq.; Ionising radiation (IR) in kBq U235 eq.; Photochemical ozone formation (POF) in kg NMVOC eq.; Particulate matter (PM) in disease incidence; Human toxicity, non-cancer (HT_{nc}) in CTU_h (Comparative Toxic Unit for humans); Human toxicity, cancer (HT_c) in CTU_h; Acidification (A) in mol H+ eq.; Eutrophication, freshwater (E_f) in kg P eq.; Eutrophication, marine (E_m) in kg N eq.; Eutrophication, terrestrial (E_t) in mol N eq.; Ecotoxicity, freshwater (ET_f) in CTU_e (Comparative Toxic Unit for ecosystems); Land use (LU) in pt (soil quality index); Water use (WU) in m3 deprived; Resource use, fossils (RU_f) in MJ; Resource use, minerals and metals (RU_{mm}) in kg Sb eq. In the classification phase, all the material and energy flows of the inventory phase are identified according to their contribution to each impact category. The EF indicators calculation is performed using Simapro software, version 9.1.1.1, applying an adapted method,

which is not suitable for conducting the EF-compliant studies, but can be used for other assessments. In this study, normalization and weighting steps are not carried out.

5.2.7 Sensitivity analysis

The sensitivity analysis is generally performed to evaluate how specific key values assumed in the inventory could influence the impact assessment results. Regarding HC derived by HTC process, its yield varies in a wide range, depending on initial SS characteristics as well as the severity of HTC conditions [43]. Moreover, combustion properties of HC (e.g., higher/lower calorific value) are generally affected by several parameters of HTC process and by feedstock characteristics [44, 45].

Thus, a combination of HC yield and LHV - named for this specific section as energy recovery (ER) - is evaluated, as reported in **equation 5.1**:

$$\text{ER (kJ kg}^{-1}_{\text{dry sludge}}) = \frac{Y_{HC}}{100} \cdot \text{LHV}_{HC} \quad (5.1)$$

where Y_{HC} is the hydrochar yield on dry basis (wt %) [46] and LHV_{HC} is the lower heating value of HC (kJ kg^{-1}_{dryHC}), calculated on the basis of HC elemental analysis [47].

Thus, at laboratory scale, five different SS anaerobically/aerobically stabilized from five WRRFs in Tuscany treating mainly municipal wastewater, were previously processed in the same HTC operational conditions here proposed (220 °C, 85 min, TS of 15 %), in addition to SS derived from the WRRF case study. Then, the couples of parameters resulting in the highest and in the lowest ER values are chosen in order to establish the range of sensitivity (**Tab. 5.6**). The minimum ER value corresponds to the parameters of the base case study. The sensitivity analysis is carried out through a Monte Carlo simulation, generating random outcomes of the ER value (1000 samples each), using a normal distribution.

Table 5.15 Sensitivity analysis range according to ER value.

Range	Y_{HC} (%)	LHV (kJ kg_{dryHC}^{-1})	ER (kJ $kg_{\ dry\ sludge}^{-1}$)
Minimum	76.60	8105	6208
Maximum	74.68	21 231	15855

5.3 Results and Discussion

LCA results are reported in the following sections according to the adapted EF 3.0 method. Further, the sensitivity analysis is described with respect to the ER parameter, as defined previously (**equation 5.1**).

5.3.1 Impact assessment

Tab. 5.7 shows the results of impact assessment expressed per functional unit (1 t of secondary SS entering into the SS treatment line on wet basis) for each investigated scenario.

Table 5.16 Results of impacts assessment for each indicator and for each investigated scenario.

Impact category	Unit	*Benchmark*	*HTC*	*HTC + AD*	*HTC + AD + P_{dry}*	*HTC + AD + P_{wet}*
Climate Change (CC)	kg CO_2 eq. $t^{-1}_{sludge\ in}$	4.77E+00	2.58E-01	**7.76E-02**	6.52E+00	4.88E+00
Ozone depletion (OD)	kg CFC-11 eq. $t^{-1}_{sludge\ in}$	9.14E-07	8.65E-07	**8.23E-07**	1.16E-06	9.93E-07
Ionising radiation (IR)	kBq U^{235} eq. $t^{-1}_{sludge\ in}$	2.86E-01	2.23E-01	1.90E-01	1.79E-01	**1.53E-01**
Photochemical ozone formation (POF)	kg NMVOC eq. $t^{-1}_{sludge\ in}$	1.47E-02	1.11E-02	**1.09E-02**	2.31E-02	2.15E-02
Particulate matter (PM)	disease incidence $t^{-1}_{sludge\ in}$	1.49E-07	9.80E-08	**1.00E-07**	1.95E-07	1.87E-07
Human toxicity, non cancer (HT_{nc})	CTU_h $t^{-1}_{sludge\ in}$	**7.37E-08**	7.65E-08	7.41E-08	8.38E-08	7.93E-08
Human toxicity, cancer ($HT_{c)}$	CTU_h $t^{-1}_{sludge\ in}$	**1.85E-09**	2.63E-09	2.50E-09	2.48E-09	2.26E-09
Acidification (A)	mol H^+ eq. $t^{-1}_{sludge\ in}$	1.63E-02	1.63E-02	**1.49E-02**	4.10E-02	3.91E-02
Eutrophication, freshwater (E_f)	kg P eq. $t^{-1}_{sludge\ in}$	1.23E-03	-1.09E-02	-1.10E-02	**-1.13E-02**	**-1.13E-02**
Eutrophication, marine (E_m)	kg N eq. $t^{-1}_{sludge\ in}$	2.36E-02	2.03E-02	**2.01E-02**	2.46E-02	2.43E-02
Eutrophication, terrestrial (E_t)	mol N eq. $t^{-1}_{sludge\ in}$	5.45E-02	3.98E-02	**3.89E-02**	1.43E-01	1.39E-01
Ecotoxicity, freshwater (ET_f)	CTU_e $t^{-1}_{sludge\ in}$	2.41E+02	2.50E+02	**2.41E+02**	3.58E+02	3.49E+02
Land use (LU)	pt $t^{-1}_{sludge\ in}$	7.28E+01	5.55E+01	**4.87E+01**	1.19E+02	1.15E+02
Water use (WU)	m^3 deprived $t^{-1}_{sludge\ in}$	3.29E-01	5.50E-01	**3.25E-01**	5.99E+00	5.93E+00
Resource use, fossils (RU_f)	MJ $t^{-1}_{sludge\ in}$	5.67E+01	1.83E+01	**1.21E+01**	4.63E+01	2.31E+01
Resource use, minerals and metals (RU_{mm})	kg Sb eq. $t^{-1}_{sludge\ in}$	**3.10E-05**	4.83E-05	4.51E-05	6.62E-05	6.23E-05

As can be observed in **Tab. 5.7**, the Benchmark scenario has better environmental performances than other configurations for three of sixteen indicators. In eleven cases on sixteen, the HTC + AD scenario provides the lowest impacts, whereas HTC + AD + P_{wet} scenario result the best configuration in the IR impact category (- 46 % with respect to the Benchmark). Further, HTC + AD + P_{wet} and HTC + AD + P_{dry} show the same impacts in case of E_f, both of which result in the lowest impacts.

Specifically, about WU category, HTC + AD + P_{dry} and HTC + AD + P_{wet} scenarios are extremely affected by the amount of water required by P acid leaching, resulting in higher impacts than all the other scenarios. In case of RU_{mm}, for the above-mentioned scenarios, the beneficial effect of SS composting, in terms of impacts, is higher than the advantage to recover P from HC. Further, avoided impacts of lignite from HC and of both EE and TE from anaerobic digestion of PW are negligible.

Thanks to HC recovery through lignite displacement and to the biogas valorization from PW through an ICE, the environmental profiles of HTC + AD scenario generally show the best environmental performances. Thus, concerning CC, HTC + AD results in an impact reduction of –98 % respect to the Benchmark scenario. The reduction of CO_2 emissions for an integrated configuration of HTC and AD, in comparison with the standalone AD, is found also in another work [6]. For CC, HTC + AD + P_{wet} shows an impact increase respect to the Benchmark equal to + 2 %, and equal to + 37 % in case of HTC + AD + $P_{dry.}$

Nevertheless, in case of HTC + AD + P_{dry} and HTC + AD + P_{wet}, the avoided impact of lignite is generally not sufficient to mitigate the direct impacts of the P recovery process. For example, in case of Acidification, these scenarios result in worst performance than Benchmark (equal to +151 %, and +139 %, respectively).

Furthermore, E_f is the only category for which the Benchmark scenario results overall in a positive impact, whereas all the others show negative scores. P recovery process slightly contributes to

reduce the impacts, while the main avoided contribution derives from the HC valorization. HTC, HTC + AD, HTC + AD + P_{dry} and HTC + AD + P_{wet} show a reduction of impacts with respect to the Benchmark scenario equal to -986, -995, -1015 and -1021 %, respectively.

As a rule, P recovery results in worst environmental profiles than other scenarios, suggesting that this process should be optimized to obtain better performances. Similar conclusions are reported by Oliver-Tomas et al. [18], whose investigation is about the environmental performances of P recovery from HC derived by HTC of organic fraction of municipal solid waste (OFMSW). Indeed, also in that study, P extraction proved to be the main limitation of the process environmental profile. However, in case of IR impact category, both HTC + AD + P_{dry} and HTC + AD + P_{wet} results in lower impacts than the other scenarios due to the displacement of P and lignite.

More detailed considerations about contribution analysis are given in the following paragraphs.

5.3.1.1 Climate change (CC)

Fig. 5.6 shows the contribution of sub-processes to CC in each scenario. For Benchmark, HTC and HTC + AD scenarios, the highest contribution to direct impacts (as positive values) is given by SS treatment line, accounting the 69, 31 and 28 % of total impact, respectively. In the Benchmark scenario, composting contribution (as positive direct impact) represents the 23 % of the total impact, while nutrients replacement (as avoided impact) accounts for -8 %. For HTC and HTC+AD scenarios, HTC process (which contains TE, EE, CO_2 and CO emissions) considering also the dewatering steps (filter-press, dryer and pelletizer) account around the 20 % of total impact in both cases, whereas the lignite replacement represents a percentage equal to -49 and -45 % of total impact, respectively. Concerning scenarios with anaerobic digestion of PW, avoided EE and TE recovered by biogas represents only around the -4 % on total impact, against a 2 % direct emissions of AD process. The avoided fertilizer from digestate composting derived by anaerobic digestion of PW negligibly contributes to the avoided impacts. In case of HTC + AD + P_{dry} and HTC + AD + P_{wet} scenarios, the highest contribution to direct impact is given by P

recovery process, which accounts for 33 and 29 % on the total impact, respectively. Otherwise, the avoided impact of P displacement is not really appreciable, since its contribution results equal to -2 % in both cases. However, the avoided impact of lignite contributes to about the -30 % in both scenarios with P recovery.

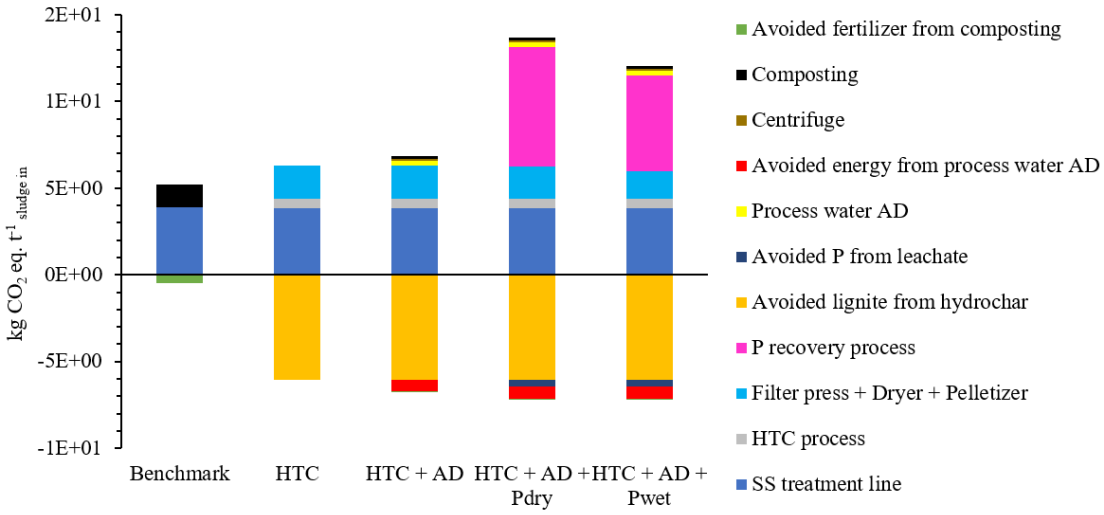

Figure 5.6 Sub-processes contribution for CC impact category.

5.3.1.2 Ionising radiation (IR)

In **Fig. 5.7** the contribution of sub-processes to IR in each scenario is reported. SS treatment line represents the highest direct impact for all the investigated scenarios, accounting a percentage of total impact equal to +55, +58, +50, +34, and +35 % for Benchmark, HTC, HTC + AD, HTC + AD + P_{dry}, and HTC + AD + P_{wet} scenario, respectively. Among the avoided impacts, the lignite replacement from HC production represents the highest contribution in case of HTC and HTC + AD, accounting a percentage of total impact equal to -28, and -24 %, respectively. In case of HTC + AD + P_{dry} and HTC + AD + P_{wet} the avoided impacts of HC results equal to about -17 % in both cases. Further, the avoided impact of P displacement in both scenarios (-17 % on total impacts) are balanced by the direct contributions of the P recovery process itself. However, all scenarios with HTC result in better environmental profile than Benchmark. Indeed, in the reference scenario, the avoided impact of fertilizer (-24 % on total impact) can not sufficiently balance the

direct contribution of SS treatment line and composting. The avoided EE and TE produced by valorization of biogas of PW anaerobic digestion through an ICE represent -9 % on total impact in case of HTC + AD scenario, while they account about -6 % in case of HTC + AD + P_{dry}, and HTC + AD + P_{wet}. Direct impacts of anaerobic digestion of PW result in negligible contribution on total impact for all scenarios (where expected).

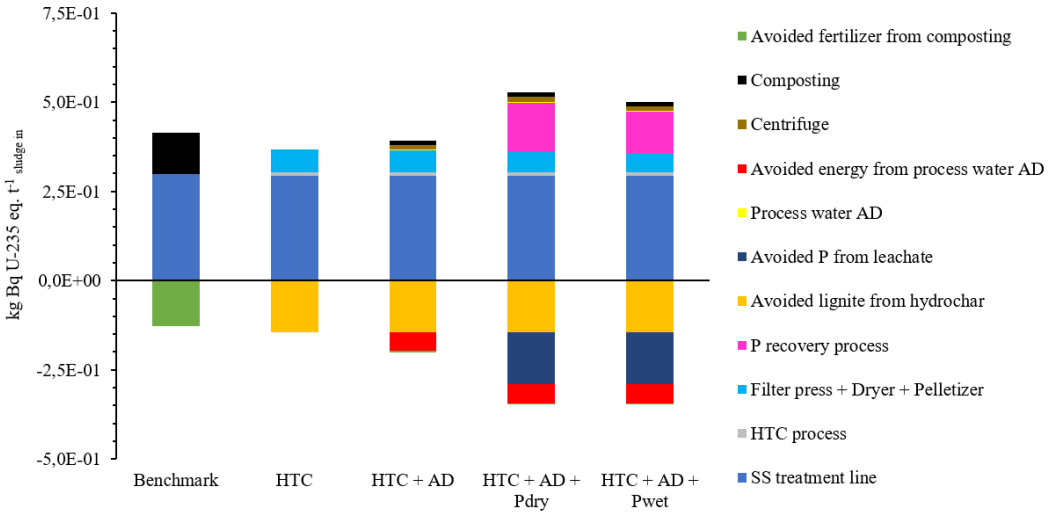

Figure 5.7 Sub-processes contribution for IR impact category.

5.3.1.3 RU_{mm}

The contribution of sub-processes to RU_{mm} impact category is depicted in **Fig. 5.8**. Direct impacts of SS treatment line are the most impactful on the environment in case of Benchmark, HTC, and HTC + AD, accounting a percentage of total impact equal to +46, +81, and +68 %, respectively. Conversely, the highest contribution in case of HTC + AD + P_{dry} and HTC + AD + P_{wet}, is accounted for P recovery process, which resulted equal to + 36, and + 35 % on total impact, respectively. For Benchmark scenario, avoided impacts of fertilizer due to the compost displacement account the -34 % of total impact, completely balancing the impact of its production (equal to 20 %). Lignite replacement by HC production represents a negligible percentage on total impact in all scenarios, whereas the P recovery significantly contributes to the avoided impacts (+21 %, and +22 %, for HTC + AD + P_{dry} and HTC + AD + P_{wet}, respectively). Conversely, the

EE and TE derived by biogas production through anaerobic digestion of PW account on total impact -7 % in case of HTC + AD, and -3 % for both HTC + AD + P_{dry} and HTC + AD + P_{wet}, while AD consumptions are negligible.

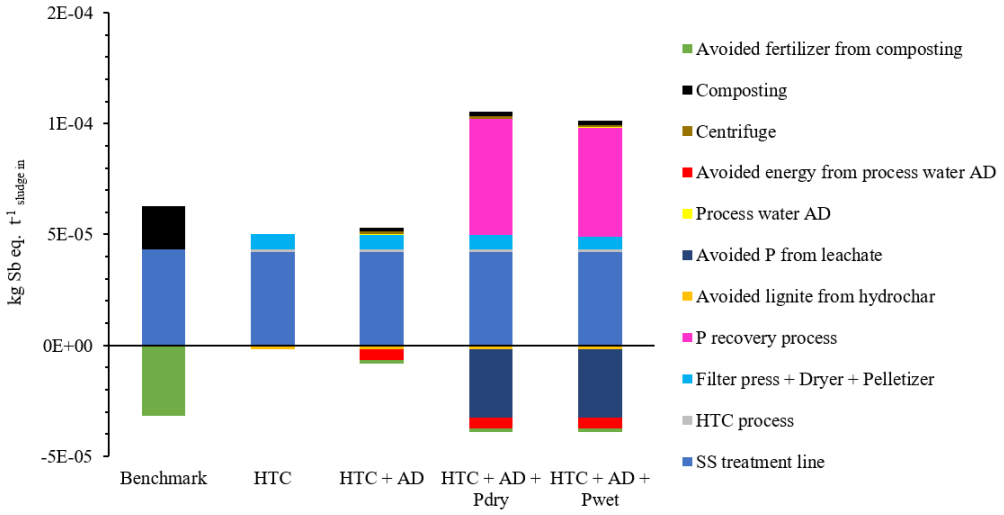

Figure 5.8 Sub-processes contribution for RU_{mm} impact category.

Details about sub-processes contribution of other impact categories are reported in **Section A2.5** of the **Appendix A2.**

5.3.2 Role of P recovery and possible routes for optimization

In the majority of impact categories HTC + AD scenario shows better environmental profile than all the others, as HTC + AD + P_{dry} and HTC + AD + P_{wet} scenarios are strongly affected by P recovery process. As expected, HTC + AD + P_{wet} results in better environmental performance than HTC + AD + P_{dry}, since the latter includes one drying step more than the first one. However, the main factor that significantly contributes to direct impacts is the HNO_3 acid consumption for all indicators (see **Fig. A2.15** in **Appendix A2**). Only in the case of WU, the highest direct contribution is observed for the water needed for P leaching. In order to optimize the P recovery process, two possible strategies are further tested. According to available experimental data, the aforementioned scenarios are adapted considering H_2SO_4 as acid solution to perform P extraction. With this change, HTC + AD + P_{dry} and HTC + AD + P_{wet} have reduced direct impacts (as positive

values) in comparison with the previous one for each impact categories, not including WU (see **Tab. A2.2** in the **Appendix A2**). HTC + AD + P_{wet} confirms its better environmental profile than HTC + AD + P_{dry} and greater reductions are observed for CC, E_t and LU. The result finds explanations in the fact that, to reach the same leaching conditions proposed for HNO_3, smaller amount of H_2SO_4 is required (0.23 mL H_2SO_4 solution g_{dryHC}^{-1}). Additionally, since the ecoinvent process associated to H_2SO_4 production has lower impacts than HNO_3 for all indicators (except for WU), direct impacts of P recovery process are generally reduced (for WU an increase of 20 % is observed) (see **Tab. A2.2** in the **Appendix A2**). Similar considerations are developed by the already cited study [18]. They report that P extraction results in negative impact scores for the following indicators: PM, Acidification (not in case of HNO_3 acid) and WU for three acids tested (HNO_3, H_2SO_4 and HCl). Here, only in case of E_f indicator, a negative impact scores occur for all scenarios with integrated HTC. However, many factors must be taken into account comparing the results of this work with that study. Indeed, Oliver-Tomas et al. [18] investigates the P recovery process with different system boundaries (no treatment plant is included nor HTC process). Further, the processed feedstock by HTC is different (here anaerobic digestate, there OFMSW), and they also include P precipitation with base after leaching. However, even though the comparison is challenging, the main conclusion is similar: P recovery demonstrates to strongly affect the environmental performance of the investigated scenarios.

Lastly, HTC + AD + P_{dry} and HTC + AD + P_{wet} scenarios with HNO_3 acid are further optimized, considering a solid/solution ratio equal to 20 %. Inventory data are adapted using laboratory information and then the impact assessment is again analyzed. An impact reduction is observed for all indicators. Specifically, WU is reduced up to an average percentage equal to 70 %, since the water needed is significantly decreased. Anyway, the P recovery process must be strongly optimized. A solid/solution ratio higher than 5 % and the use of H_2SO_4 could help in this direction. Further, the reuse of the WRRF's effluent could be used as water source instead of a conventional

one or distilled water, in order to limit the impact. Finally, it is worth pointing out that the use of H_2SO_4 on HC could add sulphur on the solid matrix, limiting its application as solid fuel [48].

As mentioned above, the P-rich leached solution was assumed to substitute the P fertilizer. As the next step, a specific characterization of this fraction should be carried out, determining the concentration of metals and evaluating the possible phytotoxic effect, which could occur as a consequence of its application on soil. However, it could be also reasonable to hypothesize a post-treatment or a dilution prior using it as fertilizer. Thus, in a future study, these possible optimization pathways could be explored.

5.3.3 Sensitivity analysis

Y_{HC} and LHV are selected as key parameters to carry out sensitivity analysis. Applying the maximum ER value (full results are reported in **Tab. A2.3** of the **Appendix A2**), the classification of environmental performances among scenarios remains unchanged for each impact category, except for HT_{nc} indicator. For the latter case, HTC + AD shows better environmental performances than other scenarios, improving the trend observed in the base case study. Thus, a sensitivity analysis is carried out for this indicator for HTC, HTC + AD, and HTC + AD + P_{dry} and HTC + AD + P_{wet}. Concerning HT_{nc}, in the base case study, which also corresponds to the minimum ER value, all scenarios show higher impacts than Benchmark, with an increase of +4, +1, +14, and +8 % for HTC, HTC +AD, HTC + AD + P_{dry} and HTC + AD + P_{wet}, respectively. Considering instead scenarios with the maximum ER value, all the aforementioned scenarios reduce their impacts in comparison to the Benchmark (except HTC + AD + P_{dry}), with percentage of -8, -12, +0.5, and -5 %, respectively. However, scenarios with the maximum ER value show better environmental performances in all impact category than the base case study, indicating that both HC yield and LHV have a relevant role on the impact of the process.

As explained above, by Monte Carlo simulation, a frequency distribution is generated on the basis of random outcomes. Here, this analysis is carried out in order to understand when a scenario results in better environmental performance than Benchmark, for a selected impact category. The

sensitivity analysis is carried out for the HT_{nc} impact category for all scenarios. For HTC, the analysis points out that this scenario results in better environmental performances than Benchmark in the 88 % of cases (as average values), for HTC + AD in the 100 % of cases (as average values), and for HTC + AD + P_{dry} in 0 % of cases (as average values). In **Fig. 5.9** the frequency curve is reported for HTC + AD + P_{wet} in case of HT_{nc}, which demonstrates to be more convenient than Benchmark in the 28 % (as average value) of times.

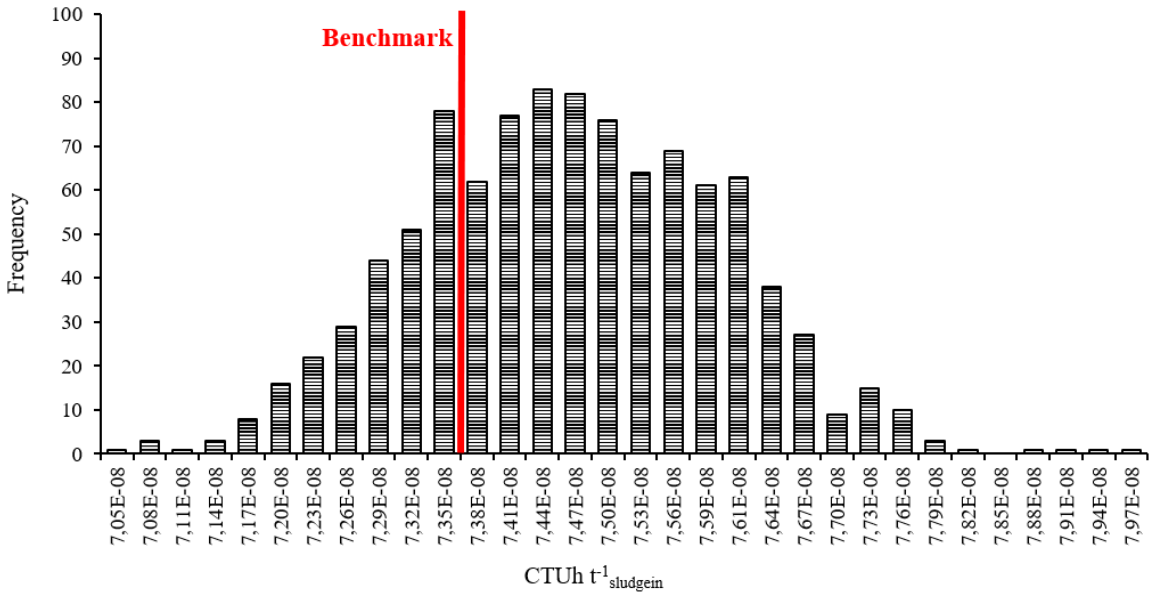

Figure 5.9 Frequency of the values for HT_{nc} indicator in Monte Carlo analysis (black bars) for HTC + AD + P_{wet} scenario and the constant value of Benchmark (7.37E-08 CTUh $t^{-1}_{sludge\ in}$).

5.4 Conclusions

In this study, the combination of a SS treatment line with HTC process for HC production, is evaluated by LCA and compared to direct composting as a benchmark option. Moreover, the HTC integrated system with PW valorization and P recovery is also assessed.

LCA results show that the scenarios with integrated HTC have lower values than Benchmark scenario, for CC impact category, with the exception for those including P recovery. Generally, HTC + AD results in the best environmental performances for eleven of sixteen impact indicators.

Conversely, scenarios with P recovery result generally in the worst performances. This fact is mainly related to the high impact of water and nitric acid required by P acid leaching, with respect to the relatively small contribution of the avoided impact of using the recovered P to displace conventional fertilizer. Thus, results suggest that future research effort should be directed toward process conditions that can reduce the impact of this process, testing for example different operational conditions or acids. Benefits of P recovery process are appreciable only in case of E_f impact category.

The additional benefits deriving from the valorization of biogas from PW through an ICE to produce EE and TE does not strongly contribute in reducing environmental impacts, whereas lignite replacement proves to be the main avoided impacts in all impact indicators, being strictly related to HC yield and its LHV. Indeed, as the sensitivity analysis showed, with higher LHV of hydrochar, more environmental benefits would occur, especially considering HT_{nc} indicator.

5.5 Supplementary information A2

Supplementary information is included into the **Appendix A2**.

5.6 References – Chapter 5

1. Langone, M., Basso, D.: Process waters from hydrothermal carbonization of sludge: Characteristics and possible valorization pathways. Int. J. Environ. Res. Public Health. 17, 1–31 (2020). https://doi.org/10.3390/ijerph17186618
2. European Commission: A Clean Planet for all. A European long-term strategic vision for a prosperous, modern, competitive and climate neutral economy. Com(2018) 773. 25 (2018)
3. Liu, B., Wei, Q., Zhang, B., Bi, J.: Life cycle GHG emissions of sewage sludge treatment and disposal options in Tai Lake Watershed, China. Sci. Total Environ. 447, 361–369 (2013). https://doi.org/10.1016/j.scitotenv.2013.01.019
4. Libra, A.J., Kammann, C., Funke, A., Berge, N.D., Neubauer, Y., Titirici, M.-M., Fuhner, C., Bens, O., Kern, J., Emmerich, K.-H.: Hydrothermal carbonization of biomass residuals : A comparative review of the chemistry , processes and appolications of wet and dry pyrolysis. 2, 89–124 (2011). https://doi.org/10.4155/bfs.10.81
5. Wang, L., Chang, Y., Li, A.: Hydrothermal carbonization for energy-efficient processing of sewage sludge: A review. Renew. Sustain. Energy Rev. 108, 423–440 (2019). https://doi.org/10.1016/j.rser.2019.04.011

6. Medina-Martos, E., Istrate, I.R., Villamil, J.A., Gálvez-Martos, J.L., Dufour, J., Mohedano, Á.F.: Techno-economic and life cycle assessment of an integrated hydrothermal carbonization system for sewage sludge. J. Clean. Prod. 277, (2020). https://doi.org/10.1016/j.jclepro.2020.122930

7. Berge, N.D., Li, L., Flora, J.R.V., Ro, K.S.: Assessing the environmental impact of energy production from hydrochar generated via hydrothermal carbonization of food wastes. Waste Manag. 43, 203–217 (2015). https://doi.org/10.1016/j.wasman.2015.04.029

8. Gievers, F., Loewen, A., Nelles, M.: Hydrothermal Carbonization (HTC) of Sewage Sludge: GHG Emissions of Various Hydrochar Applications. Springer International Publishing (2019)

9. Wang, N.Y., Shih, C.H., Chiueh, P. Te, Huang, Y.F.: Environmental effects of sewage sludge carbonization and other treatment alternatives. Energies. 6, 871–883 (2013). https://doi.org/10.3390/en6020871

10. Meisel, K., Clemens, A., Fühner, C., Breulmann, M., Majer, S., Thrän, D.: Comparative life cycle assessment of HTC concepts valorizing sewage sludge for energetic and agricultural use. Energies. 12, (2019). https://doi.org/10.3390/en12050786

11. Bora, R.R., Lei, M., Tester, J.W., Lehmann, J., You, F.: Life Cycle Assessment and Technoeconomic Analysis of Thermochemical Conversion Technologies Applied to Poultry Litter with Energy and Nutrient Recovery. ACS Sustain. Chem. Eng. 8, 8436–8447 (2020). https://doi.org/10.1021/acssuschemeng.0c02860

12. Mendecka, B., Lombardi, L., Micali, F., De Risi, A.: Energy Recovery from Olive Pomace by Hydrothermal Carbonization on Hypothetical Industrial Scale: a LCA Perspective. Waste and Biomass Valorization. 11, 5503–5519 (2020). https://doi.org/10.1007/s12649-020-01212-0

13. Zeymer, M., Meisel, K., Clemens, A., Klemm, M.: Technical, Economic, and Environmental Assessment of the Hydrothermal Carbonization of Green Waste. Chem. Eng. Technol. 40, 260–269 (2017). https://doi.org/10.1002/ceat.201600233

14. Owsianiak, M., Ryberg, M.W., Renz, M., Hitzl, M., Hauschild, M.Z.: Environmental Performance of Hydrothermal Carbonization of Four Wet Biomass Waste Streams at Industry-Relevant Scales. ACS Sustain. Chem. Eng. 4, 6783–6791 (2016). https://doi.org/10.1021/acssuschemeng.6b01732

15. European Commission: Communication from the Commission to the European Parliament, the Council, the Eurpean Economic and Social Committee and the Committee of the Regions on the 2017 list of Critical Raw Materials for the EU. Off. J. Eur. Union. COM(2017), 8 (2017)

16. Marin-Batista, J.D., Mohedano, A.F., Rodríguez, J.J., de la Rubia, M.A.: Energy and phosphorous recovery through hydrothermal carbonization of digested sewage sludge. 105, 566–574 (2020). https://doi.org/doi.org/10.1016/j.wasman.2020.03.004

17. Tasca, A.L., Mannarino, G., Gori, R., Vitolo, S., Puccini, M.: Phosphorus recovery from sewage sludge hydrochar: process optimization by response surface methodology. Water

Sci. Technol. (2020). https://doi.org/10.2166/wst.2020.485

18. Oliver-Tomas, B., Hitzl, M., Owsianiak, M., Renz, M.: Evaluation of hydrothermal carbonization in urban mining for the recovery of phosphorus from the organic fraction of municipal solid waste. Resour. Conserv. Recycl. 147, 111–118 (2019). https://doi.org/10.1016/j.resconrec.2019.04.023

19. Evangelisti, S., Clift, R., Tagliaferri, C., Lettieri, P.: A life cycle assessment of distributed energy production from organic waste: Two case studies in Europe. Waste Manag. 64, 371–385 (2017). https://doi.org/10.1016/j.wasman.2017.03.028

20. Wernet, G., Bauer, C., Steubing, B., Reinhard, J., Moreno-Ruiz, E., Weidema, B.: The ecoinvent database version 3 (part I): overview and methodology. Int. J. Life Cycle Assess. 21, 1218–1230 (2016). https://doi.org/10.1007/s11367-016-1087-8

21. Bolzonella, D., Innocenti, L., Cecchi, F.: Biological nutrient removal wastewater treatments and sewage sludge anaerobic mesophilic digestion performances. Water Sci. Technol. 46, 199–208 (2002). https://doi.org/10.2166/wst.2002.0330

22. Garrido-Baserba, M., Molinos-Senante, M., Abelleira-Pereira, J.M., Fdez-Güelfo, L.A., Poch, M., Hernández-Sancho, F.: Selecting sewage sludge treatment alternatives in modern wastewater treatment plants using environmental decision support systems. J. Clean. Prod. 107, 410–419 (2015). https://doi.org/10.1016/j.jclepro.2014.11.021

23. Francini, G., Lombardi, L., Freire, F., Pecorini, I., Marques, P.: Environmental and Cost Life Cycle Analysis of Different Recovery Processes of Organic Fraction of Municipal Solid Waste and Sewage Sludge. Waste and Biomass Valorization. 10, 3613–3634 (2019). https://doi.org/10.1007/s12649-019-00687-w

24. Bakkaloglu, S., Lowry, D., Fisher, R.E., France, J.L., Brunner, D., Chen, H., Nisbet, E.G.: Quantification of methane emissions from UK biogas plants. Waste Manag. 124, 82–93 (2021). https://doi.org/10.1016/j.wasman.2021.01.011

25. Gogolek, P.: Methane emission factors for biogas flares. J. Int. Flame Res. Found. 53-1-53–22 (2012). https://doi.org/10.1201/9781420039870.ch53

26. Teoh, S.K., Li, L.Y.: Feasibility of alternative sewage sludge treatment methods from a lifecycle assessment (LCA) perspective. J. Clean. Prod. 247, 119495 (2020). https://doi.org/10.1016/j.jclepro.2019.119495

27. Evangelisti, S., Lettieri, P., Clift, R., Borello, D.: Distributed generation by energy from waste technology: A life cycle perspective. Process Saf. Environ. Prot. 93, 161–172 (2015). https://doi.org/10.1016/j.psep.2014.03.008

28. Hong, J., Hong, J., Otaki, M., Jolliet, O.: Environmental and economic life cycle assessment for sewage sludge treatment processes in Japan. Waste Manag. 29, 696–703 (2009). https://doi.org/10.1016/j.wasman.2008.03.026

29. Basso, D.: Hydrothermal carbonization of waste biomass Daniele Basso. 1–277 (2016)

30. Lucian, M., Volpe, M., Merzari, F., Wüst, D., Kruse, A., Andreottola, G., Fiori, L.: Hydrothermal carbonization coupled with anaerobic digestion for the valorization of the

organic fraction of municipal solid waste. Bioresour. Technol. 314, 123734 (2020). https://doi.org/10.1016/j.biortech.2020.123734

31. Lucian, M., Fiori, L.: Hydrothermal carbonization of waste biomass: Process design, modeling, energy efficiency and cost analysis. Energies. 10, (2017). https://doi.org/10.3390/en10020211

32. Aragón-briceño, C., Ross, A.B., Camargo-valero, M.A.: Evaluation and comparison of product yields and bio-methane potential in sewage digestate following hydrothermal treatment. Appl. Energy. 0–1 (2017). https://doi.org/10.1016/j.apenergy.2017.09.019

33. Parmar, K.R., Ross, A.B.: Integration of hydrothermal carbonisation with anaerobic digestion; Opportunities for valorisation of digestate. Energies. 12, (2019). https://doi.org/10.3390/en12091586

34. Asunis, F., Gioannis, G. De, Francini, G., Lombardi, L., Muntoni, A., Polettini, A., Pomi, R., Rossi, A., Spiga, D.: Environmental life cycle assessment of polyhydroxyalkanoates production from cheese whey. Waste Manag. 132, 31–43 (2021). https://doi.org/10.1016/j.wasman.2021.07.010

35. Lombardi, L., Nocita, C., Bettazzi, E., Fibbi, D., Carnevale, E.: Environmental comparison of alternative treatments for sewage sludge: An Italian case study. Waste Manag. 69, 365–376 (2017). https://doi.org/10.1016/j.wasman.2017.08.040

36. Volpe, M., Fiori, L., Merzari, F., Messineo, A., Andreottola, G.: Hydrothermal carbonization as an efficient tool for sewage sludge valorization and phosphorous recovery. Chem. Eng. Trans. 80, 199–204 (2020). https://doi.org/10.3303/CET2080034

37. Pérez, C., François, J., Stina, B., Tomas, J., Jerker, G.: Acid - Induced Phosphorus Release from Hydrothermally Carbonized Sewage Sludge. Waste and Biomass Valorization. (2021). https://doi.org/10.1007/s12649-021-01463-5

38. Piccinno, F., Hischier, R., Seeger, S., Som, C.: From laboratory to industrial scale: a scale-up framework for chemical processes in life cycle assessment studies. J. Clean. Prod. 135, 1085–1097 (2016). https://doi.org/10.1016/j.jclepro.2016.06.164

39. Tambone, F., Scaglia, B., D'Imporzano, G., Schievano, A., Orzi, V., Salati, S., Adani, F.: Assessing amendment and fertilizing properties of digestates from anaerobic digestion through a comparative study with digested sludge and compost. Chemosphere. 81, 577–583 (2010). https://doi.org/10.1016/j.chemosphere.2010.08.034

40. Sherrard, J.H.: Kinetics and stoichiometry of completely mixed activated sludge. J. Water Pollut. Control Fed. 49, 1968–1975 (1977)

41. Rigamonti, L., Falbo, A., Grosso, M.: Improvement actions in waste management systems at the provincial scale based on a life cycle assessment evaluation. Waste Manag. 33, 2568–2578 (2013). https://doi.org/10.1016/j.wasman.2013.07.016

42. European Commission: Recommendation 2013/179/EU on the use of common methods to measure and communicate the life cycle environmental performance of products and organisations. Off. J. Eur. Union. 210 (2013)

43. Tasca, A.L., Stefanelli, E., Raspolli Galletti, A.M., Gori, R., Mannarino, G., Vitolo, S., Puccini, M.: Hydrothermal Carbonization of Sewage Sludge: Analysis of Process Severity and Solid Content. Chem. Eng. Technol. 43, 2382–2392 (2020). https://doi.org/10.1002/ceat.202000095

44. Peng, C., Zhai, Y., Zhu, Y., Xu, B., Wang, T., Li, C., Zeng, G.: Production of char from sewage sludge employing hydrothermal carbonization: Char properties, combustion behavior and thermal characteristics. Fuel. 176, 110–118 (2016). https://doi.org/10.1016/j.fuel.2016.02.068

45. Wang, T., Zhai, Y., Zhu, Y., Peng, C., Xu, B., Wang, T., Li, C., Zeng, G.: Influence of temperature on nitrogen fate during hydrothermal carbonization of food waste. Bioresour. Technol. 247, 182–189 (2018). https://doi.org/10.1016/j.biortech.2017.09.076

46. Aragón-Briceño, C.I., Grasham, O., Ross, A.B., Dupont, V., Camargo-Valero, M.A.: Hydrothermal carbonization of sewage digestate at wastewater treatment works: Influence of solid loading on characteristics of hydrochar, process water and plant energetics. Renew. Energy. 157, 959–973 (2020). https://doi.org/10.1016/j.renene.2020.05.021

47. Chemical Engineers' Handbook. Second edition (Perry, John H., ed.). J. Chem. Educ. 19, 449 (1942). https://doi.org/10.1021/ed019p449.2

48. Gerner, G., Meyer, L., Wanner, R., Keller, T., Krebs, R.: Sewage sludge treatment by hydrothermal carbonization: Feasibility study for sustainable nutrient recovery and fuel production. Energies. 14, (2021). https://doi.org/10.3390/en14092697

Chapter 6

Improved energy recovery from food waste through hydrothermal carbonization and anaerobic digestion

This Chapter has been published as:

Mannarino, G., Sarrion, A., Diaz, E., Gori, R., De la Rubia, M.A., Mohedano, A.F.: Improved energy recovery from food waste through hydrothermal carbonization and anaerobic digestion. Waste Manag. 142, 9–18 (2022). https://doi.org/10.1016/j.wasman.2022.02.003

Abstract

Here we studied energy valorization of food waste by hydrothermal carbonization coupled with anaerobic digestion. Hydrothermal treatment was carried out at 200°C and 230°C for 1 h, obtaining hydrochar with properties suitable for solid biofuel according to ISO/TS 17225-8. The increase in temperature improved the fuel properties of hydrochar (higher heating value 20.3 and 23.7 MJ kg^{-1}, fuel ratio 0.33 and 0.37, energy density 1.07 and 1.25). The anaerobic digestion of process water achieved methane yields around 150 mL CH_4 STP g^{-1} COD_{added} and made it possible to remove some specific recalcitrant compounds, such as 2-methylpyridine and 2-ethyl-3-methylpyrazine. Energy recovery from hydrochar and process water seems to be an interesting alternative way to sustain the process energetically and economically, despite the significant energy inputs required for hydrothermal carbonization.

6.1 Introduction

Food waste (FW) is organic waste derived from any stage of the food supply chain and it is a significant fraction of municipal solid waste. More than 2000 million tons of municipal waste were generated worldwide and production is estimated to increase by 70% to 2050.

In Europe, current legislation focuses on reducing food waste and promotes actions to minimize its impact on the environment through the so-called circular economy [1]. Indeed, many EU countries have limited the disposal of food waste in landfills, supporting effective segregation at the source and therefore facilitating its valorization [2].

As a rule, FW management can be based on biological technologies and thermochemical pathways. Regarding biological treatment, anaerobic digestion (AD) has many applications, as it can convert a significant amount of FW into biogas, potentially upgradable to bio-methane, with appreciable environmental benefits. On the other hand, anaerobic digestion is characterized by long treatment times (up to 30−40 days) and the process can be inhibited by high concentrations of free ammonia (NH_3) and cations [3]. Thermochemical conversions are another feasible route for handling food waste. Incineration is a mature technology capable of converting wastes into heat and energy, but it usually requires feedstock pre-treatments (FW is by far the wettest fraction of municipal solid wastes) and it has atmospheric emissions which generally contain dioxins and heavy metals [3, 4] requiring additional treatment of the gases produced. In this framework, hydrothermal carbonization (HTC) emerges as an environmentally friendly and energy-efficient sustainable technology, as it can be used to treat FW to obtain a product with attractive energy properties for co-firing coal [5]. Hydrothermal carbonization is an exothermic process in which the wet feedstock is treated at 170–250ºC for short times (5–240 min) under self-generated pressure. Through hydrolysis, condensation, aromatization, dehydration and decarboxylation reactions, three fractions are obtained: a solid carbonaceous product named hydrochar, process water rich in sugars and organic compounds, and a small gaseous fraction consisting mainly of CO_2 [6].

Hydrochar derived from FW is a valuable product with a high carbon content (45–93%) and energy values in the range 15–30 MJ kg^{-1} [4]. Lu et al. [7] carried out hydrothermal carbonization of FW in a batch reactor at 250°C and found that the potential energy generation of HTC of food waste was higher than that recovered by landfilling, composting, AD or incineration. Evaluations

of different HTC conditions in the conversion of FW to solid fuel have been reported in the literature. Akarsu et al. [8] performed HTC of food waste at different temperatures (175–250ºC) and with different reaction times (15–120 min), obtaining optimal conditions in terms of mass and energy efficiency at 200ºC and 60 min. On the other hand, Li et al. [9] compared the total energy recoverable from hydrochar resulting from different organic wastes as a function of HTC conditions, reporting that the highest energy generation (~17.5 MJ $kg^{-1}_{dry\ feedstock}$) was obtained from food waste at less than 200ºC for less than 150 min.

Since process water from HTC contains water-soluble organic compounds [6], its valorization through AD is a promising approach. While AD of organic wastes is a mature technology, its application to process water from food waste carbonization is new. Lucian et al. [10] recently investigated application of HTC to the organic fraction of municipal solid waste and found that coupling AD of process water with hydrochar combustion is an energy-efficient combination. Aragón-Briceño et al. [11] used the liquid fraction obtained after HTC of sewage sludge digestate at 160–250ºC for 30 min to obtain biogas by AD, also adding the resulting hydrochar to the medium, which delayed the generation of volatile fatty acids and improved the CH_4 production rate. On the other hand, Marin-Batista et al. [12, 13] hydrothermally carbonized cow manure and digestate at 170–240ºC for 1 h, evaluating energy recovery from AD of process water and combustion of hydrochar. For dairy manure carbonized at 170°C and 200°C, the energy recovery yield was at least 80% of feedstock energy content [12].

The main aim of this study was to explore the energy valorization of FW by hydrothermal carbonization coupled with anaerobic digestion of the process water, and combustion of the hydrochar. Hydrothermal carbonization of FW was carried out at 200°C and 230°C. Then hydrochar was characterized to define its combustion properties. The time-course of AD of process water was investigated, monitoring parameters such as organic matter, volatile fatty acids and recalcitrant compounds. Lastly, we calculated the energy balance of coupling hydrothermal carbonization and AD, taking the energy content of the hydrochar into account.

6.2 Materials and methods

6.2.1 Food waste

Food waste was collected from a local management plant that operates in a food supply distribution platform (Madrid, Spain). The raw food waste, which mainly consisted of fruit and vegetables, was ground and frozen in 1.5 kg portions at -20ºC to facilitate conservation, while a sample was oven dried at 105ºC for 24 h prior to analysis of its composition (**Tab. 6.1**). In each experiment, moisture of thawed FW portions was measured (91–93 wt %). The main characteristics of the feedstock (average of n=3 portions with standard deviations in brackets) were: total solids (TS) 88.2 (2.8) g kg^{-1}, volatile solids (VS) on TS 87.6 (0.2) % and total chemical oxygen demand (COD) wet basis 102.2 (2.0) g O_2 kg^{-1}.

6.2.2. Hydrothermal carbonization

Hydrothermal carbonization of food waste was conducted in an electrically heated, stirred ZipperClave pressure vessel (4 L). In each experiment, the reactor was loaded with 1.5 kg defrosted food waste. The operating temperatures (200ºC and 230ºC) were reached by heating the reactor at 3 ºC min^{-1} and holding for 1 h. The reaction was stopped by cooling at 2.5 ºC min^{-1} with an internal heat exchanger using tap water. The resulting slurry (a mixture of hydrochar and process water) was separated by filtration with a 250 μm membrane vacuum filter. The hydrochars (HC200, HC230) were obtained by oven-drying the solid fraction overnight at 105ºC, followed by grinding and sieving to a particle size between 100 and 200 μm. The process water (PW200, PW230) was filtered with 0.45 μm Scharlab glass filters and stored at 4ºC.

6.2.3. Anaerobic digestion experiments

Anaerobic digestion experiments were performed on food waste, PW200 and PW230. Batch-wise AD tests were carried out in 120 mL glass serum vials, filled with 60 mL suspension of inoculum, substrate (raw food waste or process water from HTC), deionized water and a basal medium with macro- and micronutrients, as reported elsewhere [14]. Granular anaerobic sludge from a brewery wastewater treatment plant was used as inoculum. It was characterized (average of n=3 samples

with standard deviations in brackets) as follows: TS 53.7 (0.9) g L^{-1}, VS 46.2 (0.9) g L^{-1} and COD 33.1 (2.0) g O_2 L^{-1}. The initial inoculum concentration was set at 15 g VS L^{-1} and the inoculum-to-substrate ratio at 2 on a COD basis as recommended by Villamil et al. [14]. The vials were sealed with rubber stops and metal crimps, and were flushed with N_2 for 3 min to ensure anaerobic conditions. The vials were kept under mesophilic conditions (35 ± 1 °C) in a thermostatic shaking water bath at 100 rpm. Anaerobic digestion was monitored using ten vials for each process water: three for biogas measurements (volume and composition), and the other seven were sacrificed during the experiment to monitor digestion parameters over time. Only three AD runs were performed on food waste to measure biogas. Triplicate blank samples with no substrate were run to determine the background methane yield of the inoculum, and triplicate control experiments were also performed on starch to evaluate the methanogenic activity of microorganisms. Methane yield was calculated by subtracting the amount of methane produced by blanks, and methane volume at STP (0°C, 1 atm) was recorded.

6.2.4. Analytical methods

The elemental composition (C, H, N and S) of the hydrochar and process water samples was determined on a CHNS analyzer (LECO CHNS-932). Proximate analysis was done according to ASTM methods D3173-11, D3174-11 and D3175-11 to determine moisture, ash, volatile matter (VM) and fixed carbon (FC) (by difference), respectively, of the hydrochar. Oxygen content was calculated by difference. The higher heating value (HHV) of dried solid samples was estimated by **equation 6.1**, which is a unified correlation to calculate the HHV from C, H, N, S, O and ash content according to Channiwala and Parikh [15]:

$$\text{HHV (MJ kg}^{-1}) = 0.349\,\text{C} + 1.178\,\text{H} + 0.100\,\text{S} - 0.103\,\text{O} - 0.015\,\text{N} - 0.021\,\text{Ash} \qquad (6.1)$$

Analysis of variance was performed using the MINITAB® software. Means were compared using Welch's test.

The concentration of other inorganic elements in hydrochar and process water was quantified by inductively coupled optical emission spectroscopy (ICP-OES) on an IRIS INTREPID II XDL instrument (ThermoFisher Scientific).

Inoculum and process water of AD tests were characterized by measuring TS and VS according to standard methods 2540B and 2540E [16], and COD by the method of Raposo et al. [17]. Sacrificed samples were filtered (0.45 µm) and analyzed to determine: pH (Crison 20 Basic pH meter), partial and total alkalinity (PA and TA) by pH titration to 5.75 and 4.3, respectively [18], soluble COD (SCOD) applying the closed digestion and colorimetric standard method 5220D, and total ammonia nitrogen (TAN) by distillation and titration according to standard method 4500-NH_3 [16]. Total organic carbon (TOC) was determined using an OI Analytical TOC analyzer (model 1010, Texas, USA). Individual volatile fatty acid (VFA) concentrations (C2-C7, including isoforms) were identified by gas chromatography (GC) in a Varian 430-GC instrument as described elsewhere [19]. Individual chemical species were identified by GC-MS (CP-3800/Saturn 2200 with Varian CP-8200 autosampler injection). The NIST 2018 Library was used to assess compounds. Only compounds with a probability of at least 50% were considered. Biogas production was determined using a manometric method, measuring the pressure increase in each vial with an electronic pressure monitor (ifm, PN 7097) [20]. Biogas composition (H_2, H_2S, CO_2 and CH_4) was measured by gas chromatography, using a Bruker 450-GC (Goes, The Netherlands) [19]. Biogas was subsequently exhausted to re-establish atmospheric pressure.

6.2.5 Calculations

Hydrochar mass yield (Y_{HC}), i.e., the weight ratio of hydrochar recovered (W_{HC}) to food waste feedstock (W_{FW}) on a dry basis, was calculated with **equation 6.2**:

$$Y_{HC}(\%) = \left({}^{W_{HC}}/_{W_{FW}}\right) \cdot 100 \quad (6.2)$$

Likewise, the process water yield (Y_{PW}) expresses the mass ratio of total solids in process water (W_{PW}) to that of food waste (W_{FW}) on a dry basis, and was calculated with **equation 6.3**:

$$Y_{PW}(\%) = \left({}^{W_{PW}}/_{W_{FW}}\right) \cdot 100 \quad (6.3)$$

The energy recovery efficiency was calculated with **equation 6.4**:

$$\text{Energy recovery efficiency} = Y_{HC} \cdot \frac{HHV_{HC}}{HHV_{FW}} \quad (6.4)$$

where the HHV_{HC} and HHV_{FW} are the higher heating values of hydrochar and food waste, respectively.

A more in-depth evaluation for the combustion performance is carried out from the comprehensive combustion index (CCI). The hydrochar CCI was calculated using **equation 6.5** [12]:

$$CCI(min^{-2} \cdot °C^{-3}) = \frac{DTG_m \cdot DTG_{mean}}{T_i^2 \cdot T_b} \quad (6.5)$$

where DTG_m and DTG_{mean} are the maximum and the average rate of weight loss, respectively, and T_i and T_b are the ignition and the burnout temperatures, respectively. High values of the CCI indicate a satisfactory combustion performance by an easy ignition and an efficient burnout [21].

The specific methane production (SMP, Nm^3 CH_4 kg^{-1} COD) obtained from batch anaerobic tests was converted into HHV_{PW} values using **equation 6.6**:

$$HHV_{PW}(MJ\ kg^{-1}) = 39.8 \cdot SMP \cdot {}^{COD}/_{TS} \quad (6.6)$$

where the coefficient 39.8 is the higher heating value for pure methane (MJ Nm^{-3},) and COD TS^{-1} is the COD to TS (kg COD kg^{-1} TS) in the PW.

Lastly, the total potential energy recovery was estimated with **equation 6.7:**

$$\text{Energy recovery}\left(MJ\ kg^{-1}_{\text{dry feedstock}}\right) = (HHV_{HC} \cdot Y_{HC}) + (HHV_{PW} \cdot Y_{PW}) \quad (6.7)$$

where HHV_{HC} is the HHV (MJ kg^{-1}) of hydrochar estimated with **equation 6.1**.

6.3 Results and Discussions

6.3.1 Hydrochar as solid biofuel

Tab. 6.1 collects the mean values and standard deviation of mass yield, proximate and ultimate analyses, and HHV of the raw food waste and hydrochars. Carbonization temperature showed a significant effect ($p < 0.001$) on mass yield, fixed carbon, volatile matter, ash content, and HHV. The C, N and O content were also significantly ($p < 0.05$) influenced by HTC temperature. The hydrochar yield decreased greatly at both HTC temperatures, due to the subcritical state of water induced above 200°C, which results in the transfer of components (such as proteins, amino acids and sugars) from the feedstock to the process water. This occurs at high temperatures and short reaction times [22]. The raw food waste had a low fixed carbon content, since it is mainly composed of organic compounds such as sugars, carbohydrates and proteins, and this low fixed carbon is also related to its high volatile content. The FC content in the hydrochars increased in comparison with raw feedstock, increasing the firing temperature and providing greater flame stability during combustion of these materials. High fuel ratio values maintain a less violent flame and reduce heat loss during combustion [23]. This allows hydrochar to be used as fuel in power plants, blended with coal, reducing the fossil fuel contribution to CO_2 emissions [12]. On the other hand, the ash content in hydrochar increased with temperature due to transfer of organic matter to the process water and to the high sample content of inorganic compounds, which remain in the solid phase after hydrothermal treatment [24]. The increase in ash content in hydrochar is the most concerning issue for its application as a solid fuel. Ro et al. [25] highlighted the potential of hydrochar as a renewable fuel in existing coal-fired power plants and concluded that, although fossil coals cannot be replaced entirely with hydrochar, blending up to 10% hydrochar with coal does not affect the combustion characteristics or the amount of ash for existing power plants. To reduce the ash content of hydrochar, some works have studied the blending of high-ash biomasses with other hydrochar precursors (e.g., lignocellulosic wastes) prior to HTC [26–28]. Some studies

have used acidic reagents, mainly HCl, in the HTC process to favor the extraction of the inorganic content to the process water [29, 30].

Tab. 6.1 also shows the mean values of some elements in the ash fraction of food waste and hydrochars, the most abundant being P and metals such as Na, K, Ca, Mg, Fe and Al. HTC temperature had a significant effect on P and metal content ($p < 0.001$). It can be observed that except for K and Na, which decreased in amount at higher temperature, metals mainly remained in the hydrochar. Alkali metals (K and Na), responsible for fouling, are generally transferred to the process water under severe carbonization conditions [31]. In addition, the reduction of alkali metals and the increase in alkaline earth metals (Mg and Ca) promote ash with a high melting temperature, which is easier to remove from furnaces and boilers after combustion [32].

An increase in HTC temperature generated hydrochars whose O/C and H/C atomic ratios were lower than those of raw food waste (0.56 and 1.64, respectively), indicating that the degree of hydrochar carbonization was improved by the dehydration, carboxylation and condensation reactions [8]. Thus, HC200 achieved H/C (1.41) and O/C (0.52) atomic ratios comparable to those of peat, while HC230 gave atomic ratios (1.34 and 0.4, respectively) comparable to those of lignite.

Table 6.1 Representative analysis of food waste and hydrochar (dry basis).

Sample	Proximate analysis (wt %)				Ultimate analysis (wt %)					HHV	Mineral elements (wt %)						
	Yield	FC	VM	Ash	C	N	S	H	O[6a]	(MJ kg^{-1})	Na	K	Ca	Mg	Fe	Al	P
Food waste	-	11.0 (0.2)	77.2 (0.1)	11.8 (0.1)	44.5 (0.3)	3.1 (0.2)	0.2 (0.0)	6.1 (0.8)	34.3 (0.2)	18.9 (0.1)	0.14 (0.01)	3.30 (0.03)	1.17 (0.02)	0.23 (0.01)	0.11 (0.02)	0.10 (0.04)	0.47 (0.03)
HC200	64.5 (0.2)	28.6 (0.4)	57.8 (1.6)	13.6 (0.2)	48.6 (0.3)	2.0 (0.2)	0.2 (0.0)	5.7 (0.2)	29.9 (0.2)	20.3 (0.2)	0.23 (0.02)	3.67 (0.03)	1.57 (0.06)	0.31 (0.02)	0.29 (0.01)	0.25 (0.04)	0.57 (0.02)
HC230	58.3 (1.6)	29.5 (0.9)	56.2 (0.2)	14.3 (0.2)	54.8 (0.9)	2.3 (0.3)	0.2 (0.0)	6.1 (0.1)	22.3 (0.1)	23.7 (0.1)	0.10 (0.01)	1.61 (0.02)	1.88 (0.03)	0.29 (0.01)	0.33 (0.01)	0.40 (0.03)	0.83 (0.04)

[6a] Calculated by difference O =100 - (C+H+N+S+Ash). Standard deviation is reported in brackets. Standard deviation for mineral elements is lower than 0.1 in all the cases.

Thermogravimetric analysis (TGA) was used to determine the combustion characteristics of feedstock and hydrochar (**Fig. 6.1**). The TG and first derivative (DTG) curves provide information on the thermal degradation patterns of food waste, indicating an initial mass loss up to 120°C, related to moisture evaporation. Thermal decomposition of food waste and hydrochar started at temperatures below 150°C due to the low thermal stability of sugars, resulting in an ignition temperature (T_i) of hydrochar that increased slightly from 184 to 190°C. Subsequently, the highest DTG peak or maximum weight loss rate (T_m) was associated with combustion of the samples and was found for all samples at temperatures around 280–300ºC, being higher for hydrochars obtained at higher temperatures. Before reaching this combustion peak, another earlier peak (180–220ºC) was observed only in the feedstock and HC200, related to the greater solid matrix destruction of the light carbon structures [33], and indicating that volatile matter in HC230 was largely reduced. Subsequently, a second pronounced DTG peak was recorded at 390–500ºC, attributed to the combustion of more stable structures with high molecular weight together with fixed carbon [34], the width (combustion temperature range) of which also increased with HTC temperature. A third peak was observed at 480°C with HC230 due to combustion of the remaining fixed carbon.

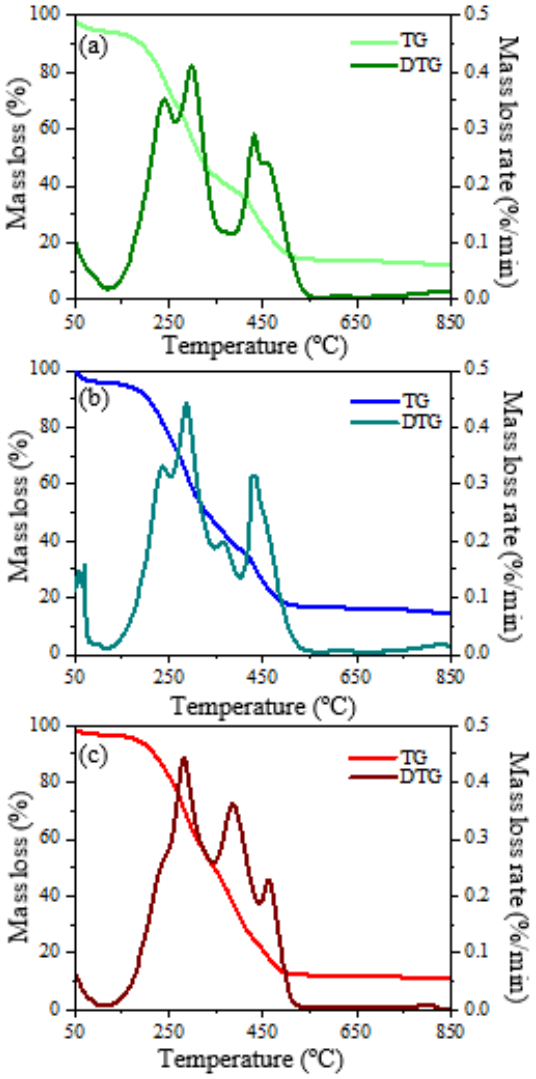

Figure 6.1 TG and DTG curves of raw food waste (a), HC200 (b) and HC230 (c).

The combustion characteristics of the hydrochars are shown in **Appendix A3** (**Tab. A3.1**). The T_i and the burnout temperature (T_b) increased and decreased, respectively, with HTC temperature, decreasing the T_m and resulting in hydrochar with a low CCI index (~$10 \cdot 10^{-7}$ min^{-2} $°C^{-3}$) (Eq. (6)), confirming high combustion as the reactivity of hydrochar increased [34]. A positive effect of temperature on HHV was observed, improving that of the feedstock, and reaching typical brown-coal values at the higher HTC temperature. Compared to the initial feedstock, the fuel ratio (FC/VM) of hydrochar doubled at the higher temperature due to the loss of volatile compounds during HTC. This indicated generation of hydrochar richer in fixed carbon, which is determinant

for improving combustion performance as solid fuel and reducing emission of pollutants [31]. The hydrochar fuel ratio was also less than 2.5, which is decisive for qualifying it as solid fuel suitable for pulverized combustion systems [35]. The energy density of hydrochar increased with HTC temperature, and considering the initial performance of food waste to hydrochar, the higher HTC temperature (230ºC) resulted in slightly more efficient energy recovery.

Fuel properties are fundamental for the viability of hydrochar as a solid fuel. Hydrochar was analyzed to check its compliance with ISO/TS 17225-8 for thermally treated and densified biomass. This standard establishes specific limits for pellets, obtained by thermal processing of non-woody biomass, to be used as solid biofuels. As there is no specific standard for solid fuel derived from food waste and since the food waste used as feedstock in this study was mainly from fruit and vegetables, the hydrochar characteristics were compared with the specification of property class TA3 for fruit biomass. The two hydrochars (Table 1) complied with the limits defined by the standard: N < 2.5% and S < 0.3%. No requirements are defined for ash, volatile matter, specific metals (e.g., Cd, Cr, Cu, Pb and Ni) or net calorific value for TA3. Nevertheless, the high HHV of both hydrochars (> 20 MJ kg^{-1}) suggests that their use as biofuels in industry is feasible, HC230 showing the best results.

6.3.2 Mesophilic anaerobic digestion of process water

The characteristics of process water samples obtained by HTC of food waste at 200 and 230°C (given as average values of three determinations with standard deviations in brackets) are reported in **Tab. 6.2**.

Table 6.2 Characterization of PW from HTC on food waste at 200 and 230 °C.

	PW200[6b]	**PW 230**[6b]
TS (g L^{-1})	38.8 (0.8)	35.9 (0.3)
VS (g L^{-1})	30.4 (0.9)	28.0 (0.4)
SCOD (g O_2 L^{-1})	68.2 (1.5)	62.4 (1.5)
TOC (g L^{-1})	24.3 (0.5)	23.6 (0.5)
TN (g L^{-1})	1.8 (0.1)	1.8 (0.1)
TP (mg L^{-1})	40.7 (0.1)	12.6 (0.1)
pH	3.9 (0.1)	3.8 (0.1)

[6b] Standard deviation of n=3 measurements is reported in brackets.

The SCOD values are consistent with ranges described in the literature, which are slightly lower than those reported for process water from carbonization of food waste from a student hostel (68–97 g O_2 L^{-1}) at 200°C for 0.5–5 h [5], and relatively higher than PW from HTC of the organic fraction of municipal solid waste (40–45 g O_2 L^{-1}) at 180–250°C for 1–6 h [10].

A decreasing trend of TS was observed with increasing temperatures, while the VS/TS ratio remained constant. Acid pH was found for both process water samples. Gupta et al. (2020) reported similar pH values for HTC process water from food waste (3.3–3.9). These pH values are consistent with the formation of a variety of organic acids during the hydrothermal process [6].

TOC concentrations were comparable to those reported in the literature. Gupta et al. [5] observed a decreasing trend of TOC (from 42 to 21 g L^{-1}) with increasing HTC reaction time (0.5–5 h) for process water derived from food waste carbonized at 200°C. The TN concentrations are slightly lower than those (2.4–4.7 g L^{-1}) reported for spent liquor obtained from HTC of food waste at 200°C (15–120 min) [8]. Phosphorus concentrations in process water decreased significantly with increasing temperature. This trend was similar to the pattern observed by Idowu et al. [36] during hydrothermal carbonization of food waste to recover nutrients, due to precipitation of phosphorus with cations (e.g., Ca, Mg, Fe and Al) and/or integration into hydrochar via sorption.

Fig. 6.2a, 6.2b show the individual time-course of VFA during anaerobic digestion of PW200 and PW230, respectively. Acetic acid (C2) accounted for about 50% of total volatile fatty acids (TVFA) (in mg acetic acid L^{-1}) for the two process waters in the early stage. In contrast, low concentrations of longer chain VFA, such as valeric (C5), isovaleric (i-C5), caproic (C6) and isocaproic (i-C6), were measured in both samples (<150 and <100 mg acetic acid L^{-1}, for the sum of C5 and i-C5 and for the sum of C6 and i-C6, respectively). Small amounts of butyric (C4) and iso-butyric (i-C4) were also detected in both process waters. During AD, the concentration of TVFA showed a decreasing trend until day 15, indicating an efficient acidogenic-acetogenic stage. At day 15, TVFA concentrations, 143 (6) and 186 (2) mg acetic acid L^{-1} for PW200 and PW230, resulted in overall reductions in TVFA of 81% and 65%, respectively. These considerable reductions in VFA concentrations show that the methanogenic phase was effective in the first 15 days, indicating a correct balance between hydrolysis and methanogenic rate. From Day 22, TVFA concentrations in PW200 samples showed a slight increase with respect to the TVFA concentration at Day 15 until the end of the experiment. In the case of PW230, TVFA concentrations remained almost constant until the end of AD tests. However, no relevant differences were detected between PW200 and PW 230 samples in the TVFA profile. In fact, the TVFA concentration showed values in the range of 150 – 350 mg acetic acid L^{-1} in both cases, starting from Day 2. These TVFA trends suggested that a good balance was reached between TVFA production/consumption producing CH_4.

Fig. 6.2c shows the time-course of SCOD (in g O_2 L^{-1}) and the TVFA/SCOD ratio (%) (both parameters expressed as g O_2 L^{-1}). Soluble COD of both process waters gradually decreased in the first 15 days, due to conversion of soluble organic matter to methane. It then remained almost constant until the end of the experiment, suggesting the presence of a non-biodegradable SCOD fraction. A slight increase in SCOD was observed in the latter stages of AD for PW200. The TVFA to SCOD ratio was around 20% for both process waters in the early stages of AD, indicating effective conversion of TVFA. About 30% of TVFA in SCOD remained constant in

the last stages of AD for both process waters (**Fig. 6.2c**), which may support the hypothesis of the presence of refractory compounds.

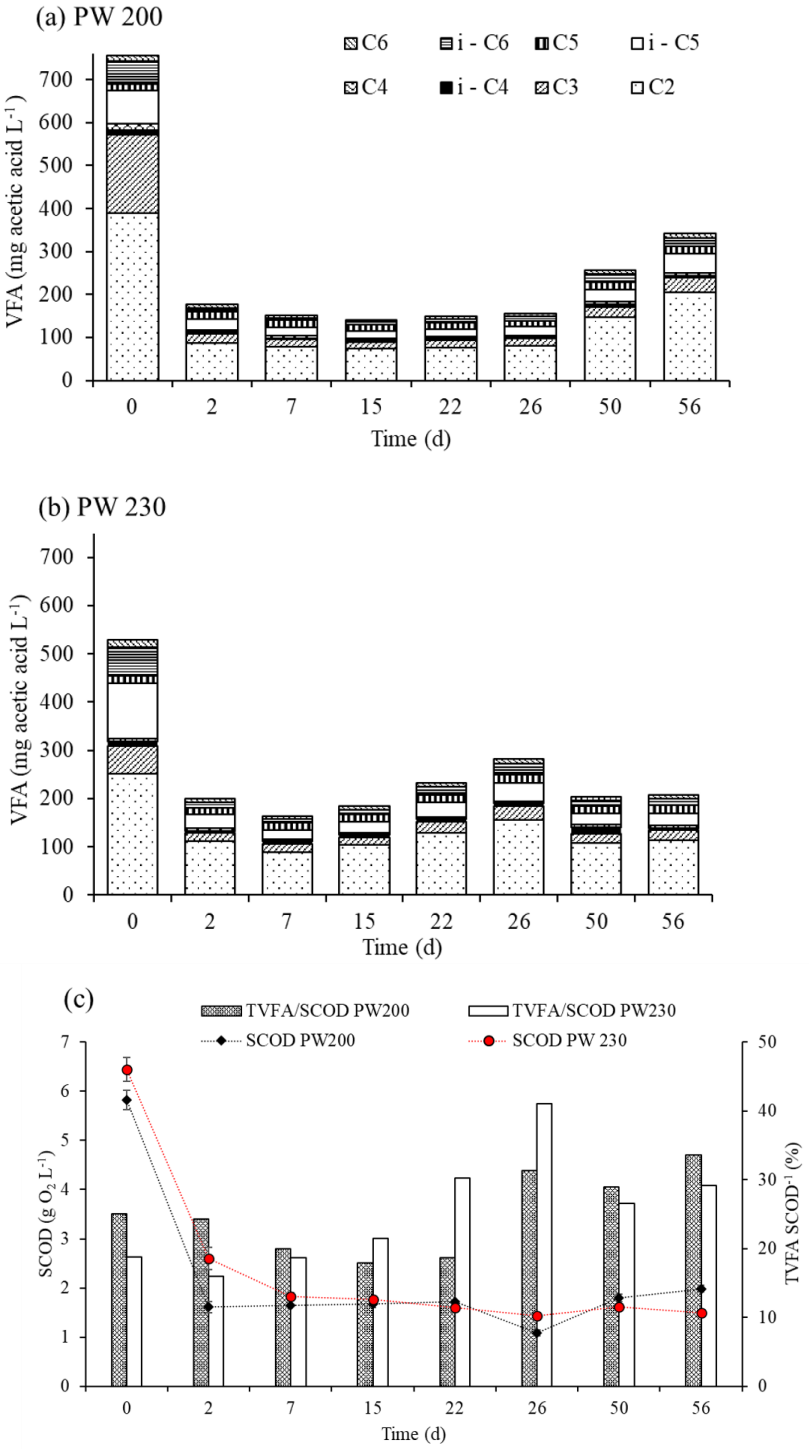

Figure 6.2 Time-course of individual VFA concentrations (in mg acetic acid L^{-1}) during anaerobic digestion for (a) PW200 and (b) PW230; (c) time-course of SCOD (in g O_2 L^{-1}) and TVFA/SCOD

ratio (%) (both parameters expressed as g O_2 L^{-1}) during anaerobic digestion of process water from HTC of food waste.

Parameters such as pH, TA and TAN are key factors for assessing the evolution of AD. For both runs, pH varied in the range 7.4–7.9. These pH values are compatible with the growth of anaerobic microorganisms [20]. TA reached values above 4.0 g $CaCO_3$ L^{-1} at the end of the experiment for both process waters, which allowed the system to provide enough buffering capacity [14]. TAN was in the range 0.2–0.3 g N L^{-1} in the early stages, increasing to 1 and 0.8 g N L^{-1} for PW200 and PW230, respectively, in the last stage. These TAN values are lower than the inhibitory concentration 1.7 g N L^{-1} [20]. These aspects could support that AD approach is promising for treating HTC-derived process water. Indeed, although this specific study was limited to batch test assays, some other works have assessed that the continuous operation of AD on HTC-derived process water from different biomasses (e.g., sewage sludge) can be successfully developed [37–39]. Particularly, Liu et al. [37] reported 71 % COD removal and 285 mL CH_4 STP g^{-1} COD_{added} can be achieved by operating an upflow anaerobic sludge blanket reactor (UASB) for 180 days using HTC-derived PW from sewage sludge.

Methane yield grew exponentially from the early stage to day 20 for all runs. The final methane yields were 140 (7) and 154 (4) mL CH_4 STP g^{-1} COD_{added} for PW200 and PW230, respectively. These methane productions were comparable to the yields reported for process water from carbonized sewage sludge (144–177 mL CH_4 STP g^{-1} COD_{added}) by Villamil et al. [14]. Cumulative methane yields at the end of the experiment proved comparable for both runs, slightly higher for PW230, while food waste showed higher methane production (228 (10) mL CH_4 STP g^{-1} COD_{added}). Lower methane yield (194 (1) mL STP CH_4 g^{-1} COD_{added}) was reported for the organic fraction of municipal solid waste by De la Rubia et al. [19] under mesophilic conditions. At day 26, SCOD declined to 81% and 78% for PW200 and PW230, respectively (calculated referring to the initial SCOD at day 0). The non-biodegradable SCOD fraction could be attributed to refractory compounds (difficult to degrade) generated during food waste carbonization. Indeed,

long-chain hydrocarbons and oxygen- and nitrogen-bearing aromatic compounds were detected in both process waters (**Fig. 6.4**).

The experimental cumulative methane yield was fitted with a first-order kinetic equation (**Fig. 6.3**), widely used to simulate methane production during AD [12]. Fitting was performed using Origin software (version 9.1). Considering the shape of the methane yield curve with no lag-phase, first-order kinetics were selected to simulate the CH_4 pattern during the AD test. The first-order kinetic equation (**equation 6.8**) used to simulate CH_4 yield was:

$$G(t) = G_{max} \cdot [1 - \exp(-k \cdot t)] \quad (6.8)$$

where G_{max} (mL CH_4 STP g^{-1} COD_{added}) is the ultimate methane yield and k (d^{-1}) is the kinetic constant.

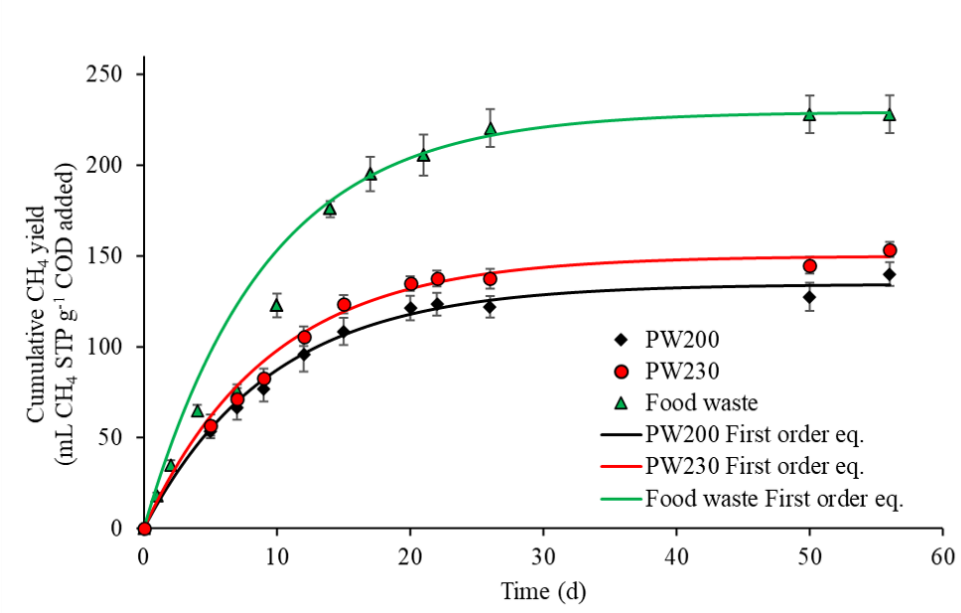

Figure 6.3 Time-course of cumulative methane yield from food waste, PW200 and PW230 during anaerobic digestion (experimental data and first-order equation values).

High values of determination coefficient R^2 (0.998 for PW200 and 0.999 for PW230 and food waste) were observed, indicating a good fit of the experimental data to the proposed model. The predicted final methane yields were also close to the experimental ones. Values of G_{max} (reported

as modelled values ± standard error) were: 135 ± 2 mL CH_4 STP g^{-1} COD_{added} for PW200, 150 ± 2 mL CH_4 STP $g^{-1}COD_{added}$ for PW230 and 229 ± 1 mL CH_4 STP $g^{-1}COD_{added}$ for food waste. The specific rate constants (k) of process water were similar (0.105 ± 0.011 and 0.106 ± 0.008 d^{-1} for PW200 and PW230, respectively). These values of k were higher than the kinetic constants described for process water obtained by HTC of sewage sludge (0.031–0.048 d^{-1}) [14]. For both process waters, all fitted parameters were comparable, sustaining the idea that there were no relevant differences between the two runs. For food waste, a comparable value of kinetic constant k (0.110 ± 0.006 d^{-1}) was obtained. Since no significant lag-phase was observed, it suggests that hydrolysis was not the limiting step in AD. The value of the first order constant was consistent with the range of k values (0.056–0.364 d^{-1}) reported elsewhere for AD of food waste using a different inoculum [2], The raw food waste, PW200 and PW230 showed similar values of the kinetic constant, and both process waters resulted in a lower G_{max} value than that estimated for food waste, which proved its higher biodegradability under anaerobic conditions compared to process waters. This may be due to recalcitrant compounds in HTC process water (**Fig. 6.4**), which could affect degradation.

Since carbonization reaction routes include hydrolysis, dehydration, decarboxylation, condensation, polymerization and aromatization, process water from HTC usually contains alkenes, phenolic and aromatic compounds [40]. A semi-quantitative analysis of chemical compounds was therefore carried out on PW200 and PW230, before (day 0) and after AD (day 56). The species were assembled into chemical groups (i.e., long-chain hydrocarbons, pyrazine, pyridine, aromatic compounds including all aromatics not grouped in the above categories, and non-aromatic N-compounds). Their concentrations were expressed as chromatogram peak area (%). **Fig. 6.4** shows the chemical species detected by GC/MS in the two process waters. In particular, PW200 showed a significantly higher percentage of long-chain hydrocarbons than PW230 at day 0. At the beginning of AD, PW200 was found to contain long-chain fatty acids with a methyl ester group (e.g., methyl ester hexadecanoic acid), whereas only 2-hexene was

observed in PW230. This suggests that the lower temperature 200°C promotes long-chain hydrocarbons, which formed other compounds at 230°C. Ring-type structures with one or two N heteroatoms were found in both at the beginning of AD. Aromatics (e.g., 1,4-benzenediamine), pyrazines (e.g., 2-ethyl-3-methylpyrazine) and pyridines (e.g., 2-methylpyridine) were observed in both process water samples. These compounds are generally formed during HTC by hydrolysis of proteins and carbohydrates [12]. In addition, PW200 showed a lower percentage of aromatics than PW230 at day 0, suggesting that the higher temperature may promote aromaticity. After AD, both process waters showed a heterogeneous composition of long-chain hydrocarbons, aromatics and N-structures. Interestingly, the removal of specific compounds was observed in both runs. As reported in **Appendix A3** (**Tab. A3.2**), up to 74% and 67% of 2-methylpyridine was removed by day 56 from PW200 and PW230, respectively. In addition, removal of 2-ethyl-3-methylpyrazine was up to 93% and 83% for PW200 and PW230, respectively, indicating that AD may remove these specific compounds. Finally, 2-methylcyclopentanone was detected in both runs at the end of the AD experiments, suggesting that this compound may be formed during anaerobic digestion.

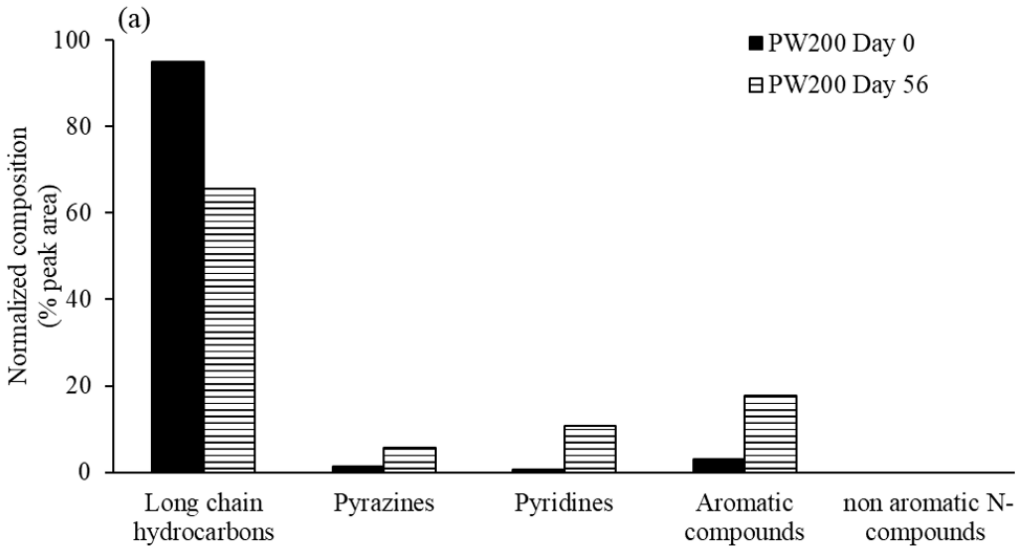

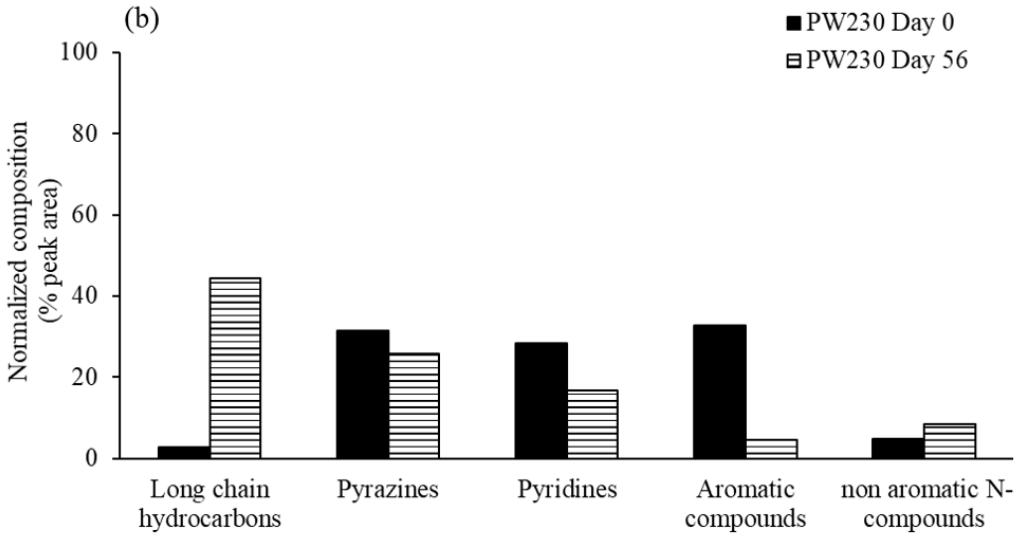

Figure 6.4 Chemical species detected by GC/MS in (a) PW200 and (b) PW230 at Day 0 and Day 56 of anaerobic digestion.

6.3.3 Energy and economic evaluation of the HTC-AD coupled process

In order to compare the performance of HTC of food waste coupled with AD of the resulting process water with the standalone AD configuration, an energy balance was performed for the different process conditions (**Tab. 6.3**). The balance was performed starting from 1 kg of food waste (dry basis) with a moisture content of ~ 93 wt %, according to the experimental data. In addition, solid and liquid yields obtained experimentally for the different operating conditions were considered. The energy input (E_{input}) for AD was ignored in all cases due to mesophilic conditions. The destination of the AD effluent will depend on its characteristics. Therefore, several options could be considered, such as direct discharge into a waterbody or into an urban sewerage system to complete water treatment. On the contrary, the energy input for HTC of food waste required initial heating of the HTC reactor (1.5 m^3) for 1 h to the selected HTC temperature, after loading the wet food waste at room temperature (25ºC): about 24 MJ $kg^{-1}_{dry\ feedstock}$ in both cases. However, as this process is designed to work continuously, we integrated the energy of the streams for heat recovery. We assumed that the hot outlet stream from the HTC reactor could be used to preheat the inlet to 100ºC, so the only energy input required was that needed to heat the

feedstock. This reduced the energy requirements to maintain the process by more than 70% for both HTC temperatures. Energy inputs were calculated using **equation 6.9 and 6.10**:

$$E_{HTC,in} = [(m_L \cdot C_L + m_s \cdot C_{FW} + C_R + h_R \cdot A \cdot \tau) \cdot (T_{HTC} - T_{298K})] \quad (6.9)$$

$$E_{preheat-HTC,in} = [m_L \cdot C_L + m_s \cdot C_{FW}] \cdot (T_{HTC} - T_{373K}) \quad (6.10)$$

where m_L is the liquid content of the food waste; C_L the specific heat of the liquid fraction of food waste, assumed equal to water (4.18 kJ kg^{-1} K^{-1}); m_S the dry solid content of food waste; C_{FW} the specific heat of food waste (2.8 kJ kg^{-1} K^{-1}), calculated with the Aspen Plus simulator using its experimental characteristics; C_R the heat capacity of the reactor (1550 kJ K^{-1}); h_R the convective heat transfer coefficient; A the surface area of the HTC reactor ($h_R \cdot A$= 0.032 kW K^{-1}) [41]; and τ the reaction time (1 h).

After carbonization of food waste, the hydrochar was assumed to be dewatered to a wet solid with a moisture content of 40 wt % using a filter-press, and then thermally dried to reach a moisture content of around 8 wt % [10, 42]. Energy consumption for hydrochar dewatering was 0.2 MJ kg^{-1} of dry food waste in all cases, using 162 kJ kg^{-1} of the resulting solid as reference value [10]. The energy input for thermal drying was calculated on the basis of the steam required to evaporate the water (1.2 kg steam (with an enthalpy of 2631 kJ kg^{-1} at 4 bar) per kg of water) from the wet hydrochar [43]. It turned out to be 10% higher at 200ºC than at 230ºC due to the greater amount of solid generated. Finally, 0.1 MJ kg^{-1} of dry feedstock was allowed for hydrochar pelletization in both cases in order to facilitate its transport and use in heating systems; 0.18 MJ kg^{-1} was the reference value used [44]. This means that the main energy requirement for the HTC system in preheating configuration was that of the HTC reaction (77% and 83% at 200°C and 230ºC, respectively).

A value of 18.9 MJ kg^{-1} of dried food waste was taken as reference for the maximum heating value that this feedstock could provide by combustion. However, direct use of food waste as solid fuel is not recommended due to the high energy requirements for drying (2.5–2.7 MJ kg^{-1} of

evaporated water) [45], in addition to the high N and S content compared to woody biomass, and the lower HHV [46]. Furthermore, the use of raw food waste as a fuel is problematic because of its heterogeneity, low mass and low energy density [47].

The energy output (E_{output}) of conventional AD depends on the amount of methane produced per kg of food waste. Therefore, since the potential energy output of AD is the entire net energy (E_{output}-E_{input}), the energy recovery yield can be up to 67% of the feedstock energy content. This was mainly due to the high methane production of this substrate (228 mL STP CH_4 g^{-1} COD_{added} or 301 mL STP CH_4 g^{-1} VS_{added}). These values are comparable with those reported in the literature, the range of which is wide, depending on substrate characteristics (158–529 mL CH_4 g^{-1} VS_{added}) [2]. On the other hand, the total energy output of the combined HTC-AD process includes combustion of the hydrochar and the methane from AD of process water, which were at least 35% higher than the energy produced by AD alone for the two HTC temperatures. The energy output of HTC at 230ºC was ~95% of the energy available in the feedstock, which was around 5% higher than that obtained for HTC at 200ºC. This is mainly due to the higher HHV of HC230, the greater amount of process water and the higher methane yield at this temperature. However, the net energy of HTC-AD depends on the energy inputs, and although the results remained positive, it is an energetically less favorable treatment (52% and 49% energy recovery at 200ºC and 230ºC, respectively) than AD of the feedstock. Nevertheless, HTC could play a key role in food waste management. Indeed, despite the energy requirements of HTC-AD, this treatment can avoid generation of a large amount of unstable digestate by AD (~ 0.5 ton $ton^{-1}_{wet\ waste}$ [48]). In addition, the energy requirements of HTC-AD can be covered by combustion of the methane and part of the hydrochar produced, while the excess can be marketed.

Although this study was mainly focused on energy recovery without going into economic aspects, product prices were taken into account. Thus, we assumed a natural gas selling price of 2.01 € GJ^{-1} (the average price in 2020 according to the U.S. Energy Information Administration), while the price of hydrochar was based on the market price established by Ingelia S.L. (9 € GJ^{-1}), which is

also comparable to the price range of wood pellets (10–12 € GJ^{-1}) [49]. Assuming these market prices, it was possible to calculate an economic value for each process. As shown in **Tab. 6.3**, the treatment providing the highest economic value was HTC from food waste at 200ºC coupled with AD of process water. In this case, the economic value proved to be three times that obtained with standalone AD.

Table 6.3 Energy and economic assessment of food waste valorization by AD and HTC-AD.

	T (ºC)	Energy $_{Input}$ (MJ kg$^{-1}_{dry\ feedstock}$)					Energy $_{Output}$ (MJ kg$^{-1}_{dry\ feedstock}$)			Economic value (€ kg$^{-1}_{dry\ feedstock}$)[6c]
							Combustion			
		HTC Reaction	Dewatering	Thermal drying	Pelletizer	Total input	Hydrochar	Methane	Total output	
HTC-AD	200	5.6	0.2	1.4	0.1	7.2	13.1	4.0	17.1	0.10
	230	7.3	0.2	1.2	0.1	8.8	13.8	4.2	18.0	0.08
AD	35	-	-	-	-	-	-	12.7	12.7	0.03

[6c] from the sale of the excess product

6.4 Conclusions

Hydrothermal carbonization emerges as alternative for valorizing food waste. Temperatures above 200 °C were suitable for improving the energetic properties of hydrochar, which has attractive characteristics (HHV and combustion properties) as a biofuel for industry. Process water is valorized by anaerobic digestion, achieving promising methane production. Although the energy assessment is strongly influenced by the energy requirements for carbonization, HTC could offer real benefits in terms of resources, particularly with regard to economic aspects. Considering the net energy and the subsequent economic value of both processes, AD coupled with HTC at 200°C seems to be optimal for food waste valorization.

6.5 Supplementary information A3

Supplementary data of this article can be found in **Appendix A3**.

6.6 References – Chapter 6

1. European Commission: A Clean Planet for all. A European long-term strategic vision for a prosperous, modern, competitive and climate neutral economy. Com(2018) 773. 25 (2018)
2. Browne, J.D., Murphy, J.D.: Assessment of the resource associated with biomethane from food waste. Appl. Energy. 104, 170–177 (2013). https://doi.org/10.1016/j.apenergy.2012.11.017
3. Pham, T.P.T., Kaushik, R., Parshetti, G.K., Mahmood, R., Balasubramanian, R.: Food waste-to-energy conversion technologies: Current status and future directions. Waste Manag. 38, 399–408 (2015). https://doi.org/10.1016/j.wasman.2014.12.004
4. Ul Saqib, N., Sharma, H.B., Baroutian, S., Dubey, B., Sarmah, A.K.: Valorisation of food waste via hydrothermal carbonisation and techno-economic feasibility assessment. Sci. Total Environ. 690, 261-276fenergy (2019). https://doi.org/10.1016/j.scitotenv.2019.06.484
5. Gupta, D., Mahajani, S.M., Garg, A.: Investigation on hydrochar and macromolecules recovery opportunities from food waste after hydrothermal carbonization. Sci. Total Environ. 749, 142294 (2020). https://doi.org/10.1016/j.scitotenv.2020.142294
6. Funke, A., Ziegler, F.: Hydrothermal carbonization of biomass: A summary and discussion of chemical mechanisms for process engineering. Biofuels, Bioprod. Biorefining. 4, 160–177 (2010). https://doi.org/10.1002/bbb.198
7. Lu, X., Jordan, B., Berge, N.D.: Thermal conversion of municipal solid waste via hydrothermal carbonization: Comparison of carbonization products to products from current waste management techniques. Waste Manag. 32, 1353–1365 (2012). https://doi.org/10.1016/j.wasman.2012.02.012
8. Akarsu, K., Duman, G., Yilmazer, A., Keskin, T., Azbar, N., Yanik, J.: Sustainable valorization of food wastes into solid fuel by hydrothermal carbonization. Bioresour. Technol. 292, 121959

(2019). https://doi.org/10.1016/j.biortech.2019.121959

9. Li, L., Flora, J.R.V., Berge, N.D.: Predictions of energy recovery from hydrochar generated from the hydrothermal carbonization of organic wastes. Renew. Energy. 145, 1883–1889 (2020). https://doi.org/10.1016/j.renene.2019.07.103

10. Lucian, M., Volpe, M., Merzari, F., Wüst, D., Kruse, A., Andreottola, G., Fiori, L.: Hydrothermal carbonization coupled with anaerobic digestion for the valorization of the organic fraction of municipal solid waste. Bioresour. Technol. 314, 123734 (2020). https://doi.org/10.1016/j.biortech.2020.123734

11. Aragón-briceño, C., Ross, A.B., Camargo-valero, M.A.: Evaluation and comparison of product yields and bio-methane potential in sewage digestate following hydrothermal treatment. Appl. Energy. 0–1 (2017). https://doi.org/10.1016/j.apenergy.2017.09.019

12. Marin-Batista, J.D., Villamil, J.A., Qaramaleki, S. V, Coronella, C.J., Mohedano, A.F., de la Rubia, M.A.: Energy valorization of cow manure by hydrothermal carbonization and anaerobic digestion. Renew. Energy. 160, 623–632 (2020). https://doi.org/10.1016/j.renene.2020.07.003

13. Marin-Batista, J.D., Mohedano, A.F., Rodríguez, J.J., De la Rubia, M.A.: Energy and phosphorous recovery through hydrothermal carbonization of digested sewage sludge. Waste Manag. 105, 566–574 (2020). https://doi.org/10.1016/j.wasman.2020.03.004

14. Villamil, J.A., Mohedano, A.F., Rodriguez, J.J., de la Rubia, M.A.: Valorisation of the liquid fraction from hydrothermal carbonisation of sewage sludge by anaerobic digestion. J. Chem. Technol. Biotechnol. 93, 450–456 (2018). https://doi.org/10.1002/jctb.5375

15. Channiwala, S.A., Parikh, P.P.: A unified correlation for estimating HHV of solid , liquid and gaseous fuels. 81, (2002)

16. APHA (American Public Health Association): APHA Standard methods for examination of water and wastewater. (2005)

17. Raposo, F., de la Rubia, M.A., Borja, R., Alaiz, M.: Assessment of a modified and optimised method for determining chemical oxygen demand of solid substrates and solutions with high suspended solid content. Talanta. 76, 448–453 (2008). https://doi.org/10.1016/j.talanta.2008.03.030

18. Jenkins, S.R., Morgan, J.M., Sawyer, C.L.: Measuring anaerobic sludge digestion and growth by a simple alkalimetric titration. 55, 448–453 (1983)

19. De la Rubia, M.A., Villamil, J.A., Rodriguez, J.J., Borja, R., Mohedano, A.F.: Mesophilic anaerobic co-digestion of the organic fraction of municipal solid waste with the liquid fraction from hydrothermal carbonization of sewage sludge. Waste Manag. 76, 315–322 (2018). https://doi.org/10.1016/j.wasman.2018.02.046

20. De la Rubia, M.A., Villamil, J.A., Rodriguez, J.J., Mohedano, A.F.: Effect of inoculum source and initial concentration on the anaerobic digestion of the liquid fraction from hydrothermal carbonisation of sewage sludge. Renew. Energy. 127, 697–704 (2018). https://doi.org/10.1016/j.renene.2018.05.002

21. Mureddu, M., Dessì, F., Orsini, A., Ferrara, F., Pettinau, A.: Air- and oxygen-blown characterization of coal and biomass by thermogravimetric analysis. Fuel. 212, 626–637 (2018).

https://doi.org/10.1016/j.fuel.2017.10.005

22. Lu, X., Jordan, B., Berge, N.D.: Thermal conversion of municipal solid waste via hydrothermal carbonization: Comparison of carbonization products to products from current waste management techniques. Waste Manag. 32, 1353–1365 (2012). https://doi.org/10.1016/j.wasman.2012.02.012

23. He, C., Giannis, A., Wang, J.Y.: Conversion of sewage sludge to clean solid fuel using hydrothermal carbonization: Hydrochar fuel characteristics and combustion behavior. Appl. Energy. 111, 257–266 (2013). https://doi.org/10.1016/j.apenergy.2013.04.084

24. Reza, M.T., Lynam, J.G., Uddin, M.H., Coronella, C.J.: Hydrothermal carbonization: Fate of inorganics. Biomass and Bioenergy. 49, 86–94 (2013). https://doi.org/https://doi.org/10.1016/j.biombioe.2012.12.004

25. Ro, K.S., Libra, J.A., Bae, S., Berge, N.D., Flora, J.R.V., Pecenka, R.: Combustion Behavior of Animal-Manure-Based Hydrochar and Pyrochar. ACS Sustain. Chem. Eng. 7, 470–478 (2019). https://doi.org/10.1021/acssuschemeng.8b03926

26. He, C., Zhang, Z., Ge, C., Liu, W., Tang, Y., Zhuang, X., Qiu, R.: Synergistic effect of hydrothermal co-carbonization of sewage sludge with fruit and agricultural wastes on hydrochar fuel quality and combustion behavior. Waste Manag. 100, 171–181 (2019). https://doi.org/10.1016/j.wasman.2019.09.018

27. Lang, Q., Zhang, B., Liu, Z., Chen, Z., Xia, Y., Li, D., Ma, J., Gai, C.: Co-hydrothermal carbonization of corn stalk and swine manure: Combustion behavior of hydrochar by thermogravimetric analysis. Bioresour. Technol. 271, 75–83 (2019). https://doi.org/10.1016/j.biortech.2018.09.100

28. Zheng, C., Ma, X., Yao, Z., Chen, X.: The properties and combustion behaviors of hydrochars derived from co-hydrothermal carbonization of sewage sludge and food waste. Bioresour. Technol. 285, 121347 (2019). https://doi.org/10.1016/j.biortech.2019.121347

29. Dai, L., Yang, B., Li, H., Tan, F., Zhu, N., Zhu, Q., He, M., Ran, Y., Hu, G.: A synergistic combination of nutrient reclamation from manure and resultant hydrochar upgradation by acid-supported hydrothermal carbonization. Bioresour. Technol. 243, 860–866 (2017). https://doi.org/10.1016/j.biortech.2017.07.016

30. Sarrion, A., Diaz, E., de la Rubia, M.A., Mohedano, A.F.: Fate of nutrients during hydrothermal treatment of food waste. Bioresour. Technol. 342, 125954 (2021). https://doi.org/10.1016/j.biortech.2021.125954

31. Wang, L., Chang, Y., Liu, Q.: Fate and distribution of nutrients and heavy metals during hydrothermal carbonization of sewage sludge with implication to land application. J. Clean. Prod. 225, 972–983 (2019). https://doi.org/10.1016/j.jclepro.2019.03.347

32. Smith, A.M., Ross, A.B.: Production of bio-coal, bio-methane and fertilizer from seaweed via hydrothermal carbonisation. Algal Res. 16, 1–11 (2016). https://doi.org/10.1016/j.algal.2016.02.026

33. Wang, T., Zhai, Y., Zhu, Y., Gan, X., Zheng, L., Peng, C., Wang, B., Li, C., Zeng, G.: Evaluation of the clean characteristics and combustion behavior of hydrochar derived from food waste towards solid biofuel production. Bioresour. Technol. 266, 275–283 (2018).

https://doi.org/10.1016/j.biortech.2018.06.093

34. Niu, S., Chen, M., Li, Y., Xue, F.: Evaluation on the oxy-fuel combustion behavior of dried sewage sludge. Fuel. 178, 129–138 (2016). https://doi.org/10.1016/j.fuel.2016.03.053

35. Sahu, S.G., Sarkar, P., Chakraborty, N., Adak, A.K.: Thermogravimetric assessment of combustion characteristics of blends of a coal with different biomass chars. Fuel Process. Technol. 91, 369–378 (2010). https://doi.org/https://doi.org/10.1016/j.fuproc.2009.12.001

36. Idowu, I., Li, L., Flora, J.R.V., Pellechia, P.J., Darko, S.A., Ro, K.S., Berge, N.D.: Hydrothermal carbonization of food waste for nutrient recovery and reuse. Waste Manag. 69, 480–491 (2017). https://doi.org/10.1016/j.wasman.2017.08.051

37. Liu, S., Wang, Y., Guo, J., Wang, W., Dong, R.: Start-up and performance evaluation of upflow anaerobic sludge blanket reactor treating supernatant of hydrothermally treated municipal sludge: Effect of initial organic loading rate. Biochem. Eng. J. 166, 107843 (2021). https://doi.org/10.1016/j.bej.2020.107843

38. Weide, T., Brügging, E., Wetter, C.: Anaerobic and aerobic degradation of wastewater from hydrothermal carbonization (HTC) in a continuous, three-stage and semi-industrial system. J. Environ. Chem. Eng. 7, (2019). https://doi.org/10.1016/j.jece.2019.102912

39. Wirth, B., Reza, T., Mumme, J.: Influence of digestion temperature and organic loading rate on the continuous anaerobic treatment of process liquor from hydrothermal carbonization of sewage sludge. Bioresour. Technol. 198, 215–222 (2015). https://doi.org/10.1016/j.biortech.2015.09.022

40. Danso-Boateng, E., Shama, G., Wheatley, A.D., Martin, S.J., Holdich, R.G.: Hydrothermal carbonisation of sewage sludge: Effect of process conditions on product characteristics and methane production. Bioresour. Technol. 177, 318–327 (2015). https://doi.org/10.1016/j.biortech.2014.11.096

41. Namioka, T., Miyazaki, M., Morohashi, Y., Umeki, K., Yoshikawa, K.: Modeling and analysis of batch-type thermal sludge pretreatment for optimal design. J. Environ. Eng. 3, (2008). https://doi.org/10.1299/jee.3.170

42. Yoshikawa, K., Prawisudha, P.: Hydrothermal Treatment of Municipal Solid Waste for Producing Solid Fuel. Presented at the (2014)

43. Werther, J.: Potentials of biomass co-combustion in coal-fired boilers. In: Proceedings of the 20th International Conference on Fluidized Bed Combustion. pp. 27–42. SpringerOpen (2009)

44. Lucian, M., Fiori, L.: Hydrothermal carbonization of waste biomass: Process design, modeling, energy efficiency and cost analysis. Energies. 10, (2017). https://doi.org/10.3390/en10020211

45. R.C. Fluck, C.D.B.: Energy requirements for agricultural inputs in agricultural energetics. (1980)

46. Kratzeisen, M., Starcevic, N., Martinov, M., Maurer, C., Müller, J.: Applicability of biogas digestate as solid fuel. Fuel. 89, 2544–2548 (2010). https://doi.org/10.1016/j.fuel.2010.02.008

47. Pradhan, P., Mahajani, S.M., Arora, A.: Production and utilization of fuel pellets from biomass: A review. Fuel Process. Technol. 181, 215–232 (2018). https://doi.org/https://doi.org/10.1016/j.fuproc.2018.09.021

48. Møller, J., Boldrin, A., Christensen, T.H.: Anaerobic digestion and digestate use: Accounting of greenhouse gases and global warming contribution. Waste Manag. Res. 27, 813–824 (2009). https://doi.org/10.1177/0734242X09344876

49. De Mena Pardo, B., Doyle, L., Renz, M., Salimbeni, A.: Industrial scale hydrothermal carbonization: new applications for wet biomass waste. (2016)

Conclusions

In this work, HTC was proposed as an alternative technology for SS and FW treatment. The research followed different investigation lines, but they were all connected with each other. Firstly, different HTC operational conditions (temperature, time, and solid content) were tested on SS, with the aim of understanding their influence on PW and HC characteristics, also considering their final application. Consequently, maintaining the same operational conditions (220 °C, 85 min, and 15 wt % of solid content), anaerobically/aerobically digested sludges were processed, and PW was characterized in detail. Its application as fertilizer on soil, or as a substrate in AD, or as an effluent to be treated into a WRRF was proposed. However, as regards its use on soil, the concentration of heavy metals was found to be the most critical parameter. PW was also tested as an acidified solution in P recovery acid leaching experiments, compared to demi water, with the aim of proposing a feasible treatment line to recover P from SS. The results demonstrated that high P recovery yield can be achieved with both nitric and sulfuric acid. The anaerobic digestion of PW was further investigated through a continuous UASB reactor. The monitored parameters (COD, VFA, TN, and TAN), together with the observed biogas production, agreed in indicating the stability of the reactor. Further, an LCA analysis was performed to understand the environmental benefits of including this technology in different configurations into SS treatment line. It suggested that HTC would improve the environmental performances of a WRRF by reducing the impacts in most indicators. Lastly, the application of HTC on FW showed that both PW and HC derived from carbonization could be energetically valorized through AD and combustion, respectively. Therefore, starting from the all collected information, it can be concluded that HTC might be a promising technology for both SS and FW treatment, since the derived products (PW, and HC) could be advantageously exploited in different fields. Below are the detailed conclusions for each Chapter:

Hydrothermal carbonization of sewage sludge: influence of process conditions

1. HC yield and C_{yield} were described by a linear relationship with the variables of temperature, reaction time, and solid content of the feedstock. Severity influenced the ash and the volatile

matter content of HC. The first one increased, while the second one decreased, respectively, with severity. H/C and O/C ratio were affected by reaction severity, and both ratios decreased with the increase of the initial solid load.

2. The dewaterability of slurry derived from carbonization of SS was strongly enhanced with respect to the raw sludge. The filtration performances of slurry were not significantly affected by reaction severity.
3. Carbon distribution depended by reaction temperature and by solid content of the initial feedstock. The concentration of C in HC decreased with the rise of temperature, while it increased at high solid load. No significant impact of reaction time on carbon distribution was observed, while the concentration in PW of specific compounds (e.g., TAN, and As) showed a linear relationship with severity, as they increased with an enhancement of reaction severity.

Phosphorous recovery from hydrochar derived by hydrothermal carbonization of sewage sludge

4. Acid leaching proved to be an efficient method to recover phosphorous from HC. Among the investigated key parameters (i.e., pH, contact time, solid/solution ratio, and type of acid), pH showed to mostly impact the P yield response.
5. The application of HNO_3 promoted a reduction of ash content on leachate HC, while H_2SO_4 determined an ash increase on HC after leaching, since calcium sulfate precipitation could occur. Thus, the use of nitric acid is preferable if HC would be applied as a solid fuel.
6. Regardless the use of PW or demi water as solution, the optimization pointed out that a pH equal to 1 must be reached to optimize the responses (P yield and ash content). However, lower acid consumptions were observed using demi water instead of PW. Regarding the application of demi water, higher P yields were obtained using H_2SO_4 instead of HNO_3, and the optimal conditions were identified as follows: HNO_3, pH equal to 1, time of 240 minutes, and solid/solution ratio equal to 5 wt %.
7. The P–rich acidified solution contains also other solubilized elements (e.g., heavy metals). Therefore, a proper characterization of this fraction should be performed prior its further applications.

Characterization of hydrothermal carbonization process water for optimizing the recovery of energy and valuable materials from sewage sludge

8. The distribution of C, N, and P between HC and PW proved to be independent of the origin of SS (anaerobically/aerobically stabilized). C and P were preferably retained into the solid matrix of HC, while N distribution showed a higher variability. The characterization of PW demonstrated that, except for specific parameters (e.g., Cr), its valorization as fertilizer might be promising in the future.
9. The anaerobic/aerobic biodegradability of COD ranged from 50 and 80 % for all PW samples investigated. This suggests that PW valorization could be feasible both through AD or by aerobic treatment into a WRRF.
10. PW derived from HTC of anaerobically digested SS resulted in a higher biodegradability in aerobic conditions, while an inverse trend was observed for PW derived from HTC on aerobically digested SS, which showed a higher biodegradability in anaerobic treatments. Thus, starting from this information, the proper treatment of PW could be designed, even if the anaerobic treatment is still the more advisable.

Performance of upflow anaerobic sludge blanket (UASB) reactor treating process water derived from hydrothermal carbonization of sewage sludge

11. The start-up strategy (i.e., feeding composed of glucose and increasing percentage of PW at a OLR equal to 5 gCOD L^{-1} d^{-1} for the whole duration of the experiments) proved to be concretely effective.
12. The UASB reactor resulted in a COD removal equal to 73 %. The removal percentages linearly decreased with the addition of PW. No accumulation of VFA was observed, while an increase in TAN concentration into the effluent was detected over time.
13. Firmicutes, Synergistetes, Bacteroidota, and Chloroflexi were identified as the most abundant bacterial phyla in granules. All collected data agreed into identifying UASB as a suitable technology to valorize PW through continuous anaerobic digestion.

Environmental Life Cycle Assessment of hydrothermal carbonization of sewage sludge and its products valorization pathways

14. The results derived from LCA analysis pointed out that the integrated scenario HTC + AD (i.e., HTC of anaerobically digested SS and subsequent anaerobic digestion of PW) showed better environmental performances than other proposed scenarios in eleven on sixteen impact categories. Lignite replacement proved to be the main avoided impacts for all indicators, being strictly related to HC yield and its LHV. Conversely, the additional benefits deriving from the valorization of biogas from PW through an ICE to produce EE and TE does not strongly contribute in reducing the environmental impacts.
15. Scenarios with P recovery (i.e., HTC + AD + P_{dry} and HTC + AD + P_{wet}) generally led to worse environmental performances than the others, due to the high impact of water and nitric acid required by acid leaching compared to the relatively small contribution of the avoided impact of using the P recovered to replace conventional fertilizer.

Improved energy recovery from food waste through hydrothermal carbonization and anaerobic digestion

16. A temperature equal to 200 °C (for 1 hour) has been identified as suitable for improving the energetic properties of HC derived from carbonization of food waste. Further, PW derived from HTC at the same process conditions resulted in a good specific CH_4 yield (140 mL CH_4 STP g^{-1} COD_{added}), comparable to that obtained from anaerobic digestion of PW derived from HTC at 230 °C (for 1 hour) (154 mL CH_4 STP g^{-1} COD_{added}).
17. Specific recalcitrant compounds (e.g., 2-methylpyridine, and 2-ethyl-3-methylpyrazine) were removed during anaerobic digestion of PW.
18. The energy balance was strongly influenced by the energy requirements for carbonization. However, this technology could be advantageous in terms of resources, especially considering the economic aspects. Thus, HTC at 200°C coupled with anaerobic digestion of PW appeared be optimal for food waste valorization, considering the net energy and the economic aspect.

Future research

This work outlines possible future developments on the application of HTC in SS and FW treatment. Firstly, since the results derived by processing PW from HTC on SS with a UASB reactor were promising, more investigations could be carried out in this direction. Further experiments could be conducted without dilution, without the addition of macro- and micro- nutrients, and at different OLRs with lab-scale reactor. Thus, more information will be collected, with the perspective of scaling-up this technology for future applications.

In addition, the environmental sustainability of the process could be deepened. Specifically, the P recovery process could be optimized to be representative of a full-scale plant. Thus, further P-leaching experiments could be carried out in this direction, evaluating also the viability of applying the P-rich leached solution as fertilizer. Additionally, a detailed economic analysis of potential HTC configurations should be carried out to understand whether, besides the environmental advantages, also an economical benefit will occur applying this technology at a full-scale level.

A1 - Appendix of Chapter 1

A1.1 SRF test

In **Fig. A1.1** is reported a discharge curve obtained filtering the slurry derived by HTC on sludge:

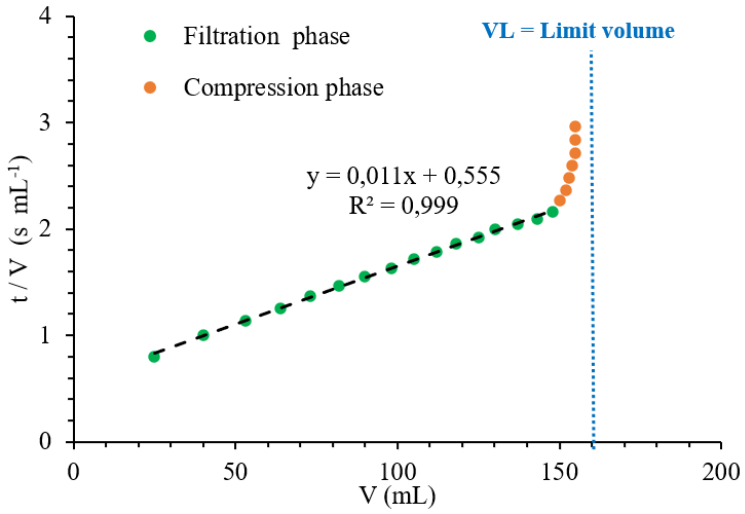

Figure A1.1 – Discharge curve performed on slurry derived for HTC performed at 205 °C, 162.5 min, and a solid concentration of ~ 2.9 wt % (Run 6).

As can be observed in the **Fig. A1.1**, the filtration phase is characterized by a linear behaviour, which is generally associated to the removal of free water. Conversely, during the compression phase, the trend is non-linear and it is generally associated to a compression of a panel, in which a further slow removal can be observed. Then, the experimental points reach an asymptotic behaviour up to the limit volume (VL), which represents the maximum volume than can be filtrated performing this test [1].

A1.2 Design of Experiments (DoE)

A brief insight about DoE is here reported. The DoE is an approach able to systematically analyze the significative elements and the goals of an experiments, in order to organize a plan in which experimental trials are ordered with the maximum efficiency. This methodology is able to evaluate the influence that a variation of an input parameter has on the outputs, developing a mathematical and probabilistic model, able to predict the responses (i.e., outputs) [2]. The DoE is a factorial design, in which the number of trials is generally minimized, and it is based on three main guidelines:

- The experiment is replicable
- The experiments are carried out in a randomised order, with the aim of reducing the systematic error
- The experiments performed with similar external factors must be clustered into blocks, in order to improve the precision and to reduce the variability.

As a rule, two different inputs can be found in a process:

- Controllable variables: X of the process
- Uncontrollable variables: Z of the process

The response (Y of the process) is a function of the all-input variables and it can be expressed as (**equation A1.1**):

$$Y = f(X) + \epsilon \quad (A1.1)$$

Where ϵ is the pure error, which depends from Z variables. The pure error ϵ must be minimized.

The software generally applied for designing the experimental plan is the Design-Expert® 11. Results obtained by DoE analysis were then analyzed through the Analysis of Variance (ANOVA) by the software, which produces a mathematical model of the responses and possible solutions for their optimization.

A development of a DoE plan is based on the following phases:

1) **Definition of the experiment's goals**
2) **Choice of factors and of their variability field**: the most relevant input factors are selected. Two types of factors could be considered: numerical and categorical. The first one is referred to a measurable variable, while the second one is referred to a not numerical variable. The variability field defines the design space, which establishes the validity field of DoE.
3) **Choice of responses**: it is based on the interested outputs.
4) **Chioce of the design**: it depends by the number of tests, number of replicates, and the type of DoE method.

After all these stages, a DoE plan, in which the operational conditions for each experiment are defined, is obtained by the software. Then, experimental trials have to be carried out in the order and with the process conditions reported in the plan. Then, once that the results are obtained, they are analyzed and the models of the responses are obtained.

Usually, three DoE should be carried out in the following order:

1) *Screening Design*: it allows to estimate which factors are actually significant;
2) *Characterization Design*: it includes only the factors that resulted significant in the *Screening Design*. It allows to evaluate if the responses linearly depend from the factors or if a curvature in the correlation occurs.
3) *RSM – Response Surface Methodology*: it allows to obtain a non-linear model of the response, in case that a curvature in the *Characterization Design* is observed. In this phase, an analytic model able to describe the experimental data and its graphical representation are obtained. Thus, the optimization of the process can be performed, in order to obtain the desired response's value.

Three types of design can be carried out (i.e., complete factorial plan, fractional factorial plan, and central composite design (CCD)). In the first one, k factors are varied on L levels (L^k tests are required). The plan is complete when all the possible combinations of the factor levels are used. The second one is carried when the number of factors is too high. Thus, only a group of the whole set of combinations is performed. Further, the third one is the CCD design, which allows to carry out tests in operational conditions out of the design space. It is a complete factorial plan (2^k tests, where k is the number of parameters), but with central and axial points. The latter, named *star points*, are points in which all parameters, without one are set on their average values. The parameters out of the average value will have a value + α with respect to the range defined into the design. It is the standard design, and it was performed in all study cases of this work. Generally, a Face Centred Design (FCD) is performed, in which α =1. As a rule, factorial, axial, and central points could be replicated to obtain a more accurate estimate of the pure error, and consequently, a higher number of trials. Usually, the required number of tests (n) (without replicates) is calculated via the following equation:

$$n = 2^k + 2k + 1 \quad \text{(A2.2)}$$

Where *k* is the number of factors (2^k are the factorial points, 2k the axial point, and 1 the central one).

An essential tool for DoE methodology is the ANOVA. It allows to compare several model fittings of a process, evaluating which is the more suitable. ANOVA is based on a hypothesis test:

- H_o (null hypothesis): all treatments have the same average
- H_1 (alternative hypothesis): not all treatments have the same average

The acceptance or the reject of the hypothesis is generally performed through the *F-statistic* value, which evaluates if the average of the two populations is statistically significant or not.

When *F-statistic* is close to 1, H_o is considered true, while when it is higher than 1 it is considered false. Alternatively, the *p-value* (i.e., the probability to observe an *F-statistic* higher or equal to that observed) can be used:

- *p-value* < 0.05: value statistically significant
- *p-value* < 0.01: value highly significant
- *p-value* > 0.05 value not statistically significant

Thus, when *p-value* is < 0.05, the probability to observe a high value of *F statistics* is higher, and consequently the null hypothesis is rejected, with a probability less than 5 % to make a mistake.

The DoE describes a factor through a mathematical model, in which the coefficients are expressed in the coded form (the sign of effects is here visible, since the increase or the decrease of the response is observed) or in the real form (where units of measure are included).

Lastly, to evaluate the goodness of fit, the determination coefficient R^2 is generally considered (it indicates the percentage variability of Y due to the variability of X in terms of sum of squares). Often the adjusted R^2 is used, since it includes also the number of variables in the set of data, with penalty for points far from the model fitting.

A1.3 References of A1

1. Marinetti, M.: CONDIZIONAMENTO E DISIDRATAZIONE FANGHI. PhD thesis - Politec. di Milano. (2007)

2. Oehlert, G.W. (University of M.: A First Course in Design and Analysis of Experiments). (2003)

A2 – Appendix of Chapter 5

A2.1 HTC Scenario

A2.1.1 Mass balance calculations

Mass balance on HTC process has been carried out on gas, solid, and liquid phase. Carbon (C) yields were applied to carry out this balance for all three fractions.

A2.1.1.1 Hydrochar (HC)

C yield (%) was calculated via **equation A2.1** using experimental data:

$$HY_C(\%) = \frac{\%C_{HC} \cdot \dot{m}_{dry\ hydrochar}}{\%C_{sludge} \cdot \dot{m}_{dry\ sludge}} \cdot 100 \quad \text{(A2.1)}$$

Where:

- $\frac{\dot{m}_{dry\ hydrochar}}{\dot{m}_{dry\ sludge}} \cdot 100$ represents the HY in terms of total solids (HY_{TS}) equal to 76.6 wt %, and $\dot{m}_{dry\ hydrochar/sludge}$ is the mass flow (t d^{-1}) in terms of dry solids (see **Chapter 3**);
- % $C_{HC/sludge}$ is the percentage of C in HC or sludge (measured experimentally and equal to 19.43 and 22.50 wt % dry basis, respectively) (see **Chapter 3**).

HY_C resulted equal to 66.09 wt %.

Thus, the mass flow of hydrochar (t d^{-1}) has been determined on dry basis, and then the total amount was calculated assuming an 8 wt % of moisture after drying.

The dry content of hydrochar after the filter press was assumed equal to 60 wt % [1].

A2.1.1.2 Process water (PW)

Total organic carbon (TOC) (mg L^{-1}) experimental values were used to calculate the process water carbon yield (LY_C), while process water flow (t d^{-1}) was determined by difference between the slurry out of HTC (t d^{-1}) and the amount of wet hydrochar (t d^{-1}) after the filter press.

$$LY_C(\%) = \frac{TOC \cdot \dot{m}_{process\ water}}{\%\ C_{sludge} \cdot \dot{m}_{dry\ sludge}} \cdot 100 \quad \text{(A2.2)}$$

Where:

- TOC (mg L^{-1}) is the concentration of total organic carbon in process water, equal to 13600 mg L^{-1};

- $\dot{m}_{process\ water}$ is the mass flow (t d^{-1}) of the liquid fraction.

LY_C resulted equal to 33.14 wt %. Process water flow resulted equal to 63.30 t d^{-1}.

A2.1.1.3 Gas phase

The gas yield in terms of C was calculated as follows:

$$GY_C\ (\%) = 100 - LY_C - HY_C \quad (A2.3)$$

Where all the terms were already defined previously.

Thus, GY_C (%) resulted equal to 0.77 wt %.

Then, the mass flow of carbon in the gas (t C d^{-1}) was calculated as:

$$\dot{m}_{C\ gas}\ (t\ C\ d^{-1}) = GY_C\ (\%) \cdot\ \%\ C_{sludge} \cdot\ \dot{m}_{dry\ sludge} \quad (A2.4)$$

Where all the terms were already known.

Further, gas was assumed to be a mixture of only CO_2 and CO according to Basso et al. [2]

$$\dot{m}_{gas}\ (t\ d^{-1}) = \frac{x_{CO_2} \cdot PM_{CO_2} + x_{CO} \cdot PM_{CO}}{PM_C} \cdot\ \dot{m}_{C\ gas} \quad (A2.5)$$

Where:

- X_{CO2} is the percentage of CO_2 in gas (92 vol %) [2];
- X_{CO} is the percentage of CO in gas (8 vol %) [2];
- PM_{CO2} is the molecular weight of CO_2 (44 g mol^{-1});
- PM_{CO} is the molecular weight of CO (28 g mol^{-1});
- PM_C is the molecular weight of C (12 g mol^{-1});
- $\dot{m}_{C\ gas}$ was calculated above.

This gas mixture has been directly emitted in atmosphere, so the emissions of biogenic CO_2 can be calculated, even if it has not been considered for the climate change impact.

Gas density has been calculated using ideal gas law (0 °C, and 1 atm):

$$\rho_{gas}\ (kg\ Nm^3) = \frac{P}{RT} \cdot (x_{CO_2}\ \cdot\ PM_{CO_2} + x_{CO}\ \cdot\ PM_{CO}) \quad (A2.6)$$

Where:

- P is equal to 101 325 Pa;
- T is the temperature of 0 °C (273.15 K);
- R is the universal gas constant (8314. 3 J $kmol^{-1}$ K^{-1});

and all the other terms were already defined above.

The gas volume was calculated as:

$$V_{gas}(Nm^3\ d^{-1}) = \frac{\dot{m_{gas}} \cdot 1000}{\rho_{gas}} \quad (A2.7)$$

Where all the terms are defined.

Lastly, CO_2 and CO emissions were calculated using these equations:

$$\dot{m}_{CO_2}\ (kg\ CO_2\ d^{-1}) = x_{CO_2} \cdot V_{gas} \cdot \frac{P \cdot PM_{CO_2}}{R \cdot T} \quad (A2.8)$$

Where all the terms are defined.

A2.1.2 Energy consumption calculations

A2.1.2.1 Volume of HTC reactor

Reactor volume was calculated considering the HTC process conditions (220 °C, 85 min). It was determined using the equation below:

$$V_{HTC}(m^3) = \frac{\dot{m_{tot}} \cdot t}{\rho_{mix} \cdot 24} \quad (A2.9)$$

Where:

- $\dot{m_{tot}}$ is the mass flow entering in HTC reactor (ton d^{-1});
- t is the reaction time (h);
- ρ_{mix}: is the density of the reaction mixture, assumed equal to the feedstock (1.050 ton $m^{3\ -1}$);
- 24 h d^{-1}.

A2.1.2.2 Thermal energy HTC

The thermal energy of HTC was calculated as the sum of the heat needed to heat the solid fraction of the feedstock, and the amount of water contained in sludge. Further, the heating loss from the reactor surface (conduction loss) were considered.

$$E_{HTCin} = E_1 + E_2 + Loss \quad (A2.10)$$

E_1 is the contribute of thermal energy required to heat the solid:

$$E_1\ (kWh \cdot\ d^{-1}) = c_{pss} \cdot \dot{m}_{ss} \cdot (T_{reaction} - T_o) \cdot 0.000278 \quad (A2.11)$$

Where:

- c_{pss} is the specific heat capacity of dry sludge [3] (kJ kg^{-1} K^{-1});

- $\dot{m}_{ss}$ is the mass of dry sludge in the inlet of the HTC reactor (kg d^{-1});
- $T_{reaction}$ is the operational temperature (220 °C);
- T_o is the entering temperature of the feedstock reached after the regenerative heat exchanger (HE), T_o = 200 °C);
- 0.000278 is the conversion factor kWh kJ^{-1}.

E_2 is the contribute of thermal energy required to heat water:

$$E_2\ (kWh \cdot\ d^{-1}) = \dot{m}_w \cdot (H_{reaction} - H_o) \cdot 0.000278 \quad (A2.11)$$

Where:

- $\dot{m}_w$: is the mass of water entering into the reactor;
- $H_{reaction}$: is the enthalpy of water at 220 °C and pressure of 24 bars (before phase transition to steam) (943.7 kJ kg^{-1});
- H_o: is the enthalpy of water at 200 °C and pressure of 24 bars (reached after the regenerative heat exchanger (HE), H_o = 852.7 kJ kg^{-1});
- 0.000278 is the conversion factor kWh kJ^{-1}.

Where:

$$Loss\ (kWh \cdot\ d^{-1}) = R_{tot}\ \cdot A_r\ \cdot \frac{(T_{reaction} - T_o)}{1000} \cdot 24 \quad (A2.12)$$

- R_{tot}: total thermal resistance (W $m^{2\ -1}$ K^{-1});
- A_r: reactor area (m^2);
- $T_{reaction}$ is the operational temperature (220 °C);
- T_o is the temperature of the external environment (25 °C);
- Conversion factor: 1000 W kW^{-1};
- 24 h d^{-1}.

Thermal resistance equation:

$$R_{tot}(W\ m^{2\ -1}\ K^{-1}) = \frac{1}{R_{insulation} + R_{steel}} \quad (A2.13)$$

$$R_{insulation/steel} = \frac{1}{(\frac{\lambda_{insulation/steel}}{s_{insulation/steel}})} \quad (A2.14)$$

$R_{insulation}$: thermal resistance of insulation material (rock fiber) ((m^2 K) W^{-1});

R_{steel}: thermal resistance of steel material ($(m^2\ K)\ W^{-1}$);

$R_{insulation/steel}$: thermal resistance of insulation/steel ($(m^2\ K)\ W^{-1}$);

$\lambda_{insulation/steel}$: thermal conductivity of insulation/steel ($W\ m^{-1}\ K^{-1}$);

$S_{insulation/steel}$: thickness of insulation/steel ($S_{insulation}$ = 0.062 m [3]; S_{steel}= 0.04 m).

$$E_{tot}(kWh \cdot d^{-1}) = \frac{E_{HTCin}}{\eta_{heat}} \quad (A2.15)$$

Where:

η_{heat} = 0.77 is the efficiency value [4].

The thermal energy required for HTC heating is partly recovered by the HE, and the remaining contribute is provided by an external heating source.

A2.1.2.3 Electric energy HTC

The electrical energy considered the energy required for stirring and for pumping.

For stirring, the following equation [4] was used:

$$EE_{stirring}\,(kWh \cdot d^{-1}) = \frac{(N_p \cdot \rho_{mix} \cdot N^3 \cdot d_{rotor}^5) \cdot 24}{\eta_{stirring} \cdot 1000} \quad (A2.16)$$

Where:

- N_p: power number of impeller (0.79);
- ρ_{mix}: is the density of the reaction mixture, assumed equal to the feedstock (1050 $kg\ m^{3\ -1}$);
- N: is the rotational speed calculated using the following equation:

  $$\pi \cdot d_{rotor} \cdot N = v_{tip} = costant$$

  assuming a tip speed (v_{tip}) equal to 1.66 $m\ s^{-1}$;
- d_{rotor}: is the diameter of the impeller, assumed equal to 1/3 of the reactor diameter;
- $\eta_{stirring}$: is an efficiency value for stirring (0.9) [4].

For pumping, the electrical energy was calculated according to head losses calculated for assumed cylindrical and steel tubes.

The diameter of the tube was calculated as:

$$d\ (m) = \sqrt{\frac{4 \cdot Q}{v \cdot 3600 \cdot 24}} \quad (A2.17)$$

Where:

- Q: is the flow of the feedstock entering in the HTC reactor ($m^3\ h^{-1}$);
- v: is the velocity inside the tube (assumed equal to 1.2 m s^{-1});
- 3600 s h^{-1} is the conversion factor.

A standardized diameter equal to 0.1 m was selected.

Losses were calculated considering as absolute turbulent flow, using equation **A2.18**:

$$\Delta H\ (m) = \Delta H_{geo} + \Delta H_{fr} + \Delta H_{st} \quad \text{(A2.18)}$$

Where:

- ΔH_{geo} depends by the height of the HTC reactor;
- ΔH_{fr} represents the distributed losses in tubes calculated as (Darcy-Weisbach equation):

$$\Delta H_{fr}\ (m) = \lambda \cdot \frac{l}{d} \cdot \frac{v^2}{2g} \quad \text{(A2.19)}$$

λ is the friction coefficient defined by Mood diagram for absolute turbulent flow (Re > 4000) and roughness equal to 0.1 mm (steel tubes), and l is the length of the pipeline. The velocity (v) was assumed equal to 1.2 m s^{-1} for both the pumps connected with HTC reactor, and equal to 1 m s^{-1} for all the other pumps.

Lastly, ΔH_{st} depends by the pressure difference:

$$\Delta H_{st}\ (m) = 10.716 \cdot (P_{HTC} - P_o) \quad \text{(A2.20)}$$

Where:

- P_{HTC} is the pressure of HTC reactor (24 bars), while P_o is the atmospheric pressure (1 bar), and 10.716 is a conversion factor bar m^{-1}.

ΔH_{geo}, and ΔH_{fr} were considered for all the studied pumps, while ΔH_{st} was taken into account only for the pump before HTC reactor.

Finally, the electrical energy required for pumping was computed by:

$$EE_{pump}\ (kWh \cdot d^{-1}) = \frac{Q \cdot g \cdot \Delta H_{tot}}{\eta_{pump} \cdot 1000} \cdot 24 \quad \text{(A2.21)}$$

Where:

- Q (kg s^{-1}) is the inlet flow in the studied pump;
- g is 9.81 m s^{-2} is the gravitational constant;

- ΔH_{tot} is the sum of the head loss of the pumping;
- η_{pump} is the efficiency of the pump (0.45 for the pump before HTC [5], and 0.75 for all the other pumps [4]);
- 24 h d^{-1}.

A safety factor of 10 % was considered for all pump studied.

Stirring and pumping equations were applied to determine electrical consumptions of this unit also in all the other scenarios.

A2.1.2.4 Electric energy for slurry dewatering

The slurry mixture was separated using a filter press. A specific energy consumption was used equal to 45 kWh $ton^{-1}_{dry\ solids}$ [1].

$$EE_{filterpress}(kWh \cdot d^{-1}) = 45 \cdot \dot{m}_{dry\ solids} \quad (A2.22)$$

Where:

- 45 kWh $ton^{-1}_{dry\ solids}$ is the specific electrical energy consumption;
- $\dot{m}_{dry\ solids}$ is the amount of dry hydrochar ($t_{dry\ hydrochar}\ d^{-1}$).

A2.1.2.5 Electric energy for screw feeder

Wet hydrochar separated by a filter press was transported by a screw feeder. A specific energy consumption was used to calculate this amount of energy. A value equal to 0.03 kWh m^{-3} was assumed [6]. The following equation was applied:

$$EE_{screw\ feeder}(kWh \cdot d^{-1}) = 0.03 \cdot \frac{\dot{m}_{wet\ hydrochar}}{\rho_{wet\ hydrochar}} \quad (A2.23)$$

Where:

- 0.03 kWh m^{-3} was the specific energy consumption;
- $\rho_{wet\ hydrochar}$ is the density of wet hydrochar (1.147 t m^{-3});
- $\dot{m}_{wet\ hydrochar}$ is the amount of wet hydrochar per day (t d^{-1}).

Process water was collected through a pump, which was sized according to the equation above, assuming a velocity of 1 m s^{-1} and not considering the contribute of $\Delta H_{st.}$

A2.1.2.6 Dryer

Drying was applied to remove the residual hydrochar moisture. After filter press, wet hydrochar (TS = 60 wt %) was dried up to a solid content equal to 8 wt %. Thus, the amount of water to be removed was obtained as the difference of the water between wet and dried hydrochar.

A2.1.2.7 Thermal energy to evaporate water

The thermal energy required to remove water was calculated as follow:

$$ET_{dryer}(kWh \cdot d^{-1}) = \frac{c_{pw}\ \dot{m}_w \cdot (T_{boil} - T_{in}) + \Delta H_{steam} \cdot \dot{m}_{steam}}{3600 \cdot \eta_{dryer}} \quad (A2.24)$$

Where:

- c_{pw} is the specific heat capacity of water at 25 °C (4.187 kJ kg^{-1} K^{-1});
- $\dot{m}_w$ is the amount of water to be evaporated (kg d^{-1});
- T_{boil} is 100 °C (373.15 K);
- T_{in} is the room temperature (25 °C equal to 298.15 K);
- ΔH_{steam} is the latent heat of water 2500 kJ kg^{-1};
- $\dot{m}_{steam}$ is the amount of steam to be produced equal to $\dot{m}_w$ (kg d^{-1});
- η_{dryer} is the efficiency factor of dryer (0.8) [4];
- $\frac{1\ kWh}{3600\ kJ}$ is the conversion factor.

To allow the evaporation of water from wet hydrochar, the air temperature is heated up to the entering temperature in the dryer (200 °C). The air was assumed to be heated up to 200 °C, and to exit from the dryer al 100 °C.

A2.1.2.8 Electric energy air blower

The required amount of air was provided by an air blower and it was calculated as follow:

$$q_{air}(kg\ s^{-1}) = \frac{ET_{dryer}}{24 \cdot c_{p\ air} \cdot (T_{air\ in} - T_{air\ out})} \quad (A2.25)$$

Where:

- ET_{dryer} is the energy required to remove the water from wet hydrochar;
- $c_{p\ air}$ is the heat specific value of air (1.003 kJ kg^{-1} K^{-1});
- $T_{air\ in}$ is the temperature of air in the dryer (200 °C in K);
- $T_{air\ out}$ is the temperature of air out the dryer (100 °C in K);

- 24 h d^{-1}.

Then:

$$Q_{air}(m^3\ s^{-1}) = \frac{q_{air}}{\rho_{air}} \quad \text{(A2.26)}$$

Where:

- q_{air} is the mass flow of air expressed as kg s^{-1};
- ρ_{air} is the air density (1.225 kg m^{-3} at 15 °C).

Lastly, the electrical energy required by the blower was calculated as follow [7]:

$$EE_{blower}(kWh \cdot\ d^{-1}) = \frac{Q_{air} \cdot \Delta P_{blower}}{\eta_{blower} \cdot 1000} \cdot 24 \quad \text{(A2.27)}$$

Where:

- Q_{air} is the flow of required air ($m^3\ s^{-1}$);
- ΔP_{blower} was assumed equal to 5000 Pa [7];
- η_{blower} in the efficiency of the blower (0.80);
- 1000 W kW^{-1};
- 24 h d^{-1}.

A2.1.2.9 Thermal energy air blower

The energy required to heat air up to 200 °C, was calculated as follows:

$$ET_{air}(kWh \cdot\ d^{-1}) = c_{p\ air} \cdot q_{air} \cdot (T_{air\ out} - T_{air\ in}) \cdot 24 \quad \text{(A2.28)}$$

Where:

- $c_{p\ air}$ is the heat specific value of air (1.003 kJ kg^{-1} K^{-1});
- q_{air} is the mass flow of required air (kg s^{-1});
- $T_{air\ out}$ is the temperature of air out the mix heater (100 °C in K);
- $T_{air\ in}$ is the temperature of air in the mix heater (25 °C in K);
- 24 h d^{-1}.

A2.1.2.10 Electric energy pelletizer

Hydrochar was at the end pelletized. A specific energy consumption was used equal to 51 kWh $ton_{dry\ solids}^{-1}$ [7].

$$EE_{pelletization}(kWh \cdot\ d^{-1}) = 51 \cdot \dot{m}_{dry\ solids} \quad \text{(A2.29)}$$

Where:

- 51 kWh $ton_{dry\ solids}^{-1}$ is the specific electrical energy consumption;
- $\dot{m}_{dry\ solids}$ is the amount of dry hydrochar ($t_{dry\ hydrochar}\ d^{-1}$).

A2.1.2.11 Heat exchanger

In all the scenarios including HTC, energy from the slurry suspension exiting the HTC is recovered to preheat the feedstock entering into the HTC reactor, in a regenerative heat exchanger operating in continuous mode. A temperature difference (ΔT) equal to 20 °C has been established between the temperature of the hot slurry entering in HE and the feedstock out of HE, to avoid large exchanges surfaces.

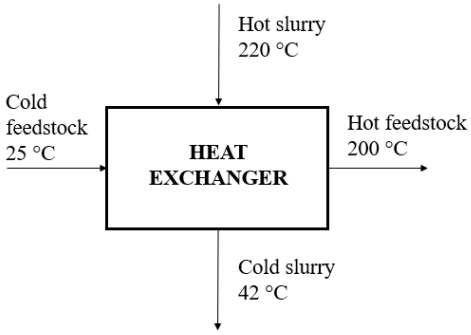

Figure A2.1 Scheme of heat exchanger in which feedstock is heated by hot slurry.

$$\dot{m}_{ss} \cdot c_{p\,ss} \cdot (T_{in\ HTC} - T_o) + \dot{m}_w \cdot (H_{w\ in\ HTC} - H_{w\ o}) = \dot{m}_{slurry} \cdot (H_{slurry\ in\ HE} - H_{slurry\ out\ HE}) \quad \text{(A2.30)}$$

Where:

- c_{pss} is the specific heat capacity of dry sludge ($kJ\ kg^{-1}\ K^{-1}$);
- $\dot{m}_{ss}$ is the mass of dry sludge in the inlet of the HTC reactor ($kg\ d^{-1}$);
- $T_{in\ HTC}$ equal to 200 °C (473.15 K);
- T_o is the initial temperature of the feedstock (25 °C) (298.15 K);
- $\dot{m}_w$ is the mass of water in the inlet of the HTC reactor ($kg\ d^{-1}$);
- $H_{w\ in\ HTC}$ is the enthalpy of water at 200 °C in non-saturated conditions (at a pressure of 24 bars) (852.7 $kJ\ kg^{-1}$);

- $H_{w\,o}$ is the enthalpy of water at 25 °C in non-saturated conditions (at a pressure of 24 bars) (107.8 kJ kg^{-1});
- $\dot{m}_{slurry}$ is the mass flow out of HTC reactor, it was assumed considering only the amount of water (neglecting the energy required to heat the solid) (kg d^{-1});
- $H_{\text{slurry in HE}}$ is the enthalpy of water at 220 °C in non-saturated conditions (943.7 kJ kg^{-1});
- $H_{\text{slurry out HE}}$ is the enthalpy of water in non-saturated conditions at the temperature out of the heat exchanger (HE).

From the **equation A2.30**, $H_{\text{slurry out HE}}$ was calculated. From linear interpolation, the temperature of the slurry out of the heat exchanger was determined (42 °C).

Energy heat from slurry out of HE at 42 °C could be recovered including a second heat exchanger, to pre-heat the air of the dryer. This configuration was initially considered, but then abandoned, since no real advantage was observed (the temperature of air increased of only 2 °C).

A2.2 HTC + AD Scenario

A2.2.1 Mass balance calculations

A2.2.1.1 Anaerobic digestion of process water

Process water is supposed to be treated by anaerobic digestion in HTC+AD Scenario. The balance is based on experimental data reported in the following Table:

Table A2.1 Experimental parameters of anaerobic digestion of PW

Parameter	Unit of measure	Value
COD	mg L^{-1}	31 000
SMP	Nm^3 CH_4 kg^{-1}COD	0.192
CH_4	%	71
TS digestate	%	1.90
TVS TS^{-1}	%	49.7

Biogas is considered as a gas mixture of only CH_4 and CO_2. Using these data, the mass flow (t d^{-1}) of biogas and digestate are determined. After anaerobic digestion (AD), a centrifuge was hypothesized to separate digestate (specific polyelectrolyte consumption of 18 kg $t_{\text{TS digestate}}^{-1}$; % TS in exiting digestate

equal to 20 %) [8]. The digestate was assumed to be treated by composting. A specific composting TS removal yield was assumed equal to 70 wt % [9], and a TS content equal to 60 % was applied for compost [10]. Nutrient contents of compost (as N, P_2O_5, and K_2O) are considered as depicted in the main text. Emissions of CH_4 and N_2O are taken into account according to Garrido – Baserba [11], while CO_2 and H_2O emissions were calculated as follows (**equation A2.31**):

$$\text{Emission } CO_2 + H_2O \text{ (t d}^{-1}) = Q_{\text{out centrifuge}} - Q_{\text{compost}} - \text{Emission } CH_4 - \text{Emission } N_2O \quad \text{(A2.31)}$$

The process losses are calculated as the sum of all emissions (CH_4, N_2O, CO_2, and H_2O). The ICE stack emissions were calculated as reported in the main text.

A2.2.2 Energy consumptions calculations

A2.2.2.1 Anaerobic digestion reactor – Thermal energy

The anaerobic digestion reactor was designed considering a hydraulic retention time of 20 d (the cumulative CH_4 yield at day 20 is ≅ 80 % of the latest CH_4 yield).

$$V\ (m^3) = \dot{m}_{\text{in AD}} \cdot t \quad \text{(A2.32)}$$

Where:

- $\dot{m}_{\text{in AD}}$ is the flow in the AD reactor ($m^3\ d^{-1}$);
- t is the HRT (20 d).

A safety factor is then considered (10 %), and a cylindrical reactor (in which the diameter is equal to the height) is supposed.

In principle, the thermal energy required by the reactor should be calculated as the sum of the energy required to heat the feedstock (assumed equal to water) and losses. The following equation was used:

$$E_{\text{AD in}} = E_1 + \text{Loss} \quad \text{(A2.33)}$$

In which:

$$E_1 = \frac{\dot{m}_{\text{in AD}} \cdot c_{p\,w} \cdot (T_{AD} - T_o)}{1000} \cdot 24 \quad \text{(A2.34)}$$

Where:

- $\dot{m}_{\text{in AD}}$ is the flow in the AD reactor converted in kg s^{-1} (ρ_{PW} assumed equal to ρ_{H2O} = 1000 kg m^{-3};

- $c_{p\,w}$ is the heat specific capacity of water (4187 J kg^{-1} K^{-1});
- T_{AD} is the operational temperature (35 °C);
- T_o is the initial temperature of the feedstock;
- 24 h d^{-1}.

Further, losses from AD reactor were considered using the equation reported above, assuming that the reactor surface is made of a layer of reinforced concrete with 1% of steel (0.25 m) ($\lambda_{concrete}$ = 2.3 W m^{-1} K^{-1} according to UNI EN ISO 10456:2008), and a coat of extruded polyurethane foam (0.05 m) ($\lambda_{polyurethane}$ = 0.034 W m^{-1} K^{-1} UNI 10351:2015).

However, E1 was considered negligible since PW out of HE has a temperature higher than 35 °C. Thus, no further heating of AD feedstock has been taken into account. Hence, thermal energy requirements consider only the losses through AD reactor.

Thus, the total thermal energy was calculated using:

$$E_{tot\,AD}(kWh \cdot d^{-1}) = \frac{E_{AD\,in}}{\eta_{heat}} \quad \text{(A2.35)}$$

Where:

- $E_{AD\,in} = Loss$
- η_{heat} is 0.94 [4].

A2.2.2.2 Anaerobic digestion reactor – Electric energy

Electric energy for pumping and stirring are considered using the equations already reported above. Specific energy consumptions were also used for centrifugation (5 kWh t^{-1}) [8].

Composting electric energy consumption were calculated using 70 kWh $t^{-1}_{TSdigestate}$ as reference value [10].

A2.3 HTC + AD + P_{dry} Scenario

A2.3.1 Mass balance calculations

This scenario considers P recovery from hydrochar by acid leaching with HNO_3 (65 %, ρ_{HNO3} = 1.4 g cm^{-3}) on the dry solid. The mass balance has been carried out using lab-scale data (see **Chapter 2**).

Hydrochar contains a 55 611 mg P kg^{-1} and a solid/solution ratio equal to 5 wt % was chosen, according to the experiments carried out. Further, a ratio of 0.30 mL HNO_3 $g^{-1}_{dry\ hydrochar}$ was applied to calculate

the amount of acid required. A mass loss of 17 wt % was observed on hydrochar mass, whereas an increase of the same extent was observed for LHV. Thus, these values were used to calculate the mass flow of hydrochar after acid leaching and the subsequent LHV. The P yield was set equal to 78 %, according to experimental results.

A2.3.2 Energy consumption calculations

A2.3.2.1 Electric energy screw feeder

See above.

A2.3.2.2 Electric energy grinding

A specific energy consumption of grinding equal to 16 kWh t^{-1} was used [4].

A2.3.2.3 Electric energy mixing

See above (stirring).

A2.3.2.4 Electric energy filter press

See above.

A2.3.2.5 Electric and thermal energy dryer

See above.

A2.3.2.6 Electric energy pump

See above.

A2.3.2.7 Electric energy pelletizer

See above.

A2.4 HTC + AD + P_{wet} Scenario

A2.4.1 Mass balance calculations

This scenario considers P recovery from hydrochar by acid leaching with HNO_3 (65 %, ρ_{HNO3} = 1.4 g cm^{-3}) on the wet solid (before the air dryer).

In this scenario, the ratio of mL HNO_3 g $_{\text{dry hydrochar}}^{-1}$ remains constant, while the amount of water to be added is less than the previous scenario due to the water already contained in wet hydrochar. However, this difference resulted to be small, and therefore negligible.

A2.4.2 Energy consumption calculations

Electric energy consumption of grinding, mixing, filter press, screw feeder, pumps, dryer and the thermal energy consumption of the air dryer were calculated as already described above.

A2.5 Results - Contribution of each sub-processes for impact categories not shown in the main text of Chapter 5

A2.5.1 Ozone depletion (OD)

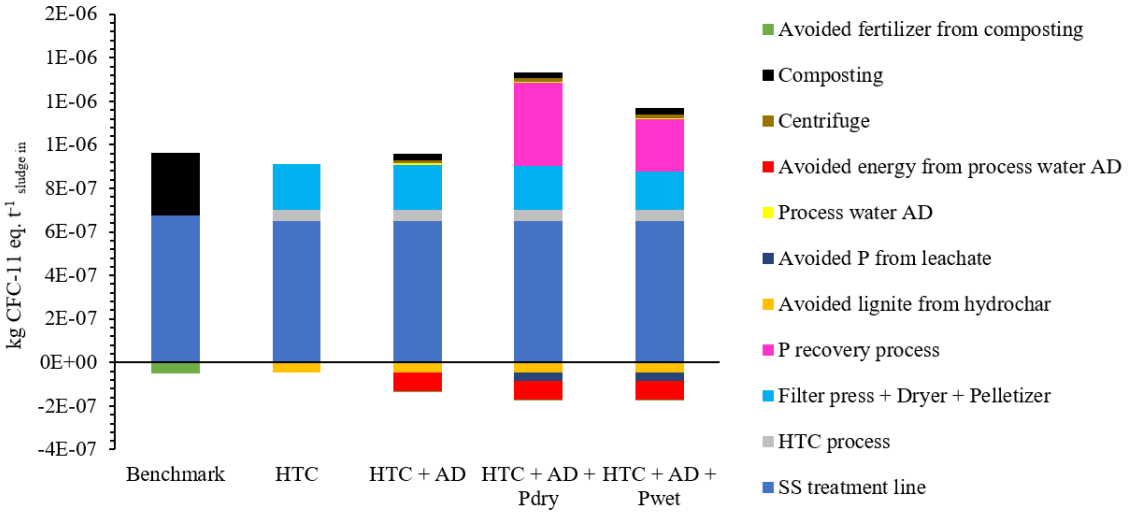

Figure A2.2 Sub-processes contribution for OD impact category.

A2.5.2 Photochemical ozone formation (POF)

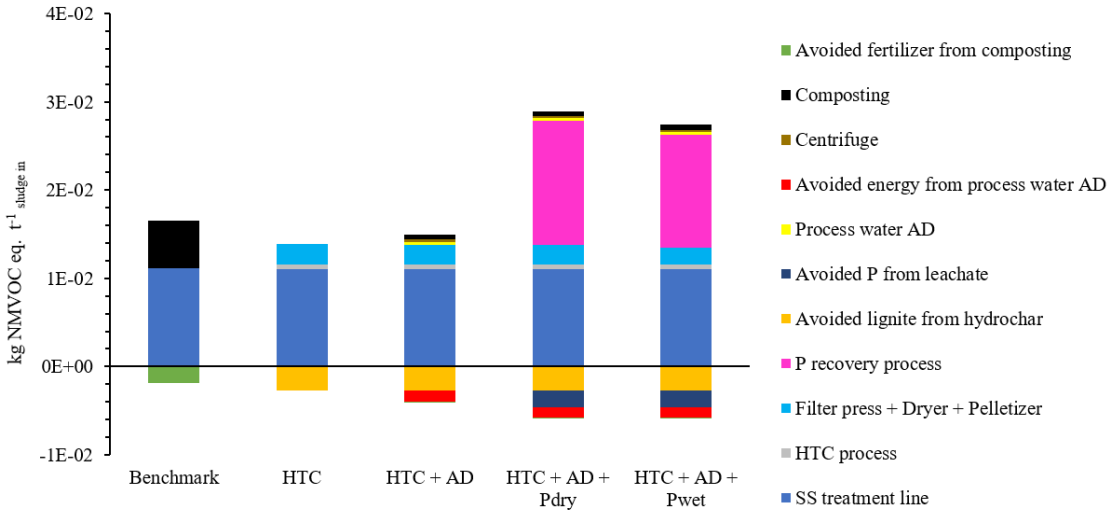

Figure A2.3 Sub-processes contribution for POF impact category.

A2.5.3 Particulate matter (PM)

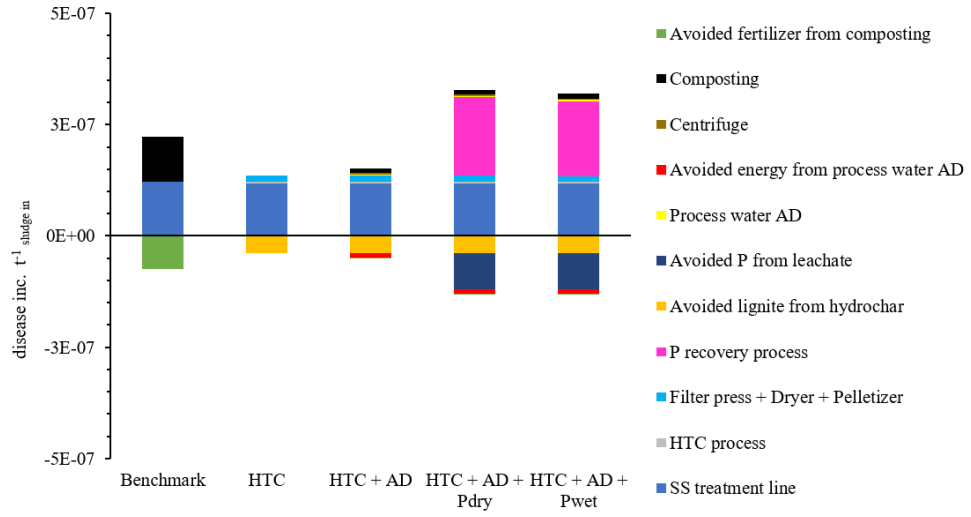

Figure A2.4 Sub-processes contribution for PM impact category.

A2.5.4 Human toxicity, non – cancer (HT_{nc})

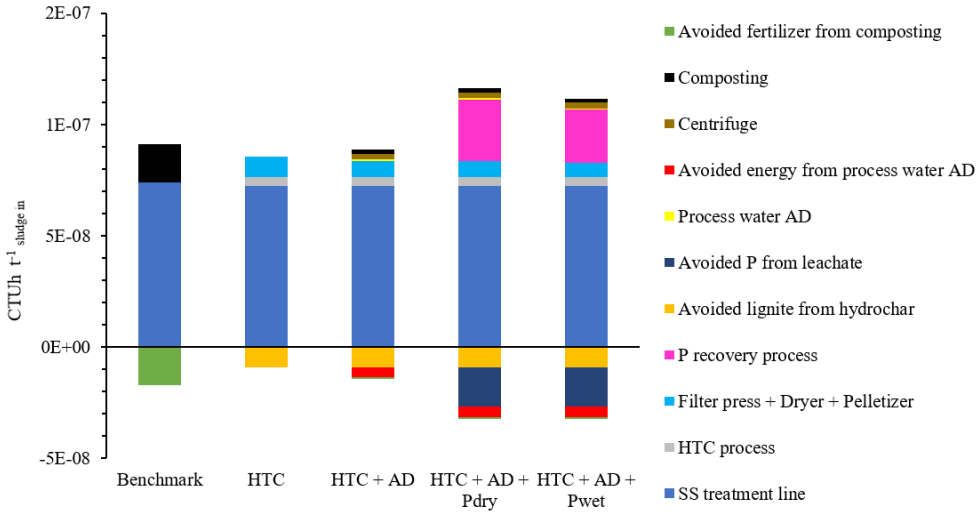

Figure A2.5 Sub-processes contribution for HT_{nc} impact category.

A2.5.5 Human toxicity, cancer (HT_c)

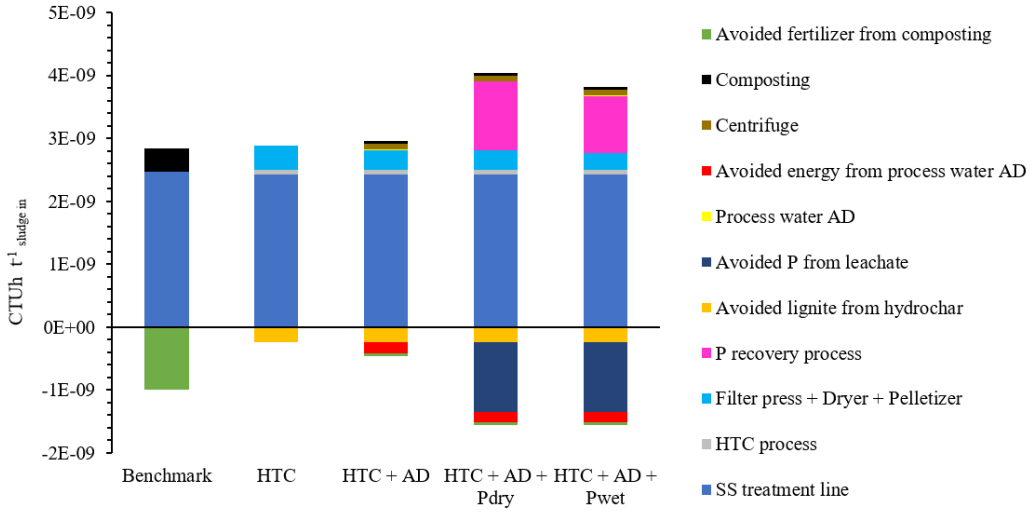

Figure A2.6 Sub-processes contribution for HT_c impact category.

A2.5.6 Acidification (A)

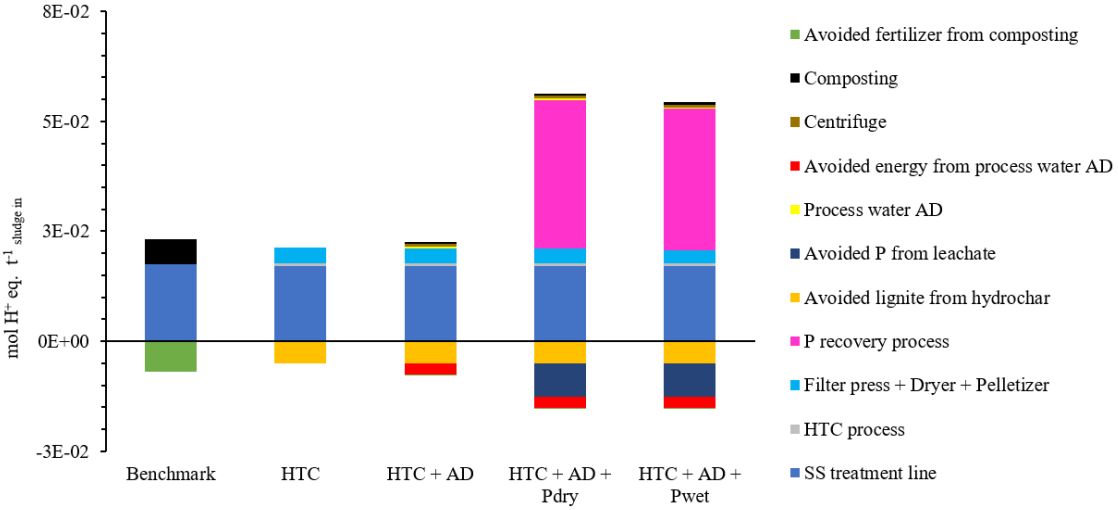

Figure A2.7 Sub-processes contribution for A impact category.

A2.5.7 Eutrophication, freshwater (E_f)

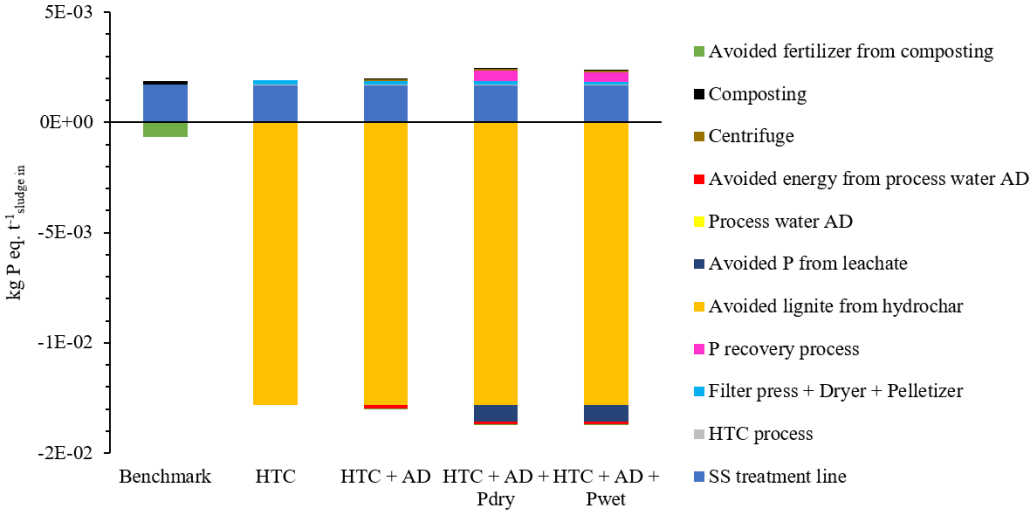

Figure A2.8 Sub-processes contribution for E_f impact category.

A2.5.8 Eutrophication, marine (E_m)

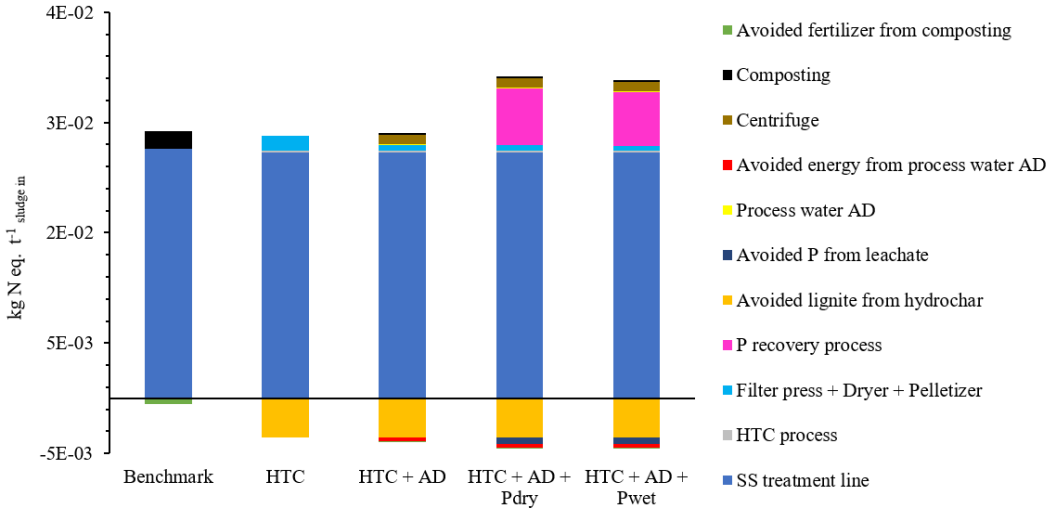

Figure A2.9 Sub-processes contribution for E_m impact category.

A2.5.9 Eutrophication, terrestrial (E_t)

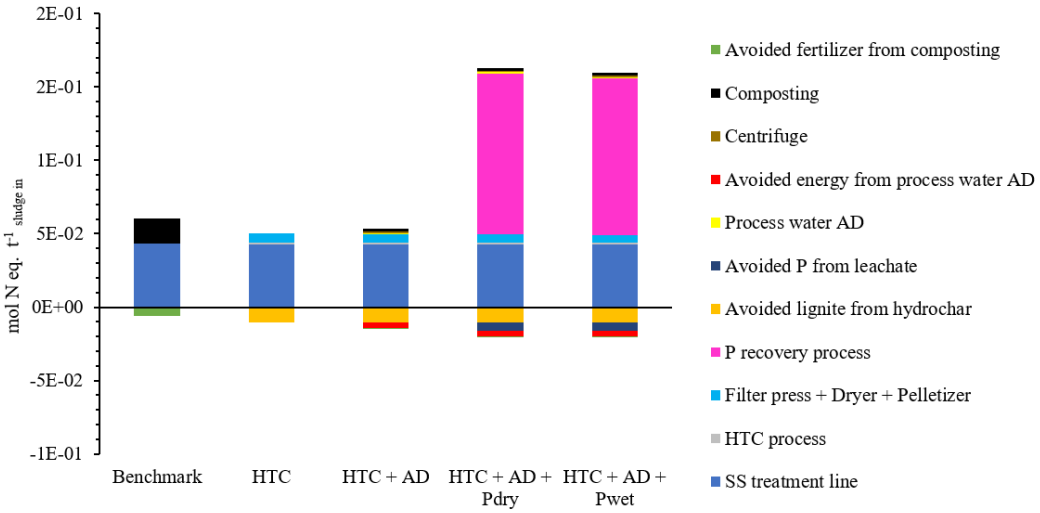

Figure A2.10 Sub-processes contribution for E_t impact category.

A2.5.10 Ecotoxicity, freshwater (ET_f)

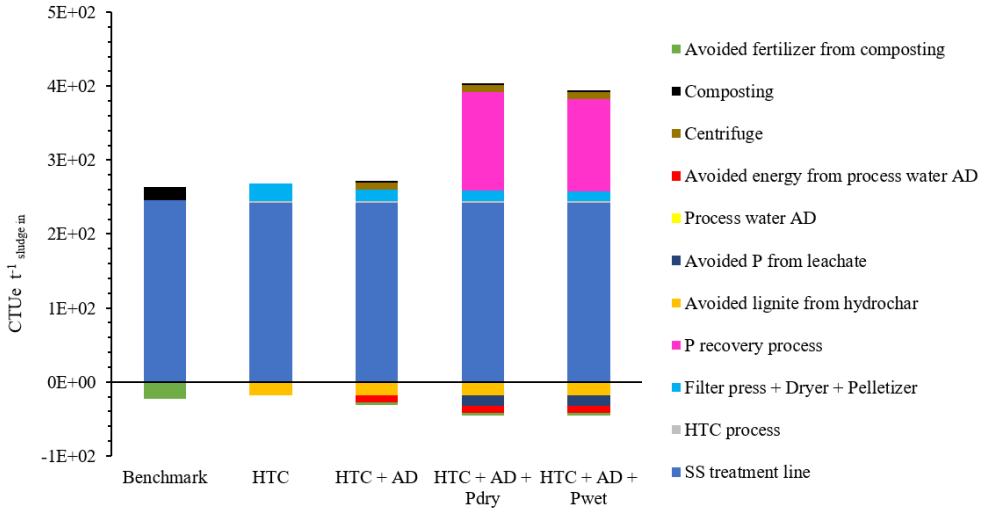

Figure A2.11 Sub-processes contribution for ET_f impact category.

A2.5.11 Land use (LU)

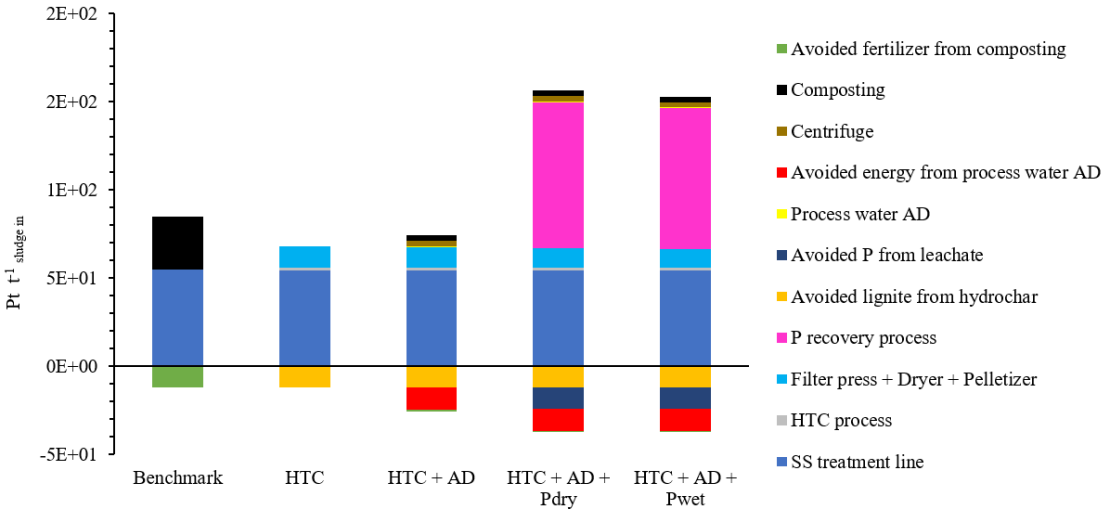

Figure A2.12 Sub-processes contribution for LU impact category.

A2.5.12 Water use (WU)

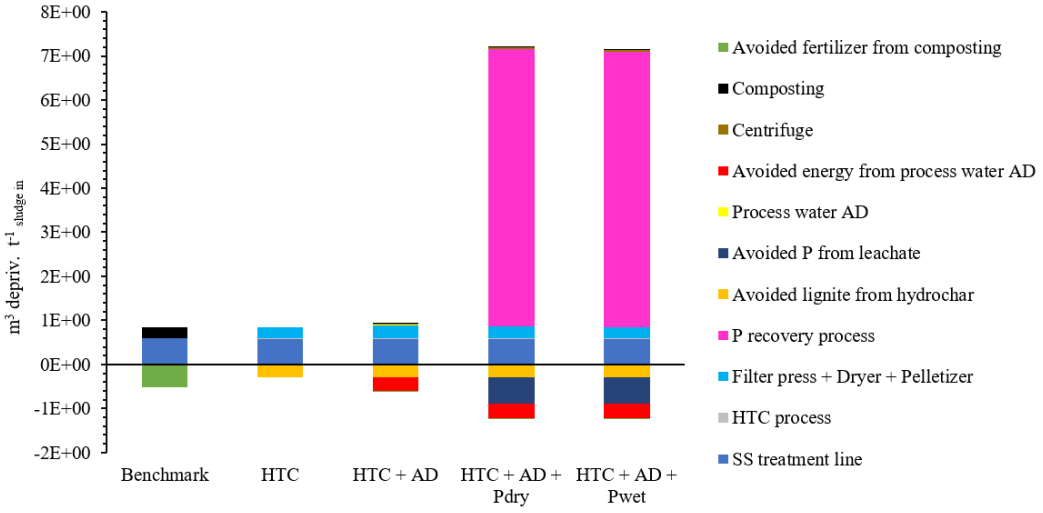

Figure A2.13 Sub-processes contribution for WU impact category.

A2.5.13 Resource use, fossil (RU_f)

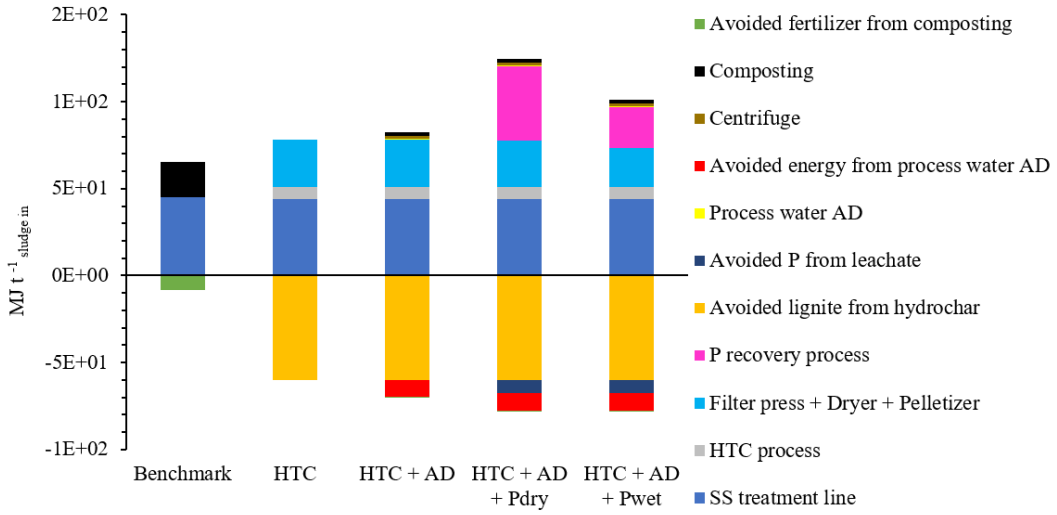

Figure A2.14 Sub-processes contribution for RU_f impact category.

A2.6 Results - Nitric acid impact

Nitric acid shows the highest percentage contribution to direct impacts in 15 of 16 impact categories for the P extraction process, in both scenarios with integrated P recovery process (**Fig. A2.15**).

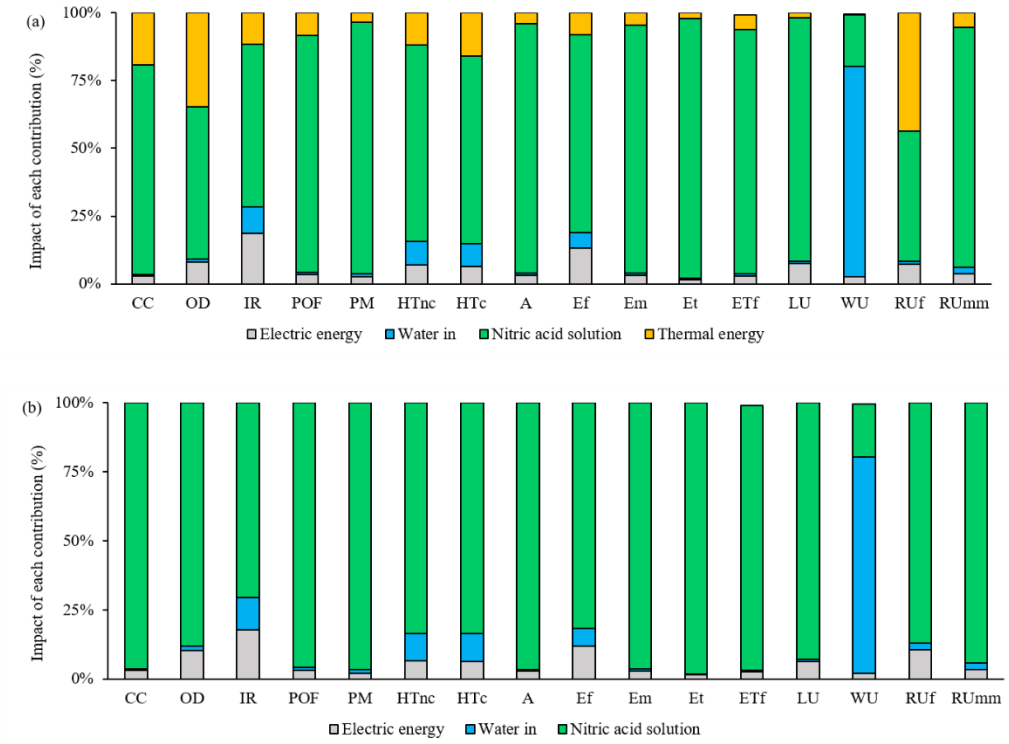

Figure A2.15 Percentage distribution of impacts of P recovery process for HTC + AD + P_{dry} (a) and HTC + AD + P_{wet} (b) scenarios.

A2.7 Results - Comparison between nitric and sulfuric acid impacts

In **Tab. A2.2** the comparison of direct impacts (as positive values) of HTC + AD + P_{dry} and HTC + AD + P_{wet} scenarios, using sulfuric or nitric acid for the P extraction, is reported:

Table A2.2 Comparison of direct impacts of HTC + AD + P_{dry} and HTC + AD + P_{wet} scenarios with both sulfuric and nitric acid.

Direct impacts	**CC**	**OD**	**IR**	**POF**	**PM**	**HT_{nc}**	**HT_c**	**A**	**E_f**	**E_m**	**E_t**	**ET_f**	**LU**	**WU**	**RU_f**	**RU_{mm}**
HTC + AD + P_{dry} nitric acid	1.37 E+01	1.33 E-06	5.27 E-01	2.89 E-02	3.28 E-07	1.16 E-07	4.04 E-09	5.64 E-02	2.44 E-03	2.92 E-02	1.63 E-01	4.03 E+02	1.56 E+02	7.22 E+00	1.24 E+02	1.05 E-04
HTC + AD + P_{dry} sulfuric acid	8.86 E+00	1.18 E-06	4.88 E-01	2.09 E-02	3.29 E-07	1.10 E-07	3.72 E-09	5.26 E-02	2.26 E-03	2.54 E-02	6.75 E-02	2.98 E+02	9.19 E+01	8.65 E+00	1.18E+ 02	9.81E-05
Reduction of sulfuric acid respect to nitric acid	-35%	-12%	-7%	-28%	**0%**	-5%	-8%	-7%	-8%	-13%	-59%	-26%	-41%	**20%**	-5%	-7%
HTC + AD + P_{wet} nitric acid	1.20 E+01	1.17 E-06	5.01 E-01	2.74 E-02	3.19 E-07	1.12 E-07	3.81 E-09	5.44 E-02	2.38 E-03	2.88 E-02	1.60 E-01	3.94 E+02	1.53 E+02	7.16 E+00	1.01E +02	1.01E-04
HTC + AD + P_{wet} sulfuric acid	7.22 E+00	1.01 E-06	4.62 E-01	1.93 E-02	3.21 E-07	1.05 E-07	3.49 E-09	5.07 E-02	2.19 E-03	2.50 E-02	6.41 E-02	2.89 E+02	8.85 E+01	8.59 E+00	9.44E +01	9.42E-05
Reduction of sulfuric acid respect to nitric acid	-40%	-13%	-8%	-29%	**0%**	-6%	-8%	-7%	-8%	-13%	-60%	-27%	-42%	**20%**	-7%	-7%

Table A2.3 Total impacts for the investigated scenarios and for each impact category applying the maximum ER value.

Impact category		*Benchmark*	*HTC*	*HTC + AD*	*HTC + AD + P_{dry}*	*HTC + AD + P_{wet}*
Climate Change (CC)	kg CO_2 eq. $t^{-1}_{sludge\ in}$	4.77E+00	-1.29E+00	**-1.47E+00**	4.80E+00	3.20E+00
Ozone depletion (OD)	kg CFC-11 eq. $t^{-1}_{sludge\ in}$	9.14E-07	7.91E-07	**7.48E-07**	1.08E-06	9.13E-07
Ionising radiation (IR)	kBq U^{235} eq. $t^{-1}_{sludge\ in}$	2.86E-01	-2.16E-03	-3.49E-02	-4.92E-02	**-7.42E-02**
Photochemical ozone formation (POF)	kg NMVOC eq. $t^{-1}_{sludge\ in}$	1.47E-02	7.08E-03	**6.80E-03**	1.86E-02	1.71E-02
Particulate matter (PM)	disease incidence $t^{-1}_{sludge\ in}$	1.49E-07	**3.77E-08**	3.79E-08	1.28E-07	1.20E-07
Human toxicity. non cancer (HT_{nc})	$CTU_h\ t^{-1}_{sludge\ in}$	7.37E-08	6.76E-08	**6.49E-08**	7.40E-08	6.96E-08
Human toxicity. cancer (HT_c)	$CTU_h\ t^{-1}_{sludge\ in}$	**1.85E-09**	2.24E-09	2.11E-09	2.07E-09	1.85E-09
Acidification (A)	mol H^+ eq. $t^{-1}_{sludge\ in}$	1.63E-02	8.41E-03	**6.99E-03**	3.23E-02	3.04E-02
Eutrophication. freshwater (E_f)	kg P eq. $t^{-1}_{sludge\ in}$	1.23E-03	-3.09E-02	-3.10E-02	-3.12E-02	**-3.13E-02**
Eutrophication. marine (E_m)	kg N eq. $t^{-1}_{sludge\ in}$	2.36E-02	1.48E-02	**1.46E-02**	1.90E-02	1.87E-02
Eutrophication. terrestrial (E_t)	mol N eq. $t^{-1}_{sludge\ in}$	5.45E-02	2.39E-02	**2.28E-02**	1.24E-01	1.21E-01
Ecotoxicity. freshwater (ET_f)	$CTU_e\ t^{-1}_{sludge\ in}$	2.41E+02	2.21E+02	**2.12E+02**	3.26E+02	3.17E+02
Land use (LU)	pt $t^{-1}_{sludge\ in}$	7.28E+01	3.61E+01	**2.93E+01**	9.73E+01	9.39E+01
Water use (WU)	m^3 deprived $t^{-1}_{sludge\ in}$	3.29E-01	1.01E-01	**-1.23E-01**	5.50E+00	5.45E+00
Resource use. fossils (RUf)	MJ $t^{-1}_{sludge\ in}$	5.67E+01	-7.54E+01	**-8.15E+01**	-4.84E+01	-7.11E+01
Resource use. minerals and metals (RU_{mm})	kg Sb eq. $t^{-1}_{sludge\ in}$	**3.10E-05**	4.52E-05	4.20E-05	6.19E-05	5.81E-05

A2.8 References of A2

1. Lucian, M., Volpe, M., Merzari, F., Wüst, D., Kruse, A., Andreottola, G., Fiori, L.: Hydrothermal carbonization coupled with anaerobic digestion for the valorization of the organic fraction of municipal solid waste. Bioresour. Technol. 314, 123734 (2020). https://doi.org/10.1016/j.biortech.2020.123734
2. Basso, D.: Hydrothermal carbonization of waste biomass Daniele Basso. 1–277 (2016)
3. Danso-Boateng, E., Holdich, R.G., Martin, S.J., Shama, G., Wheatley, A.D.: Process energetics for the hydrothermal carbonisation of human faecal wastes. Energy Convers. Manag. 105, 1115–1124 (2015). https://doi.org/10.1016/j.enconman.2015.08.064
4. Piccinno, F., Hischier, R., Seeger, S., Som, C.: From laboratory to industrial scale: a scale-up framework for chemical processes in life cycle assessment studies. J. Clean. Prod. 135, 1085–1097 (2016). https://doi.org/10.1016/j.jclepro.2016.06.164
5. Mendecka, B., Lombardi, L., Micali, F., De Risi, A.: Energy Recovery from Olive Pomace by Hydrothermal Carbonization on Hypothetical Industrial Scale: a LCA Perspective. Waste and Biomass Valorization. 11, 5503–5519 (2020). https://doi.org/10.1007/s12649-020-01212-0
6. Grobelak, A., Grosser, A., Kacprzak, M., Kamizela, T.: Sewage sludge processing and management in small and medium-sized municipal wastewater treatment plant-new technical solution. J. Environ. Manage. 234, 90–96 (2019). https://doi.org/10.1016/j.jenvman.2018.12.111
7. Lucian, M., Fiori, L.: Hydrothermal carbonization of waste biomass: Process design, modeling, energy efficiency and cost analysis. Energies. 10, (2017). https://doi.org/10.3390/en10020211
8. Lombardi, L., Nocita, C., Bettazzi, E., Fibbi, D., Carnevale, E.: Environmental comparison of alternative treatments for sewage sludge: An Italian case study. Waste Manag. 69, 365–376 (2017). https://doi.org/10.1016/j.wasman.2017.08.040
9. Teoh, S.K., Li, L.Y.: Feasibility of alternative sewage sludge treatment methods from a lifecycle assessment (LCA) perspective. J. Clean. Prod. 247, 119495 (2020). https://doi.org/10.1016/j.jclepro.2019.119495
10. Hong, J., Hong, J., Otaki, M., Jolliet, O.: Environmental and economic life cycle assessment for sewage sludge treatment processes in Japan. Waste Manag. 29, 696–703 (2009). https://doi.org/10.1016/j.wasman.2008.03.026
11. Garrido-Baserba, M., Molinos-Senante, M., Abelleira-Pereira, J.M., Fdez-Güelfo, L.A., Poch, M., Hernández-Sancho, F.: Selecting sewage sludge treatment alternatives in modern wastewater treatment plants using environmental decision support systems. J. Clean. Prod. 107, 410–419 (2015). https://doi.org/10.1016/j.jclepro.2014.11.021

A3 - Appendix of Chapter 6

Table A3.1 Energy properties of food waste and hydrochars.

	T_i (ºC)	T_b (ºC)	T_m (ºC)	DTG_m (% min^{-1})	CCI·10^{-7} (min^{-2} ºC^{-3})	HHV (MJ kg^{-1})	Fuel ratio	Energy density	Energy recovery efficiency
Food waste	175	543	298	41.6	10.2	18.9	0.18	-	-
HC200	184	536	287	42.3	10.3	20.3	0.33	1.07	0.69
HC230	190	518	282	42.3	10.0	23.7	0.37	1.25	0.73

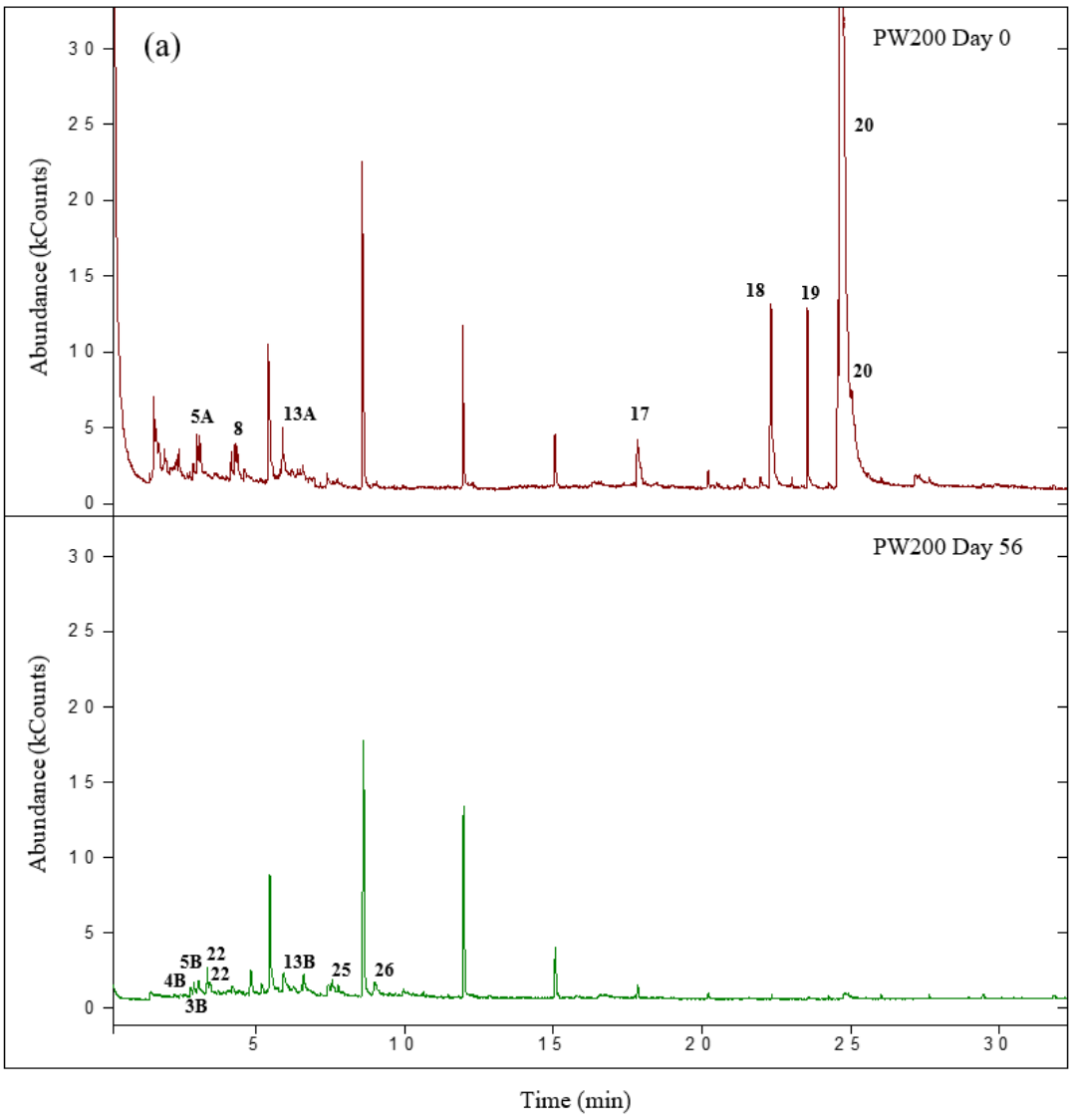
(a)
PW200 Day 0
Abundance (kCounts)
5A
8
13A
17
18
19
20
20
PW200 Day 56
Abundance (kCounts)
4B
5B
3B
22
22
13B
25
26
Time (min)

.

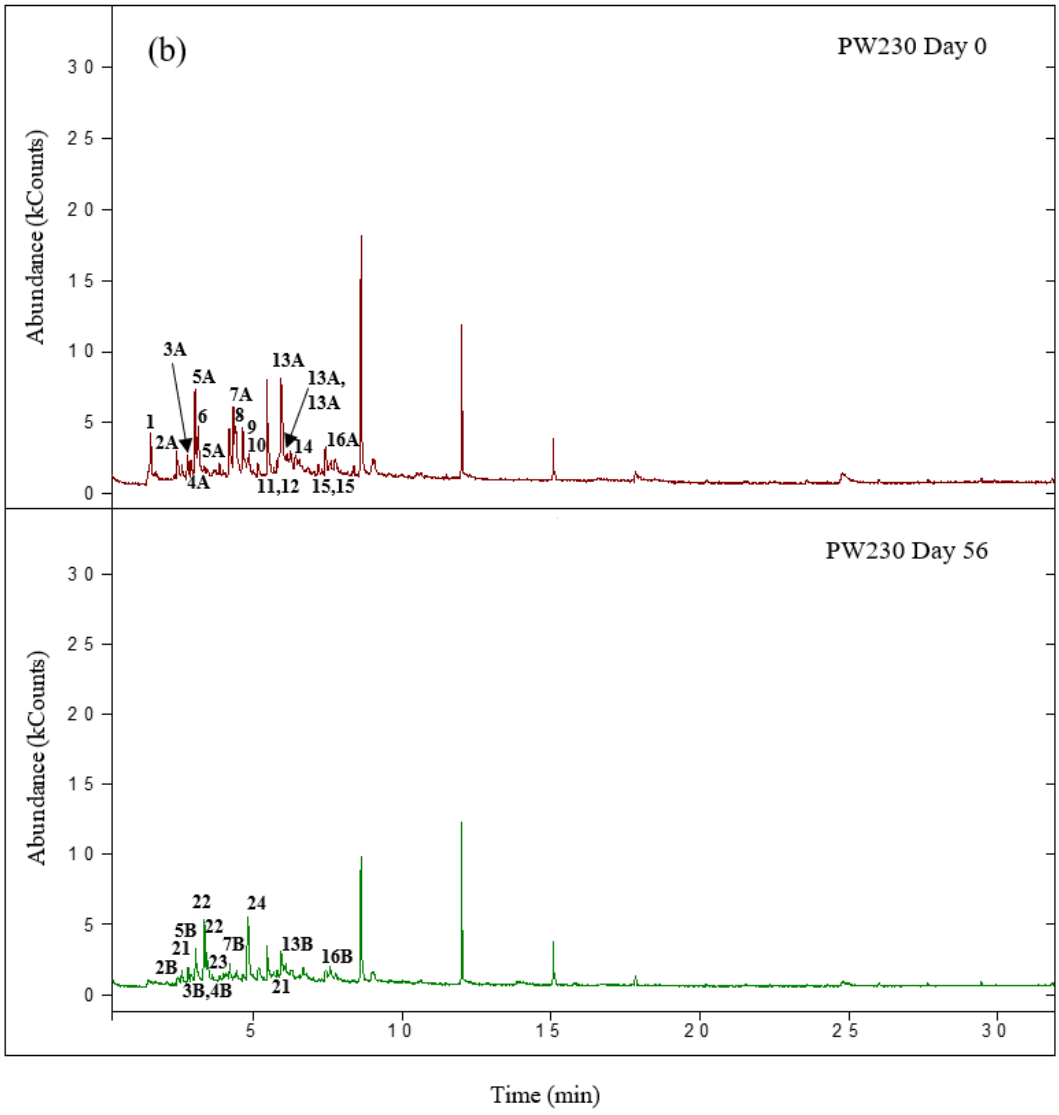

Figure A3.1 GC/MS chromatograms of PW200 (a) and PW230 (b) at Day 0 and Day 56 of anaerobic digestion experiment from HTC on food waste.

Table A3.2 Compounds identified by GC/MS in process water (PW200 and PW230) obtained from HTC (200 and 230°C, 1 h) at the beginning and end of anaerobic digestion.

Peak number	Category	Compound	Removal PW200 (%)	Removal PW230 (%)
1	non aromatic N-compounds	trimethylamine	-	> 99
2A	Pyridines	pyridine	-	81
2B	Pyridines	pyridine	-	
3A	Long-chain hydrocarbons	2-hexene	-	47
3B	Long-chain hydrocarbons	2-hexene	gen	
4A	Aromatic compounds	2,3,6-trichlorobenzaldehyde	-	67
4B	Aromatic compounds	2,3,6-trichlorobenzaldehyde	gen	
5A	Pyridines	2-methyl-pyridine	74	67
5B	Pyridines	2-methyl-pyridine		
6	Pyridines	3-aminopyridine	-	> 99
7A	Pyrazines	2,6-dimethyl-pyrazine	-	72
7B	Pyrazines	2,6-dimethyl-pyrazine		
8	Aromatic compounds	1,4-benzenediamine	> 99	> 99
9	Aromatic compounds	N-methylaniline	-	> 99
10	Aromatic compounds	N,4-dimethyl-benzenamine	-	> 99
11	Pyridines	2,4,6-trimethylpyridine	-	> 99
12	Pyridines	3-(1-methyl-2-pyrrolidinyl)-(S)-pyridine	-	> 99
13A	Pyrazines	2-ethyl-3-methyl-pyrazine	93	83
13B	Pyrazines	2-ethyl-3-methyl-pyrazine		

14	Aromatic compounds	N,3-dimethyl-benzenamine	-	> 99
15	Aromatic compounds	2,4,5-trimethylbenzenamine	-	> 99
16A	Pyrazines	2,3-diethyl-pyrazine	-	31
16B	Pyrazines	2,3-diethyl-pyrazine		
17	Long-chain hydrocarbons	dodecanoic acid	> 99	-
18	Long-chain hydrocarbons	methyl ester hexadecanoic acid	> 99	-
19	Aromatic compounds	2-ethyl-9,10-anthracenedione	> 99	-
20	Long-chain hydrocarbons	methyl ester (Z)-9-octadecenoic acid	> 99	-
21	non aromatic N-compounds	2-ethylpiperidine	-	gen
22	Long-chain hydrocarbons	2-methyl-cyclopentanone	gen	gen
23	Aromatic compounds	ethylbenzene	-	gen
24	Long-chain hydrocarbons	1-octanol	-	gen
25	Aromatic compounds	4,5-dimethyl-ortho-phenylenediamine	gen	-
26	Long-chain hydrocarbons	octahydro-4,4,8,8-tetramethyl-4a,7-methano-4aH-naphth[1,8a-b]oxirene	gen	-

gen: generated

Acknowledgment

I met a lot of people during this journey! Each of them, gave a contribute!

Thank you to my supervisors, Prof. Riccardo Gori and Prof. Angel F. Mohedano, you always find a moment for giving me the right advice, you are great people. Thanks to Prof. Lidia Lombardi, for your valuable help in the LCA world. A big thank you to Prof. M. Angeles de la Rubia and Prof. Elena Diáz, you were always helpful and kind with me. Thanks to Prof. Monica Puccini, Prof. S. Vitolo, and their research group at University of Pisa, collaborating with you was a great opportunity for me to learn a lot. Thanks to the whole people of SLUDGE4.0 project, it was a big challenge, but being part of it was extraordinary!

Thank you to the DICEA team, I am grateful to all of you! Thanks to Benedetta and Letizia, you were the perfect mates to make this journey easier when it got difficult. Thank you to Riccardo and Tommaso, you always had the right answer to my (many) questions. I would like to thank you also the UAM group, especially Andrés and Paul, because you were always friendly and ready to give me your help. Thanks to Martina, you were the friend that I needed during the Spanish stay, and thanks also to Marco and Matteo for sharing with me the period in Madrid. Thank you also to all the people that I met at UNALAB joint laboratory.

I am grateful to my family; you always support me! Thanks to my old and new friends. Thank you to Giovanni, you were patient and you are the person that always understood me. Last, but not least, you were the right advisor for LCA analysis!